12-2013

# Design and Synthesis of Novel Sultams as Non-nucleoside Inhibitors of HIV Reverse Transcriptase

Brian Chadwick LeCroix
*University of Tennessee, Knoxville*, blecroix@utk.edu

To the Graduate Council:

I am submitting herewith a dissertation written by Brian Chadwick LeCroix entitled "Design and Synthesis of Novel Sultams as Non-nucleoside Inhibitors of HIV Reverse Transcriptase." I have examined the final electronic copy of this dissertation for form and content and recommend that it be accepted in partial fulfillment of the requirements for the degree of Doctor of Philosophy, with a major in Chemistry.

David C. Baker, Major Professor

We have read this dissertation and recommend its acceptance:

Shawn R. Campagna, David Jenkins, Hong Guo

Accepted for the Council:

Carolyn R. Hodges

Vice Provost and Dean of the Graduate School

(Original signatures are on file with official student records.)

# Design and Synthesis of Novel Sultams as Non-nucleoside Inhibitors of HIV Reverse Transcriptase

A Dissertation Presented for the

Doctor of Philosophy

Degree

The University of Tennessee, Knoxville

Brian Chadwick LeCroix

December 2013

## Dedication

To my wife, Becky LeCroix, who has been with me throughout my entire time at the University of Tennessee even in these last two years we spent eight hours apart. Thank you for being my support through it all. I love you and I dedicate this to you.

To both my parents, who have supported me through my whole life. For helping me throughout my undergraduate studies with whatever you could. I wouldn't be here today if it wasn't for you two, "Not letting me work on the farm so that I couldn't end up enjoying it and becoming a farmer."

## Acknowledgements

I first want to give acknowledgments to Dr. David C. Baker, my major professor, for giving this farm boy from Alabama the guidance and teaching needed to complete my studies at the University of Tennessee. You were always there to offer any kind of advice, help, or joke to aid in the laboratory; whether it be fixing equipment, offering a new idea for a reaction, just sitting in your office talking stories about anything from chemistry to farming. Thank you for giving me this project to sort of speak, “add the final chapter to the book.” You are an amazing chemist, and I am proud to follow in your footsteps. To this day, I do not regret and will never regret choosing the University of Tennessee and in choosing you as my advisor. I hope that although I may leave here to move across the country we will stay in contact through e-mail or phone.

I would also like to mention my committee members, Dr. Shawn Campagna, Dr. David Jenkins, and Dr. Hong Guo. Thank you for your time in helping me through my first research proposal in my second year. And thank you for any advice you gave along the way.

Now I would like to acknowledge former and current members of the Baker group. To Dr. Samson Francis and Dr. Julio Gutierrez for being there to show me the ropes of the lab when I first joined. To Dr. Samson Francis for being my host when I came to Knoxville for the Open House weekend, and brewing great cups of coffee. To Dr. Julio Gutierrez for helping out in showing me the ropes of the NMR. I also want to mention Dr. Costyl Njiojob and Dr. Irene Abia who had to deal with me throughout their

time at UT; you two made the lab entertaining in either just someone to talk to and laugh with or in providing someone to play pranks on, Costyl.

To the current members of the Baker group, Yundi Gan and Bo Meng, keep at it; you'll reach your goals soon. Thank you guys for always making me jealous of your lunch with the Chinese food you'd bring in everyday.

To all the undergraduates that passed through the Baker group in my time at UT. To first off Andy Hahn for just being around to talk to about whatever and for turning red at any of Dr. Baker's jokes. To Andy Rowe for helping with the project and for harassing me via text messaging during Alabama Tennessee football games even though you knew Alabama would end up winning. To Andrew Moss, who started off in my third year in the program as just a freshman. You're definitely an intelligent student who would make a fine chemist, it's a shame the field will lose you to the medical field.

I also want to acknowledge Dr. Carlos Steren. You helped me in training me on the new 500 MHz NMR and were always willing to talk about anything with NMR experiments or analysis. I enjoyed learning how to maintain the NMR under your tutelage and just discussing things about Argentina as we performed helium fills on the magnet.

I would also like to mention the friends I had coming into UT and the ones I made at UT. So many of you to name, but John West, Cal Woodruff, Aaron Edwards, Chuck Smith, Bob Kress, Adam Condra, Evan Jones, Chris and Allyn Milojevich, Blake and Andy Hicks, Stefanie Bragg, and Kelly Hall thank you for just being around to provide a stress outlet with either a night out drinking or just talking about old times at either BSC or in high school.

I also want to thank Dr. David J.A. Schedler for inspiring me to go into the field of Organic Chemistry from your lectures and your research projects at Birmingham-Southern College.

Finally, I want to thank all in the Department of Chemistry at the University of Tennessee. So many things could not function within the department if it weren't for so many of you.

It has been a long road to this day, but I have finally made it. I thank all of you, and even some I have not mentioned. And last but not least, Roll Tide.

## Abstract

The compound 2-methyl-3-phenyl-2,3-dihydro-1,2-benzisothiazole 1,1-dioxide (NSC 108406) was identified as an HIV-1 reverse transcriptase inhibitor by the National Cancer Institute. Using this lead, the Baker group has developed a series of analogues with various groups at the 3-position that show a spectrum of biological activities. In the end, the substituents used could not compare to the biological activity of the inhibitor efavirenz (Sustiva® [trademark]), and so it was decided to synthesize sultams with alkylethynyl substituents at the 3-position of the sultams in an attempt to mimic the activity of efavirenz.

Previous research analyzed the proposed novel sultams in the modeling program FlexiDock contained in the SYBYL package. The FlexiDock modeling performed by Riyam Kafri gave evidence for unique binding of the proposed sultams in both wild type and Y181C reverse transcriptase. Another in silico method applied to the novel sultams was the CoMFA analysis, which looks at the similarities between common compounds with known biological activities and uses this information to calculate predicted activities for untested compounds.

Synthesis of the novel ethynyl sultams is achieved by reacting the desired lithiated alkylethynyl reagent with 3-chloro-1,2-benzoisothiazole 1,1-dioxide, *pseudo*-saccharin chloride. Methods were designed to yield either the mono-alkylated or the bis-alkylated products. Various methods for reducing the mono-substituted compounds were applied to attempt to achieve the desired *S* enantiomer. Other methods resulted in the production of a racemic mixture of the reduced compounds. The reduced mono-

sultams or the bisalkylated sultams are then methylated to yield the desired final product.

An aryl sultam was also synthesized in a similar method employed by Baker and co-workers by reacting saccharin with two equivalents of a Grignard reagent of 3-bromostyrene. The compound was reduced with the catalyst (*R*)-Cp*RhCl[(1*S*,2*S*)-*p*-TsNCH($C_6H_5$)CH($C_6H_5$)$NH_2$] [(*R*)-pentalmethylcyclopentadienylrhodium chloride-(1*S*,2*S*)-*p*-toluenesulfonyl-1,2-diphenylethylenediamine] and alkylated with base and iodomethane. The vinyl group was reacted in a modified Simmons–Smith fashion to produce a cyclopropyl group in the *meta* position on the phenyl ring.

# Table of Contents

# List of Tables

# List of Figures

# List of Schemes

# List of Mechanisms

# Abbreviations

| | |
|---|---|
| AIDS | Acquired Immunodeficiency Syndrome |
| Arg | Arginine |
| Asn/N | Asparagine |
| Asp/D | Aspartic Acid |
| AZT | Azidothymidine |
| BAF | Barrier-to-Autointegration Factor |
| BINAL-H | Lithium 2,2’-dihydroxy-1,1’-binapthylethoxyaluminum hydride |
| CADA | Cyclotriazadisulfonamide |
| Cbz | Carboxybenzyl |
| CD4 | Cluster of Differentiation 4 |
| CDC | Center for Disease Control |
| $CeCl_3 \bullet 7H_2O$ | Cerium trichloride heptahydrate |
| $CH_2I_2$ | Diiodomethane |
| $Co_2(CO)_8$ | Dicobalt octacarbonyl |
| CoMFA | Comparative Molecular Field Analysis |
| CRC5 | C-C chemokine receptor type 5 |
| $Cs_2CO_3$ | Cesium Carbonate |
| CXCR4 | C-X-C chemokine receptor type 5 |
| Cys/C | Cysteine |
| DCM | Dichloromethane |
| DDDP | DNA dependent DNA polymerase |

| | |
|---|---|
| DFT | Density Functional Therapy |
| DNA | Deoxyribonucleic Acid |
| EtOH | Ethanol |
| FDA | Food and Drug Administration |
| Glu | Glutamine |
| Gly | Glycine |
| GNA | *Galanthus nivalis* |
| gp | Glycoprotein |
| HEPT | 1-[(2-hydroxyethoxy)methyl]-6-(phenylsulfanyl)thymine |
| HHA | *Hippeastrum* hybrid |
| HIV-1/2 | Human Immunodeficiency Virus 1 or 2 |
| HMB | High mobility group |
| HONO | Nitrous Acid |
| HPLC | High-Performance Liquid Chromatography |
| DARTHRMS | High Resonance Direct Analysis in Real Time Mass Spectrometry |
| HTLV-1 | Human T-Cell Leukemia Virus Type-1 |
| IDAV-1/2 | Immune Deficiency Associated Virus |
| Ile/I | Isoleucine |
| *i*-$Pr_2EtN$ | Diisopropylethylamine |
| LAH | Lithium aluminum hydride |
| Leu/L | Leucine/L |

| | |
|---|---|
| Lys/K | Lys/K |
| MeOH | Methanol |
| MM3 and MM4 | Molecular Mechanics Type 3 and 4 |
| $NaBH_4$ | Sodium Borohydride |
| *n*-BuLi | *n*-Butyllithium |
| $NaCNBH_3$ | Sodium cyanoborohydride |
| NCI | National Cancer Institute |
| NMR | Nuclear Magnetic Resonance |
| NNIBP | Non-Nucleoside Reverse Transcriptase Inhibitor Binding Pocket |
| NNRTI | Non-Nucleoside Reverse Transcriptase Inhibitor |
| NRTI | Nucleoside Reverse Transcriptase Inhibitor |
| NtRTI | Nucleotide Reverse Transcriptase Inhibitor |
| PBS | Primer Binding Site |
| Phe | Phenylalanine |
| PR | Protease |
| Pro | Proline |
| PyBOP | Benzotriazole-1-yl-oxytripyrrolidinophosphonium hexafluorophosphate |
| QSAR | Quantitative Structure–Activity Relationship |
| RDDP | RNA Dependent DNA Polymerase |
| RNA | Ribonucleic Acid |
| RNase H | Ribonuclease H |

| | |
|---|---|
| RT | Reverse Transcriptase |
| Ru | Ruthenium |
| S:C | Substrate-to-Catalyst Ratio |
| Ser | Serine |
| SIV | Simian Immunodeficiency Virus |
| $SO_2$ | Sulfur Dioxide |
| THF | Tetrahydrofuran |
| Thr | Threonine |
| TIBO | 4,5,6,7-Tetrahydroimidazole[4,5,1-*jk*][1,4]benzodiazepine-2(1*H*)-one |
| Trp/W | Tryptophan |
| TsDPEN | *N*-*p*-Toluenesulfonyl-1,2-diphenylethylenediamine |
| Tyr/Y | Tyrosine |
| Val | Valine |
| wt RT | wild type Reverse Transcriptase |

# I. Introduction

## A. AIDS and HIV—The Beginning

The human immunodeficiency virus, or HIV, is a virus that is an ongoing menace to mankind, with several million people either being HIV positive or living with AIDS (acquired immunodeficiency syndrome), the full-blown disease that it produces. Since HIV was first reported in 1981, it has become a pandemic, and approximately 34 million people in the world were living while infected with HIV, while there were 1,700,000 deaths from AIDS in 2011 alone.[1] Of the 34 million plus living with HIV in the world in 2012, approximately 9.7 million people were receiving antiretroviral therapy in the lower- or middle-income countries.[1]

When the world became knowledgeable of HIV and AIDS, people believed it targeted specific groups of people. Since then, it has been determined that HIV is a virus with no discrimination and the ability to infect anyone. HIV is predominately transmitted through sexual acts, but can also be transmitted through other methods such as contaminated blood transfusions and the sharing of used narcotic needles.[1]

HIV may not have been discovered as the causative agent of AIDS as early as it was if not for the work by Robert Gallo and co-workers in the 1970s at the National Cancer Institute, NCI, with the Human T-Cell Leukemia Virus Type 1 (HTLV-1) and its discovery as a retrovirus that affects humans.[2, 3]

In June of 1981, the Center for Disease Control (CDC) reported in the *Morbidity and Mortality Weekly Report* of cases of five men with a rare *Pneumocystis* pneumonia. The pneumonia was reported to the CDC by Dr. Michael Gottlieb and colleagues who had noticed the infection in several homosexual men.[4] What made the pneumonia so

unique was that the patients had a lack of CD4 T-cells, helper T-cells, preventing the body from fighting the infection. It was found that by the time the CDC released the report, already 250,000 Americans were infected with the disease, which came to be known as AIDS.[4] With the first discoveries in the United States (U.S.) being reported on homosexual men, the disease began to be known as "the gay disease" and having ties with the homosexual lifestyle. However, in New York in the same year, Dr. Gerald Friedland and Dr. Arye Rubenstein began seeing the disease in non-gay men in injection drug users, and in some cases symptoms in their children.[4] After reading the article by the CDC, two European doctors reported seeing similar cases in their patients: primarily heterosexual, with the most notable cases including heterosexual women in Belgium originally from central Africa.[4]

Further support arose against the idea of AIDS being a homosexual disease when Dr. Margaret Fischl reported cases to the CDC in 1982 of non-homosexual male and female Haitians having both *Pneumocystis* pneumonia and Kaposi's sarcoma. However, Dr. Fischl reports the CDC initially did not believe her findings.[4]

The first signs of AIDS being a viral related situation arose when three heterosexual men with hemophilia developed symptoms of *Pneumocystis* pneumonia. The significance of this comes from the treatment of hemophiliacs with plasma from donors that is processed through a filtration system that only a virus is small enough to slip through.[4] Another case was found in a 20-month-old infant who had received several blood transfusions that developed immunosuppressant symptoms. It was discovered that one out of the nineteen donors of blood for the child had already passed away from AIDS.[4]

With more and more cases giving evidence to AIDS being caused by a virus, researchers began an investigation to find the cause of the newly discovered disease. Gallo began to claim that the source of AIDS could be a retrovirus like HTLV-1. His initial tests showed patients diagnosed with AIDS as having positive test results for a retrovirus. It was found later that these patients also had HTLV-1, but at the time Gallo's team was convinced that they had discovered a new retrovirus responsible for the disease, AIDS, and worked to find out more about the retrovirus.[5] Gallo goes on to state in a review from 2004 that it was difficult declaring HIV as the causative agent of AIDS because AIDS has been known to show signs of infection typically after years since the actual date of infection, followed by the fact that once AIDS was shown to be present, a patient already had numerous other infections that could have been confused as the causative agent.[3]

After Gallo's group released information regarding a new retrovirus as the causative agent in AIDS, a group at the Pasteur Institute in Paris led by Luc Montagnier were prompted to lead studies on the new retrovirus.[5] The group obtained the biopsy of a lymph node of a homosexual patient with multiple lymphadenopathies and symptoms that had become known to be early signs of AIDS. The initial studies found that a retrovirus was present in the lymph node biopsy with ionic requirements of a viral reverse transcriptase related to that of HTLV, but it had viral core proteins not immunologically related to the p24 and p19 proteins of sub-group 1 of HTLV.[6] Further studies included comparing the proteins of the newly discovered retrovirus with proteins of other HTLV species isolated from various cases, which resulted in seeing a relation between various HTLV species and the new retrovirus, but with some very clear

differences. With personal communication with Gallo, Montagnier reported that studies show the nucleic acid sequences of the new virus have less than 10% homology with that of other HTLV isolates.[6] Even with this new information, Montagnier's group did not link the new retrovirus to AIDS at the time because the patient was not diagnosed with "frank" AIDS.[5]

Montagnier's group later went on to collect several isolates of a retrovirus from AIDS-positive patients and labeled them as IDAV-1 and -2 for immune deficiency associated virus. However, before Montagnier published information involving IDAV-1 and -2 in 1984, Gallo's group isolated viruses that did not display immunological cross-reactions with HTLVs, and they began to have two isolates continue to grow through cell-line cultures.[5] Gallo et al. would use the experiments involved in the cell-line cultures to develop a blood test that was later used to confirm the presence of the newly discovered virus, termed HTVL-III, in 48 different patients.[5, 7, 8] From their collection of evidence through their studies, Gallo's group was able to determine that HTVL-1, which was later termed HIV, was the single cause of the disease, AIDS.

With the development of the first conclusive blood test for HIV from Gallo et al., donated blood for transfusions could be tested for infection to prevent the further spread of the virus. Furthermore, with the development of the continuous cell-line cultures, testing for anti-HIV drugs could be performed such as with azidothymidine (3'-azido-3'-deoxythymidine, AZT), the first moderately successful anti-HIV drug.[5, 9]

**B. Possible Origins of HIV**

The primate lentivirus group consists of the two strands of HIV and various simian immunodeficiency viruses (SIV). Among the primate lentivirus group are five

different lineages, with HIV-1 and HIV-2 coming from two different lines.[10] Since documentation of the two serotypes of HIV, it has been found that HIV-1 can be accounted for a majority of infections around the world.[11] Viral cluster experiments show that HIV-1 clusters with that of $SIV_{CPZ}$, chimpanzee SIV, suggesting that the source of HIV-1 comes from the chimpanzee subspecies *Pan troglodyte troglodytes* with evidence pointing to wild species of *P. t. troglodytes* in southern Cameroon being the likely original source.[10, 12] This leads to theories of the origin of HIV-1 and 2 as being in the area of West Africa.

One counter theory from Carel Mulder argues that the differences between HIV 1 and 2 sequences from that of SIV are so distinct that the origin could not have occurred recently.[13] Instead, Mulder argues that HIV has been around for much longer and evolving with primates along the way.

Studies of the origin of HIV-1 have been estimated to date back as far as the 1920s with the use of molecular clocks, and samples obtained in 1960 has corroborated this time scale through the analysis of the diversified group M strains of HIV-1.[14] It was also found in the study that a common ancestor of HIV-1, HIV-2, and $SIV_{AGM}$ existed about 150 years ago instead of the millions of years mentioned by Mulder.[10] The use of the molecular clock study investigates the viral sequences and notes the different mutations through time, allowing a rate of change to be estimated. However, there is the idea of host-dependent evolution and the molecular clock model does not take this into account.[10]

## C. The Lifecycle of HIV

### 1. Overview

There are several methods of treatment for HIV as of now with up to 20 different clinical pharmaceuticals on the market, but to understand how these methods of treatment work, HIV's life cycle of infection to reproduction should be discussed. The infection begins with the virus attaching to and becoming a parasite on a target cell (Figure 1). The virus binds via its glycoprotein-120 (gp120) to the CD4 receptors on T-lymphocytes, macrophages, monocytes, and/or dendritic cells. From here, the gp120 that bonded to the CD4 receptors binds to one of the chemokine receptors, CXCR4 or CRC5, which leads to the insertion and uncoating of the virus and insertion of its RNA and key enzymes for reverse transcription and nucleic acid integration.[5] Once inside the cell, the viral RNA goes through reverse transcription with the HIV enzyme, reverse transcriptase, to generate a complimentary DNA strand of the viral RNA. Next a double-stranded HIV–DNA is then produced and then proceeds to integrate into the cellular genome through the enzyme HIV integrase. The infected cell then becomes activated, resulting in the production of messenger RNA encoding for viral proteins, and then, within approximately 2.5 days of infection, virus particles begin budding out of the cell. Once out of the cell, viral polyproteins are cleaved by HIV protease, which results in the release of individual viral particles to infect other cells.[5]

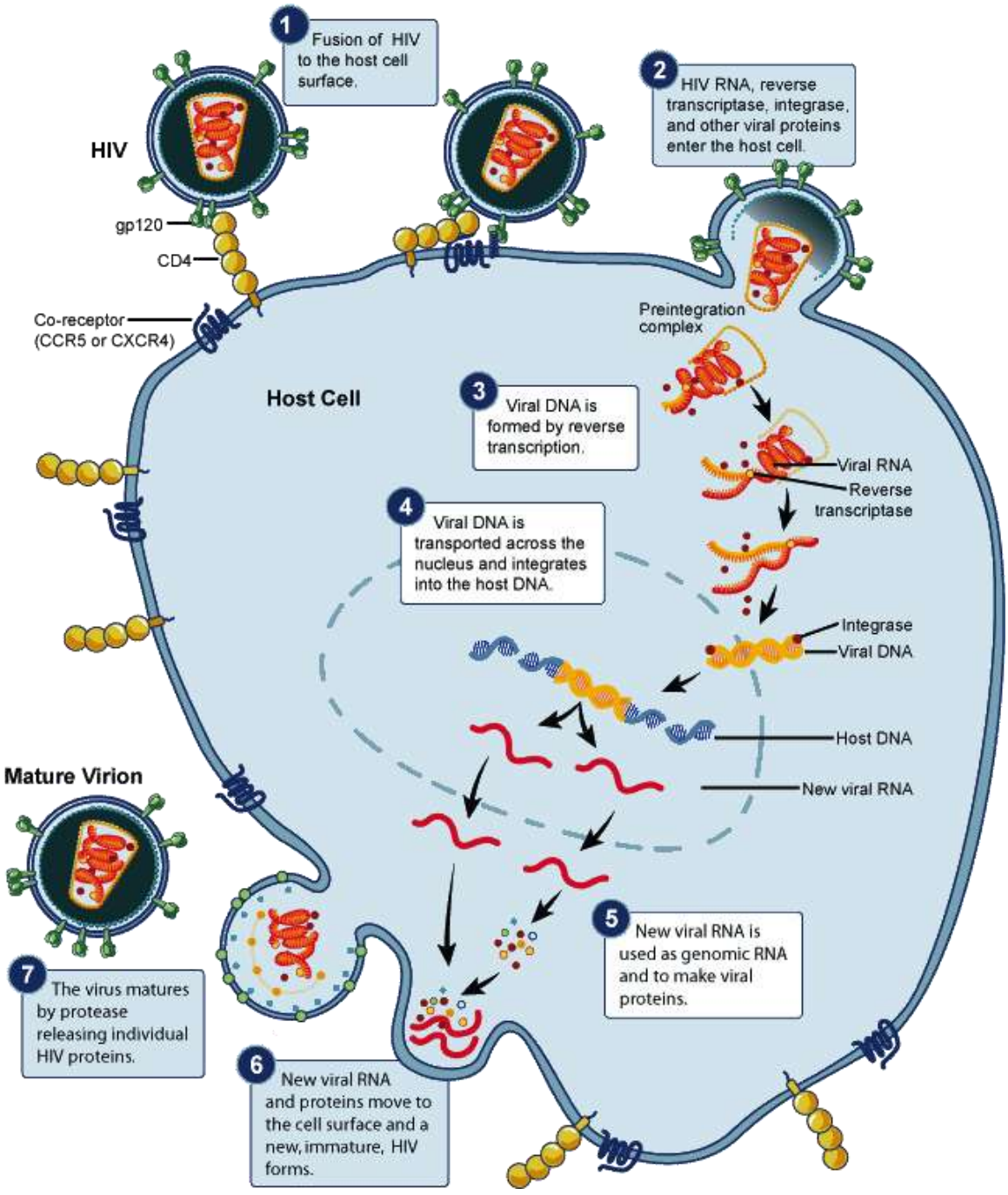


**Figure 1. The HIV life cycle, from fusion to budding.[15]**

**2. Viral Entry—Fusion**

For the virus to infect a host cell, it must first gain entry into the cell, and this begins with a process known as attachment followed by fusion. The virus first begins by the cleavage of glycoprotein 160 (gp160) into glycoprotein 120 (gp120) and gp41.[16] This step is followed by the binding of the subunit (gp120) of the viral envelope to the CD4 receptor site on the host cell (T-lymphocyte) wall.[17] Once the gp120–CD4 interaction has occurred, the virus proceeds next to binding to either a CCR5 (HIV strains that infect macrophages, M-tropic or R5 strains) or CXCR4 (strains that infect T-cells, T-tropic or X4 strains) chemokine co-receptor.[18] Following the gp120 and coreceptor binding, the gp41 subunit is altered to prepare itself for the formation of the pre-fusion intermediate designated the extended coiled-coil.[17] Before the coiled-coil inserts into the target cell membrane, a six-helix bundle, nicknamed the hairpin conformation, forms from what is known as the C- and the N-terminal heptad repeats of gp41 coming into a tight association together as the fusion peptide and the transmembrane domain of gp41 come into apposition bringing the two membranes, viral and target, close to each other allowing the merger to proceed.[17] This six-helix bundle forms a fusion pore that allows the release of the viral capsid into the cytosol of the target cell.[17]

**3. Reverse Transcription**

The reverse transcriptase enzymes of retroviruses perform up to three enzymatic activities. These enzymatic activities include: an RNA-dependent DNA polymerase (RDDP), ribonuclease H (RNase H), and a DNA-dependent DNA polymerase (DDDP). The enzymes execute the steps in the order of copying a plus-strand RNA genome to

produce a minus strand of DNA (RDDP), removal of the plus-strand RNA template (RNase H), and the synthesis of a plus-strand of DNA with the minus-strand of DNA acting as a template (DDDP).[19]

The RT of HIV is a heterodimer consisting of a large p66 subunit (66-kDa) 560 amino acids in length and a small p51 subunit (51-kDa) 440 amino acids in length with common N termini.[19, 20] Both p66 and p51 contain the polymerase domain of RT (RDDP and DDDP), while a C-terminal fragment that is removed from the p66 subunit is involved with the RNase H domain of RT.[19] In the activity of the two subunits, it has been found as homodimers, they remain active, but as a monomer, both subunits become inactive.[21] Furthermore, altering the p51 subunit by mutation shows little effect on the activity, while mutating the p66 subunit in some way causes the heterodimer to be inactive.[22]

The structure of HIV-1 RT, as seen in an X-ray crystal structure, shows that overall the enzyme is asymmetric, but both p66 and p51 contain subdomains labeled as “finger,” “palm,” “thumb,” and “connection.” The p66 subunit is positioned such that the finger, palm, and thumb domains are open in a sense of forming a cleft, termed a “hand” shown to be the active site of the enzyme (Figure 2). The p51 subunit and the p66 are joined at the connection domain, which is rotated such as that the palm of p51 is hidden within the enzyme.[19] This shape supports the activity discussed previously of it appearing the p66 subunit being largely responsible for reverse transcription to proceed.

Both the polymerase and the RNAse H of RT reside in the p66 subunit. The two active sites are located as such that a (+)-strand RNA template ($tRNA^{Lys}$) enters “through” the fingers and thumb of RT where it attaches to the 18 nucleotide primer

binding site (PBS).[23-25] The RNA strand passes through the RDDP enzyme to be transcribed into a (-)-strand of DNA starting from the 5' end of the (+)-strand RNA. From here the combined RNA/DNA strand is fed into RNAse H, which removes the RNA strand so that the (-)-DNA strand could be used as a template to form a complete double stranded helix of viral DNA as it is passed through the DDDP. It has been theorized that the RDDP and the DDDP are one in the same.[19] After the DNA replication process has completed, the integration process begins.

Since its discovery, there have been crystal structures analyzed and characterized of RT as it is bound with an inhibitor, a double-stranded DNA, and a polypurine RNA:DNA double strand and unbounded RT. Through each structure, it was seen the flexibility of the thumb and fingers of the RT active site.[26-28] The shape of the RT enzyme is altered at the thumb position when RT is either bound or unbound. When RT is unbound, the thumb is placed in an upright position, residing in close proximity of the finger subdomains.[29] It was found that there are two small and weak interactions between the thumb and fingers at the Arg78 amino acid of the fingers with the main chain of the thumb and a nonpolar interaction between Phe61 in the fingers and Leu289 of the thumb. These interactions allow for the mobility of the thumb to be flexible and free because of their weak interactions. The shape of the active site with the presence of either a double-stranded DNA or the RNA:DNA double strand showed a similar shape with the finger and palm subdomains interacting heavily with the substrates present in the cavity.[27, 28]

The ability for the catalytic site to be so flexible has allowed for RT to be a viable target for inhibition (Figure 2). (The mechanism for NNRTIs shall be discussed in detail in the section on non-nucleoside reverse transcriptase inhibitors below.)

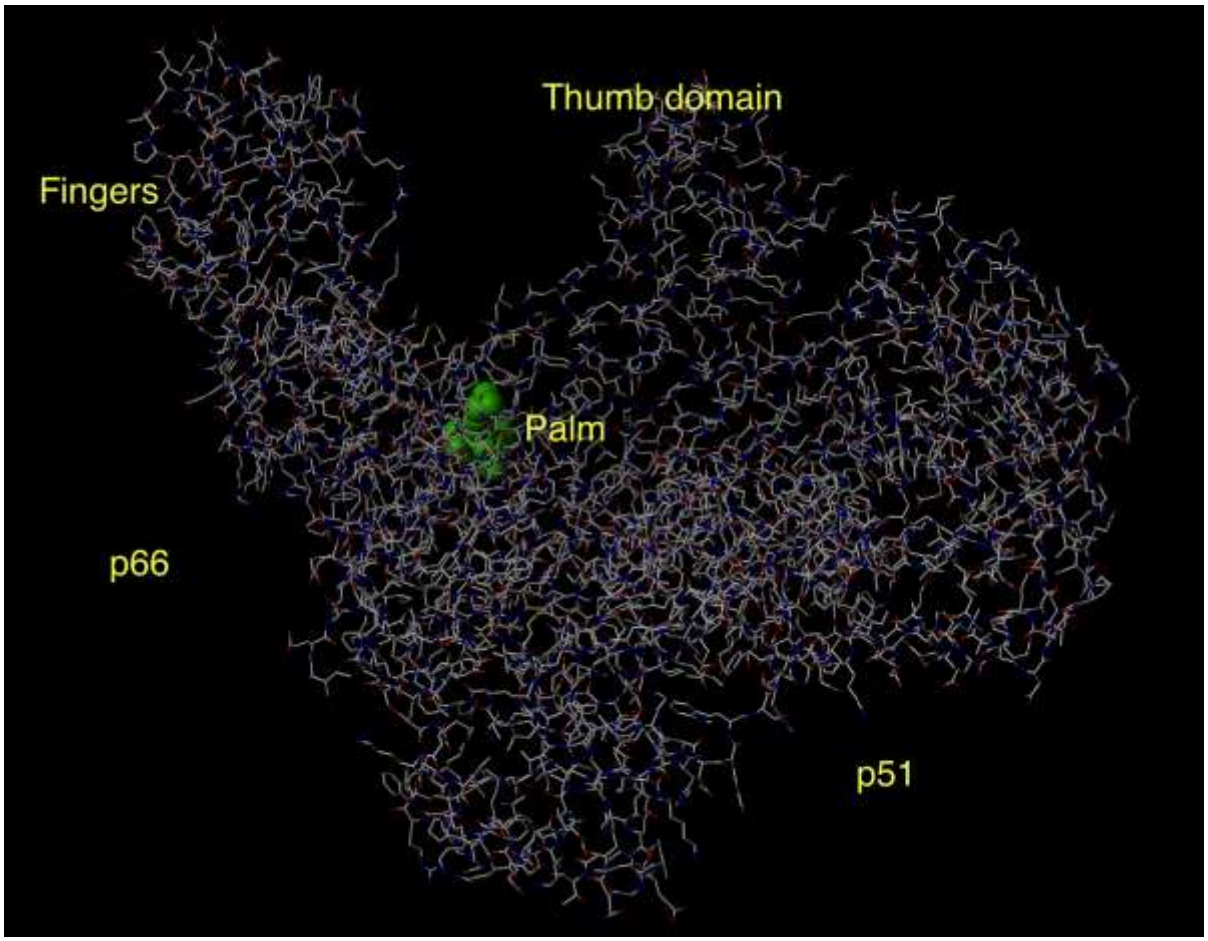


**Figure 2. Reverse transcriptase with efavirenz (green) in binding pocket of palm. (pdb code 1ikw).**

**4. Integration**

Integration is an important step in the viral replication cycle, in that it is responsible for ensuring a stable relationship between the viral DNA from reverse transcription and that of the host–cell chromosome.[19] Before integration begins, a pre-integration complex forms, which isolates show the complex involving the linear viral DNA, reverse transcriptase, nucleocapsid integrase, and two cellular proteins (high-mobility-group, HMB-I(Y), and barrier-to-autointegration factor, BAF). Once formed, the pre-integration complex of HIV-1 enters the nucleus through the nuclear pore, where it then catalyzes integration.[30]

Integrase is responsible for cleaving the 3'-end groups of the viral DNA to expose hydroxyl groups at the 3'-ends so that host DNA can connect to the viral DNA. Once connected, the exposed viral DNA is inserted into the cellular DNA of the host, and this action can occur at any location on the host cellular DNA.[31]

After integration is complete, a viral polyprotein is synthesized by use of cellular machinery within the host cell.[32] Once synthesized, the viral polyprotein is subject to cleavage by the enzyme HIV protease.

**5. Protease Interaction**

As previously stated, the next step in the replication process is cleaving of the polyproteins in the protease (PR) enzyme to form mature viral particles. The HIV PR is composed of 99 amino acids, and belongs to the aspartyl protease class. All retroviral PRs, especially those of HIV, are monomers that contain a single conserved active-site triplet, Asp-Thr/Ser-Gly, and upon activation the PRs become a dimer.[19] As stated, the protease is responsible for cleaving the polyproteins, but so far no distinctive primary

sequence of amino acids has been found within a substrate polyprotein at the cleavage sites. Some common characteristics to be found are that the area around the cleavage sites are hydrophobic sequences, and a strongly conserved feature is at the N-terminal side of the cleaved bond.[33] The protease of HIV is an attractive target for inhibition, because each kind of retrovirus has to rely on its own PR for maturation to occur.[34]

**D. Methods of Treatment: Chemotherapy**

These processes necessary for the reproduction of HIV provide several points of pharmaceutical intervention, and several treatments have been developed involving inhibitors for the different processes. However, HIV has a high rate of mutation through its replication, with reverse transcriptase having the highest affinity for error. With this being the case, when a patient is treated with anti-virals that are active against wild-type HIV, the mutant strains that develop with a resistance to the inhibitor proceed on to replicate further making treatment difficult. Nevertheless, given the fact that an anti-HIV vaccine has eluded researchers for more than 30 years, and even today there seems to be little hope for an effective vaccine,[35, 36] chemotherapy is in reality the only method for combating the virus.

As previously discussed, the method of HIV reproduction is the act of the virus attaching to the cell at the CD4 receptor, binding to a co-receptor, fusion of the cell membrane, reverse transcription, integration, and the synthesis of new viral particles from the cleavage of polyproteins by protease. Each step in the replication process has been studied with the intent of designing inhibitors for treatment in anti-HIV therapy, with some inhibitors already on the market for patient use.

## 1. Virus Attachment and Fusion Inhibitors

### i. CD4 Receptor Inhibitors

As already discussed, the initial action of viral replication is the attachment to the CD4 receptor on the host cell wall. There are currently no pharmaceutically compounds approved on the market for inhibiting cellular CD4 receptors; however, there are classes of compounds showing inhibitory activity in studies. A series of analogues of cyclotriazadisulfoamide (Figure 3) are being investigated for preventing the viral attachment to the CD4 receptor.[37, 38] The inhibitors do so by down-modulating the CD4 receptor expression on cell surfaces without affecting other receptors, CXCR4 and CCR5.[39, 40] CADA has been found to be able to work alongside with other anti-HIV inhibitors such as NNRTIs, NRTIS, and protease inhibitors, which allows it to be added to the current method of HIV treatment by a cocktail of inhibitors.[41]

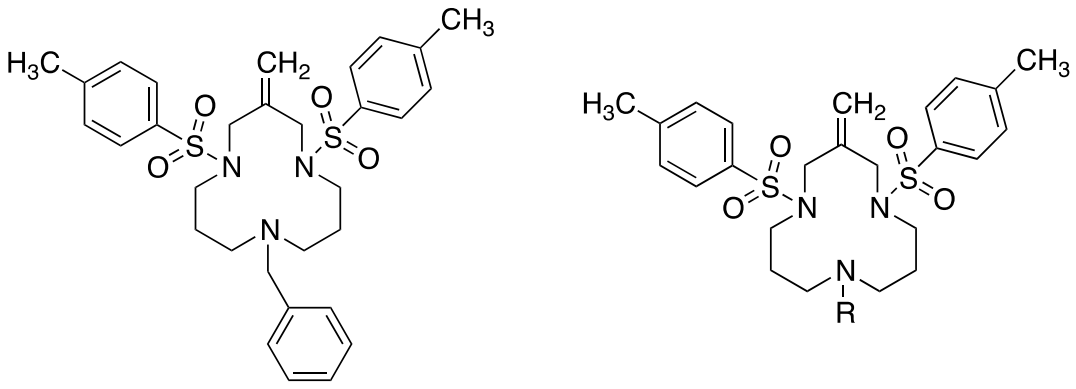


CADA

**Figure 3. CADA, a potential inhibitor of CD4, and the general structure of analogues.**

### ii. gp120 and gp41 Inhibition

A series of inhibitors has been identified for activity in preventing the gp120 from attaching to the CD4 receptor. It has been assumed that whether the inhibitor is naturally occurring or synthesized it acts by shielding off the positively charged sites in the V3 loop of the viral envelope of gp120, therefore preventing viral attachment.[18] Among these is a group of plant lectins from *Galanthus nivalis* (GNA) and *Hippeastrum* hybrid (HHA) that are mannose specific. The lectins have low toxicity and are considered to act as topical microbicides.[42] One microbicide being investigated is the protein cyanovirin-N isolated from the cyanobacterium *Nostoc ellipsosporum*.[43] Another potential highly active lectin isolated from red algae, *Griffithsia,* being studied is griffinsin.[44, 45] Both cyanovirin-N and griffithsin bind to the gp120 and inhibit the binding to the CD4 receptor both dependently and independently. Another potential gp120 inhibitor for viral attachment to CD4 is BMS-378806 [(4-benzoyl-1-[4-methoxy-1*H*-pyrrol[2,3-*b*]pyridine-3-yl]oxyacetyl)-2-(*R*)-methylpiperazine]. Unlike the two lectins, BMS-378806 has shown to be only active with dependent binding with CD4; this means it only affects the CD4—gp120 interaction.[46, 47] The three gp120 inhibitors discussed are shown in Figure 4.

Another type of viral attachment inhibitors is that of the gp41 class of inhibitors. Most notable of these is enfuvirtide, as it has been FDA approved for HIV treatment as of March 2003. Enfuvirtide (Figure 5) is a linear, 36 amino acid synthetic peptide resembling part of the HR2 region of gp41 causing it to act as a competitive inhibitor against HR1 binding.[48] A series of smaller molecule peptidic fusion inhibitors (Figure 5)

are being investigated and are currently showing better pharmacodynamics than enfuvirtide.[18]

$(NH_2)$Ser-Leu-Thr-His-Arg-Lys-Phe-Gly-Gly-Ser-Gly-Gly-Ser-Pro-Phe-Ser-Gly-Leu-Ser-Ser-Ile-Ala-Val-Arg-Ser-Gly-Ser-Tyr-Asp-X-Ile-Ile-Ile-Asp-Gly-Val-His-His-Gly-Gly-Ser-Gly-Gly-Asn-Leu-Ser-Pro-Thr-Phe-Met-Thr-Ile-Arg-Ser-Gly-Asp-Tyr-Ile-Asp-Asn-Ile-Ser-Phe-Glu-Thr-Asn-Met-Gly-Arg-Arg-Phe-Gly-Pro-Tyr-Gly-Gly-Ser-Gly-Gly-Ser-Ala-Asn-Thr-Leu-Ser-Asn-Val-Lys-Val-Ile-Gln-Ile-Asn-Gly-Ser-Ala-Gly-Asp-Tyr-Leu-Asp-Ser-Leu-Asp-Ile-Tyr-Tyr-Glu-Gln-Tyr(COOH)

**Griffithsin**

$(NH_2)$Leu-Gly-Lys-Phe-Ser-Gln-Thr-Cys-Tyr-Asn-Ser-Ala-Ile-Gln-Gly-Gly-Ser-Val-Leu-Thr-Ser-Thr-Cys-Glu-Arg-Thr-Asn-Gly-Gly-Tyr-Asn-Thr-Ser-Ser-Ile-Asp-Lew-Asn-Ser-Val-Ile-Glu-Asn-Val-Asp-Gly-Ser-Leu-Lys-Trp-Gln-Pro-Ser-Asn-Phe-Ile-Glu-Thr-Cys-Arg-Asn-Thr-Gln-Leu-Ala-Gly-Ser-Ser-Glu-Lew-Ala-Ala-Glu-Cys-Lys-Thr-Arg-Ala-Gln-Gln-Phe-Val-Ser-Thr-Lys-Ile-Asn-Lew-Asp-Asp-His-Ile-Ala-Asn-Ile-Asp-Gly-Thr-Lew-Lys-Try-Glu(COOH)

**Cyanovirin-N**

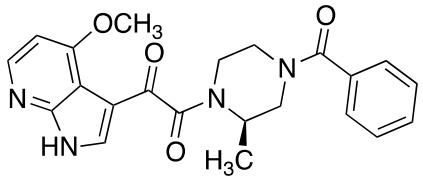


**BMS-378806**

**Figure 4. Viral attachment inhibitors.**

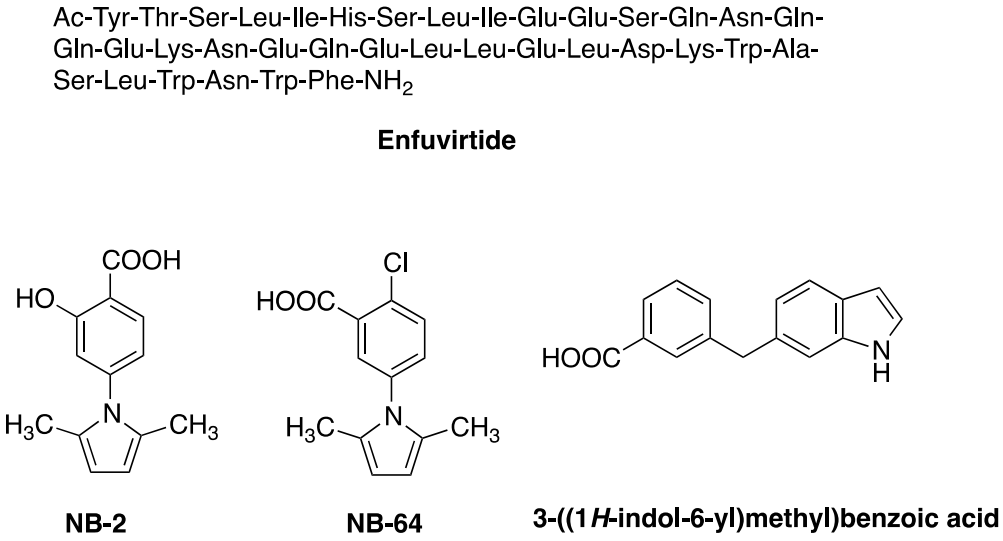


**Figure 5. gp41 Inhibitors.**

### iii. Co-receptor Inhibitors

As previously discussed, after the viral gp120 has been bound to the CD4 receptor, the virus then attaches to either of two co-receptors, CCR5 or CXCR4. The class of co-receptor inhibitors has included proteins, small molecules, and antibodies. The inhibitors interact with either the CCR5 or CXCR4 receptors or the viral envelope in order to prevent the interaction of the co-receptor with the viral envelope. Among the inhibitors developed, the first one was TAK 779 as an inhibitor of the CCR5 co-receptor (Figure 6). Compound SCH351125 has shown activity, but is not yet in clinical trials. The inhibitor maraviroc was approved by the FDA in August of 2007 and is currently part of treatment methods for co-receptor inhibition of HIV. Vicriviroc is currently in Phase III clinical trials.

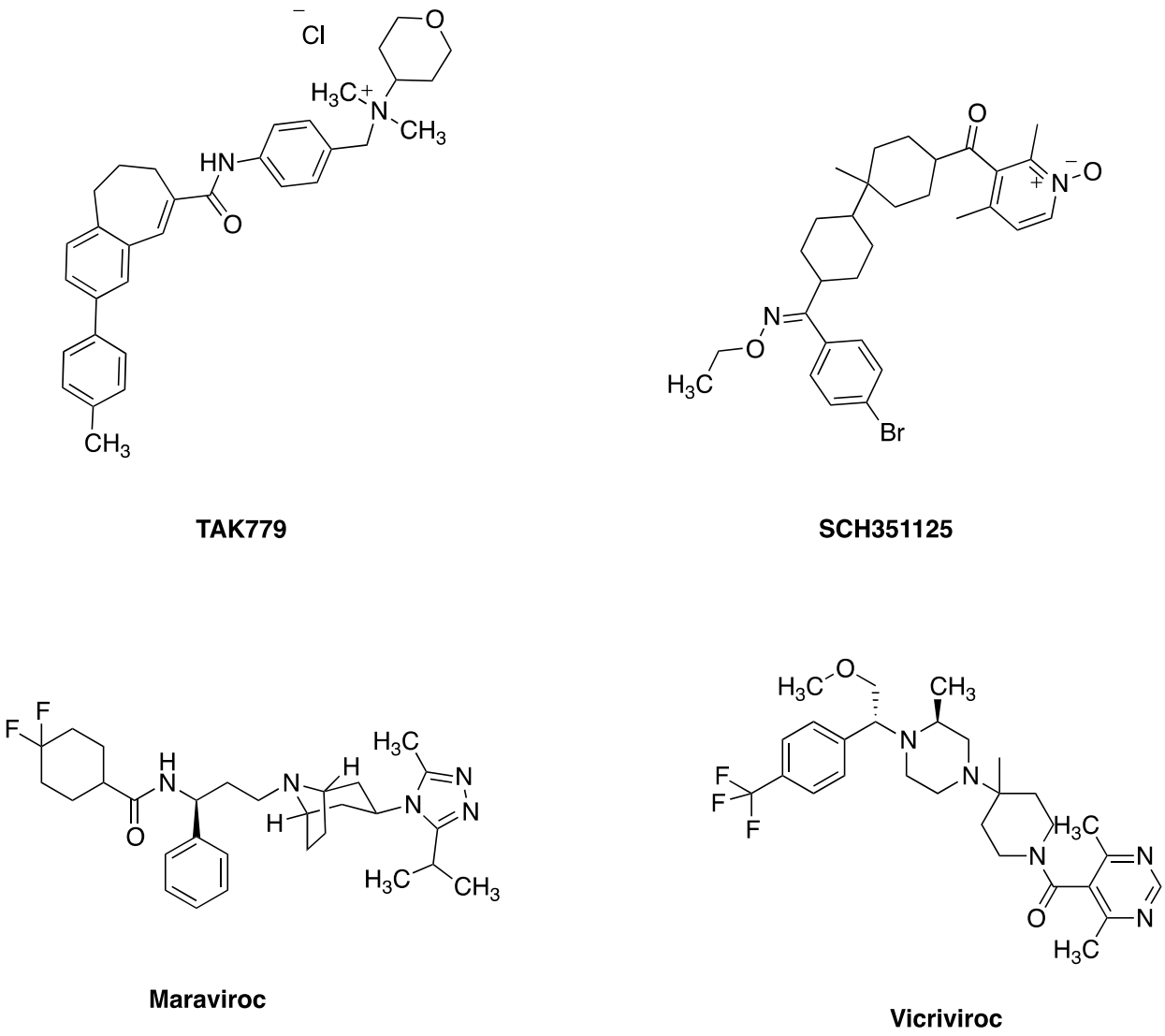


**Figure 6. Inhibitors affecting CXCR4 and CCR5.**

## 2. Integrase Inhibitors

Inhibitors for integration are relatively new for HIV treatment. The compound raltegravir (Figure 7) was approved by the FDA in October of 2007. Raltegravir acts by inhibiting the final step of the integration process, blocking the strand transfer of viral

DNA to the host cell DNA.[18] Another integrase inhibitor is elvitegravir, which was approved by the FDA as recently as August 2012.[49]

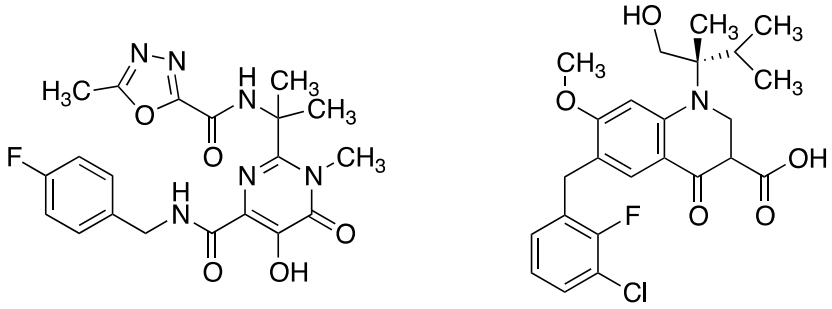


**Figure 7. Integrase inhibitors.**

### 3. Protease Inhibitors

Unlike the previous groups of inhibitors, protease inhibitors are a larger class of FDA-approved compounds. The protease inhibitors act as competitive inhibitors against the protease enzyme in its action to cleave viral polyproteins. The inhibitors are substrates of CYP3A4, and they either act by inhibiting or inducing specific CYP isoenzymes at varying degrees.[18] The earliest FDA-approved protease inhibitors were indinavir and saquinavir (Figure 8) approved in December of 1995, and most recently the protease inhibitor darunavir (Figure 8) was approved in June 2006.

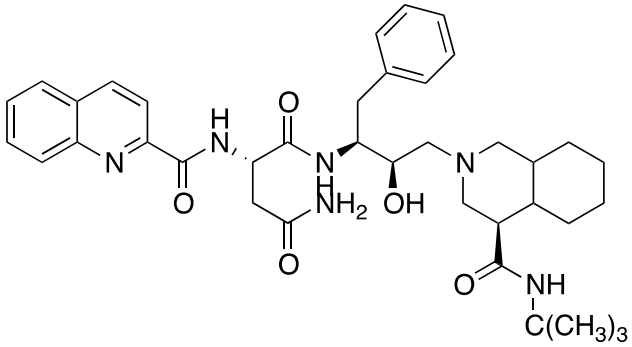

**Saquinavir**

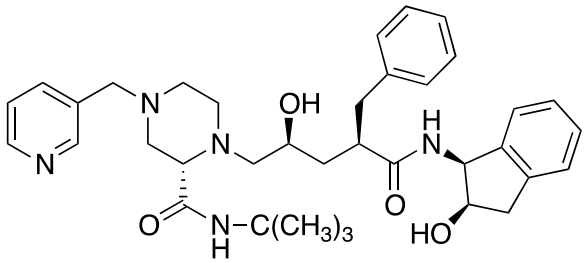

**Indinavir**

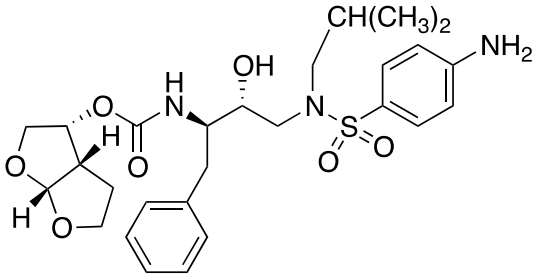

**Darunavir**

**Figure 8. Protease inhibitors.**

## 4. Reverse Transcriptase Inhibitors

The process of reverse transcription has been highly investigated for inhibition studies of the RT enzyme.[9] Reverse transcriptase has been found to have three types

of inhibitors: nucleoside reverse transcriptase inhibitors (NRTIs), nucleotide reverse transcriptase inhibitors (NtRTIs), and non-nucleoside reverse transcriptase inhibitors (NNRTIs).

NRTIs and NtRTIs are competitive inhibitors that require activation to their triphosphate forms by the host cell kinase enzymes.[18] Once activated, the NRTIs bind to reverse transcriptase at the active site and cause chain-termination of the viral DNA by mutating reverse transcriptase.[6, 50] These inhibitors are also able to be integrated into the viral DNA being synthesized in RT causing the chain elongation to be terminated because of the lack of a 3-OH preventing the formation of phosphodiester linkages.[18, 51] The NRTIs have shown toxicity because of the partial inhibition of human DNA polymerase, but the level of toxicity is dependent on each NRTI.[18, 51]

Figure 9 shows five of the NRTIs and an NtRTI on the market as of 2012. The first compound in the figure, AZT, was the first anti-HIV drug approved by the FDA for treatment.[52] After the discovery of AZT, various NRTIs were synthesized by either adjusting the nucleobase, the attached sugar moiety, or both. This method lead to the design and synthesis of emtricitabine, as one of the more potent NRTIs on the market, especially in conjecture with the NRTI stavudine, and the NNRTI efavirenz (will be discussed later).[52]

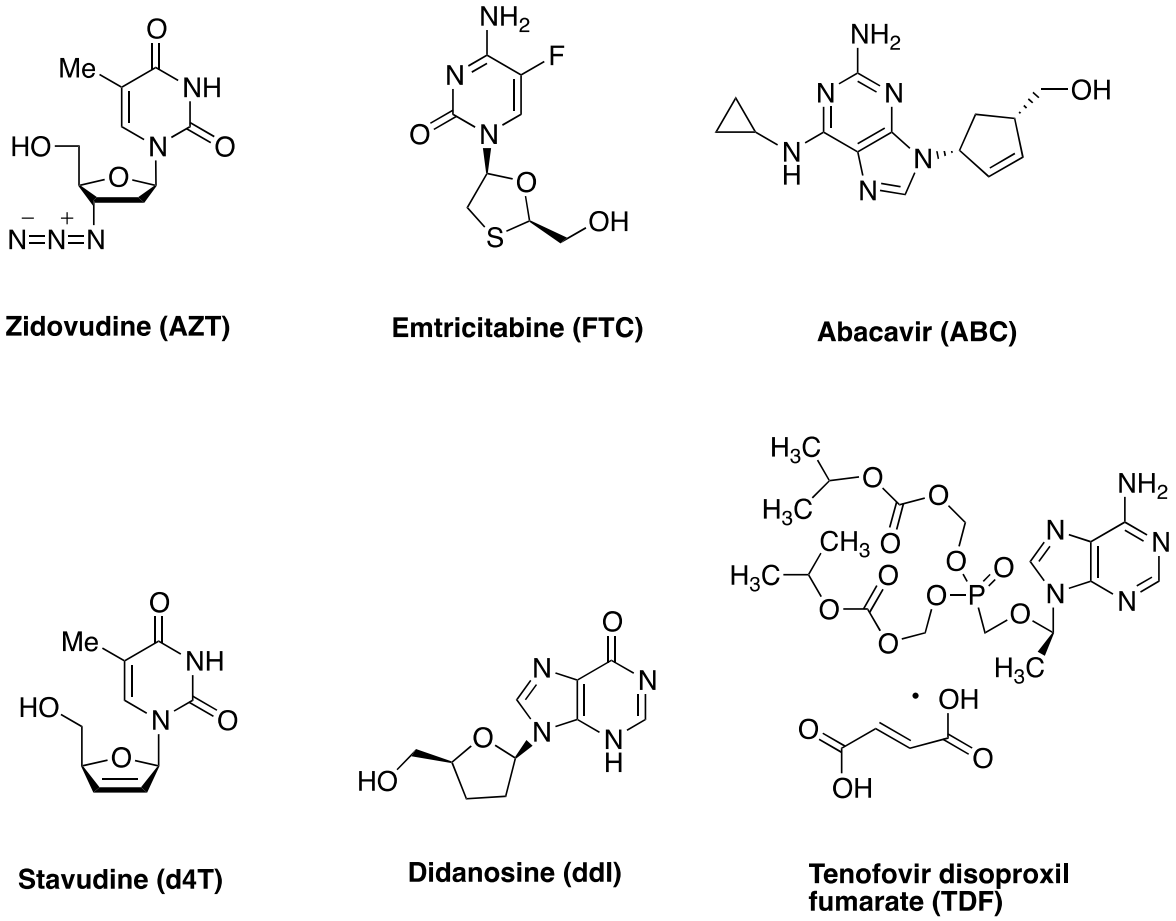


**Figure 9. NRTIs and the NtRTI TDF.**

Non-nucleoside reverse transcriptase inhibitors (NNRTIs) are highly specific, noncompetitive inhibitors and require no activation for them to bind to RT. NNRTIs are able to be structurally diverse in their make-up, while most share a butterfly wing shape when bound in the NNIBP.[53] NNRTIs have been shown to bind to a site distinct from the NRTIs on reverse transcriptase known as the non-nucleoside inhibitor binding pocket (NNIBP) (to be discussed in more detail in section E).[5, 50] The NNRTI class have shown to bind specifically to the RT of HIV-1 and not of HIV-2 or other retroviruses' RT.[54] The

reason for inactivity with HIV-2 is due to the residues making up the allosteric binding pocket of HIV-2 compared to HIV-1. The pocket of HIV-1 consists of hydrophobic aromatic residues, while the wild type HIV-2 pocket has primarily aliphatic residues.[55] The NNRTIs have been shown to have effective concentration ($EC_{50}$) as inhibitors at concentrations 50% lower than that of the cytotoxic concentration ($CC_{50}$).[54]

The first class of NNRTIs to be discovered belong to the TIBO, tetrahydroimidazo[4,5,1-*jkj*][1,4]benzodiazepine-2(1*H*)-one and -thione, group. The studies involved the screening of around 600 molecules led to the TIBO ring system with a ketone, R14458, and after alterations to the compound by changing the ketone to the thione, the allyl group to 3-methyl-2-butenyl, and adding a chloro group to the aromatic ring produced R82913 with $IC_{50}$ 1.5 nm, a potency 41,000-fold greater than R14458.[56, 57] The TIBO group were then used in the investigation of the mechanism of inhibition of RT to better understand the act of inhibition for further development of compounds.[58]

Although the TIBO group had been the first class to be designated as NNRTIs, they weren't the first NNRTIs discovered. The HEPT, 1-[(2-hydroxyethoxy)methyl]-6-(phenylsulfanyl)thymine) compounds had first been discovered in 1989 by Baba et al.; however, they were first described as NRTIs.[58, 59] Kinetic studies were performed with HEPT compounds, and it was eventually found that they did not compete with the thymidine triphosphate during the polymerization step. Furthermore, the triphosphate of HEPT was a weaker inhibitor than that of HEPT itself. It was not until the investigation of the mechanism of inhibition of the TIBO class that it was suggested that HEPT could also be an NNRTI.[56]

Since the discovery of TIBO and HEPT as NNRTIs, they have been discontinued in clinical use, but there have since been several generations of new NNRTIs.[60] Among the first generation of NNRTIs are the compounds nevirapine and efavirenz. Since their approval by the FDA, HIV-1 has resulted in mutant strains of RT that have shown resilience to the first generation. The second generation of NNRTIs, for example, etravirine or rilpivirine, were designed to combat the effect of the Y181C or K103N mutation with emphasis on interactions with the conserved residues of RT like W229.[52] Compounds such as efavirenz inhibit the RT process at concentrations in the nanomolar range. Structures of the mentioned NNRTIs can be seen in Figure 10.

As mentioned earlier, once bound in the NNIBP, the inhibitors take on a folded "butterfly" wing-like shape. The later inhibitors such as nevirapine and efavirenz were designed to abate the formation of this shape.[61] To better adapt the butterfly wing shape, the inhibitors must meet three criteria: two $\pi$-systems, a body or bridge that connects the two $\pi$-systems, typically made up of a thiocarbonyl, a carbonyl, or a sulfonyl moiety, and a methyl or some other alkyl group at the *meta*-position of the extended $\pi$-system. In the end, the NNRTIs that meet this criteria form a rigid structure.[53]

Some NNRTIs do not exhibit the butterfly shape or it isn't as obvious. In opaviraline and UC-781, the top wing (the $\pi$-system that interacts with the residues Tyr 181, Tyr 188, and Trp229) is decreased in size or even nearly absent compared to other NNRTIs. The compounds delavirdine and TSAO-T do not even seem to resemble the butterfly shape.[54]

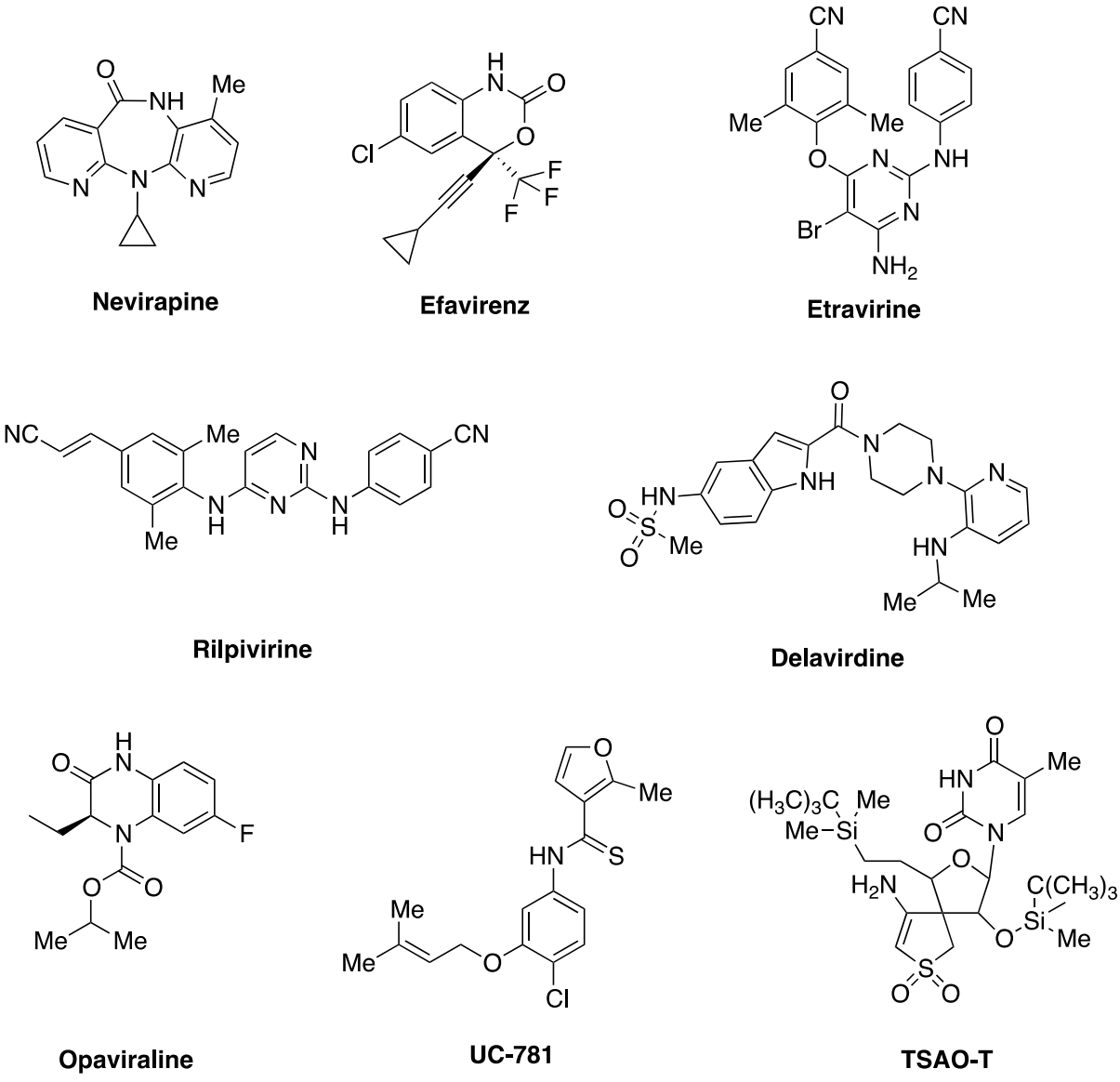


**Figure 10. NNRTIs.**

## E. The Non-Nucleoside Reverse Transcriptase Inhibitor Binding Pocket

The NNIBP (Figure 11), as discussed, is the site for attachment of NNRTIs. It is an allosteric, hydrophobic site that is roughly 15 Å away from the catalytic site of RT and is between 620 to 720 $Å^3$ in size.[52, 58] The site is located within the palm of the p66

subunit of RT. The pocket is comprised of amino acid residues 105–110 and 179–191 of the beta-sheets β4, β7, and β8, residues 224–241 of the sheets β9, β10, and β11, residues preceding the β4, 98–104, and the amino acid residues 59, 132, 138, 139, 141, and 318.[54, 58] The pocket mouth contains the two residues Pro225 and Pro236 which have been theorized as “closing the door” of the pocket once the NNRTI has entered.[54] Specifically, the roof of the pocket is formed by the aromatic residues Tyr 181, Tyr 188, and Trp 229, and the walls are made up of Leu 100, Val 106, and Leu 234. The floor of the pocket consists of a chain of three lysines: Lys 101, Lys 102, and Lys 103.[54]

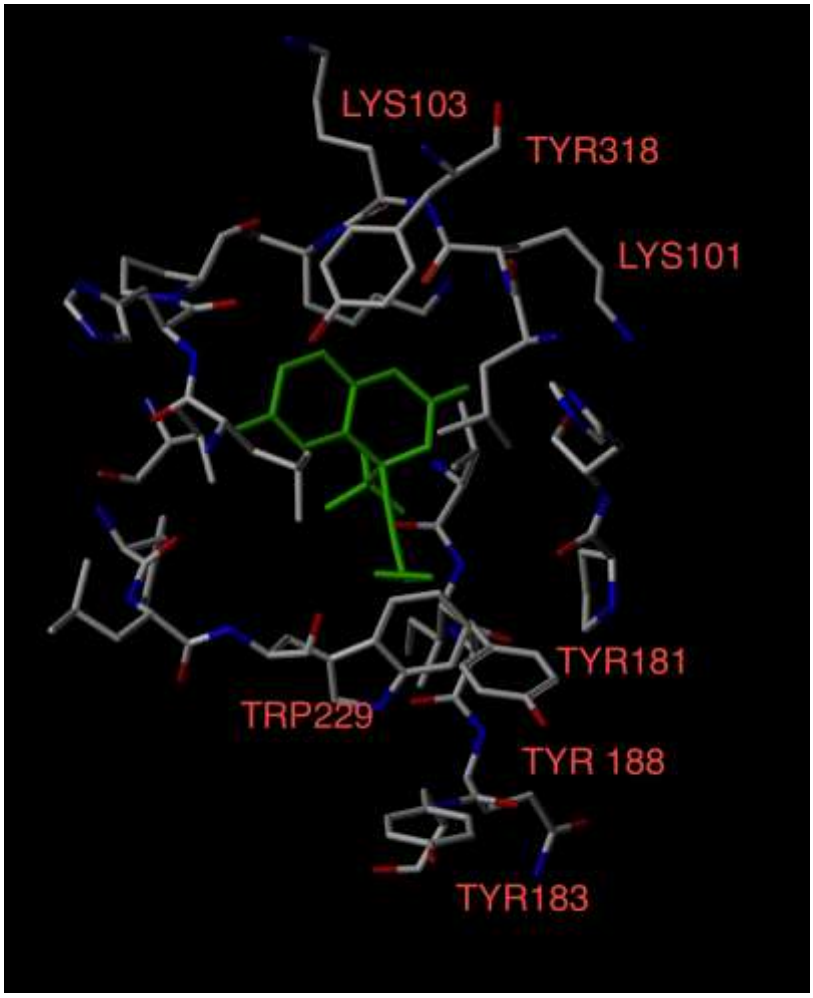


**Figure 11. The non-nucleoside reverse transcriptase inhibitor binding pocket.**

Interestingly, crystal studies of RT without a ligand attached found the absence of the NNIBP, and it was found only to exist when bound with an inhibitor.[26] The formation of the pocket results in the induction of a conformational change of the side chains of Y181 and Y188 in the direction of the catalytic site, resulting in a related movement of the β4-β7-β8 sheet and three of the amino acid residues at the catalytic cite by 2 Å.[62] It is theorized the inhibition is caused from this change in the beta-sheets and the catalytic

triad. The pocket will typically conform to a similar shape independent of the structure of chemically different NNRTIs.[58]

The NNRTIs each have their own unique interaction within the binding pocket, but the differences are quite minor from each other. The most important interaction for the NNRTIs to exhibit is the $\pi$–$\pi$ interaction felt with one or more of the residues Tyr 181, Tyr 188, Trp 229, and/or Tyr 318, with the more interactions occurring the better. Another interaction is the electrostatic charges occurring with residues Lys 101, Lys 103, and Glu 138 with the aromatic wing of an NNRTI. A third interaction to occur with ligands and the pocket is the van der Waals interaction that occurs with resiudes Leu 100, Val 106, Val 179, Tyr 181, Gly 190, Trp 229, Leu 234, and Tyr 318. A potential final interaction are hydrogen bonds that occur with the ligand to the main chain peptide bonds of Lys 101 and/or Lys 103.[54]

**F. Mutations Induced by NNRTIs**

Since the use of NNRTIs began, several mutations arose leading to drug resistance of NNRTIs. These mutations differ from those formed from NRTI treatment; furthermore, NNRTI induced mutant strains retain sensitivity to NRTI treatment and *vice versa*.[63] Unlike NRTI-induced mutations that can occur throughout RT, NNRTI induced mutations occur only in the NNIBP.[63] Most mutations are as simple as one amino acid being changed to another with variability on whether one inhibitor is made inactive or not. The first two resistant mutations seen were the K103N (Lys 103 → Asn 103) and the Y181C (Tyr 181→ Cys181) strains, both of which rendered almost all known NNRTIs inactive. In some extreme cases, double mutations have occurred. The more prevalent double mutations are K103N/Y181C, L100I/K103N, and K101D/K103N.[64]

Table 1 shows a list of possible mutations and the NNRTI that was used in the treatment that led to the mutation.

A valid question arises, “Since NNRTIs give rise to rapid mutation, are these viable inhibitors to develop.” Two schools of thought offer discordant opinions. One is, yes, mutations seriously impede these drugs and they should be abandoned. The other is, no, we need a succession of ever-more potent NNRTIs to meet the challenge of mutant strains. Moreover, NNRTIs seem most effective as components of 3- or 4-way cocktail regiments for long-term therapy.[65]

**Table 1. Mutations with resistance to NNRTIs and the NNRTI used in treatment. nevirapine (NEV), deliviradine (DLV), and efavirenz (EFV).[54]**

| Amino Acid Mutations in RT | NNRTI used to cause mutation |
|---|---|
| 98-Ala-->Glu | NEV |
| 100-Leu-->Ile | NEV, DLV, EFV |
| 101-Lys-->Glu | EFV |
| 103-Lys-->Asn/Thr | NEV, DLV, EFV |
| 106-Val-->Ala | NEV,DLV |
| 108-Val-->Ile | NEV,DLV |
| 135-Ile-->Met/Thr/Leu | EFV |
| 179-Val-->Asp/Glu | EFV |
| 181-Tyr-->Cys/Ile | NEV, DLV, EFV |
| 188-Tyr-->Cys/His/leu | NEV, DLV, EFV |
| 190-Gly-->Glu/Ala/Ser | NEV, DLV, EFV |
| 225-Pro-->His | EFV |
| 233-Glu-->Val | DLV |
| 236-Pro-->Leu | DLV |
| 238-Lys-->Thr | DLV |

## G. Sultams: A novel class of NNRTIs

### 1. The Discovery of Sultams as NNRTIs

The initial design of the sultam class of NNRTIs resulted from Gussio et al. developing a structure for the NNIBP with an all-atom model from a crystal structure of reverse transcriptase complexed with the inhibitor nevirapine.[66] The group used the known C-$\alpha$ coordinates from the crystal structure with only a resolution of 2.9 Å. After a series of tests using structural probes based on nevirapine and nevirapine analogs with known structure–activity relationships, a reasonably accurate and complete NNIBP was developed. From here, new NNRTIs could be analyzed in this more complete binding pocket model.[66]

After comparisons of nevirapine analogs, a 3-D QSAR (quantitative structure–activity relationship) model was developed. Using the 3-D QSAR and density functional theory (DFT), a stereoelectronic pharmacophore was designed to use in designing new inhibitors.[66] With this newly designed pharmacophore, Gussio and co-workers at the National Cancer Institute (NCI) conducted a search of its database of over 200,000 compounds. After several runs through the database with parameters designed to narrow the field each run, a list of 33 potentially active molecules with 26 of these being structurally novel molecules. Among the 33 molecules were the compounds nevirapine and NSC-119833 (Figure 12).[66]

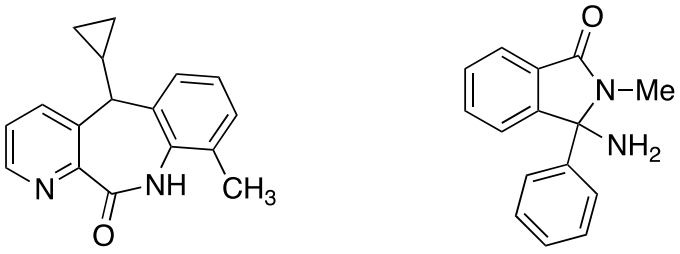


**Nevirapine** **NSC-119833**

**Figure 12. Two compounds discovered in NCI database search.**

Another search through the NCI database produced a few new results of active compounds. One compound to come out of this was NSC-108406 (Figure 13). NSC-108406 showed inhibition activity with an $IC_{50}$ of 0.5 ± 0.3 μM and an $EC_{50}$ of 1.5 ± 1.0 μM.[67] NSC-108406 belongs to a family of compounds known as sultams, which the first synthesis of a similar compound was discussed by Hauser and co-workers, and other methods were developed by Baker and co-workers, unpublished work, to produce over 65 analogues of NSC-108406.[68-72]

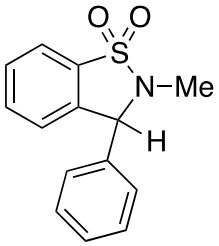


**NSC108406**

**Figure 13. Sultam discovered by NCI database search.**

## 2. The Synthesis of Sultams

The sultams discussed here are derivatives of isothiazoles with an aromatic ring being fused at the C4 and C5 positions with numbering starting with 1 at the sulfur atom. The Baker lab developed sultams resembling that of the compound shown in Figure 10 with the aromatic ring attached to the isothiazole ring being ring A, Ring B the heterocycle, and Ring C another aromatic ring. The initial studies had the nitrogen atom being either secondary or tertiary depending on whether $R^1$ was a hydrogen or an alkyl group, and with various substituents at either C6 or C7 in ring A. It was later discovered that altering groups at C6 or C7 decreased activity, and it was the effect of using various substituents at the *meta* position of Ring C, labeled $R^2$, that enhanced activity. The original method by the Baker group to synthesize the sultams is shown in Scheme 1.

**Scheme 1**

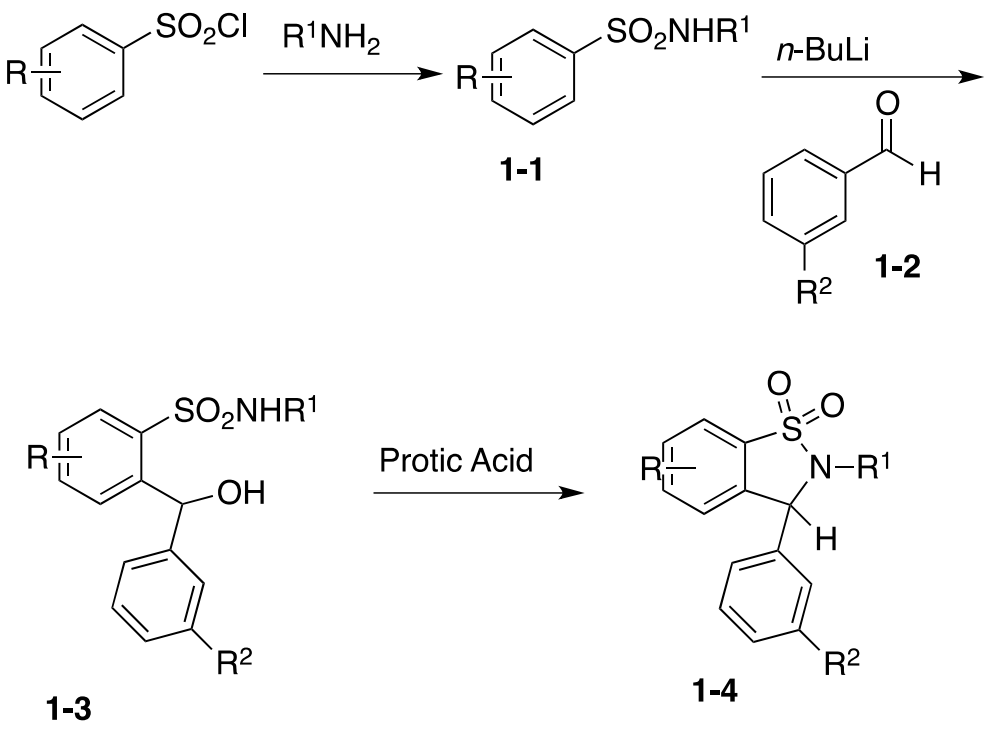


In Scheme 1, the first step is the coupling of a primary amine with a substituted benzenesulfonyl chloride to form compound **1-1**. When **1-1** is reacted with *n*-butyllithium, the hydrogen at the *ortho* position is lithiated, which reacts with a *meta*-substituted benzaldehyde (**1-2**) to produce **1-3**. Upon reaction of **1-3** with a protic acid, the racemic final compound **1-4** is formed from the cyclization of **1-3**. Initial methods used a chiral semi-preparative column on HPLC to separate the enantiomers, where they were sent to NCI for biological testing.[68, 70]

The original method for synthesizing the sultams was flawed when analogues with a halogen as a substituent was desired because of the tendency of alkyllithium to perform a lithium–halogen exchange reaction. To circumvent the production of side

products, a new method was developed, Scheme 2. A halogen-substituted *ortho*-aminobenzophenone (**2-1)** was first reacted with HONO to produce a diazonium compound, which upon reaction with $SO_2$ in ionic copper produced **2-2**. Ammonia was used to perform a condensation on **2-2** to produce **2-3**, which was then hydrogenated to form racemic **2-4**. The final step involved the alkylation of the nitrogen to produce racemic **2-5**.[69, 73]

**Scheme 2**

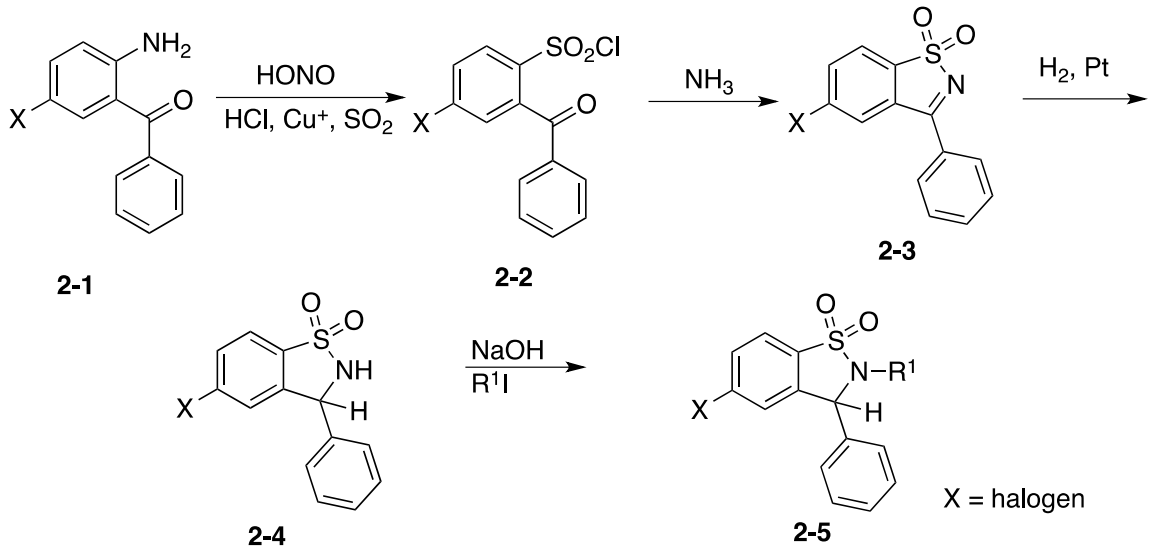


In the early days of the project other methods were designed, patented, and employed in the laboratory as shown in Scheme 3. Compound **3-1**, 2,4-(dimethoxyphenyl)-(4-methoxyphenyl)methylamine was reacted with benzenesulfonyl chloride in the presence of a base to form **3-2**. After *ortho*-lithiation of the aromatic ring attached to the sulfur, benzaldehyde or substituted benzaldehyde was added to yield a

mixture of **3-3** and **3-4**. Sulfuric acid was then used to cyclize the ring to produce the sultam **3-5**.[69]

**Scheme 3**

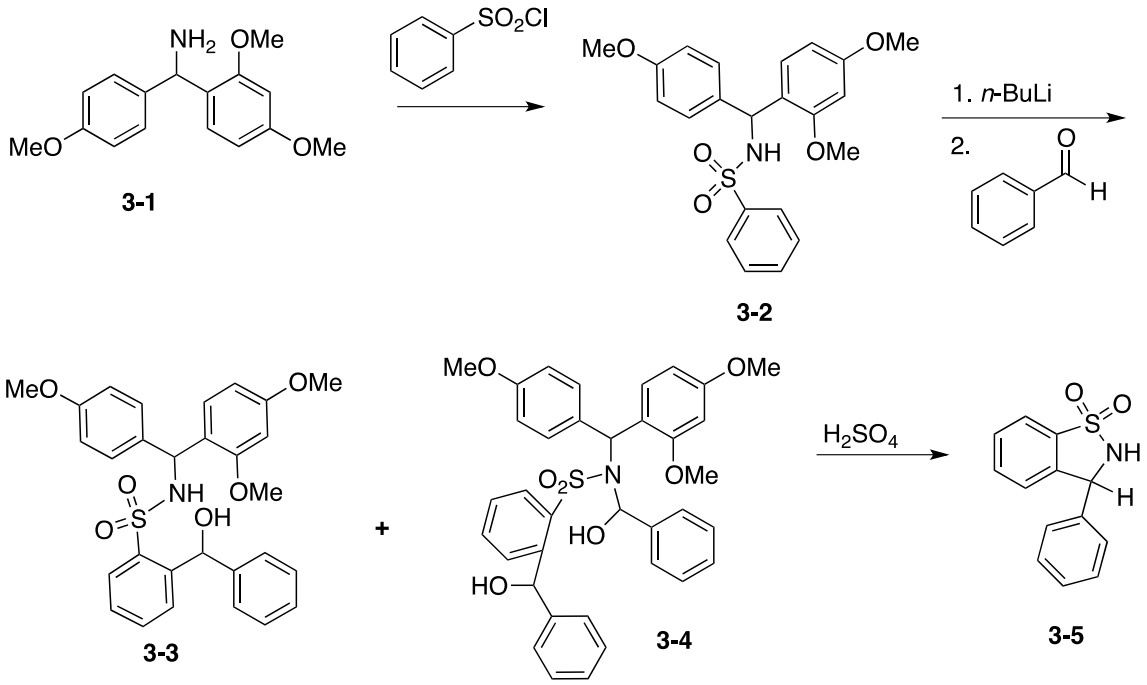


A fourth method was developed to involve a $-CF_3$ group at the C3 position in ring B, Scheme 4. The method starts with reacting *tert*-butylamine with benzenesulfonyl chloride to yield **4-1**. The nitrogen atom in **4-1** is deprotonated with sodium hydride, which the negative charge performs an $S_N2$ reaction on iodomethane to form **4-2**. Compound **4-2** is *ortho*-lithiated with *n*-BuLi and then reacted with 2,2,2-trifluoro-1-phenylethanone to produce **4-3**, which is cyclized with sulfuric acid to produce the racemic compound **4-4**.[69]

**Scheme 4**

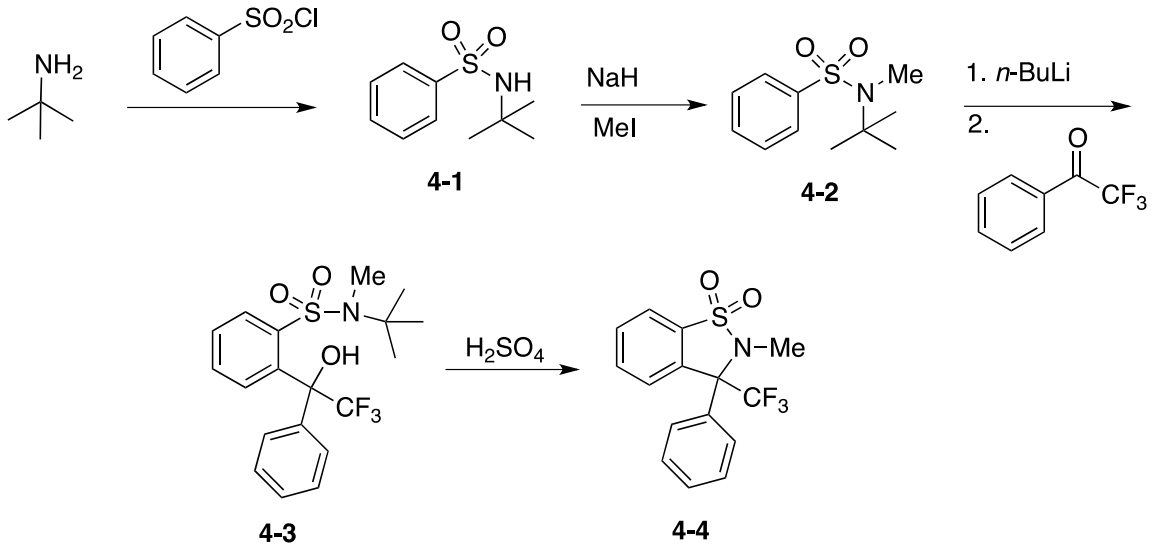


**4-1** **4-2** **4-3** **4-4**

As it was done with the final compound in Scheme 1, the final compounds in Schemes 2–3 (**2-5**, **3-5**, and **4-4**) were purified into the desired enantiomer predominately with chiral separation with a Chiralcel OD column on HPLC. Some enantiomers were purified with derivitization into the respected diastereomer and then separated with liquid chromatography and recrystallization.

Initial biological studies showed a decrease in activity of compounds with altered substitution on Ring A as directed by models supplied by the NCI team. When these diminished activities were realized, the Baker group re-evaluated the model and determined that Ring C was the more likely candidate for insertion into the NNIBP of the enzyme; hence, modifications were made on this part of the molecule. Since Ring A was to only be unsubstituted, the Baker group developed a method of synthesizing analogues with various substituents on Ring C starting initially from saccharin. Using methods developed by Abramovitch and co-workers, saccharin was reacted with 2

equivalents of an aryl magnesium bromide or chloride to yield **5-1**.[74] Initially, **5-1** was reduced with a ruthenium chiral catalyst developed by Noyori et al. to yield the desired enantiomer **5-2**.[75, 76] The nitrogen atom was deprotonated with $Cs_2CO_3$ and alkylated with a methyl group from iodomethane giving the final enantiopure compound **5-3**.

**Scheme 5**

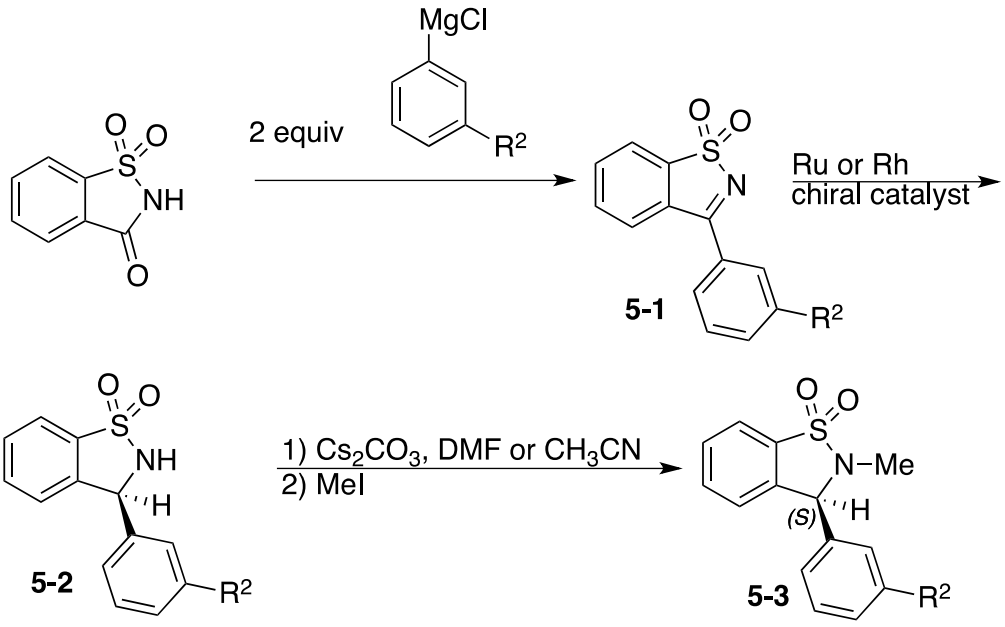


As shown in Scheme 5, a chiral TsDPEN-Cp*rhodium chloride catalyst was also used in the asymmetric reduction of **5-1** to **5-2**. The idea of the use of rhodium came from an article in *C & E News* about the use of rhodium being used to reduce imines to amines effectively.[77] The Baker group set forth on the synthesis of a chiral rhodium catalyst with related ligands to the Noyori catalyst previously used. The rhodium catalyst was prepared by reacting pentamethylcyclopentadienylrhodium chloride dimer with either (1*R*,2*R*)-*N*-*p*-toluenesulfonyl)-1,2-diphenylethylenediamine [(1*R*,2*R*)-TsDPEN] or

[(1*S*,2*S*)-TsDPEN] to form the red *R,R*-catalyst or the *S,S*-catalyst, respectively.[78] As one can see in Figure 14, the catalyst has three chiral centers: the two carbons in the TsDPEN ligand and the rhodium metal; however, the catalyst will be referred to as either *R,R* or *S,S*. The catalyst was characterized by single-crystal X-ray diffraction analysis of the *R,R* isomer of the catalyst.[78] Experiments were performed with a 5:2 formic acid–triethylamine azeotrope as the hydrogen source to test the viability of the catalyst on various imines, differing solvents, time, and different substrate-to-catalyst ratios. It was found the catalyst resulted in better enantioselectivity in polar solvents, and the preferred solvent of choice was dry dichloromethane. In some cases, the catalyst performed the reduction in as little as 10 minutes at room temperature, but it was safe to run the reaction up to say 30 minutes. The catalyst performed well with a S:C ratio of 200:1 compared to the Noyori catalyst with Ru of 100:1. It was found that in most cases it could be said that the *R,R* catalyst resulted in the *S* enantiomer of the product, and vice versa, but this result was dependent on the substitution on the imine substrate. In a case of 3-phenyl-1,2-benzisothiazole 1,1-dioxde, the resulting product was the *S* enantiomer with the use of the *R,R* catalyst, while 3-(2-chlorophenyl)-1,2-benzisothiazole 1,1-dioxide with the same catalyst would result in the *R* enantiomer illustrating a play on Cahn–Ingold–Prelog priorities.[78]

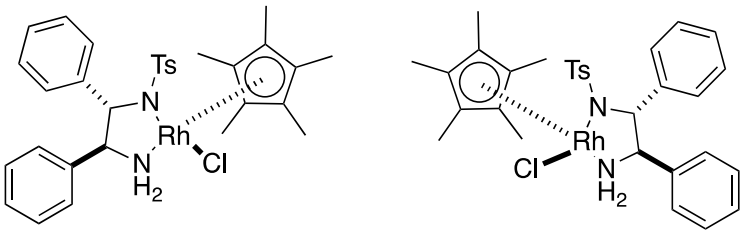


(*S,S*) (*R,R*)

**Figure 14. The *S,S* and *R,R* isomers of Rh catalyst for asymmetric reduction.**

The catalyst was found to be quite stable at room temperature, and it even was found to be effective at cold or warm temperatures with little effect on the enantioselectivity.

With the new method involving saccharin as the starting material, and the highly effective rhodium catalyst, the possibility of synthesizing more and new sultams with defined stereochemistry could be investigated for potential anti-HIV activity.

**3. The First Sultams with Enhanced Activities**

As previously mentioned, it was found that the most active compounds involved substituents on the *meta* position of the C ring. Among the substituents synthesized and tested, four stood out as having the highest inhibition activity (Figure 15). All four compounds were synthesized as is shown in Scheme 5. The activities of the compounds can be viewed in Table 5, but the most active of the four is the compound (*S*)-3-(3-methylphenyl)-2,3-dihydro-2-methyl-1,2-benzisothiazole 1,1-dioxde with an $EC_{50}$ of 0.037 μM (work unpublished).[72] However, the compound Efavirenz from Sustiva® showed higher activity, and the Baker group sought out a way to make a comparable compound to efavirenz with similar if not better activity (work unpublished).[72]

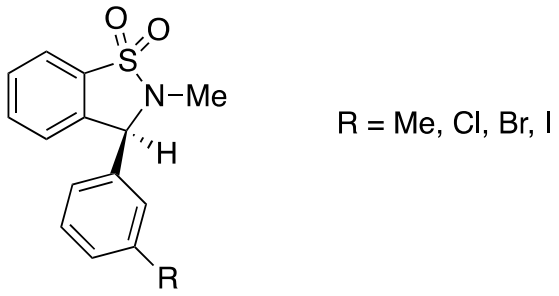


**Figure 15. General structure of sultams with enhanced activities.**

## H. FlexiDock Modeling

To begin the process to look for similiarly active sultams to efavirenz, Dr. Kafri used the FlexiDock modeling tool of the program SYBYL as an investigative resource for potentially interesting binding in the NNIBP of HIV RT with new compounds.[79] Kafri prepared each novel compound designed for the project in the SYBYL modeling program (Figure 16). Each compound was drawn and minimized with the Tripos Force Field and Gasteiger–Hückel charges. Each compound was docked into the NNIBP of the modeled RT crystal structure with the inhibitor efavirenz by superimposing the sultam on top of efavirenz. After preparing the FlexiDock file to process the sultam's effect in the pocket, the potential hydrogen bonds, the hydrogen bond angles, and distances of the hydrogen bonds in the pocket to the sultam were observed. In Kafri's findings, the sultams showed unique binding in the pocket that had some similarities and some differences compared to efavirenz's binding in the pocket.[79]

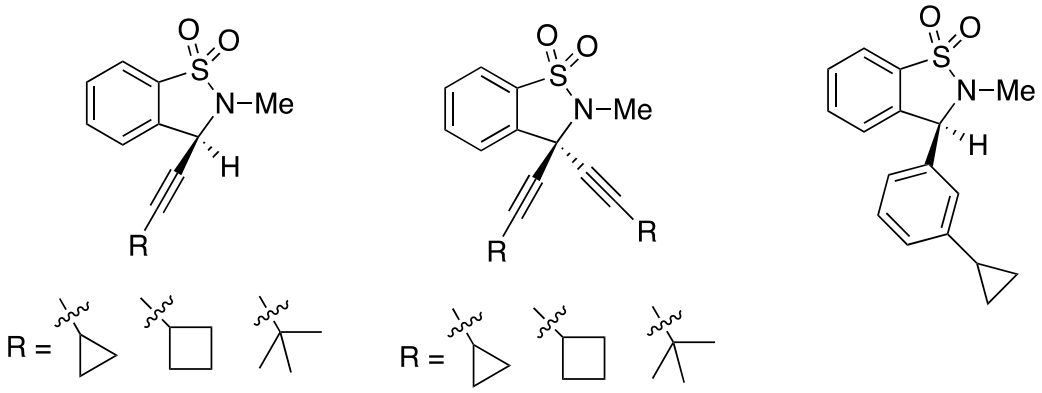


**Figure 16. Sultams to be modeled in FlexiDock.**

Table 2 shows the comparison of efavirenz to the mono-alkylated sultams: cyclopropylethynyl, cyclobutylethynyl and *tert*-butylethynyl, within the NNIBP as studied by Kafri. In binding studies, it is generally expected that a strong hydrophobic interaction should show a distance between residue and ligand being less than 4 Å, a moderate interaction being 4–5 Å, and anything larger than 5 Å is considered a weak interaction.[80] With this knowledge, the three mono-alkylated sultams have some form of interaction within the binding pocket with the interaction with Tyr 183 being the weakest at roughly 7.5 Å with all four inhibitors. The cyclopropyl sultam shows the closest similarity with efavirenz interaction with Lys 101 at 2.10 Å compared to efavirenz 2.06 Å, but both the cyclobutyl- and *tert*-butylethynyl sultams still showed at least a moderate or strong interaction respectively to Lys 101. The substituents at the end of each ethynyl group: cyclopropyl, cyclobutyl, and *tert*-butyl, all shared similar distances from Tyr 188 and Trp 229 with almost stronger interactions occurring throughout the sultam group. Interestingly, only the cyclopropyl sultam showed a hydrogen bond present at an angle

**Table 2. Distance of NNIBP residues to ligands and angles of hydrogen bonds if present with wt RT (wt RT). (CP = cyclopropyl; Ar = aromatic ring; CB = cyclobutyl; t-Bu = *tert*-butyl.[79]**

| **wt RT** | **Efavirenz** | | | **Cyclopropylethynyl Sultam** | | | **Cyclobutylethynyl Sultam** | | | ***tert*-Butylethynyl Sultam** | | |
|---|---|---|---|---|---|---|---|---|---|---|---|---|
| **Residue in wt RT** | | Distance (Å) | Angle of H-bond | | Distance (Å) | Angle | | Distance (Å) | Angle | | Distance (Å) | Angle |
| **Lys 101** | C=O | 2.06 | 98.55° | $SO_2$ | 2.10 | 115° | $SO_2$ | 4.27 | -- | $SO_2$ | 3.00 | -- |
| **Tyr 181** | CP | 2.54 | | CP | 4.20 | | CB | 4.61 | | *t*-Bu | 5.09 | |
| **Tyr 183** | | 7.23 | | | 7.85 | | | 7.54 | | | 7.88 | |
| **Tyr 188** | | 5.96 | | | 5.60 | | | 4.6 | | | 4.30 | |
| **Trp 229** | | 4.49 | | | 4.54 | | | 4.01 | | | 4.55 | |
| **Tyr 318** | Ar | 5.84 | | Ar | 6.11 | | Ar | 5.95 | | Ar | 4.91 | |

**Table 3. Distance of NNIBP residues to ligands and angles of hydrogen bonds if present with mutant RT Y181C (Y181C). (CP = cyclopropyl; Ar = aromatic ring; CB = cyclobutyl; t-Bu = *tert*-butyl.[79]**

| | **Efavirenz** | | | **Cyclopropylethynyl Sultam** | | | **Cyclobutylethynyl Sultam** | | | ***tert*-Butylethynyl Sultam** | | |
|---|---|---|---|---|---|---|---|---|---|---|---|---|
| **Residue in Y181C** | | Distance (Å) | Angle of H-bond | | Distance (Å) | Angle | | Distance (Å) | Angle | | Distance (Å) | Angle |
| **Lys 101** | C=O | 2.31 | 97.76° | $SO_2$ | 2.19 | 119.06° | $SO_2$ | 2.31 | 124° | $SO_2$ | 2.13 | 127° |
| **Cys 181** | CP | -- | | CP | -- | | CB | -- | | *t*-Bu | -- | |
| **Tyr 183** | | 7.26 | | | 7.86 | | | 7.7 | | | 7.19 | |
| **Tyr 188** | | 3.99 | | | 4.32 | | | 4.41 | | | 4.19 | |
| **Trp 229** | | 4.04 | | | 5.24 | | | 4.87 | | | 4.75 | |
| **Tyr 318** | Ar | 5.00 | | Ar | 4.86 | | Ar | 4.85 | | Ar | 4.74 | |

of 115° compared to efavirenz at 98.55°. An example of a sultam binding in the NNIBP can be seen in Figure 17.

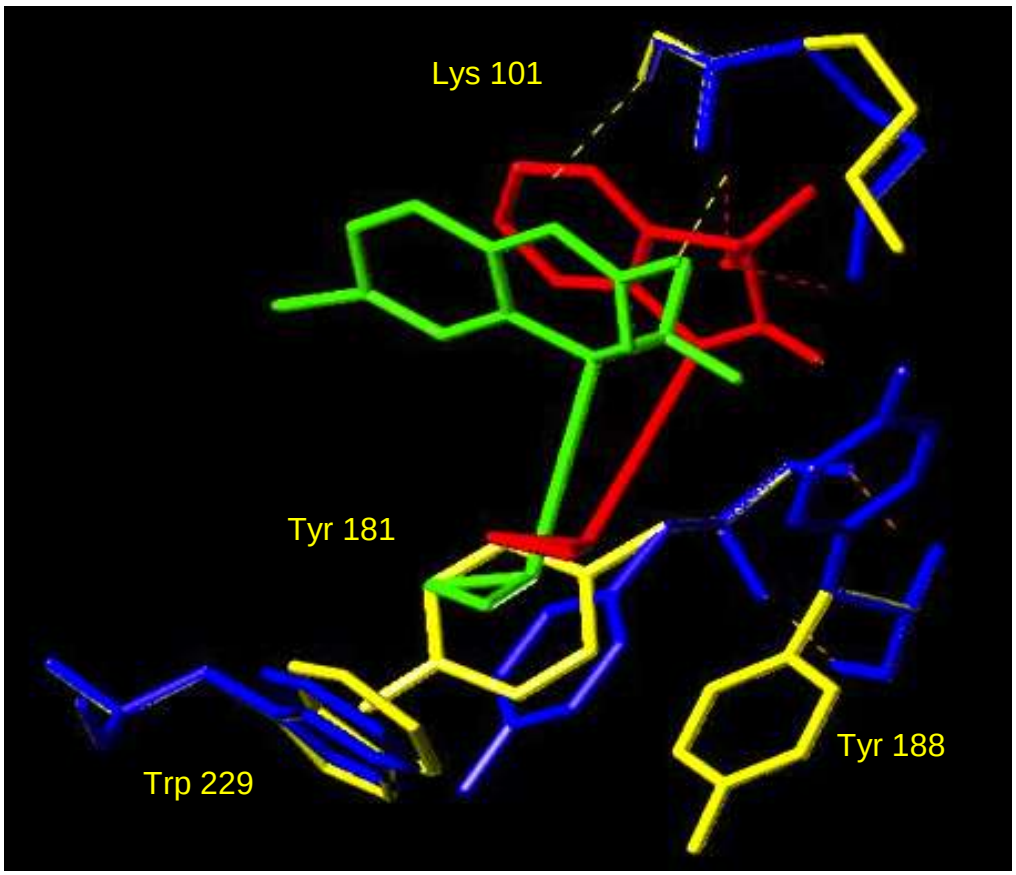


**Figure 17. Efavirenz (green) and cyclopropylethynyl sultam (red) in the NNIBP of wt RT.**

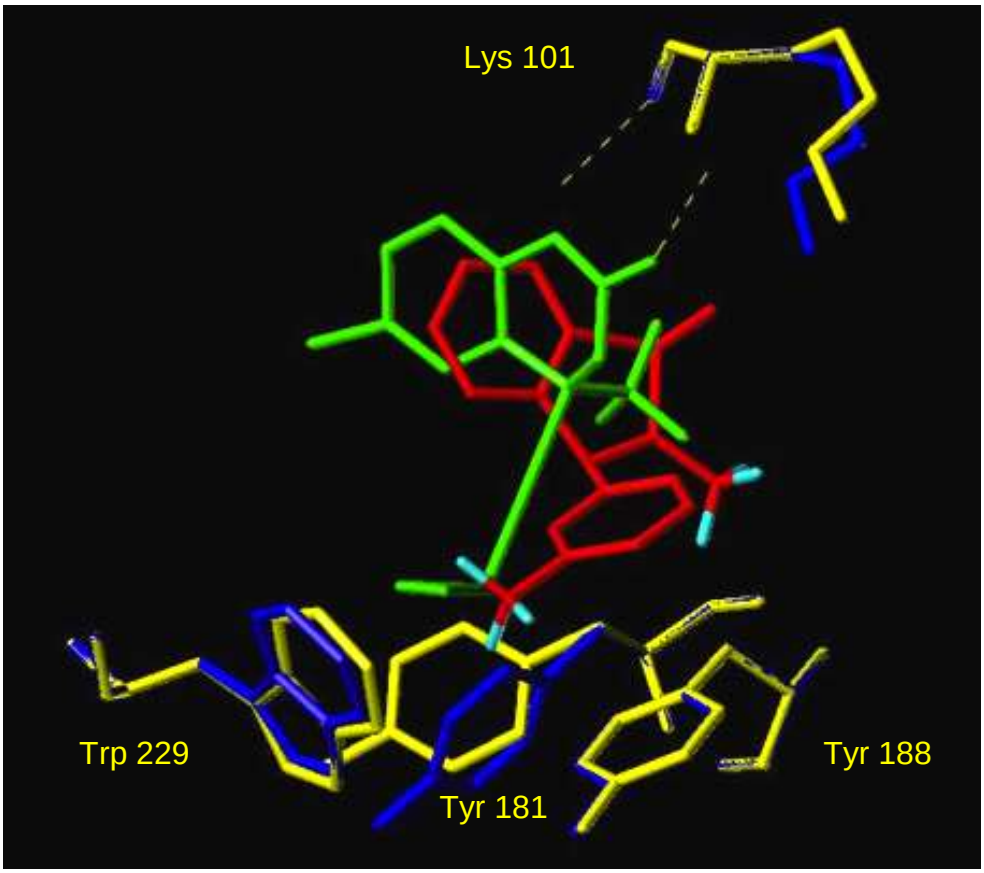


**Figure 18. Efavirenz (green) with 3-methylphenyl sultam (red) in NNIBP of wt RT.**

Figure 18 shows the sultam (*S*)-3-(3-methylphenyl)-2,3-dihydro-2-methyl-1,2-benzisothiazole 1,1-dioxide in the NNIBP of wt RT with efavirenz. Compared to efavirenz, it is located in a different configuration in the binding pocket while still conforming to the traditional butterfly wing shape. The 3-methylphenyl sultam is the most biologically active sultam synthesized to date with an $EC_{50}$ of 0.037 μM, while efavirenz has activity in the nanomolar range. However, if the 3-methylphenyl sultam is compared to the cyclopropylethynyl derivative sultam in Figure 17 and efavirenz, the cyclopropylethynyl looks to interact in a similar fashion as that of efavirenz but with its

own unique binding interactions. The results shown in Figure 17 gave a positive reinforcement of the pursuit to synthesize the alkylethynyl sultams.

Table 3 shows the data of efavirenz and the three sultams within the NNIBP of the mutant strain of RT Y181C (Tyr 181 → Cys 181). The first point to notice with the mutant interaction is that all three sultams have strong interactions with Lys 101 either being closer or equal to that of efavirenz at 2.31 Å. The presence of cysteine has changed the interaction of the sultams greatly, although there is a lack of interaction with cysteine itself with the absence of an aromatic ring in the amino acid residue. The other interactions occurring throughout the pocket seem to resemble that of efavirenz relatively closely. With the mutant strain, each sultam shows a hydrogen-bond interaction with angles roughly between 120 and130° compared to efavirenz at 97.76°. Figure 19 shows the theoretical binding structure of the ethynylcyclopropyl sultam with efavirenz in the mutant Y181C RT. The sultam is in red and efavirenz is white. The two have very similar positioning within the NNIBP of the mutant RT. Efavirenz is one of the few NNRTIs that can still be partially active with the mutant strain, and looking at the similar bonding of the sultam leads to the possibility that the sultam could be active as well.

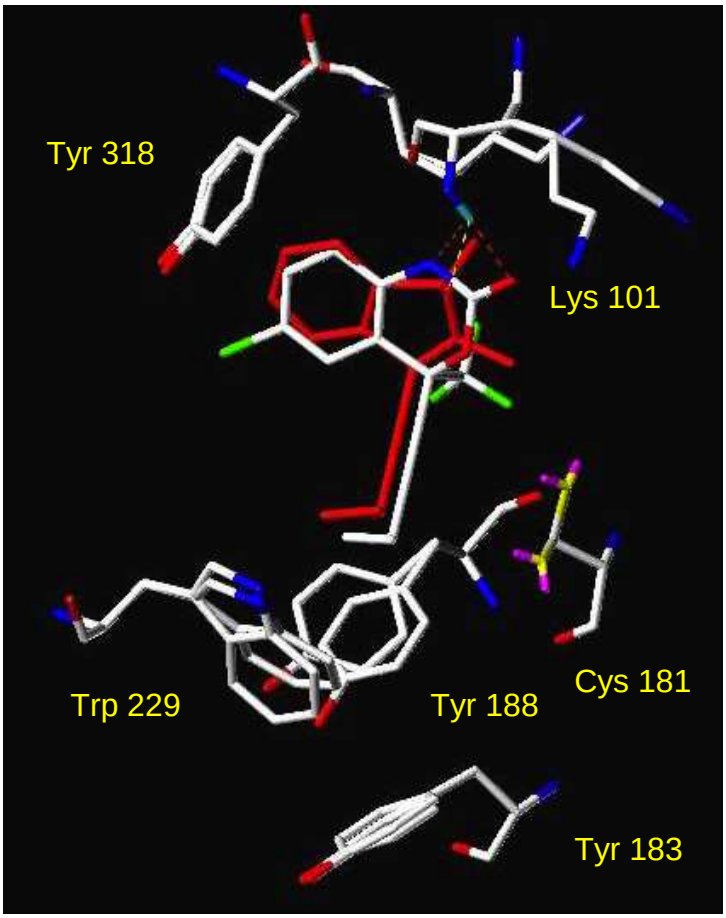


**Figure 19. Efavirenz (white) and cyclopropylethynyl sultam (red) in NNIBP of mutant RT Y181C.[79]**

The bis-alkylated sultams were too large to perform docking studies in wt RT, but were able to be docked into the Y181C RT pocket.[79] Table 4 shows the distances of the sulfonyl and the alkyl groups attached to the alkyne of the bis-alkylated sultams to the important residues of the Y181C binding pocket. Interestingly, the modeling program did not show a result of the distance between the mono-alkylated sultams and the Cys 181 residue, but the bis-alkylated compounds are within the distance to be considered a strong interaction; however, there is a loss of the $SO_2$ to Lys 101 interaction. Figure 20

shows the shape the bis-alkylated compounds form to within the binding pocket. The overall confirmation is very different than that of efavirenz leading to the inability to predict the possible binding accurately.

**Table 4. Distances between biscyclopropyl and bis-*tert*-butylethynyl sultams and key residues in Y181C rt. CP = cyclopropyl and *t*-Bu = *tert*-butyl**

| | **biscyclopropylethynyl** | | **bis-*tert*-butylethynyl sultam** | |
|---|---|---|---|---|
| **Residue in Y181C** | | Distance (Å) | | Distance (Å) |
| **Cys 181** | $SO_2$ | 3.96 | $SO_2$ | 2.37 |
| **Tyr 183** | CP (A) | 5.72 | *t*-Bu (A) | 7.32 |
| **Tyr 188** | | 5.77 | | 5.01 |
| **Trp 229** | | 4.33 | | 4.42 |
| **Tyr 318** | CP (B) | 3.75 | *t*-Bu (B) | 3.26 |

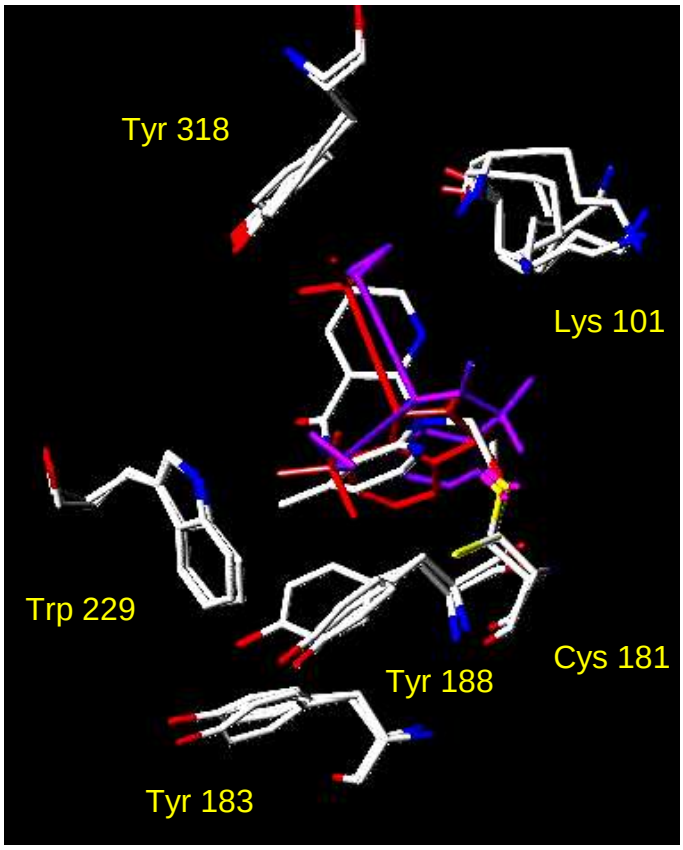


**Figure 20. Bis-cyclopropylethynyl sultam (purple) and bis-*tert*-butylethynyl sultam (red) in the Y181C binding pocket with nevirapine (white).[79]**

Figure 21 shows the compound (*S*)-3-(3-cyclopropylphenyl)-2,3-dihydro-2,methyl-1,2-benzisothiazole 1,1-dioxide in the NNIBP of wt RT with efavirenz. Compared to the similar structure of 3-methylphenyl sultam in Figure 18, the cyclopropylphenyl sultam shows a closer fit to efavirenz. Rings A and B of the sultam are closer to overlapping the efavirenz Rings A and B, and the cyclopropyl group of the sultam. Although it is not in the same position, it is in the same area as the cyclopropyl group of efavirenz, with the cyclopropyl groups essentially competing for the same space.

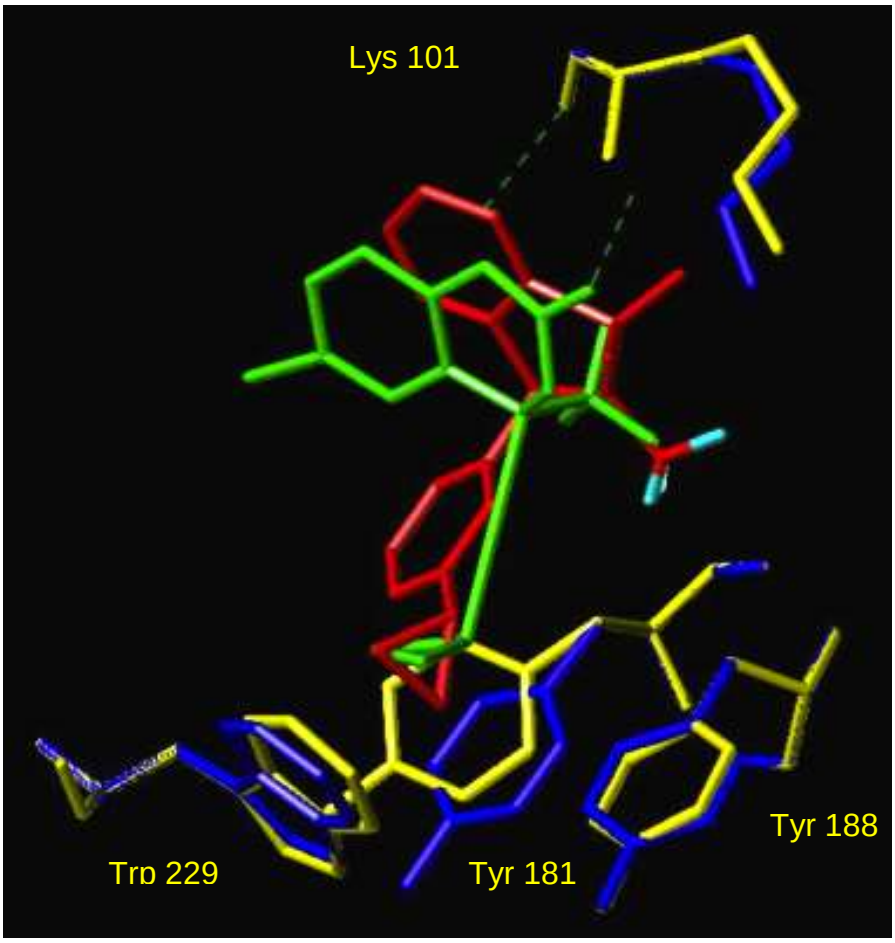


**Figure 21. 3-Cyclopropylphenyl sultam (red) with efavirenz (green) in NNIBP of wt RT.**

The binding studies give a theoretical insight to the ability for the sultams to inhibit RT, and in most cases indicate a probable chance of high activity.

## I. CoMFA Modeling

### 1. CoMFA

Comparative molecular field analysis (CoMFA) is a useful tool in *in silico* quantitative structure–activity relationship (QSAR) studies to aid in predicting possible biological behaviors of new compounds using a method derived from the relationships

of a set of already tested compounds with known properties.[81] The idea of CoMFA came from three points of observations in QSAR like studies: most relevant numerical property values would be shape-dependent, non-covalent interactions produce observed biological effects, and molecular mechanic force fields, typically steric and electrostatic forces, account for a variety of observed molecular properties.

CoMFA collects data from field values at lattice intersections of automatically calculated parameters of energies of sterics (van der Waals) and electrostatic (coulombic) interactions between the compound of interest and a "probe atom" placed at various intersections of a regular three-dimensional lattice large enough to surround all of the compounds in the series (Figure 22).[81] The van der Waals values are dependent on the force field applied (Tripos, MM3, MM4. etc.) and the atomic charges are dependent on what charges are applied to the series (Gasteiger–Marsili, Gasteiger–Hückel, etc.). The probe atom is diagnosed by default with the properties of an $sp^3$ carbon and a charge +1.0. When the probe atom experiences a steric repulsion greater than what is called the "cut-off," the steric interaction is set to the value of that "cut-off," and the electrostatic interaction is set to the average of the other molecules' electrostatic interactions at the same location.[81] From here, a partial least-squares (PLS) method is employed to extract QSAR data from the data table, and a QSAR equation is generated.

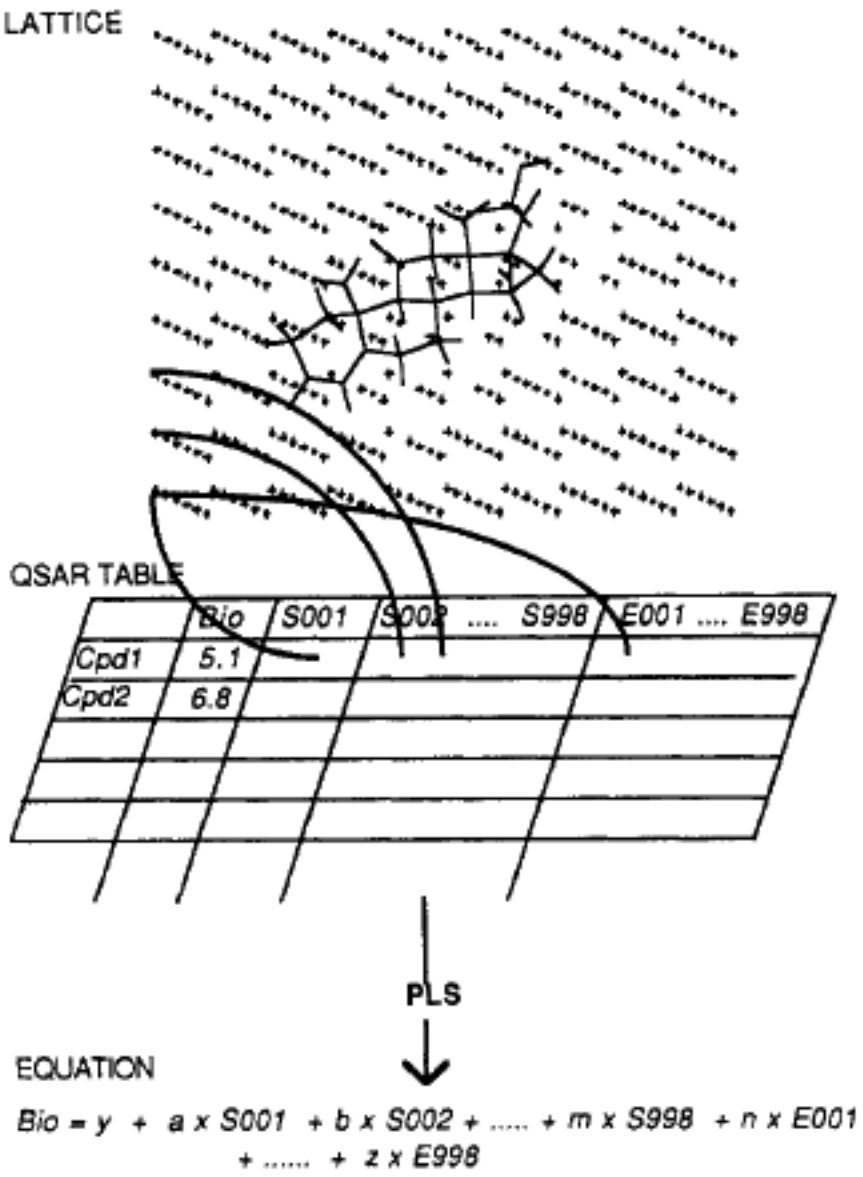


**Figure 22. The CoMFA process.**[81]

After setting the force field and the charges, CoMFA's most important input variable in positioning of the molecular model within the lattice is highly dependent on what is called the "alignment rule," because of the dependence of the relative interaction

energies on relative molecular positions. The molecules in the series are to be aligned together through space in a “field-fit” manner in order to set the molecules in positioning of the fixed lattice.[81] Once the “alignment rule” has been met, the last of the input data is the known biological activity value of each compound. This is entered into the program in a table as the log of each value of biological activity. From here, CoMFA outputs data that includes a cross-validated $r^2$, the “coefficient contour” map displays, and the desired prediction values of compounds with unknown data.[82]

**2. MM4 Force Field**

The minimalization force field applied to the sultams in this project was the molecular mechanics 4 (MM4) force field. The MM4 force field was developed to improve upon the calculation of vibrational frequencies, rotational barriers, and various relatively small errors found in the MM3 force field.[83] Since MM3 was already useful and decent with few substantial errors, it was used as the template for the design of the MM4 force field. An accurate force field of compounds is dependent on three moderately coupled parts: structure, vibrational spectra, and the heats of formation. The MM3 force field was developed in 1989 to improve upon the MM2 force field developed in 1977 that only gave a good interpretation of organic compounds. From here, the MM3 force field allowed the calculation of vibrational spectra with fair accuracy and thus allowed the calculation of certain thermodynamic properties. The MM3 force field has been labeled as a class 2 force field with its use of harmonic terms, explicit diagonal effects, cubic and higher terms, and explicit off-diagonal elements to the force constant matrix (mechanical terms). A class 3 force field would take into account these mechanical terms while also including chemical effects such as electronegativity and

hyperconjugation. From here, the MM4 force field was developed to improve the MM3's insufficient accuracy of vibrational spectra, rotational barriers for congested molecules low calculations, the lack of vibrational energy being taken into account for heats of formation calculations, and small improvements on structures of simple compounds on the whole.[84]

Following the improvements on the MM3 model, a set of cross terms was added to the MM4 force field to improve the force field. The cross terms involved were bend-torsion-bend, torsion-improper torsion-improper torsion, and stretch-stretch terms. These new terms work together to improve upon the method without taking away the effect of each other. The new terms work to improve the coupled in-plane bending, the out-of-plane bending, and stretching vibrational frequencies, in that order.[85]

### 3. Gasteiger–Marsili Charges

Atomic charges can be calculated through several methods in computer modeling programs by characterizing the atoms by their orbital electronegativies. The Gasteiger–Marslili method goes on to include the effect of the connectivities of the atoms in a molecule to further advance the calculation of charges based on electronegativity. Using the connectivities, not only are the orbitals of a particular atom involved in the calculation, but the effect of neighboring orbitals as well, therefore involving the inductive effect.[86]

## J. Summary

With the identification of HIV as the causative agent of AIDS,[3] which is one of the landmark discoveries in the history of medicine, the challenge was put into the hands of the medicinal chemist to develop therapies to either eradicate[87] or at least limit the

development of the virus. By making use of a precise knowledge of the lifecycle of the HIV virus, a number of points for pharmaceutical intervention were identified, among them the reverse transcriptase process.[23] To this end, medicinal chemists have worked, using molecular modeling and QSAR studies to design non-nucleoside reverse transcriptase inhibitors (NNRTIs) that have shown substantial activity against HIV. These, and a handful of other drugs acting on other points of attack, either alone or in combination, are today the only successful anti-HIV therapies, given that fact that a vaccine against the virus remains elusive.[88]

That which remains to do in the Baker group is to extend the molecular modeling and CoMFA studies on the binding of a class of non-nucleoside RT inhibitors called "sultams" to improve both potency and activity toward resistant HIV strains.[72, 79] The Baker group has developed methods to selectively synthesize specific enantiomers for a large number of sultams and has developed considerable structure–derivatives of 3-substituted-1,2-benzisiothiazole 1,1-dioxides. Taking the lead of efavirenz, a successful drug from Merck and Co., a new set of NNRTIs is planned.

# Chapter II. Statement of the Problem

AIDS is still a large problem throughout the world today, with HIV being the cause of the epidemic. Many forms of treatment have come along to help reduce the mortality rate of the disease with inhibition of reverse transcriptase being a popular method of inhibition. It is our hope that our proposed compounds will be effective against wt RT and mutant strains of RT. After FlexiDock modeling work performed by Dr. Kafri, the use of another modeling method called CoMFA is to be used to further aid in predicting possible activities of the proposed compounds. Using calculations to analyze compounds with known biological activities, an $r^2$ value, a coefficient of determination, is to be determined to help predict theoretical $EC_{50}$ values for the sultams to be designed and synthesized in this project.

Previous research by Dr. Kafri looked into synthesizing the three bis-alkynyl compounds shown in Figure 16 along with the three mono-substituted compounds. In her research, she declares success in the synthesis of 3,3-bis(cyclopropylethynyl)-2,3-dihydro-2-methyl-1,2-benzisothiazole 1,1-dioxide, 3,3-bis(cyclobutylethynyl)-2,3-dihydro-2-methyl-1,2-benzisothiazole 1,1-dioxide, 3,3-bis(*tert*-butylethynyl)-2,3-dihydro-2-methyl-1,2-benzisothiazole 1,1-dioxide, and (*S*)-3-(*tert*-butylethynyl)-2,3-dihydro-2-methyl-1,2-benzisothiazole 1,1-dioxide, none of which required reduction following the initial organometallic addition (Scheme 6).

**Scheme 6**

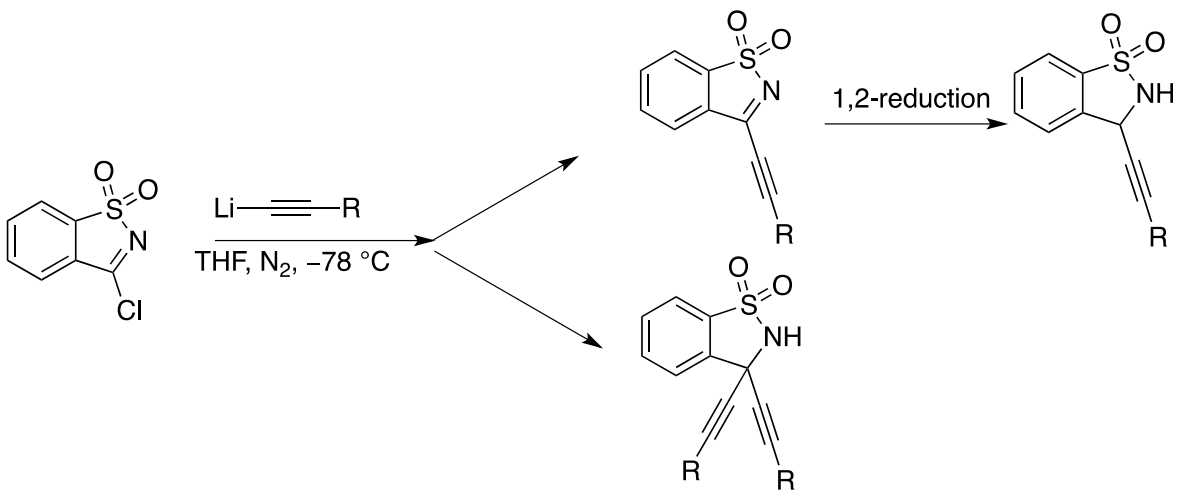


In addition were also synthesized compounds of complete reduction (*S*)-3-(cyclobutylethyl)-2,3-dihydro-2-methyl-1,2-benzisothiazole 1,1-dioxide and (*S*)-3-(cyclopropylethyl)-2,3-dihydro-2-methyl-1,2-benzisothiazole 1,1-dioxide. Evidence suggests that in the time since Dr. Kafri has left the department, the bis compounds have degraded, and further studies of her data suggests that the mono *tert*-butylethynyl sultam has not been synthesized. This project looks to reproduce her compounds while also adding to the database the compounds 3-(*tert*-butylethynyl)-2,3-dihydro-2-methyl-1,2-benzisothiazole 1,1-dioxide, 3-(cyclobutylethynyl)-2,3-dihydro-2-methyl-1,2-benzisothiazole 1,1-dioxide, 3-(cyclopropylethynyl)-2,3-dihydro-2-methyl-1,2-benzisothiazole 1,1-dioxide, and (*S*)-3-(3-cyclopropylphenyl)-2,3-dihydro-2-methyl-1,2-benzisothiazole 1,1-dioxide, all of which require selective 1,2-reduction of the intermediate imine.

In previous research on the sultams, methods for synthesizing the alkylated sultam in the first step resulted in low yields and without selectivity of a mono or bis product. This project will work towards the improvement of the methodology of the addition of a lithiated or Grignard reagent to saccharin or *pseudo*-saccharin chloride reaction step of the synthesis to achieve methods with selectivity of one product over the other in the case of mono- vs. bis-alkynyl derivatives. The purpose of the research into the novel methodology was to improve the yields of the preferred product over the undesired side product.

A third issue discussed in this project involved how previous research showed that the *S*-enantiomer of the sultam class of NNRTIs as the more active enantiomers, and the previously discussed Rh catalyst for asymmetric reduction was used to attain the desired product. However, once the chiral Rh catalyst was applied to the alkynyl sultams, previous research shows that a 1,4-reduction of the $\alpha,\beta$-conjugated system resulted. From this problem, research was performed towards the goal of performing the 1,2-reduction or possibly isolation of the *S*-enantiomer. Various methods included, other asymmetric reducing reagents, employing the Luche reduction (a racemic reduction favoring 1,2- over 1,4-reduction), isolation of the desired *S*-isomer via chiral resolution methods, or protection of the alkynes as cobalt derivatives.

The final problem to solve was the development of a procedure for the synthesis of (*S*)-3-(3-cyclopropylphenyl)-2,3-dihydro-2-methyl-1,2-benzisothiazole 1,1-dioxide, a compound of compelling interests from its FlexiDock model and CoMFA predictions. Methods involved looking into performing traditional Simmons–Smith reactions first, which later would be altered as to form the cyclopropane ring in the last step with an

iodomethylzincphenoxide reagent. From here, issues arose with the separation of the (*S*)-3-(3-vinylphenyl)-2,3-dihydro-2-methyl-1,2-benzisothiazole 1,1-dioxide and the final compound 3-cyclopropylphenyl sultam.

# Chapter III. Results and Discussion

## A. CoMFA Modeling

### 1. Preparing Sultams with Known Activities

Each sultam with known activity was drawn in the Sketch Molecule menu of SYBYL 8.0. The sultams sketched resembled the structure in Figure 23 where $R^1$ and $R^2$ are shown in Table 5. Hydrogen atoms were added, and the MM4 force field minimalization was applied followed by the Gasteiger–Marsili charges. The structures were then superimposed onto each other to form a database with the common sub-structure of (*S*)-3-phenyl-2,3-dihydro-2-methyl-1,2-benzisothiazole 1,1-dioxide, Figure 23, as the aligning model.

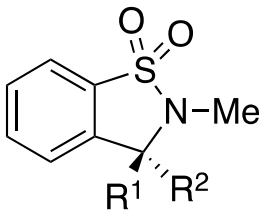


**Figure 23. Common substructure of sultams with known activities modeled into SYBYL 8.0. The positions of $R^1$ and $R^2$ are shown in Table 5.**

**Table 5. Sultams with known activities, their $EC_{50}$ and the $pEC_{50}$ for CoMFA studies with validation data**

| sultam | | $EC_{50}$ (uM) | $pEC_{50}$ | predicted $pEC_{50}$ | predicted $EC_{50}$ | Difference $pEC_{50}$ | Difference $EC_{50}$ |
|---|---|---|---|---|---|---|---|
| $R^1$ | $R^2$ | | | | | | |
| **phenyl** | **H** | 0.471 | 6.327 | 6.148 | 0.711 | 0.179 | -0.240 |
| ***m*-vinylphenyl** | **H** | 0.86 | 6.066 | 6.524 | 0.299 | -0.458 | 0.561 |
| ***m*-hydoxymethyl phenyl** | **H** | 6.04 | 5.219 | 5.101 | 7.925 | 0.118 | -1.885 |
| ***m*-CHO-phenyl** | **H** | 1.41 | 5.851 | 5.726 | 1.879 | 0.125 | -0.469 |
| ***m*-OMs phenyl** | **H** | 1.91 | 5.719 | 5.703 | 1.982 | 0.016 | -0.072 |
| ***m*-methylphenyl** | **H** | 0.037 | 7.432 | 6.821 | 0.151 | 0.611 | -0.114 |
| ***m*-Fphenyl** | **H** | 0.179 | 6.747 | 6.797 | 0.160 | -0.050 | 0.019 |
| ***m*-Clphenyl** | **H** | 0.086 | 7.066 | 7.060 | 0.087 | 0.006 | -0.001 |
| ***m*-Brphenyl** | **H** | 0.074 | 7.131 | 7.170 | 0.068 | -0.039 | 0.006 |
| ***m*-Iphenyl** | **H** | 0.076 | 7.119 | 7.167 | 0.068 | -0.048 | 0.008 |
| ***o*-methylphenyl** | **H** | 4.68 | 5.33 | 5.589 | 2.576 | -0.259 | 2.104 |
| ***p*-methylphenyl** | **H** | 1.53 | 5.815 | 5.894 | 1.276 | -0.079 | 0.254 |
| ***m*-ethylphenyl** | **H** | 0.12 | 6.921 | 7.038 | 0.092 | -0.117 | 0.028 |

**2. Data Input**

A spreadsheet was designed resembling Table 5 with each sultam designed being represented by a number in a row and its respective $EC_{50}$ and calculated $pEC_{50}$. The CoMFA interaction energies were calculated for each compound, and a partial least squares analysis was performed to produce the correlation value, $R^2$. Using a non-validation calculation with three components, an $R^2$ value of 0.890 was determined. The manual for use of CoMFA states that an $R^2$ value above 0.65 and below 0.95 to be substantial for predictability, with any value above 0.95 as being too ideal to be usable data.

To test the viability of the $R^2$ value from the known sultam compounds used for the CoMFA analysis, a cross validation was performed on the same biologically active compounds shown in Table 5. The cross-validation results produced predicted activities within a 0.001–2.1 micromolar range of the known values. The *m*-halogenated phenyl sultams resulted in excellent predictability of the CoMFA analysis with differences in the nanomolar range. A few cases resulted in larger differences in the micromolar range, such as the *o*-methylphenyl sultam, which CoMFA predicted a higher activity for this compound. The validation results predicted some values to have greater activity in some cases and lower activity in others; however, the values were without further analysis deemed generally applicable for calculating predicted activities of novel compounds.

### 3. Preparation of Sultams with Unknown Activities

The sultams to be analyzed for a predicted activity were prepared in a similar fashion as those with known activities in Section 4 with the MM4 force field, Gasteiger–Marsili charges, and the superimposing with a common substructure of 2,3-dihydro-2-methyl-1,2-benzisothiazole 1,1-dioxide (Figure 24). They shared the same common structure of Figure 5, with the $R^1$ and $R^2$ shown in Table 6.

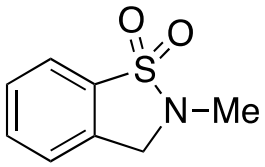


**Figure 24. Common sub-structure of novel sultams.**

### 4. Data Output

The data output from the CoMFA analysis produced predicted $pEC_{50}$ values for the novel sultams. These values were converted to the $EC_{50}$ value giving predicted activities of the sultams. The predicted most active sultam is the (*S*)-3-cyclopropylethynyl-2,3-dihydro-2-methyl-1,2-benzisothiazole with an $EC_{50}$ of 0.148 μM. The bis-alkylethynyl compounds were predicted with $EC_{50}$ values around 0.33 to 0.38 μM. These predictions are only a general idea of the activity of the novel sultams. The CoMFA analysis was comparing mainly sultams with an aryl substituent as compared to the alkynyl substituents of the novel sultams.

**Table 6. Novel sultams with calculated and predicted $EC_{50}$ and $pEC_{50}$ values.**

| Sultam | | $EC_{50}(\mu M)$ | $pEC_{50}$ |
|---|---|---|---|
| $R^1$ | $R^2$ | | |
| **cyclopropylethynyl** | **H** | 0.148 | 6.831 |
| **cyclopropylphenyl** | **H** | 0.167 | 6.776 |
| **cyclopropylethynyl** | **cyclopropylethynyl** | 0.333 | 6.477 |
| ***tert*-butylethynyl** | **H** | 0.160 | 6.795 |
| ***tert*-butylethynyl** | ***tert*-butylethynyl** | 0.344 | 6.464 |
| **cyclobutylethynyl** | **cyclobutylethynyl** | 0.378 | 6.422 |

## B. Synthesis

### 1. Overview

The original synthetic method to yield the ethynyl sultams resembles that as designed by Baker and co-workers to synthesize (*S*)-3-aryl-2,3-dihydro-2-methyl-1,2-benzisothiazole 1,1-dioxide, which was expanded from that of Abramovitch et al where two equivalents of an aryl magnesium chloride or bromide Grignard reagent were coupled to one equivalent of saccharin to produce the respected 3-(aryl)-1,2-benzisothiazole 1,1-dioxide (Scheme 5).[69, 70, 74] Using this method, a synthesis was designed using 2 equivalents of alkynyllithium reagents with saccharin to yield the desired 3-(alkylethynyl)-1,2-benzisothiazole 1,1-dioxides (**7-1**). From here, the carbon–nitrogen double bond would be asymmetrically reduced by the (*R,R*)-[TsDPEN]RhCp* catalyst developed by Baker and co-workers to yield the (*S*)-3-

alkylethynyl)-1,2-benzisothiazole 1,1-dioxide product (**7-2**). The nitrogen atom would be deprotonated by cesium carbonate, and the resulting negative charge on the nitrogen atom would act as a nucleophile towards the methyl iodide producing the methylated nitrogen atom in the product (*S*)-3-(alkylethynyl)-2,3-dihydro-2-methyl-1,2-benzisothiazole 1,1-dioxide (**7-3**) (Scheme 7).

**Scheme 7**

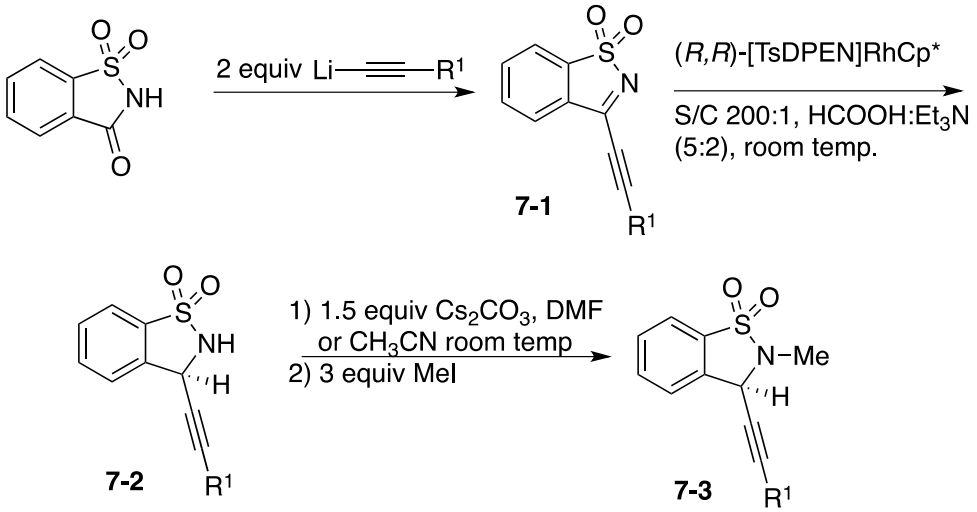


When the project began, methodologies were to be investigated to synthesize the compounds (*S*)-3-(cyclopropylethynyl)-2,3-dihydro-2-methyl-1,2-benzisothiazole 1,1-dioxide, (*S*)-3-(cyclobutylethynyl)-2,3-dihydro-2-methyl-1,2-benzisothiazole 1,1-dioxide, and (*S*)-3-(3-cyclopropylphenyl)-2,3-dihydro-2-methyl-1,2-benzisothiazole 1,1-dioxide, as shown respectively, in Figure 25. Furthermore, the project was to also look into samples developed by Dr. Riyam Kafri (Figure 26), which upon analysis, signs of

possible degradation may have occurred, and the compounds would need to be synthesized again to be used for biological testing.[79]

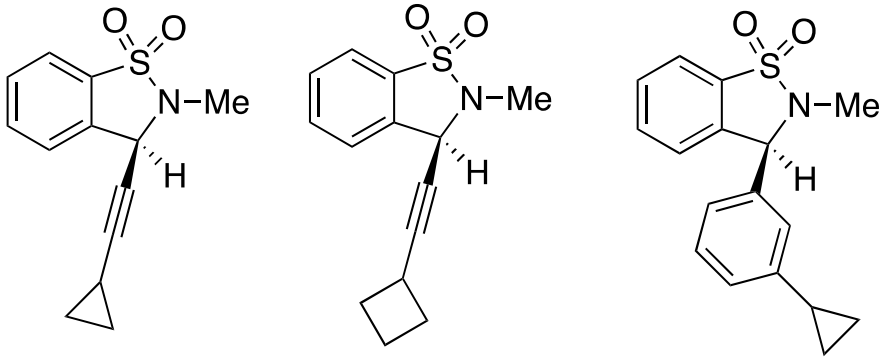

**Figure 25. Novel Sultams intended to be synthesized**

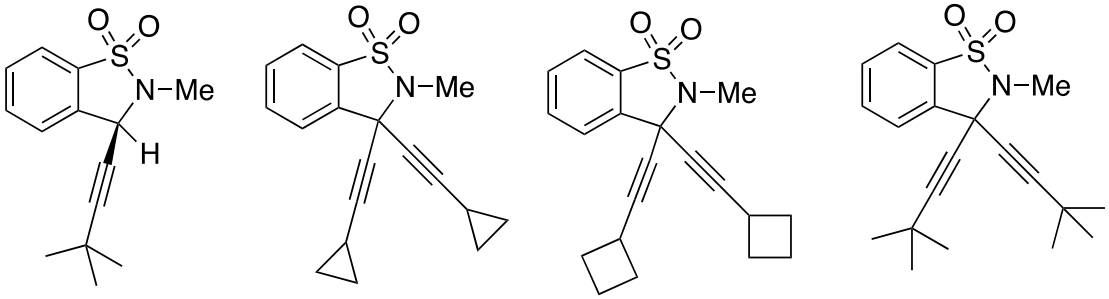

**Figure 26. Sultams developed by Dr. Riyam Kafri**

**2. 3-(Alkylethynyl)-1,2-benzisothiazole 1,1-dioxide (10-1–10-3)**

Two issues arose in the above-proposed method to synthesizing the alkylethynyl sultams. Firstly, the lithiated alkynyl compounds, when reacted with saccharin, produced the mono-alkynyl sultams in low yield, while also resulting in the production of bis-alkylated products. The second issue was that the use of the rhodium catalyst for

the asymmetric reduction would result in 1,4-reduction instead of the desired 1,2-reduction. The first problem that will be discussed is the development of a method to improve the synthesis of mono-alkylethynyl-1,2-benzisothiazole 1,1-dioxide while limiting the production the bis-alkylethynyl-2,3-dihydro-1,2-benzisothiazole 1,1-dioxide.

As stated previously, when performing the addition of the lithiated alkynes to saccharin, the yield of the mono-substituted sultam (**8-1**) was substantially low compared to the addition of aryl magnesium bromides. The product of the bis-alkylated product (**8-2**) was also detected as determined by DARTHRMS and $^{1}H$ and $^{13}C$ NMR spectroscopy (Scheme 8). It was determined that from here a new method was to be developed that improved the selectivity of the product and the yield of the mono-substituted product. A goal was to also design another method to produce the bis-substituted product in higher yield as well.

**Scheme 8**

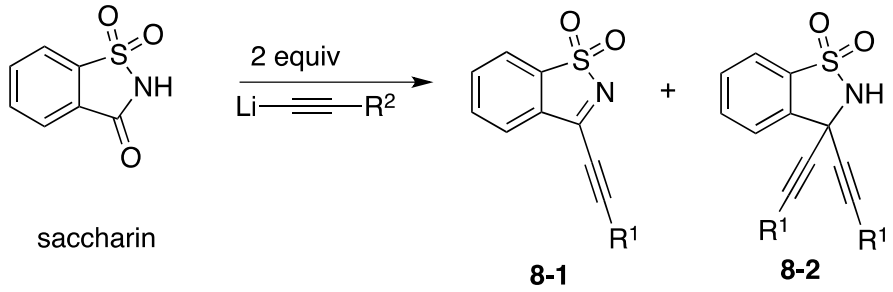


As discussed by Abramovitch et al.,[74] another compound named 3-chloro-1,2-benzisothiazole 1,1-dioxide (saccharin *pseudo*-chloride) was shown to react with lithiated alkanes to produce similar compounds. To produce the saccharin *pseudo*-

chloride (**9-1**), saccharin was dissolved in 1,4-dioxane, and an excess of thionyl chloride was added to the solution. A catalytic amount of *N*,*N*-dimethylformamide was added to perform the reaction under Vilsmeier-like conditions (Scheme 8).[89] The reaction was stirred at reflux for two days, and brought back to room temperature. The reaction mixture was rotary evaporated to remove solvent, and then recrystallized using hot toluene producing white crystals of the chloro derivative.

**Scheme 9**

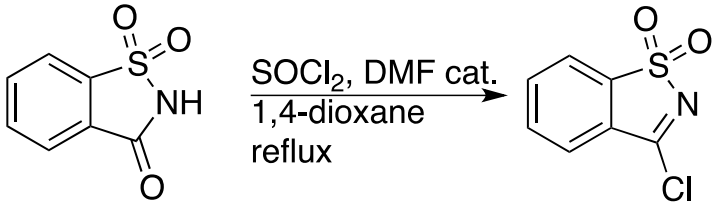


Saccharin **9-1**

The reactivity of the saccharin *pseudo*-chloride (**9-1**) was shown to be greater than that of saccharin itself, which resulted in the production of the bis-alkylated product in higher yield under the right conditions. From here, methodology was designed to favor the mono- over the bis-product and another method to favor the bis- over the mono-product.

In an attempt to produce more of the mono-alkylated product relative to the bis-product, because of the saccharin *pseudo*-chloride's (**9-1**) higher activity, it was decided to use 1.5 equivalents of the chloride **9-1** to 1.0 equivalent of the lithiated alkyne. Furthermore, the reaction was performed by slowly injecting the lithiated alkyne into a solution of the saccharin *pseudo*-chloride (**9-1**) over a period of 1 hour at −78 °C. Under these conditions, the saccharin *pseudo*-chloride (**9-1**) always would be at a substantially

much higher concentration than the lithiated alkyne at cold temperatures, resulting in the nucleophile to favor a mono-addition over the bis-addition (Scheme 9). This method on average produced around 60% yield of the desired mono-product when the alkyne was commercially available in high purity (**10-1** (70%) and **10-3** (59%)).

In the case of the cyclobutylethynyl derivative **10-2**, the ethynylcyclobutane precursor was synthesized from 6-chlorohexyne (**11-1**) with 2 equivalents of *n*-BuLi under anhydrous conditions starting at −78 °C with warming to room temperature overnight.[90] It was found that the product of that reaction, before work-up, was typically cyclobutylethynyl lithium (**11-2**) and was therefore added directly to a solution of 1.5 equivalents of saccharin *pseudo*-chloride (**9-1**) (Scheme 10). Due to the boiling point of ethynylcyclobutane being so close to THF, the purification by distillation of the compound from THF proved impossible, thus limiting its purity for the lithiation reagent. Because of the immediate addition of the synthesized lithiated ethynylcyclobutane (**11-2**), with the presence of impurities, the percent yield was typically around 15%.

**Scheme 10**

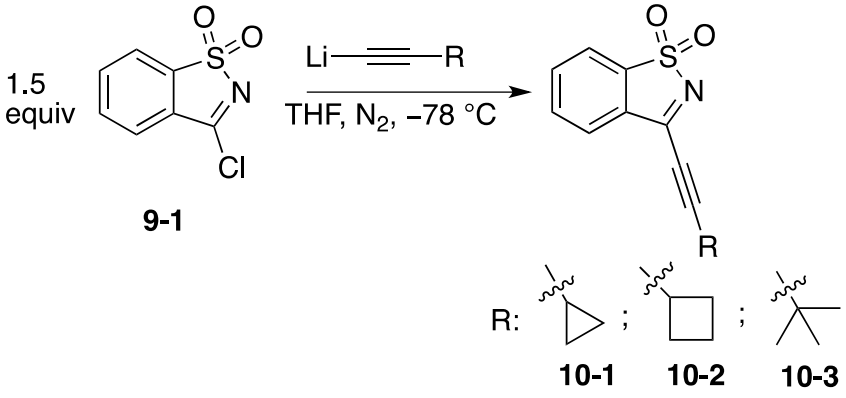

**Scheme 11**

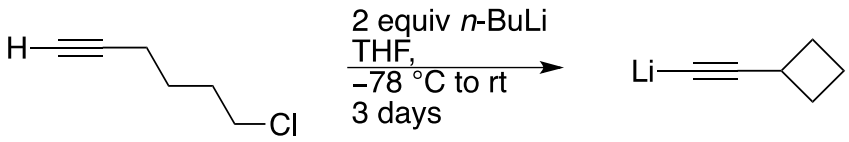


**6-Cl-hexyne 11-1** **11-2**

In steps taken toward producing the bis-alkylated products, a number of factors were considered in adjusting the conditions for the synthesis of the mono-alkylated products in order to reverse the outcome. After performing the steps to produce the lithium–hydrogen exchange on the alkynes, 0.5 equivalents of saccharin *pseudo*-chloride (**9-1**) were slowly added dropwise to the solution of the lithiated alkyne at –78 °C (inverse addition), which was warmed to 10 °C over a period of 1 hour (Scheme 12). This method allowed the lithiated alkyne to be greater in concentration compared to the saccharin *pseudo*-chloride (**9-1**) at all times. After the work-up and column chromatography, the method produced close to a 70% yield for bis-derivatives **12-1** (69.5%) and **12-3** (88%), while that for **12-2** was lower (15%) due to the impure lithium reagent as for **10-2.**

**Scheme 12**

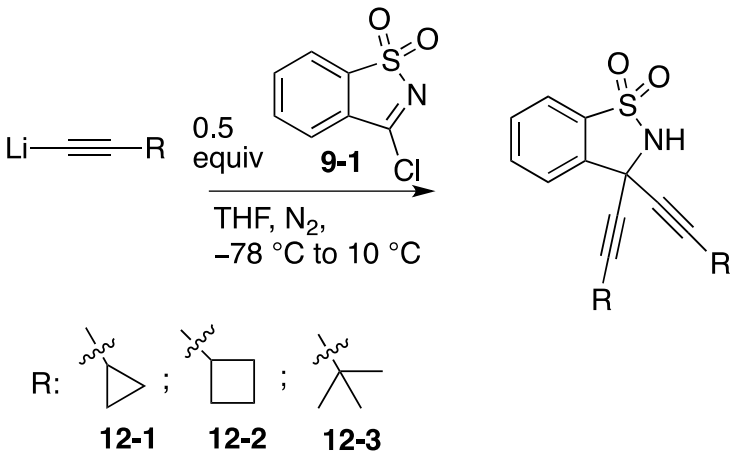


As shown in Mechanism 1, the mono-imine product is postulated to form by the addition of the alkyne at the electrophilic carbon atom attached to the nitrogen atom and the chlorine atom, thereby pushing electrons onto the nitrogen atom. From here, the electrons re-form the double bond resulting in the chlorine–carbon bond breaking and the $Cl^-$ leaving. For the mono-substituted product, work-up with satd $NH_4Cl$ is used to quench any remaining base. The second line in Mechanism 1 shows how the second equivalent of the alkyne is added to the same carbon atom center pushing the electrons onto the nitrogen atom once more, but from here, the use of a slightly acidic work-up protonates the nitrogen atom and ends the reaction. To confirm that this was how the formation of the bis-alkylated product was proceeding, a reaction was designed where pure 3-cyclopropylethynyl-1,2-benzisothiazole 1,1-dioxide was dissolved in dry THF, brought to –78 °C, and one equivalent of lithiated ethynylcyclopropane was added to the solution. Formation of the bis-product was seen showing how the second equivalent of the lithiated alkyne could add once more in the

reaction to the same electrophilic center without a need for a proton source such as water.

**Mechanism 1**

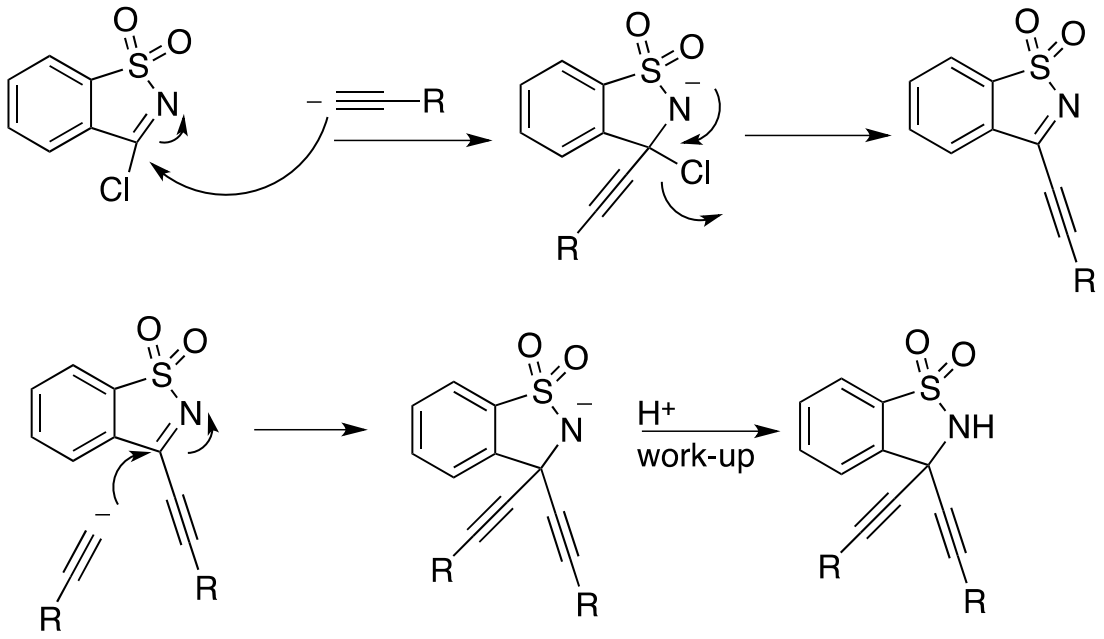


As discussed by Abramovitch et al., the methodology for the synthesis of the bis-alkylated versus the mono-alkylated product needed improvement.[74] Abramovitch et al. typically produced 10% of the mono-alkylated product and 24% of the bis-alkylated product by their methods.[74] The method employed by Kafri produced around 40% yields and showed no selectivity in mono- versus bis-product production.[79] By the change in the order and speed of addition, temperature control, and taking advantage of concentration ratios, the yields of the bis- versus the mono-products were adjusted to favor one product over the other successfully and in greater yields. At this point, a

methodology for performing 1,2-reductions on the mono-alkylethynyl sultams would be investigated.

### 3. 3-(Alkylethynyl)-2,3-dihydro-1,2-benzisothiazole 1,1-dioxide (16-1–16-3)

As previously discussed, a paper by Baker and co-workers addressed the design and synthesis of a novel catalyst employing the ligands as used by Noyori et al. with the reactivity of rhodium towards the reduction of imines.[75, 78] Noyori's catalyst used (1*S*,2*S*)-*p*-TsNCH($C_6H_5$)-CH($C_6H_5$)$NH_2$ and various aromatic groups as ligands on ruthenium chloride as an asymmetric catalyst for hydrogenation of ketones with high ee.[75] Noyori's catalyst was shown to work on imine double bonds with varying high ee, however, with long reaction times.[75] It was found by Dr. Jianmin Mao, while in Dr. Baker's lab, that rhodium-based catalysts showed strong affinity for reactions with imines.[77, 78] The rhodium catalyst performed asymmetric hydrogenation with a 5:2 formic acid–triethylamine azeotrope on the 3-aryl-1,2-benzisothiazole 1,1-dioxides (**13-1**) with high yield and a high ee around 95% (Scheme 13).

**Scheme 13**

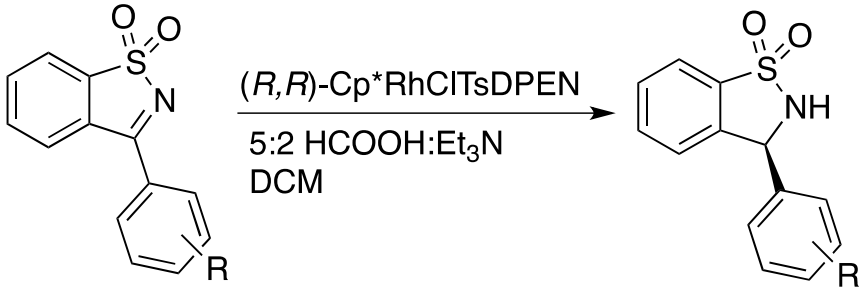


**13-1** **13-2**

In Dr. Kafri's research it was found that when used to reduce two of the 3-alkylethynyl-1,2-benzisothiazole 1,1-dioxides (**10-1** and **10-2**), the chiral rhodium catalyst (Figure 14) would not only reduce the imine bond in a 1,2-reduction fashion, but also the triple bond due to the $\alpha,\beta$-conjugated system in these compounds, performing a complete reduction.[79] This would result in the production of 3-alkylethyl-2,3-dihydro-1,2-benzisothiazole 1,1-dioxides (**14-1**) (Scheme 14). However, Dr. Kafri stated that when the rhodium catalyst was used to reduce 3-(*tert*-butylethynyl)-1,2-benzisothiazole 1,1-dioxide (**10-3**), the 1,2-reduction was performed to produce **15-1**, as shown in Scheme 15.[79] As with the bis-alkylated sultams, the material for **15-1** had degraded; therefore, the synthesis of **15-**1 would also be a part of the work performed. Further studies by performing the reaction and investigating as per Dr. Kafri's methods did not yield **15-1**. Upon a more detailed investigation of the $^{1}H$ and $^{13}C$ NMR of (*S*)-3-(*tert*-butylethynyl)-2,3-dihydro-1,2-benzisothiazole 1,1-dioxide (**15-1**) doubts in the synthesis of the desired product arose. This led to the inclusion of compound **10-3**, the *tert*-butyl imine, in the search of a method to yield only the 1,2-reduction and not the 1,4-reduction for all three compounds **10-1**–**10-3**.

**Scheme 14**

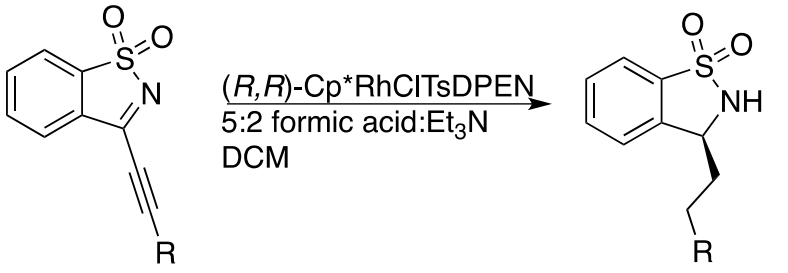


**10-1–10-2** **14-1–14-2**

**Scheme 15**

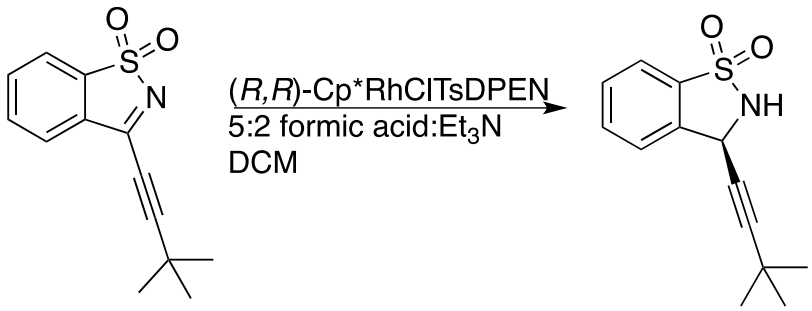


**10-3** **15-1**

The first attempt to perform the 1,2-reduction was to use a mild reducing agent such as $NaCNBH_3$ in methanol with the idea that it would not be reactive enough to perform the 1,4-reduction. However, this, too, would perform the 1,4-reduction while also performing the racemic reduction resulting in the 50:50 mixture of 3-alkyl-2,3-dihydro-1,2-benzisothiazole 1,1-dioxide. Seeing as this was not a desired product, the method was abandoned.

After further investigation, the Luche reduction, which has been shown to perform a racemic 1,2-reduction of $\alpha,\beta$-conjugated ketone systems, was attempted.[91] Further hopes for the application of the Luche reduction was found in a reaction of a patent for pyrazolyl-amino substituted pyrazines where the conditions for the Luche reduction were applied to an imine bond adjacent to an aromatic ring.[92] From here, the Luche reduction was applied to compound **10-1** first to test usefulness of the reaction. Results found that the Luche reduction can also be applied to an imine functionality with $\alpha,\beta$-conjugation to give an alkyne in a heterocyclic system with high yield of approximately 75% (Scheme 16). This was unique at the time, because the only application of the

Luche reduction to imines involved the imine in conjugation with aromatic rings instead of alkynes or alkenes.

Due to the lower reactivity of the nitrogen atom in an imine bond, when compared to the oxygen in a carbonyl bond, the method involved reacting the 3-alkylethynyl-1,2-benzisothiazole 1,1-dioxides (**10-1–10-3**) with 1.5 equivalents of $CeCl_3$ for 1 hour at room temperature before addition of 1.5 equivalents of $NaBH_4$ in 100% ethanol at 0 °C. The reaction was stirred at 0 °C for 30 minutes before warming to room temperature and stirring for one hour. It was later investigated to attempt the Luche reduction with $CeCl_3 \bullet 7H_2O$, a cheaper alternative to the anhydrous $CeCl_3$, with positive results. Since the application of the Luche reduction in this project, a paper was published in 2012 discussing the procedure of using Luche reduction conditions on hexaazamacrocycles-like compounds to reduce conjugated imines, but again, the conjugation was with aromatic rings instead of an alkyne or alkene that risked the chance be reduced in a 1,4 fashion.[93] This gives evidence that the application of the Luche reduction to α,β-conjugated imines to perform 1,2-reductions as a novel methodology.

**Scheme 16**

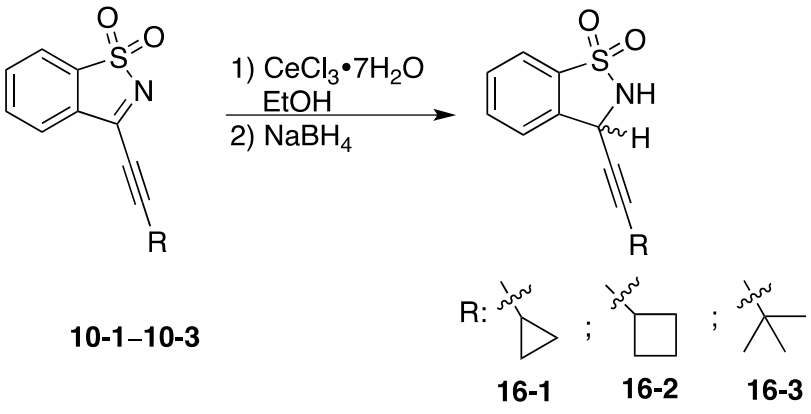


**10-1–10-3**

**16-1** **16-2** **16-3**

Upon the synthesis of racemic **16-3**, a comparison of its NMR spectra to those of Dr. Kafri for the purported **15-1**, it was concluded that the compound had not been synthesized. In Dr. Kafri's $^{13}C$ spectrum of **15-1**, the carbon peak of the C=N is still present; furthermore, in her $^{1}H$ spectrum, there is a singlet proton peak around 6.2 ppm, which, the proton spectrum for **16-3** shows two proton peaks at 4.81 ppm for the hydrogen atom on the nitrogen atom in **16-3**, and 5.41 ppm for the hydrogen atom on the carbon atom adjacent to the nitrogen.[79]

As discussed previously, this method produced a high yield of the racemic products (**16-1**–**16-3**), and a procedure was sorely needed for synthetically producing the pure (*S*)-enantiomer of the desired 3-(alkylethynyl)-2,3-dihydro-1,2-benzisothiazole 1,1-dioxides.

From here, methods were explored to attempt coupling of the now 3-alkylethynyl-2,3-dihydro-1,2-benzisothiazole 1,1-dioxides (**16-1**–**16-3**) with an amino acid with defined stereochemistry as an attempt to induce a chiral resolution that can be used to manipulate the presence of diastereomers in column separations. The amino acid L-phenylalanine was chosen for coupling with the nitrogen atom of the heterocycle in attempts to form a peptide bond.

The first attempt in the project for coupling the nitrogen atom of the sulfonamide functionality was to look at the use of amino acid coupling reagents. According to Backes and Ellman, the coupling reagent PyBOP, has shown substantially good results when coupling Ellman's modification of Kenner's sulfonamide linker (Figure 27) resin with a Boc-protected L-phenylalanine with a yield of 90% in DCM at –20 °C with *i*-

$Pr_2EtN$ as the base.[94] When compared to other peptide coupling agents, Ellman's modification has also been used by Marcaurelle and Bertozzi to synthesize deptericin and by Mende and Seitz to synthesize peptide $\alpha$-thioesters with protection by Fmoc instead of Boc.[95, 96] The idea was investigated to look into the idea of a heterocyclic sulfonamide reacting under similar conditions as the primary alkanylsulfonamide in the resin. The same conditions were maintained for the first attempt, and 3-cyclopropylethynyl-2,3-dihydro-1,2-benzisothiazole 1,1-dioxide (**16-1**) was reacted with L-Boc-Phe-OH with PyBOP as the coupling reagent (Scheme 17). Using the DART-MS, evidence of the mass of the product appeared, but subsequent column chromatography produced very little of the coupled product. Alterations of time and temperature also proved to not yield a substantial amount of product, leading to a pursuit of alternate methods.

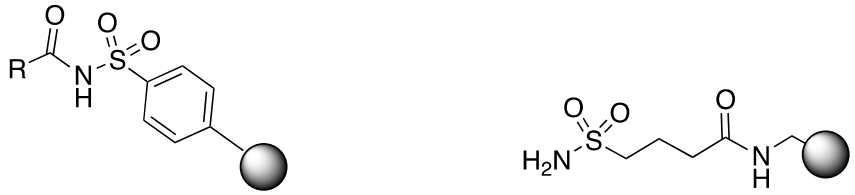


**Figure 27. Kenner's Sulfonamide and Ellman's modification, respectively.**

**Scheme 17**

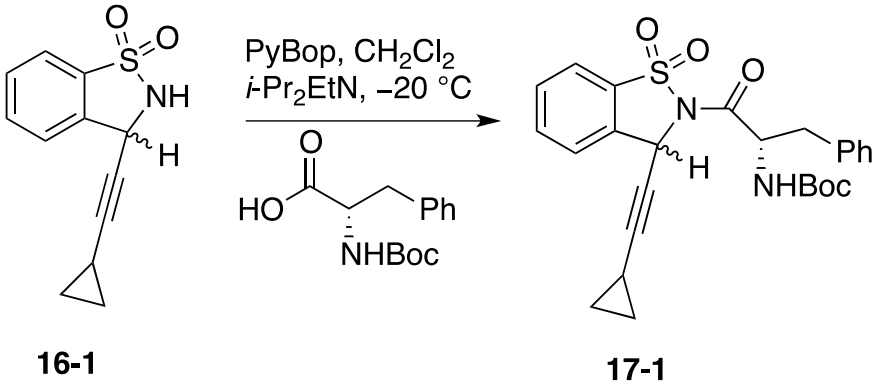


**16-1** **17-1**

A different approach was attempted when several papers presented the idea of reacting the 3-alkylethynyl-2,3-dihydro-1,2-benzisothiazole 1,1-dioxide (**16-1**–**16-3**) with a base to deprotonate the nitrogen, which would then react with an acyl chloride to form the peptide bond.[97, 98] Oppolzer et al. performed various methods of acylating either (*S*)-3-methyl-2,3-dihydro-1,2-benzisothiazole 1,1-dioxide or camphorsultam with either acyl chlorides or with trimethylaluminum and an ester.[97] One attempt used the (*S*)-methyl sultam **19-1** with propionyl chloride (Scheme 19). Seeing as Oppolzer used a sultam very similar to **16-1** instead of a primary solid-phase sulfonamide like those in Figure 25, the same method was attempted with racemic 3-cyclopropylethynyl-2,3-dihydro-1,2-benzisothiazole 1,1-dioxide (**16-1**) with *N*-Cbz-L-phenylalanine acyl chloride. Triethylamine was used to deprotonate the nitrogen atom of the heterocycle, which would then be expected to attack the carbonyl carbon of the acyl chloride producing the peptide bond (Scheme 18).

**Scheme 18**

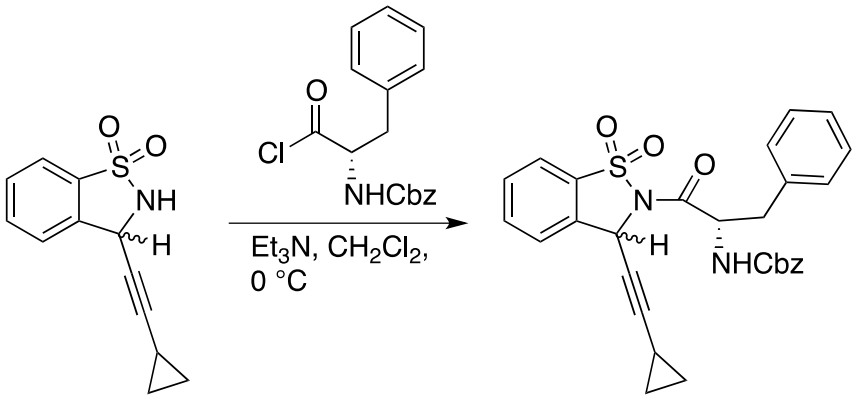


**16-1** **18-1**

The coupling with the use of the acyl chloride of the amino acid and the racemic 3-cyclopropylethynyl-2,3-dihydro-1,2-benzisothiazole 1,1-dioxide (**16-1**) gave no positive results. When compared with the method of Oppolzer et al., the sulfonamide **19-1** already had defined stereochemistry with only a methyl group at the 3-position as compared to the racemic cyclopropylethynyl substituent.[97] Furthermore, Oppolzer et al. performed the coupling with propionyl chloride to form **19-2** as opposed to the bulkier *N*-Cbz-L-phenylalanine acyl chloride (Scheme 19). It is believed that the sterics of the racemic ethynyl sultam compared to the *S* methyl sultam and the sterics of the Cbz-phenylalanine to the propionyl chloride prohibited the reaction from occurring.

**Scheme 19**

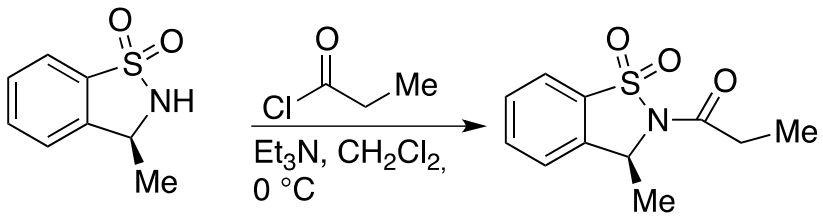


**19-1** **19-2**

From here, a look into other possibilities for performing the amino acid coupling with the racemic 3-cyclopropylethynyl-2,3-dihydro-1,2-benzisothiazole 1,1-dioxide (**16-1**) was investigated to discover that Oppolzer and co-workers and various other groups also performed the acylation with the use of trimethylaluminum to couple sulfonamides with the carbonyl of an ester.[99-103] To achieve the ester of the *N*-Cbz-L-phenylalanine, the Cbz protected amino acid was reacted with thionyl chloride in methanol. From here, the sultam was reacted with trimethylaluminum in anhydrous toluene under argon followed by the *N*-Cbz-L-phenylalanine methyl ester to attempt to synthesize **20-1** (Scheme 20).[102]

**Scheme 20**

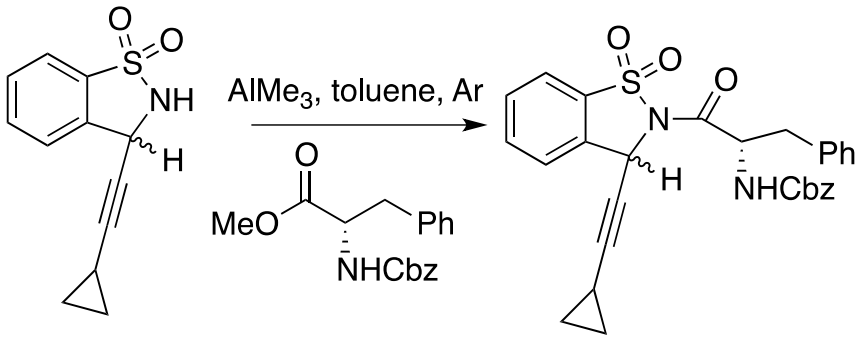


**16-1** **20-1**

As with the use of the acyl chloride, this reaction was not successful, with theories believing it was also because of steric hindrance. It was decided to attempt the same procedure with varying protecting groups on the nitrogen atom of the amino acid. Of the protecting groups attempted were a Boc-group, dibenzyl-, and methyl- and benzyl-protected amines. The method failed to produce positive results in any of the varying compounds, except the Boc-protected group did react, however, not at the methyl ester site as shown by NMR analysis. The first indication of the product not occurring at the methyl ester was the presence of a single methyl peak integrating to 3H as compared to the integration of the single proton in the sultam ring. Furthermore, using 2-D NMR analysis, it was determined that a peptide bond was formed at the carbonyl carbon atom of the Boc protecting group because the hydrogen on C3 in the sultam ring correlated to a carbonyl carbon. The carbonyl carbon did not show a correlation to the $CH_2$ group in the phenylalanine as it should if the carbonyl were bonded to the nitrogen atom was from the methyl ester carbonyl. Therefore, the reaction occurred at the Boc carbonyl and the *tert*-butoxide group acted as a leaving group, producing the sulfonylurea sultam **21-1** (Scheme 21).

**Scheme 21**

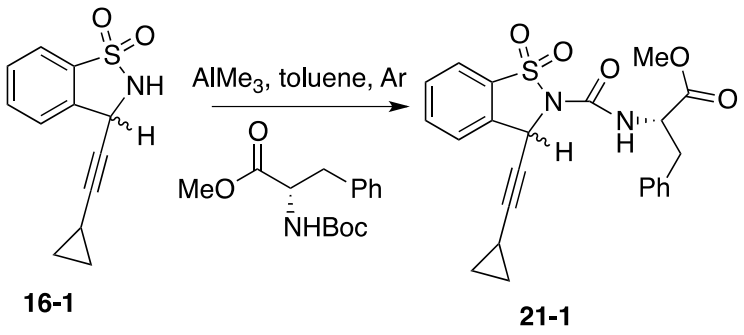


In the end, it seemed the use of L-phenylalanine, protected or not, would not couple to the racemic 3-cyclopropylethynyl-2,3-dihydro-1,2-benzisothiazole 1,1-dioxide (**16-1**). The issue of sterics arises with the reasoning of the coupling not occurring. In the works cited,[97, 98, 101-103] the authors either used a sultam with a defined stereocenter with only a methyl substituent versus our racemic cyclopropylethynyl group, or an alkanesulfonamide. Most of the authors also used a group for the acylation that was not itself defined with stereochemistry but rather small and/or flat near the acylating carbonyl.

From here, different methods were considered for reducing the imine bond without affecting the triple bond. The use of a compound nicknamed BINAL-H (*R* isomer in Figure 26) by Noyori, comprised of reacting LAH with either the *R* or *S* isomer of 2,2'-dihydroxy-1,1'-binapthol and a simple alcohol (MeOH or EtOH) was considered.[104] Noyori et al. found that BINAL-H with ethanol could reduce various ketones asymmetrically with high ee under cold conditions. When applied to an $\alpha,\beta$-conjugated system, BINAL-H showed a preference for asymmetric reduction while also performing the 1,2-reduction over the 1,4-reduction. BINAL-H has been applied to the asymmetric

reduction of phosphinyl imines, which gave hope to it working on the cyclic sulfonyl imine.[105] It was with this knowledge that the method and reagent would be applied to the reduction of 3-cyclopropylethynyl-1,2-benzisothiazole 1,1-dioxide (**10-1**) (Scheme 22). After several attempts, the analysis of the results of the reaction in Scheme 22 showed that no reaction took place. Conditions were altered to longer reaction times and/or warmer conditions than discussed in the Noyori paper, which also yielded negative results.

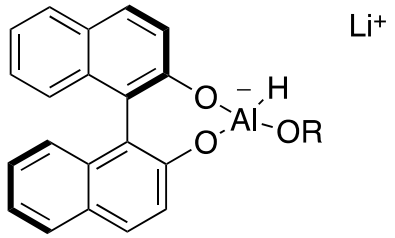


**Figure 28. (*R*)-BINAL-H.**

**Scheme 22**

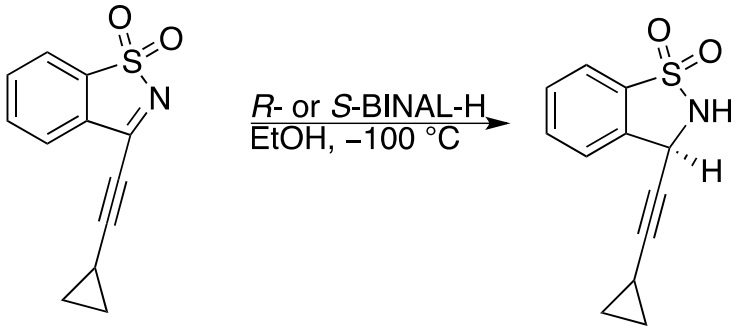


**10-1** **22-1**

The next attempt was to use $Co_2(CO)_8$ as a protecting group on the alkyne. Upon reacting the 3-cyclopropylethynyl-1,2-benzisothiazole 1,1-dioxide (**10-1**) with $Co_2(CO)_8$,

the complex **23-1** with the alkyne was formed according to what appeared as broadening of peaks in the NMR due to the presence of the cobalt that matched with the proton shifts of the cyclopropylethynyl sultam proton spectrum (Scheme 23).[106-108] After seeing the presence of the cobalt complex, the asymmetric reduction was attempted with the chiral rhodium catalyst designed by Baker and co-workers.[78] The reaction appeared to occur only by evidence in the spectrum from the DARTMS with a trace of a $^{+}$H *m/z* of 234, the mass of **16-1** without the presence of the cobalt protecting group. Column chromatography failed to produce a tangible amount of pure material. Looking at the 3-D shape of the cobalt-complexed sultam (Figure 29), the three carbonyl groups on the cobalt tend to point in various directions of the structure leading one to believe that they could cause steric interference with the ligands of the rhodium catalyst, thus preventing interaction of the nitrogen atom to rhodium. At this point a new method was pursued.

**Scheme 23**

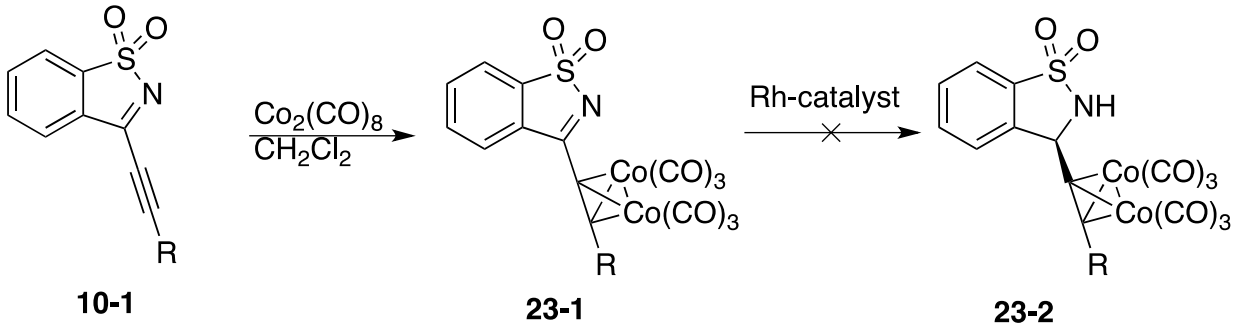


**10-1** **23-1** **23-2**

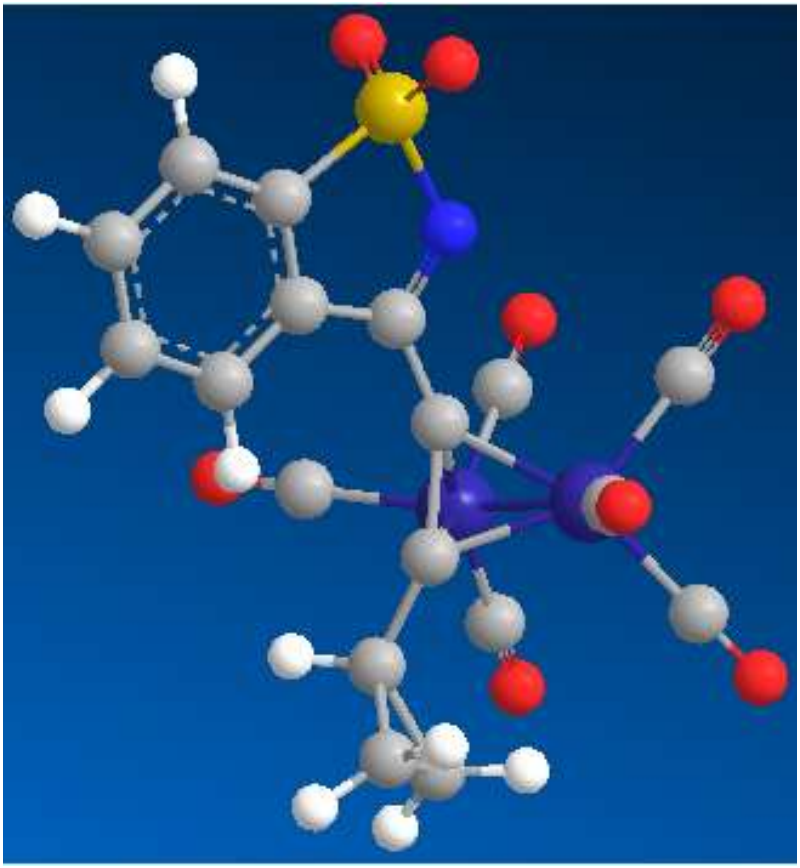

**Figure 29. Compound 23-1, the cyclopropylethynyl sultam with the alkyne protected with the cobalt carbonyl complex.**

After a search through the literature, one paper by Corey and co-workers showed the use of a chiral oxazaborolidine with catelcholborane to perform the 1,2-reduction on α,β-ynones asymmetrically with high ee without affecting the triple bond.[109, 110] With the Luche reduction occurring primarily on ketones, but also being a feasible method for the reduction of α,β-conjugated imines (Scheme 16), the use of the oxazaborolidine was applied to the reduction of the sultam as well. The catalytic oxazaborolidine **24-1** was prepared from (*S*)-α,α-diphenyl-2-pyrrolidinemethanol and $Me_3SiCH_2B(OH)_2$. It was reacted with the cyclopropylethynyl sultam **10-1** with catelcholborane at −78 °C to room

temperature over night (Scheme 24). After work-up and column chromatography, NMR spectra and DARTMS indicated a 20% yield for the reduced sultam **24-2**, and the triple bond was not affected, therefore the 1,2-reduction occured. To test for the asymmetric reduction the sample was analyzed with a polarimeter to assess the optical activity. Polarimetery at multiple wavelengths showed no rotation, leading one to believe there was no optical activity; therefore, the reduction occurred, but not asymmetrically. This method was no longer pursued as it performed the same racemic reduction as the Luche reduction but lower yield.

**Scheme 24**

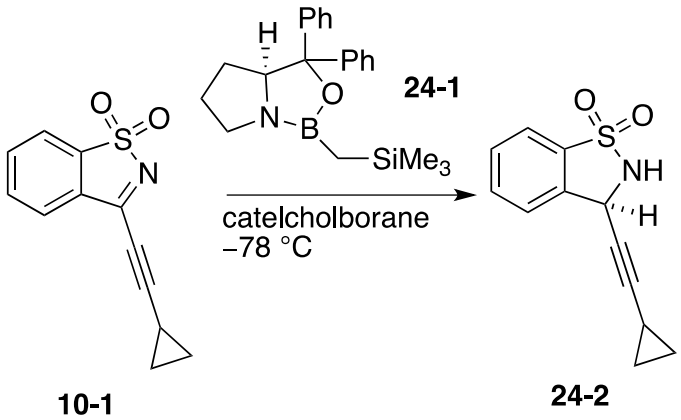


After the above-mentioned attempts had been ruled out as viable methods for a selective 1,2-asymmetric reduction, it was decided to rely on the Luche reduction and to evaluate the biological activity of the racemic mixtures. Once the biological activity data are collected, if the data seems worth pursuing the pure enantiomers, the use of chiral columns for HPLC will be investigated for the purification of the enantiomers. As of this time, some limited chiral separations have been attempted using the available ChiralCel

D column, which was used in the Baker group to separate the racemic mixtures of the 3-methylphenyl and similar derivatives by the original method, and a ChiralCel AD analytical chiral column. No meaningful separations were achieved. More extensive work using a set of chiral columns, followed by selective (and expensive) semipreparative columns would be necessary.

Mechanistically, the Luche reduction proceeds by the lone pair on the nitrogen atom forming a complex with the $CeCl_3$, resulting in the carbon in the imine bond becoming more electrophilic. Furthermore, the presence of the ethanol causes the sodium borohydride to become a harder nucleophile by replacing the hydrides with ethoxide groups. From here, the hydride adds the hydrogen to the carbon of the imine bond pushing electrons to the nitrogen atom, where after work-up the product is formed (Mechanism 2).

**Mechanism 2**

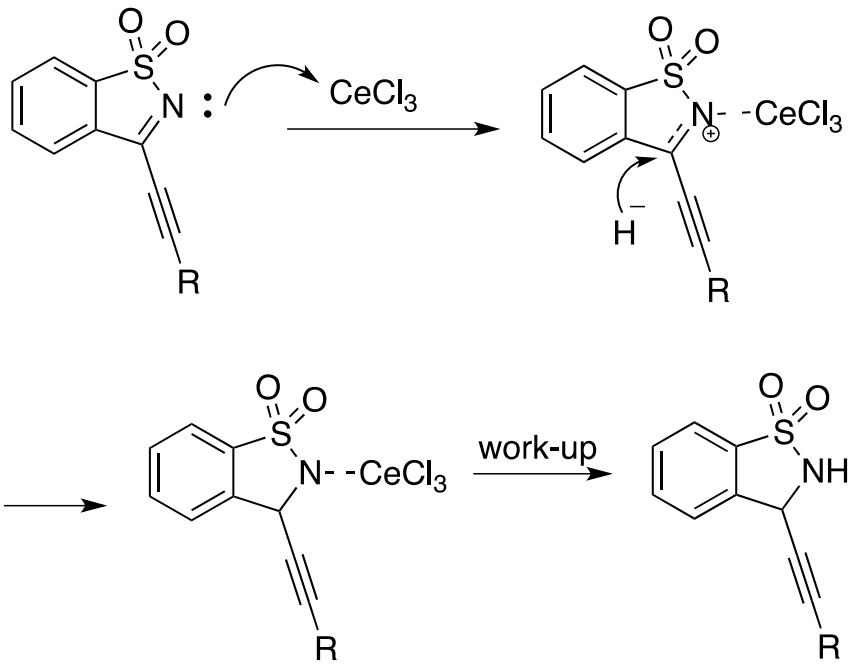


4. **3-Alkylethynyl-2,3-dihydro-3,methyl-1,2-benzisothiazole 1,1-dioxide and 3,3-bis(alkylethynyl)-2,3-dihydro-3-methyl-1,2-benzisothiazole 1,1-dioxide (25-1–25-6)**

The final step for the product of the mono-alkylethynyl sultams (**25-1**–**25-3**), including the bisalkylated-products (**25-4**–**25-6**), involved methylating the nitrogen atom. The process involved the use of the inorganic base $Cs_2CO_3$ in an organic solvent in which it was soluble, acetonitrile or *N*,*N*-dimethylformamide. The base deprotonates the nitrogen atom, where after the addition of iodomethane, the electrons attack the carbon in the methyl group displacing the iodo group, resulting in the *N*-alkyl product (Scheme 25).

**Scheme 25**

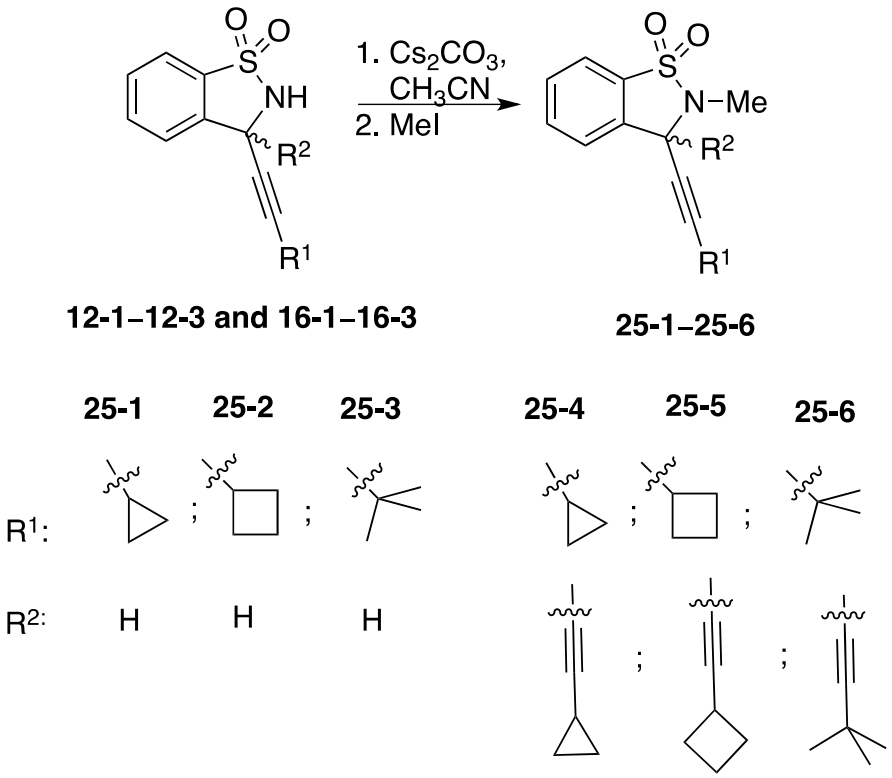


**5. (*S*)-3-(3-Cyclopropylphenyl)-2,3-dihydro-2-methyl-1,2-benzisothiazole 1,1-dioxide (26-4)**

Original methods to synthesize compound **26-4** involved initially performing the Simmons–Smith cyclopropanation on 3-bromostyrene. This was performed via a traditional Simmons–Smith method with a zinc–copper couple and diiodomethane. The cyclopropanation occurred as evidenced by the presence of the mass of the product in a GC/MS spectrum; however, upon attempts to form the organometallic form of the compound (lithiated or Grignard reagent), the organometallic was not formed. Past results showed use of *n*-BuLi possibly opened the cyclopropane ring or formed a

dimeric linked version of the compound, and evidence suggests that the Grignard reagent, 3-cyclopropylphenylmagnesium bromide was never formed. From here, it was decided to attempt the cyclopropanation reaction in the last step of the synthesis to **26-4**.

The method for preparing 3-(3-vinylphenyl)-1,2 benzisothiazole 1,1-dioxide (**26-1**) follows a method similar to that designed by Baker and co-workers, which resembles that of Abramovitch et al.[74] While a Grignard reagent of 1.0 equivalent of 3-bromostyrene is synthesized with magnesium turnings, a solution of 0.9 equivalents of saccharin in THF is reacted with 0.9 equivalent of phenylmagnesium bromide to deprotonate the nitrogen atom of saccharin. Once one equivalent of the 3-vinylphenyl magnesium bromide was prepared, it was added to the deprotonated solution of saccharin to act as a nucleophile at the carbonyl carbon, and the product was formed after work-up followed by column chromatography. Compound **26-1** was obtained in a 62.2% percent yield (Scheme 26, **26-1**).[35]

The asymmetric reduction was carried out with the chiral rhodium catalyst developed by Baker and Mao as it had produced high yields and high ee values in the past on various other derivatives of the 3-phenylsultams.[78] The compound **26-1** was dissolved in dry DCM, and the catalyst was added with a ratio of 200:1 S:C. An azeotrope of 5:2 formic acid to triethylamine was added to act as the hydride source, and after a short reaction time of 30 min to 1 h, the reaction was complete and worked-up the compound (*S*)-3-(3-vinylphenyl)-2,3-dihydro-1,2-benzisothiazole 1,1-dioxide (**26-2**) was yielded after column chromatography in 93% yield (Scheme 26).

The nitrogen atom was methylated as discussed in previous methods with $Cs_2CO_3$ and iodomethane in acetonitrile to give **26-3** at 39% yield (Scheme 26).

The vinyl group on **26-3** was reacted under Simmons–Smith conditions to form a cyclopropyl ring at the 3-position of the phenyl ring. The first attempt was tried with the standard Simmons–Smith method using a copper–zinc couple in THF with $CH_2I_2$ as it was conducted on 3-bromostyrene. This method yielded little product, leading to a search for other methods. Charette et al. have reported the use of various phenoxides with diethyl zinc and diiodomethane to synthesize an iodomethylzinc phenoxide as a cyclopropanating reagent.[111] The paper discussed several phenols with halides in the ortho and para positions as being effective reagents, along with pentafluorophenol having similar reactivity to perform the cyclopropanation on styrene.[111] Following this lead, pentafluorophenol was reacted with diethylzinc, followed by $CH_2I_2$, to produce the cyclopropanating reagent that was then added to a solution of compound **26-3** in dry DCM and allowed to react for two days producing **26-4** in 53% yield. (Scheme 26).

An issue arose with the purification of **26-4** in that the rf values of **26-4** and **26-3** are identical under various solvent system methods. By analysis of NMR integration and HPLC, the purity of **26-4** appears to be around 90%, and this is adequate enough for biological analysis as the biological activity of **26-3** is already known. Compound **26-4** is characterized as a mixture of ca. 9:1 **26-4**:**26-3**.

**Scheme 26**

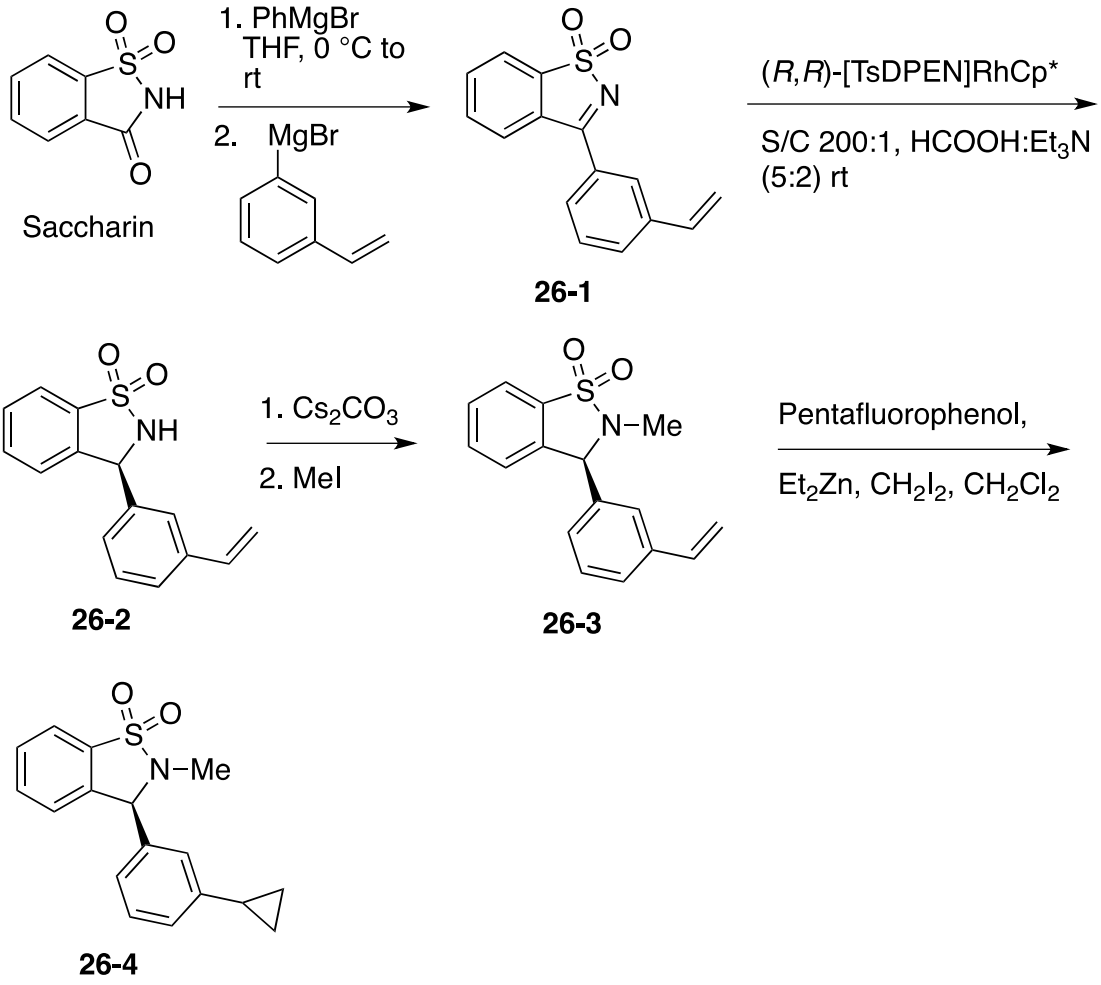


**26-1**

**26-2**

**26-3**

**26-4**

# Chapter IV. Experimental Procedures

## General

All reactions were monitored by thin-layer chromatography (TLC). Adsorption chromatography was carried out using Sorbent Technologies silica gel products: (a) TLC on 0.2 mm aluminum-backed plates, (b) column chromatography using 60–200 μm mesh silica gel. Visualization of the TLC plates was by 254 nm UV light and by dip–heat development using a *p*-anisaldehyde–sulfuric acid reagent.[112] All reactions were carried out under a nitrogen atmosphere.

For every procedure involving dry solvents (THF, DCM, DMF, $CH_3CN$), solvents were dried using alumina columns in a PureSolv system, with THF also being distilled from sodium–benzophenone ketyl, and DMF was distilled from calcium carbonate and stored in a nitrogen-purged flask with 4 Å molecular sieves.

*n*-butyllithium was purchased from Sigma–Aldrich as 2.5 M in hexanes, but was titrated with a solution of diphenylacetic acid in dry THF to determine the molarities shown in the procedures.[113]

All NMR spectroscopy was performed on Varian 500-MHz and 125-MHz NMR instrument in $CDCl_3$. Chemical shifts (δ-values) are reported downfield from tetramethylsilane (TMS). Mass spectrometry was performed with a JEOL AccuTOF Direct Analysis in Real Time (DART) Mass Spectrometer.

All glassware and stir bars were dried in an oven overnight at 150 °C, and cooled in a desiccator before use in reactions.

**Synthesis of 3-chloro-1,2-benzisothiazole 1,1-dioxide (9-1)**

In a large 1-L round-bottom flask was added 55.2325 g (0.301520 mol) of saccharin dissolved 250 mL of 1,4-dioxane. Approximately 90.0 mL (1.25 equiv) of $SOCl_2$ was added with 4.0 mL of DMF as a catalyst. The reaction was stirred at reflux for 3 days. It was concentrated under vacuum and recrystallized in hot toluene. $^1$H NMR: $\delta$ 7.80–7.95 (4H, m, Ar**H**); $^{13}$C NMR: $\delta$ 122.44, 125.10, 129.86, 134.46, 134.97, 140.51 (Ar), 166.11 (N**C**Cl); DARTHRMS: Calcd for $C_7H_4ClNO_2S$ *m/z* 200.96513; found $[M + H]^+$ *m/z* 201.97317 (calcd *m/z* 201.97295).[89, 114]

**Synthesis of 3-(cyclopropylethynyl)-1,2-benzisothiazole 1,1-dioxide (10-1)**

In a dry flask was dissolved 0.5656 mg (8.557 mmol) of ethynylcyclopropane (Organic Technologies) in 10 mL of dry THF. The solution was stirred and cooled to –78 °C under a nitrogen atmosphere. One equiv of 2.3 M *n*-BuLi solution in hexanes (3.720 mL) was added via syringe. The reaction was left to stir for 4 h at –78°C. A second solution of dry THF and 2.5900 g (12.845 mmol, 1.5011 equiv) of 3-chloro-1,2-benzisothiazole 1,1-dioxide (**9-1**) was cooled to a temperature of –78 °C under a nitrogen atmosphere. It was at this time that the lithiated alkyne solution was added dropwise via syringe to the benzisothiazole solution over a period of 1 h at –78 °C. After the addition was complete, the reaction was left to stir at –78 °C for 1 h, at which time it was quenched with satd aq $NH_4Cl$ at –78 °C. The mixture was left to warm to room temperature. The product was extracted with $Et_2O$ in a separatory funnel, and the organic layer was dried with anhyd $MgSO_4$, vacuum filtered, and rotary evaporated. The desired product was purified on two separate silica gel columns. The first elution used a 3:1 mixture of $Et_2O$ to hexane. This method separated the mono- and bis-

formations of the product effectively; however, some compounds coeluted with the mono-substituted product in this method. The second column was eluted with a 3:1 mixture of DCM to hexane to purify the desired product at 1.3868 g (70.111% yield). $^{1}$H NMR: $\delta$ 1.09–1.25 (4H, m, CHC**H**$_2$), 1.64–1.73 (1H, m, C**H**CH$_2$), 7.72–7.78 (3H, m, Ar**H**), 7.83–7.94 (1H, m, Ar**H**); $^{13}$C NMR: $\delta$ 0.80 (**C**HCH$_2$), 11.01 (CH**C**H$_2$), 68.51 (C**C**), 116.09 (**C**C), 122.06, 124.94, 131.60, 133.76, 133.96, 138.62 (Ar), 156.62 (**C**=N); DARTHRMS: Calcd for $C_{12}H_9NO_2S$ *m/z* 231.27036; found $[M + H]^+$ *m/z* 232.04424 (calcd *m/z* 232.04322).

**Synthesis of 3-(cyclobutylethynyl)-1,2-benzisothiazole 1,1-dioxide. (10-2)**

In a dry flask was dissolved 665.1 mg (5.705 mmol) of 6-chloro-1-hexyne (**11-1**) (Sigma–Aldrich) in 10 mL of dry THF. The solution was stirred and cooled to –78 °C under a nitrogen atmosphere. Two equiv of 2.3 M *n*-BuLi solution in hexanes (5.209 mL) were added dropwise via syringe over 20 min. After addition was complete, the reaction stirred at –78 °C for an additional 20 min, whereupon it was brought to room temperature and stirred under nitrogen overnight. The next day, a second solution of dry THF and 1.7844 g (1.5512 equiv, 8.8499 mmol) of 3-chloro-1,2-benzisothiazole 1,1-dioxide (**9-1**) was cooled to a temperature of –78 °C under a nitrogen atmosphere, and the lithiated ethynylcyclobutane (**11-2**) solution was added dropwise over 1 h. After standing for 1 h at –78 °C under a nitrogen atmosphere, the solution was quenched with satd aq $NH_4Cl$ at –78 °C. The biphasic mixture was extracted with $Et_2O$, and the organic layer was separated and dried with anhyd $MgSO_4$, vacuum filtered, and rotary evaporated. The desired product was purified on silica gel chromatography by eluting with a 3:1 mixture of $Et_2O$ to hexane, followed by a second silica gel chromatography by

eluting with 3:1 mixture of DCM to hexane to give the desired product at 245.1 mg (17.51% yield). $^{1}$H NMR: δ 2.00–2.15 (2H, m, $CH_2C\mathbf{H}_2CH_2$), 2.32–2.42 (2H, m, $CHC\mathbf{H}_2CH_2$), 2.44–2.52 (2H, m, $CHC\mathbf{H}_2CH_2$), 3.41–3.48 (1H, m, $CH_2C\mathbf{H}CH_2$), 7.73–7.78 (3H, m, Ar**H**), 7.86–7.89 (1H, m, Ar**H**); $^{13}$C NMR: δ 19.45 ($CH_2\mathbf{C}H_2CH_2$), 25.61 ($CH_2\mathbf{C}HCH_2$), 29.33 ($CH\mathbf{C}H_2CH_2$), 73.45 (**C**C), 114.30 (C**C**), 122.18, 125.04, 131.34, 133.86, 133.99, 138.71 (Ar), 156.81 (**C**=N) DARTHRMS: Calcd for $C_{13}H_{11}NO_2S$ *m/z* 245.29694; found $[M + H]^+$ *m/z* 246.05816 (calcd *m/z* 246.05887).

**Synthesis of 3-(*tert*-butylethynyl)-1,2-benzisothiazole 1,1-dioxide (10-3)**

In a dry flask was dissolved 405.9 mg (4.941 mmol) of 3,3-dimethylbutyne (Sigma–Aldrich) in 10 mL of dry THF. The solution was stirred and cooled to –78 °C under a nitrogen atmosphere. One equiv of 2.5 M *n*-BuLi solution in hexanes (1.98 mL) were added via syringe. The reaction was left to stir for 4 h at –78 °C. A second solution of dry THF and 1.992 g (9.882 mmol, 2.000 equiv) of 3-chloro-1,2-benzisothiazole 1,1-dioxide (**9-1**) was cooled to a temperature of –78 °C under a nitrogen atmosphere, and the lithiated alkyne solution was added dropwise via syringe to the benzisothiazole solution over 20 min. After the addition was complete, the reaction was left to stir at –78 °C for 1 h, at which time it was quenched with satd aq $NH_4Cl$ at –78 °C. The mixture was left to warm to room temperature whereupon the product was extracted with $Et_2O$. The mixture was then separated in a separatory funnel, and the organic layer was dried with anhyd $MgSO_4$, vacuum filtered, and rotary evaporated. The desired product was purified on silica gel chromatography by eluting with a 3:1 mixture of $Et_2O$ and hexane to purify the desired product to give 719.9 mg (58.99% yield). $^{1}$H NMR: δ 1.46 (9H, s, $C(C\mathbf{H}_3)_3$), 7.72–7.78 (3H, m, Ar**H**), 7.85–7.93

(1H, m, Ar**H**); $^{13}$C NMR: δ 28.76 (**C**$(CH_3)_3$), 29.91 (C(**C**$H_3)_3$), 71.68 (**C**C), 118.76 (C**C**), 122.26, 125.00, 131.44, 133.73, 133.92, 138.85 (Ar), 156.79 (**C**=N) DARTHRMS: Calcd for $C_{13}H_{13}NO_2S$ *m/z* 247.31282; found $[M + H]^+$ *m/z* 248.07567 (calcd *m/z* 248.07452).

**Synthesis of 3-(cyclopropylethynyl)-2,3-dihydro-1,2-benzisothiazole 1,1dioxide (16-1)**

In a dry flask, 0.9651 g (4.178 mmol) of 3-(cyclopropylethynyl)-1,2-benzisothiazole 1,1-dioxide (**10-1**) was dissolved in 100% EtOH at room temperature. While stirring, 2.326 g (6.242 mmol, 1.494 equiv) of $CeCl_3$•$7H_2O$ was added to the solution with stirring for 2 h at room temperature. After 2 h, 0.2305 g (6.093 mmol, 1.458 equiv) of $NaBH_4$ was added to the solution at room temperature with stirring for 3 h. The reaction was worked up with DOWEX-50 in $[H^+]$ form and stirred for 1 h. The resin was filtered off, and the EtOH was rotary evaporated off leaving a solid. The solid was dissolved in DCM, and was washed with $H_2O$ (3 × 10 mL). The organic layer was dried with anhyd $MgSO_4$ and filtered. The solvent was rotary evaporated, and the desired product was purified on silica gel chromatography by eluting with a 4:1 mixture of DCM and hexane to purify the desired product to give 0.5660 g (58.14% yield). $^1$H NMR: δ 0.69–0.72 (2H, m, CHC**H**$_2$C**H**$_2$), 0.78–0.83 (2H, m, CHC**H**$_2$C**H**$_2$), 1.23–1.30 (1H, m, $CH_2$C**H**$CH_2$), 4.99 (1H, s, N**H**), 5.37 (1H, d, *J* = 5.5 Hz C**H**NH), 7.52–7.55 (2H, t, Ar**H**), 7.637 (1H, t, *J* = 7.5 Hz, Ar**H**), 7.74 (1H, d, *J* = 8.0 Hz, Ar**H**); $^{13}$C NMR: δ -0.47 (**C**H$CH_2$), 8.39 (**C**$H_2$CH), 49.02 (**C**HNH), 69.92 (**C**C), 90.57 (C**C**), 121.06, 124.91, 129.72, 133.45, 135.06, 138.37 (Ar) DARTHRMS: Calcd for $C_{12}H_{11}NO_2S$ *m/z* 233.05105; found $[M + H]^+$ *m/z* 234.05850 (calcd *m/z* 234.05887).

**Synthesis of 3-(cyclobutylethynyl)-2,3-dihydro-1,2-benzisothiazole 1,1-dioxide (16-2)**

In a dry flask, 117.2 mg (0.4763 mmol) of 3-(cyclobutylethynyl)-1,2-benzisothiazole 1,1-dioxide (**10-2**) was dissolved in 100% EtOH at room temperature. While stirring, 226.2 mg (0.7145 mmol, 1.500 equiv) of $CeCl_3 \bullet 7H_2O$ was added to the solution, and the mixture was stirred for 2 h at room temperature. The reaction was then cooled to 0 °C, and 37.3 mg (0.986 mmol, 2.07 equiv) of $NaBH_4$ was added to the solution at 0 °C, and the mixture was stirred for 30 min. The reaction was brought to room temperature and stirred for an additional 1 h, at the end of which time it was worked up with DOWEX-50 in [$H^+$] form and stirred for 1 h. The resin was filtered off, and the EtOH was rotary evaporated off leaving a solid. The solid was dissolved in DCM, and was washed with $H_2O$ (3 × 10 mL). The organic layer was dried with anhyd $MgSO_4$ and filtered. The solvent was rotary evaporated, and the desired product was purified on silica gel chromatography by eluting with a 4:1 mixture of DCM to hexane to purify the desired product to give 87.3 mg (74.1% yield). $^1$H NMR: $\delta$ 1.82–1.97 (2H, m, $CH_2C\mathbf{H}_2CH_2$), 2.01–2.14 (2H, m, $CHC\mathbf{H}_2CH_2$), 2.16–2.30 (2H, m, $CHC\mathbf{H}_2CH_2$), 3.04 (1H, quintet, *J* = 8.5 Hz, $CH_2C\mathbf{H}CH_2$), 4.97 (1H, s, CHN**H**), 5.44 (1H, s, C**H**NH), 7.50–7.56 (2H, m, Ar**H**), 7.65 (1H, t, *J* = 8.0 Hz, Ar**H**), 7.74 (1H, d, *J* = 7.0, Ar**H**); $^{13}$C NMR: $\delta$ 18.99 ($CH_2\mathbf{C}H_2CH_2$), 24.44 ($CH_2\mathbf{C}HCH_2$), 29.26 ($CH\mathbf{C}H_2CH_2$), 29.28 ($CH\mathbf{C}H_2CH_2$), 48.69 (**C**HNH), 75.30 (**C**C), 90.94 (C**C**), 120.81, 124.76, 129.50, 133.27, 134.86, 138.25 (**Ar**); DARTHRMS: Calc for $C_{13}H_{15}NO_2S$ *m/z* 247.06670; found $[M + H]^+$ *m/z* 248.07540 (calcd *m*/z 248.07452).

**Synthesis of 3-(*tert*-butylethynyl)-2,3-dihydro-1,2-benzisothiazole 1,1-dioxide (16-3)**

In a dry flask, 315.5 mg (1.277 mmol) of 3-(*t*-butylethynyl)-1,2-benzisothiazole 1,1-dioxide (**10-3**) was dissolved in 100% EtOH at room temperature. While stirring, 713.9 mg (1.916 mmol, 1.500 equiv) of $CeCl_3 \bullet 7H_2O$ was added to the solution, and the mixture was stirred for 2 h at room temperature. After 2 h, 72.5 mg (1.92 mmol, 1.50 equiv) of $NaBH_4$ was added to the solution at room temperature, and stirring continued for 3 h. The reaction was worked up with DOWEX-50 in [$H^+$] form and stirred for 1 h. The resin was filtered off, and the EtOH was rotary evaporated off leaving a solid. The solid was dissolved in DCM and was washed with $H_2O$ (3 × 10 mL). The organic layer was dried with anhyd $MgSO_4$ and filtered. The solvent was rotary evaporated, and the desired product was purified on silica gel chromatography by eluting with 3:1 DCM to petroleum ether to give the purified desired product at 238.5 mg (74.9% yield). $^1$H NMR: δ 1.22 (9H, s, C(C**H**$_3$)$_3$), 4.81 (1H, s, N**H**), 5.41 (1H, d, C**H**NH), 7.53–7.56 (2H, t, Ar**H**), 7.64–7.67 (1H, td, Ar**H**), 7.75 (1H, d, Ar**H**); $^{13}$C NMR: δ 27.59 (**C**(CH$_3$)$_3$), 30.46, (C(**C**H$_3$)$_3$), 48.86 (**C**HNH), 73.14, (**C**C), 95.77 (C**C**), 120.93, 124.78, 129.58, 133.33, 135.24, 138.86 (Ar); DARTHRMS: Calc for $C_{13}H_{15}NO_2S$ *m/z* 249.08235; found [M + H]$^+$ *m/z* 250.08992 ( calcd *m/*z 250.09017).

**Synthesis of 3-(cyclopropylethynyl)-2,3-dihydro-2-methyl-1,2-benzisothiazole 1,1-dioxide (25-1)**

In a dry flask, 139.0 mg (0.5958 mmol) of 3-(cyclopropylethynyl)-2,3-dihydro-1,2-benzisothiazole 1,1-dioxide (**16-1**) was dissolved in dry acetonitrile. The temperature was brought to 0 °C, and 581.0 mg (1.788 mmol, 3.001 equiv) of $Cs_2CO_3$ was added,

followed by dropwise addition of 0.19 mL (3.1 mmol, 5.1 equiv) of $CH_3I$. After 45 min at 0 °C, the ice bath was removed and the reaction was stirred at room temperature for 2 h. The solution was quenched with satd aq $NH_4Cl$ and extracted with EtOAc. The organic layer was washed with $H_2O$ (2 × 15 mL) and a solution of brine. The organic layer was separated, dried with anhyd $MgSO_4$, and rotary evaporated. The desired product was purified on silica gel chromatography with an elution of 2:1 petroleum ether to EtOAc to give the desired product at 104.8 mg (71.15% yield). $^1$H NMR: δ 0.66–0.72 (2H, m, CHC**H**$_2$), 0.74–0.83 (2H, m, CHC**H**$_2$), 1.22–1.31 (1H, m, C**H**$CH_2$), 2.95 (3H, s, NC**H**$_3$), 5.01 (1H, s, C**H**N), 7.52–7.77 (4H, m, Ar**H**); $^{13}$C NMR: δ -0.61 (**C**$HCH_2$), 8.51 (CH**C**$H_2$), 27.67 (N**C**$H_3$), 54.37 (**C**$HNCH_3$), 68.40 (**C**C), 91.44 (C**C**), 121.13, 124.72, 129.66, 133.10, 134.02, 135.47 (Ar); DARTHRMS: Calcd for $C_{13}H_{13}NO_2S$ *m/z* 247.31282; found $[M + H]^+$ *m/z* 248.07506 (calcd *m/z* 248.07452).

**Synthesis of 3-(cyclobutylethynyl)-2,3-dihydro-2-methyl-1,2-benzisothiazole 1,1-dioxide (25-2)**

In a dry flask, 181.8 mg (0.7351 mmol) of 3-(cyclobutylethynyl)-2,3-dihydro-1,2-benzisothiazole 1,1-dioxide (**16-2**) was dissolved in dry acetonitrile and brought to 0 °C. Once at 0 °C, 726.6 mg (3.041 equiv, 2.236 mmol) of $Cs_2CO_3$ was added, followed by dropwise addition of 0.23 mL (5.0, equiv, 3.7 mmol) of $CH_3I$. After 45 min at 0 °C, the ice bath was removed and the reaction stirred for 3 h. The solution was quenched with satd aq $NH_4Cl$ and extracted with EtOAc. The organic layer was washed with $H_2O$ (2 × 15 mL) and a brine solution. The organic layer was dried with anhyd $MgSO_4$, filtered, and rotary evaporated. The desired product was purified on silica gel chromatography

by eluting with 2:1 petroleum ether to EtOAc to give the desired product at 141.3 mg (73.56%). $^{1}$H NMR: δ 1.86–1.98 (2H, m, C**H**$_2$), 2.08–2.16 (2H, m, C**H**$_2$), 2.24–2.30 (2H, m, C**H**$_2$), 2.98 (3H, s, NC**H**$_3$), 3.03–3.09 (1H, m, $CH_2$C**H**$CH_2$), 5.08 (1H, s, NC**H**), 7.53–7.58 (2H, m, Ar**H**), 7.65 (1H, td,*J* = 5 Hz, *J* = 1.25, Ar**H**), 7.78 (1H, d, *J* = 10 Hz, Ar**H**); $^{13}$C NMR: δ 19.22 ($CH_2$**C**$H_2CH_2$), 24.76 ($CH_2$**C**$HCH_2$), 27.71 (N**C**$H_3$), 29.67 (CH**C**$H_2CH_2$), 54.42 (N**C**H), 73.98 (**C**C), 91.92 (C**C**), 121.15, 124.73, 129.65, 133.10, 134.05, 135.05 (Ar); DARTHRMS: Calcd for $C_{14}H_{15}NO_2S$ *m/z* 261.33940; found [M + H]$^+$ *m/z* 262.09133 (calcd *m/z* 262.09017).

**Synthesis of 3-(*tert*-butylethynyl)-2,3-dihydro-2-methyl-1,2-benzisothiazole 1,1-dioxide (25-3)**

In a dry flask, 238.6 mg (0.9570 mmol) of 3-(*t*-butylethynyl)-2,3-dihydro-1,2-benzisothiazole 1,1-dioxide (**16-3**) was dissolved in dry acetonitrile. To the mixture was added 460.1 mg (1.479 equiv, 1.416 mmol) of $Cs_2CO_3$ at room temperature and was stirred for 45 min. After 45 min., 0.30 mL (5.0 equiv, 4.8 mmol) of $CH_3I$ was added to the solution dropwise at room temperature, and the mixture was stirred for 1 h. The solution was quenched with $H_2O$ and rotary evaporated on the high vacuum. The remaining oil was dissolved in DCM and washed with $H_2O$ (2 × 5 mL) and dried with anhyd $MgSO_4$. The drying agent was filtered off, and the solvent was rotary evaporated off leaving a yellow oil. The desired product was purified with an elution of 2:1.5:0.1 mixture of hexanes to EtOAc to $CHCl_3$ on silica gel chromatography to give 118.5 mg (47.0% yield) $^{1}$H NMR: δ 1.22 (9H, s, C(C**H**$_3$)$_3$), 2.94 (3H, s, NC**H**$_3$), 5.03 (1H, s, C**H**$NCH_3$), 7.51–7.76 (4H, m, Ar**H**); $^{13}$C NMR: δ 27.52 (**C**$(CH_3)_3$, 27.63 (N**C**$H_3$), 30.74 (C(**C**$H_3$)$_3$), 54.35 (**C**$HNCH_3$), 71.74 (**C**C), 96.48 (C**C**), 121.03, 124.64, 129.61, 133.10,

134.02, 135.69 (Ar); DARTHRMS: Calcd for $C_{14}H_{17}NO_2S$ *m/z* 263.09800; found $[M + H]^+$ *m/z* 264.10690 (calcd *m/z* 264.10582).

**Synthesis of 3-(*m*-vinylphenyl)-1,2-benzisothiazole 1,1-dioxide (26-1)**

In an oven dried 2-necked flask, addition funnel, and reflux column was added 100.8 mg (1.000 equiv, 4.147 mmol) $Mg^0$ turnings, and the apparatus was purged with nitrogen for 20 min. After 20 min. of purging, dry THF was added to the flask, and the mixture was purged for 20 min and stirred vigorously. After bringing the mixture to reflux, a solution of 0.7595 g (4.149 mmol) of 3-bromostyrene (Matrix Scientific) in dry THF was added dropwise to the solution. The reaction was stirred at reflux until the solution turned a yellow-brown color, and the magnesium turnings no longer remained. In a oven-dried round-bottom flask was dissolved 722.3 mg (0.9503 equiv, 3.943mmol) of saccharin in dry THF, and the solution was purged with nitrogen and brought to 0 °C. At 0 °C, 3.95 mL of a 1.0 M solution of phenyl magnesium bromide (Sigma–Aldrich) (0.952 equiv, 3.95 mmol) was added dropwise at 0 °C to the saccharin solution to deprotonate the saccharin. After stirring for some time at 0 °C, the (3-vinylphenyl)magnesium bromide solution was added dropwise to the solution of deprotonated saccharin at 0 °C with warming to room temperature. The solution was allowed to stir overnight under nitrogen. The reaction was quenched with ice water and then brought to pH 1 with 1 N HCl. The organic compound was extracted with $Et_2O$, and washed with a 10% $NaHCO_3$ solution to remove unreacted saccharin. The organic layer was dried with anhyd $MgSO_4$, filtered, and rotary evaporated to produce a yellow solid. The desired product was purified on silica gel chromatography with an elution of 2:1 mixture of petroleum ether to EtOAc to give 660.4 mg (62.19% yield). $^1$H NMR: $\delta$ 5.42 (1H, d, *J* = 10 Hz CH=C**H**$_2$), 5.89 (1H, d,

*J* = 20 Hz, CH=C**H**$_2$), 6.81 (1H, quartet, *J* = 10 Hz, *J* = 20 Hz, C**H**=CH$_2$), 7.58 (1H, t, *J* = 10 Hz, Ar**H**), 7.72-7.85 (4H, m, Ar**H**), 7.89-7.91 (1H, m, Ar**H**), 7.99 (1H, t, *J* = 5.0 Hz, Ar**H**), 8.02-8.04 (1H, m, Ar**H**); $^{13}$C NMR: δ 116.23 (CH=**C**H$_2$), 123.10 (Ar), 126.51 (Ar), 127.18 (Ar), 128.54 (Ar), 129.36 (Ar), 130.54 (Ar), 130.75 (Ar), 130.89 (Ar), 133.42 (Ar), 133.66 (Ar), 135.43 (**C**H=CH$_2$), 138.85 (Ar), 141.10 (Ar), 170.99 (**C**=N). DARTHRMS: Calcd for $C_{15}H_{12}NO_2S$ *m/z* 269.31834; $[M+H]^+$ *m/z* 270.06044 (calcd *m/z* 270.05887).

**Synthesis of (*S*)-3-(*m*-vinylphenyl)-2,3-dihydro-1,2-benzisothiazole 1,1-dioxide (26-2)**

In an oven-dried flask, 660.4 mg (2.452 mmol) of 3-(*m*-vinylphenyl)-1,2-benzisothiazole 1,1-dioxide (**26-1**) was added to dry DCM. With a ratio of 200:1 imine to catalyst, 8.9 mg (0.014 mmol) of pre-formed Cp*RhCl[(1*R*,2*R*)-*p*-TsNCH($C_6H_5$)CH($C_6H_5$)NH$_2$] was added, and the mixture was stirred at room temperature under nitrogen. At this time, 0.4 mL of an azeotropic mixture of 5:2 formic acid–triethylamine was added, and the reaction was stirred for 30 min. After evidence that the substrate had disappeared by TLC, the reaction was worked-up with 1 M $NaHCO_3$ and extracted with DCM. The combined organic phase was washed with brine, dried over $MgSO_4$, and concentrated to give a crude product. The desired product was purified on silica gel chromatography with an elution of 2:1 mixture of hexanes to EtOAc to give 620.0 mg (93.16%) $[\alpha]_D^{23}$ +119° (c=0.1, $CHCl_3$); $^1$H NMR: δ 5.05 (1H, s, N**H**), 5.28 (1H, d, *J* = 10 Hz, CH=C**H**$_2$), 5.71 (1H, d, *J* = 5 Hz, C**H**NH), 5.76 (1H, d, *J* = 20 Hz, CH=C**H**$_2$), 6.68 (1H, quartet, *J* = 10 Hz, *J* = 20 Hz, C**H**=CH$_2$), 7.13-7.83 (8H, m, Ar**H**); $^{13}$C NMR: δ 61.28 (**C**HNH), 115.12 (CH=**C**H$_2$), 121.15 (**C**H=CH$_2$), 125.33, 125.40, 126.76, 126.87, 129.47, 129.51, 133.33,

134.78, 136.01, 138.64, 139.00, 139.65 (Ar); Calcd for $C_{15}H_{13}NO_2S$ *m/z* 271.06670; found $[M + H]^+$ *m/z* 272.07352 (calcd *m/z* 272.07452).

**Synthesis of (*S*)-3-(*m*-vinylphenyl)-2,3-dihydro-2-methyl-1,2-benzisothiazole 1,1-dioxide (26-3)**

To a solution of 620.0 mg (2.285 mmol) (*S*)-3-(*m*-vinylphenyl)-2,3-dihydro-1,2-benzisothiazole 1,1-dioxide (**26-2**) in dry acetonitrile was added 1.4800 g (1.9929 equiv, 4.5538 mmol) of $Cs_2CO_3$. The mixture stirred for 1 h, at which time 0.29 mL (2.1 equiv, 4.7 mmol) of $CH_3I$ were added, and the mixture stirred until completion of the reaction as shown by TLC. The reaction was quenched with water, and the mixture was rotary evaporated under high vacuum. The product was taken up in DCM, and washed with water (3 × 15 mL) followed by a brine wash. The organic phase was dried with anhyd $MgSO_4$, and rotary evaporated. The desired product was purified on silica gel chromatography with an elution of 2:1 hexanes to EtOAc to give 254.8 mg (39.08% yield). $[\alpha]_D^{20}$ +138° (c=0.1, $CHCl_3$); $^1$H NMR: δ 2.78 (3H, s, NC**H**$_3$), 5.18 (1H, s, C**H**N), 5.29 (1H, d, *J* = 10 Hz, CH=C**H**$_2$), 5.77 (1H, d, *J* = 20 Hz, CH=C**H**$_2$), 6.70 (1H, quartet, *J* = 10 Hz, *J* = 20 Hz, C**H**=CH$_2$), 7.03-7.86 (8H, m, Ar**H**); $^{13}$C NMR: δ 27.51 (N**C**H$_3$), 66.94 (**C**HN), 115.01 (CH=**C**H$_2$), 121.12 (**C**H=CH$_2$), 124.98, 125.91, 126.84, 127.50, 129.33, 129.40, 132.97, 134.06, 136.07, 136.99, 138.24, 138.58 (Ar); DARTHRMS: Calcd for $C_{16}H_{15}NO_2S$ *m/z* 285.36080; found $[M + H]^+$ *m/z* 286.09156 (calcd *m/z* 286.09017).

**Synthesis of (*S*)-3-(*m*-cyclopropylphenyl)-2,3-dihydro-2-methyl-1,2-benzisothiazole 1,1-dioxide (26-4)**

In an oven-dried flask was dissolved 180.6 mg (2.002 equiv, 0.9812 mmol) of pentafluorophenol in dry dichlorohmethane under nitrogen. The solution is brought to

–40 °C, and 0.98 mL of 1 M $Et_2Zn$ (2.0 equiv, 0.98 mmol) is added to the solution to stir for 15 min. After 15 min. has passed, 0.10 mL (2.5 equiv, 1,2 mmol) of $CH_2I_2$ is added to the solution to continue stirring for 15 min. at –40 °C. After 15 min has passed, a solution of 140.0 mg of sultam **26-3** (1.000 equiv, 0.4901 mmol) in dry dichloromethane is added, and the cold bath is removed to allow the reaction to warm to room temperature. The reaction was stirred for 18 h. The reaction was washed with 10% aq HCl (2 × 25 mL), satd aq $NaHCO_3$ (2 × 25 mL), satd aq $Na_2SO_3$ (25 mL), and satd aq NaCl (25 mL). The organic layer was dried over $MgSO_4$, filtered, and rotary evaporated. The product was purified on silica gel chromatography with an elution of 2:1 hexanes to EtOAc to give 78.1 mg (53.2% yield). $[\alpha]_D^{21}$ +117° (c=0.1, $CHCl_3$); $^1$H NMR δ 0.68 (2H, m, CHC**H**$_2$C**H**$_2$), 0.97 (2H, m, CHC**H**$_2$C**H**$_2$), 1.88 (1H, m, C**H**$CH_2CH_2$), 2.76 (3H, s, NC**H**$_3$), 5.13 (1H, s, C**H**N), 7.01-7.84 (8H, m, Ar**H**); $^{13}$C NMR δ 9.57 (CH**C**$H_2CH_2$), 9.62 ($CHCH_2$**C**$H_2$), 15.36 ($CH_2$**C**$HCH_2$), 27.42 (N**C**$H_3$), 67.04 (**C**$HNCH_3$), 121.06, 124.99, 125.20, 125.67, 125.85, 129.07, 129.25, 132.92, 134.01, 136.09, 138.44, 145.31 (Ar); DARTHRMS: Calcd for $C_{17}H_{17}NO_2S$ *m/z* 299.38738; found $[M + H]^+$ *m/z* 300.10610 (calcd *m/z* 300.10582).

**Synthesis of 3,3-bis(cyclopropylethynyl)-2,3-dihydro-1,2-benzisothiazole 1,1-dioxide (12-1)**

In a dry flask was dissolved 301.0 mg (4.554 mmol) of ethynylcyclopropane in 10 mL of dry THF. The solution was stirred and cooled to –78 °C under a nitrogen atmosphere. At this time, 1.90 mL (4.56 mmol, 1.00 equiv) of 2.4 M *n*-BuLi solution in hexanes were added via syringe. The reaction was left to stir for 4 h at –78 °C. A second solution of

dry THF and 457.7 mg (0.4985 equiv, 2.270 mmol) of 3-chloro-1,2-benzisothiazole 1,1-dioxide (**9-1**) was added dropwise to the solution of lithiated ethynylcyclopropane at –78 °C. The mixture was allowed to warm to 10 °C over an hour, and the reaction was worked up with satd aq $NH_4Cl$ and allowed to warm up to room temperature. The solid was filtered off, and the two layers were separated. An $Et_2O$ extraction was performed on the aqueous layer, and combined with the organic layer. The organic layer was dried with anhyd $MgSO_4$, which was filtered off, and the solvent was rotary evaporated off leaving a solid. The desired product was purified on silica gel chromatography by eluting with a 3:1 mixture of $Et_2O$ to hexane to purify the product to give 472.3 mg (69.53% yield). $^1$H NMR: $\delta$ 0.62-0.78 (8H, m, CHC**H**$_2$C**H**$_2$), 1.17-1.26 (2H, m, $CH_2$C**H**$CH_2$), 5.17 (1H, s, N**H**), 7.44-7.57 (1H, m, Ar**H**), 7.64-7.70 (3H, m, Ar**H**); $^{13}$C NMR: $\delta$ -0.74 ($CH_2$**C**H$CH_2$), 8.35 (CH**C**H$_2$**C**H$_2$), 52.29 (**C**N), 72.11 (**C**C), 88.59 (C**C**), 120.95, 124.90, 134.04, 133.29, 133.99, 140.73 (Ar); DARTHRMS: Calcd for $C_{17}H_{15}NO_2S$ *m/z* 297.37150; found $[M + H]^+$ *m/z* 298.08973 (calcd *m/z* 298.09017).

**Synthesis of 3,3-bis(cyclobutylethynyl)-2,3-dihydro-1,2-benzisothiazole 1,1-dioxide (12-2)**

In a dry flask was dissolved 3.7623 g (0.032270 mol) of 6-chlorohexyne in dry THF. The mixture was brought to −78 °C and 29.8 mL (0.0685 mol, 2.12 equiv) of 2.3 M *n*-BuLi was slowly injected for 20 min, whereupon the mixture was kept at −78 °C for at least 20 min afterwards. This solution was warmed to room temperature overnight, quenched with $NH_4Cl$, extracted with $Et_2O$, dried with anhyd $MgSO_4$, and the $Et_2O$ was distilled of to leave the product in THF. 4 Å Molecular sieves were added to the solution, and it was cooled to −78 °C. At this time, 14.0 mL (0.0323 mol, 1.00 equiv) of 2.3 M *n*-BuLi was

added to the solution dropwise, and the mixture was stirred for 4 h at −78 °C. A solution of 3.2482 g (0.016110 mol, 0.50000 equiv) of 3-chloro-1,2-benzisothiazole 1,1-dioxide (**9-1**) in dry THF was added dropwise to the solution of lithiated ethynylcyclobutane, and the mixture was allowed to warm to 10 °C over 1 h. The reaction mixture was worked up with satd aq $NH_4Cl$ and allowed to warm up to room temperature. The solid was filtered off, and the two layers were separated. An $Et_2O$ extraction was performed on the aqueous layer, and combined with the organic layer. The organic layer was dried with anhyd $MgSO_4$, which was filtered off, and the solvent was rotary evaporated off leaving a solid. The desired product was purified on silica gel chromatography with an elution of a 2:1 petroleum ether and EtOAc to purify the desired product at 0.7764 g (14.81% yield). $^1$H NMR: δ 1.79-1.93 (4H, m, $CH_2C\mathbf{H}_2CH_2$), 2.03-2.15 (4H, m, $CHC\mathbf{H}_2CH_2$), 2.15-2.24 (4H, m, $CHC\mathbf{H}_2CH_2$) 2.98-3.05 (2H, quintet, $CH_2C\mathbf{H}CH_2$), 5.06 (1H, s, CN**H**), 7.53-7.57 (1H, m, Ar**H**), 7.66-7.70 (2H, m, Ar**H**), 7.71-7.73 (1H, d, Ar**H**); $^{13}$C NMR: δ 19.15 ($CH_2\mathbf{C}H_2CH_2$), 24.67 ($CH_2\mathbf{C}HCH_2$), 29.30 ($CH\mathbf{C}H_2CH_2$), 29.31 ($CH\mathbf{C}H_2CH_2$), 52.41 (**C**NH), 78.18 (**C**C), 89.13 (C**C**), 120.95, 124.98, 130.08, 133.46, 134.00, 140.97 (Ar). DARTHRMS: Calcd for $C_{19}H_{19}NO_2S$ *m/z* 325.11365; found $[M + H]^+$ *m/z* 326.12147 (calcd *m/z* 326.12124).

**Synthesis of 3,3-bis(*tert*-butylethynyl)-2,3-dihydro-1,2-benzisothiazole 1,1-dioxide (12-3)**

In a dry flask was dissolved 473.2 mg (5.761 mmol) of 3,3-dimethylbutyne in 10 mL of dry THF. The solution was stirred and cooled to –78 °C under a nitrogen atmosphere. At −78 °C, 2.51 mL (1.00 equiv, 5.77 mmol) 2.3 M *n*-BuLi solution in hexanes were added via syringe. The reaction was left to stir for 4 h while at −78 °C. A second

solution of dry THF and 580.8 mg (0.5000 equiv, 2.881 mmol of 3-chloro-1,2-benzisothiazole 1,1-dioxide (**9-1**) was added dropwise to the solution of lithiated 3,3-dimethylbutyne at –78 °C. The reaction mixture was allowed to warm to 10 °C over 1 h, and the reaction was worked up with satd aq $NH_4Cl$ and allowed to warm up to room temperature. The solid was filtered off, and the two layers were separated. An $Et_2O$ extraction was performed on the aqueous layer, and combined with the organic layer. The organic layer was dried with anhyd $MgSO_4$, which was filtered off, and the solvent was rotary evaporated off leaving a solid. The desired product was purified on silica gel chromatography by eluting with a 2:1 mixture of petroleum ether to EtOAc to purify the product to give 837.1 mg 88.21% yield. $^1$H NMR: $\delta$ 1.18 (18H, s, C(C**H**$_3$)$_3$), 5.00 (1H, s, N**H**), 7.53-7-72 (4H, m, Ar**H**); $^{13}$C NMR: $\delta$ 27.37 (**C**(CH$_3$)$_3$, 30.36 (C(**C**H$_3$)$_3$), 52.21 (**C**NH), 76.49 (**C**C), 93.43 (C**C**), 120.85, 124.76, 129.93, 133.47, 133.90, 141.41 (Ar); DARTHRMS: Calcd for $C_{19}H_{23}NO_2S$ *m/z* 329.14495; found $[M + H]^+$ *m/z* 330.15426 (calcd *m/z* 330.15277).

**Synthesis of 3,3-bis(cyclopropylethynyl)-2,3-dihydro-2-methyl-1,2-benzisothiazole 1,1-dioxide (25-4)**

In a dry flask was dissolved 856.3 mg (2.880 mmol) of sultam **12-1** in dry $CH_3CN$. Once dissolved, the mixture was brought to 0 °C, whereupon 2.7962 g (2.987 equiv, 8.604 mmol) of $Cs_2CO_3$ was added to the solution, followed by dropwise addition of 0.90 mL (5.0 equiv, 14 mmol) of $CH_3I$. The reaction was stirred at 0 °C for 45 min, and the ice bath was removed to warm the mixture to room temperature for 3 h. The mixture was quenched with $NH_4Cl$ and extracted with EtOAc. The organic layer was washed with $H_2O$ (2 × 15 mL) and a wash of brine. The organic layer was dried with anhyd $MgSO_4$

and filtered. The organic solvent was rotary evaporated, and the product was purified on silica gel chromatography with an elution of 2:1 petroleum ether to EtOAc to give 845.7 mg (94.30 % yield). $^{1}$H NMR: $\delta$ 0.61-0.69 (4H, m, C**H**$_2$CHC**H**$_2$), 0.72-0.78 (4H, m, C**H**$_2$CHC**H**$_2$), 1.20-1.26 (2H, m, CH$_2$C**H**CH$_2$), 2.93, (3H, s, NC**H**$_3$), 7.52, (1H, t, Ar**H**), 7.62-7.71 (3H, m, Ar**H**); $^{13}$C NMR: $\delta$ -0.59 (CH$_2$**C**HCH$_2$), 8.48 (**C**H$_2$CHCH$_2$), 8.52 (CH$_2$CH**C**H$_2$), 25.02 (N**C**H$_3$) 56.32 (**C**NCH$_3$), 70.20 (**C**C), 89.70 (C**C**), 120.94, 124.66, 129.93, 132.70, 133.53, 138.66 (Ar); DARTHRMS: Calcd for $C_{18}H_{17}NO_2S$ *m/z* 311.39808; found $[M + H]^+$ *m/z* 312.10698 (calcd *m/z* 312.10582).

**Synthesis of 3,3-bis(cyclobutylethynyl)-2,3-dihydro-2-methyl-1,2-benzisothiazole 1,1-dioxide (25-5)**

In a dry flask was dissolved 89.4 mg (0.275 mmol) of sultam **12-2** in dry $CH_3CN$, and the solution was brought to 0 °C. At 0 °C, 134.4 mg of $Cs_2CO_3$ (1.503 equiv, 0.4135mmol) was added, followed by the dropwise addition of 0.10 mL (5.8 equiv, 1.6 mmol) of $CH_3I$. After 45 min of stirring at 0 °C, the ice bath was removed, and the mixture was stirred for 3 h at room temperature. The reaction was quenched with satd aq $NH_4Cl$ and washed with EtOAc. The organic layer was washed with $H_2O$ (2 $\times$ 15 mL) and a brine solution. The organic layer was dried with anhyd $MgSO_4$ and filtered. The organic solvent was rotary evaporated, and the product was purified on silica gel chromatography with an elution of 2:1 hexanes to EtOAc to give the desired product at 70.4 mg (75.4% yield). $^{1}$H NMR: $\delta$ 1.84-1.97 (4H, m, CH$_2$C**H**$_2$CH$_2$), 2.07-2.16 (4H, m, CHC**H**$_2$CH$_2$), 2.22-2.28 (4H, m, CHC**H**$_2$CH$_2$), 3.01 (3H, m, NC**H**$_3$), 3.04 (2H, quintet, *J* = 9.0 Hz CH$_2$C**H**CH$_2$), 7.57 (1H, t, *J* = 7.5 Hz, Ar**H**), 7.68 (1H, t, *J* = 7.5 Hz, Ar**H**), 7.74 (1H, d, *J* = 10.0 Hz, Ar**H**), 7.78 (1H, d, *J* = 10.0 Hz, Ar**H**); $^{13}$C NMR: $\delta$ 19.18

($CH_2$**C**$H_2CH_2$), 24.74 ($CH_2$**C**$HCH_2$), 25.08 (CN**C**$H_3$), 29.52 (CH**C**$H_2CH_2$), 56.47 (**C**$NCH_3$), 75.98 (**C**C), 90.07 (C**C**), 121.06, 124.69, 129.85, 132.82, 133.46, 138.93 (Ar) DARTHRMS: Calcd for $C_{20}H_{21}NO_2S$ *m/z* 339.12930; found $[M + H]^+$ *m/z* 340.13720 (calcd *m/z* 340.13712).

**Synthesis of 3,3-bis(*tert*-butylethynyl)-2,3-dihydro-2-methyl-1,2-benzisothiazole 1,1-dioxide (25-6)**

In a dry flask was dissolved 837.1 mg (2.541 mmol) of sultam **12-3** in dry $CH_3CN$. Once dissolved, the solution was brought to 0 °C, and 2.4916 g (3.0171, 7.6665 mmol) of $Cs_2CO_3$ was added to the solution, followed by the dropwise addition of 0.80 mL (5.1 equiv, 13 mmol) of $CH_3I$ to the solution. The mixture was stirred for 45 min at 0 °C, and the ice bath was removed allowing the reaction to warm to room temperature for 3 h. The reaction was quenched with satd aq $NH_4Cl$, and the mixture was extracted with EtOAc. The organic layer was washed with $H_2O$ (2 × 15 mL) and then a brine solution. The organic layer was separated, dried with anhyd $MgSO_4$, and filtered. The organic solvent was rotary evaporated, and the compound was purified on silica gel chromatography with an elution of 4:1 petroleum ether to EtOAc to give 749.0 mg (85.82% yield). $^1$H NMR: δ 0.61-0.71 (4H, m, C**H**$_2$CHC**H**$_2$), 0.72-0.79 (4H, m, C**H**$_2$CHC**H**$_2$), 1.20-1.26 (2H, m, $CH_2$C**H**$CH_2$), 2.93 (3H, s, NC**H**$_3$), 7.52 (1H, t, Ar**H**), 7.62-7.71 (3H, m, Ar**H**); $^{13}$C NMR: δ -0.59 ($CH_2$**C**$HCH_2$), 8.62 (**C**$H_2$CH**C**$H_2$), 25.00 (N**C**$H_3$), 56.27 (**C**$NCH_3$), 70.30 (**C**C), 89.74 (C**C**), 121.05, 124.53, 129.78, 132.41, 133.49, 138.75 (Ar); DARTHRMS: Calcd for $C_{20}H_{25}NO_2S$ *m/z* 343.48300; found $[M + H]^+$ *m/z* 344.17032 (calcd *m/z* 344.16842).

**5:2 Formic acid: triethylamine azeotrope**

A distillation apparatus was set up with a Vigreux column (15 cm) between the round-bottom flask and the distilling head, and a water condenser leading to a bent vacuum adapter with a bent dropper attached to a distillation cow. An approximate ratio of 5:2 molar mixture of 98% formic acid and triethylamine were poured into the round-bottom flask with triethylamine being poured first. The round-bottom flask was placed in a sand bath that was brought to approximately 200 °C. The first fraction to come off was triethylamine at 88 °C, followed by formic acid at 100.8 °C. The thermometer for some time showed a distillate at approximately 110 °C. Once this distillate was collected, the air condenser was removed, placing the still head directly on the round-bottom flask. As the temperature rose up to 190 °C, these fractions were collected separately. Once 190 °C was reached, the distillation cow was turned so that a clean collector would collect the azeotrope. The azeotrope was collected until either a change in temperature or before all liquid was distilled to prevent distilling to dry. An NMR spectrum was performed on the azeotrope to confirm the 5:2 ratio. The formyl H in formic acid has a shift at 8.25 ppm, and the triethylamine has the 3 $CH_2$ groups with a shift at 3.0 ppm, and the 3 $CH_3$ groups with a shift at 1.2 ppm. The integrations on these peaks were normalized so that the methyl groups integrated to 18.00, resulting in the $CH_2$ groups integrated to 12.13, and the formyl group integrated to 4.46.

# Literature Cited

1. Nevins, N.; Allinger, N. L. Molecular mechanics (MM4) vibrational frequency calculations for alkenes and conjugated hydrocarbons. *J. Comput. Chem.* **2004,** *17*, 730-746.
2. Gallo, R. C. Viewpoint: Historical essay: The early years of HIV/AIDS. *Science (Washington, DC, United States)* **2002,** *298*, 1728-1730.
3. Gallo, R. C. HIV-1: A look back from 20 years. *DNA and Cell Biology* **2004,** *23*, 191-192.
4. Cramer, R. D. R-group template CoMFA combines benefits of "ad hoc" and topomer alignments using 3D-QSAR for lead optimization. *J. Comput.-Aided Mol. Des.* **2012,** *26*, 805-819.
5. Gallo, R. C. Human retroviruses after 20 years: a perspective from the past and prospects for their future control. *Immunol. Rev.* **2002,** *185*, 236-265.
6. Barre-Sinoussi, F.; Chermann, J. C.; Rey, F.; Nugeyre, M. T.; Chamaret, S.; Gruest, J.; Dauguet, C.; Axler-Blin, C.; Vezinet-Brun, F.; Rouzioux, C.; Rozenbaum, W.; Montagnier, L. Isolation of a T-lymphotropic retrovirus from a patient at risk for acquired immune deficiency syndrome (AIDS). *Science* **1983,** *220*, 868-71.
7. Safai, B.; Sarngadharan, M. G.; Groopman, J. E.; Arnett, K.; Popovic, M.; Sliski, A.; Schupbach, J.; Gallo, R. C. Seroepidemiological studies of human T-lymphotropic retrovirus type III in acquired immunodeficiency syndrome. *Lancet* **1984,** *1*, 1438-40.
8. Sarngadharan, M. G.; Popovic, M.; Bruch, L.; Schupbach, J.; Gallo, R. C. Antibodies reactive with human T-lymphotropic retroviruses (HTLV-III) in the serum of patients with AIDS. *Science* **1984,** *224*, 506-8.
9. Mitsuya, H.; Weinhold, K. J.; Furman, P. A.; St. Clair, M. H.; Lehrman, S. N.; Gallo, R. C.; Bolognesi, D.; Barry, D. W.; Broder, S. 3'-Azido-3'-deoxythymidine (BW A509U): an antiviral agent that inhibits the infectivity and cytopathic effect of human T-lymphotropic virus type III/lymphadenopathy-associated virus in vitro. *Proc. Natl. Acad. Sci. U. S. A.* **1985,** *82*, 7096-100.
10. Sharp, P. M.; Bailes, E.; Gao, F.; Beer, B. E.; Hirsch, V. M.; Hahn, B. H. Origins and evolution of AIDS viruses: estimating the time-scale. *Biochem. Soc. Trans.* **2000,** *28*, 275-282.
11. Schupbach, J.; Gallo, R. C. Human retroviruses. *Clin. Virol. Man. (3rd Ed.)* **2000**, 513-560.
12. Keele, B. F.; Van Heuverswyn, F.; Li, Y.; Bailes, E.; Takehisa, J.; Santiago, M. L.; Bibollet-Ruche, F.; Chen, Y.; Wain, L. V.; Liegeois, F.; Loul, S.; Ngole, E. M.; Bienvenue, Y.; Delaporte, E.; Brookfield, J. F. Y.; Sharp, P. M.; Shaw, G. M.; Peeters, M.; Hahn, B. H. Chimpanzee Reservoirs of Pandemic and Nonpandemic HIV-1. *Science (Washington, DC, United States)* **2006,** *313*, 523-526.
13. Mulder, C. Human AIDS virus not from monkeys. *Nature* **1988,** *333*, 396.
14. Sharp, P. M.; Hahn, B. H. The evolution of HIV-1 and the origin of AIDS. *Philos. Trans. R. Soc., B* **2010,** *365*, 2487-2494.
15. Cramer Richard, D. R-group template CoMFA combines benefits of "ad hoc" and topomer alignments using 3D-QSAR for lead optimization. *J. Comput. Aided Mol. Des.* **2012,** *26*, 805-19.

16. Hallenberger, S.; Bosch, V.; Angliker, H.; Shaw, E.; Klenk, H. D.; Garten, W. Inhibition of furin-mediated cleavage activation of HIV-1 glycoprotein gp160. *Nature (London, United Kingdom)* **1992,** *360*, 358-61.
17. Markovic, I. Advances in HIV-1 entry inhibitors: strategies to interfere with receptor and coreceptor engagement. *Curr. Pharm. Des.* **2006,** *12*, 1105-1119.
18. Kashid, A. M.; Murumkar, P. R.; Dube, P. N.; Alkutkar, P. G.; Bhatia, M. S.; Dhawale, S. C. Antiretroviral drugs: a perspective. *J. Pharm. Res.* **2012,** *5*, 2837-2845.
19. Katz, R. A.; Skalka, A. M. The retroviral enzymes. *Annu. Rev. Biochem.* **1994,** *63*, 133-73.
20. Sarafianos, S. G.; Marchand, B.; Das, K.; Himmel, D. M.; Parniak, M. A.; Hughes, S. H.; Arnold, E. Structure and function of HIV-1 reverse transcriptase: Molecular mechanisms of polymerization and inhibition. *J. Mol. Biol.* **2009,** *385*, 693-713.
21. Restle, T.; Mueller, B.; Goody, R. S. Dimerization of human immunodeficiency virus type 1 reverse transcriptase. A target for chemotherapeutic intervention. *J. Biol. Chem.* **1990,** *265*, 8986-8.
22. Le Grice, S. F. J.; Naas, T.; Wohlgensinger, B.; Schatz, O. Subunit-selective mutagenesis indicates minimal polymerase activity in heterodimer-associated p51 HIV-1 reverse transcriptase. *EMBO J.* **1991,** *10*, 3905-11.
23. Jonckheere, H.; Anne, J.; De Clercq, E. The HIV-1 reverse transcription (RT) process as target for RT inhibitors. *Med. Res. Rev.* **2000,** *20*, 129-154.
24. Liu, S.; Harada, B. T.; Miller, J. T.; Le Grice, S. F. J.; Zhuang, X. Initiation complex dynamics direct the transitions between distinct phases of early HIV reverse transcription. *Nat. Struct. Mol. Biol.* **2010,** *17*, 1453-1460.
25. Puglisi, E. V.; Puglisi, J. D. Secondary structure of the HIV reverse transcription initiation complex by NMR. *J. Mol. Biol.* **2011,** *410*, 863-874.
26. Kohlstaedt, L. A.; Wang, J.; Friedman, J. M.; Rice, P. A.; Steitz, T. A. Crystal Structure at 3.5 Angstrom Resolution of HIV-1 Reverse Transcriptase Complexed with an Inhibitor. *Science* **1992,** *256*, 1783-1790.
27. Sarafianos, S. G.; Das, K.; Tantillo, C.; Clark, A. D., Jr.; Ding, J.; Whitcomb, J. M.; Boyer, P. L.; Hughes, S. H.; Arnold, E. Crystal structure of HIV-1 reverse transcriptase in complex with a polypurine tract RNA:DNA. *EMBO J.* **2001,** *20*, 1449-1461.
28. Jacobo-Molina, A.; Ding, J.; Nanni, R. G.; Clark, A. D., Jr.; Lu, X.; Tantillo, C.; Williams, R. L.; Kamer, G.; Ferris, A. L.; Clark, P.; et al. Crystal structure of human immunodeficiency virus type 1 reverse transcriptase complexed with double-stranded DNA at 3.0 A resolution shows bent DNA. *Proc Natl Acad Sci U S A* **1993,** *90*, 6320-4.
29. Rodgers, D. W.; Gamblin, S. J.; Harris, B. A.; Culp, J. S.; Hellmig, B.; Woolf, D. J.; Debouck, C.; Harrison, S. C.; Ray, S. The structure of unliganded reverse transcriptase from the human immunodeficiency virus type 1. *Proc. Natl. Acad. Sci. U. S. A.* **1995,** *92*, 1222-6.
30. Hindmarsh, P.; Leis, J. Retroviral DNA integration. *Microbiol. Mol. Biol. Rev.* **1999,** *63*, 836-843.
31. Craigie, R. HIV integrase, a brief overview from chemistry to therapeutics. *J. Biol. Chem.* **2001,** *276*, 23213-23216.

32. Gale, M., Jr.; Tan, S.-L.; Katze, M. G. Translational control of viral gene expression in eukaryotes. *Microbiol. Mol. Biol. Rev.* **2000,** *64*, 239-280.
33. Pettit, S. C.; Simsic, J.; Loeb, D. D.; Everitt, L.; Hutchison, C. A., III; Swanstrom, R. Analysis of retroviral protease cleavage sites reveals two types of cleavage sites and the structural requirements of the P1 amino acid. *J. Biol. Chem.* **1991,** *266*, 14539-47.
34. Kaplan, A. H.; Zack, J. A.; Knigge, M.; Paul, D. A.; Kempf, D. J.; Norbeck, D. W.; Swanstrom, R. Partial inhibition of the human immunodeficiency virus type 1 protease results in aberrant virus assembly and the formation of noninfectious particles. *J. Virol.* **1993,** *67*, 4050-5.
35. Arasappan, A.; Njoroge, F. G.; Girijavallabhan, V. M. Preparation of prolyl peptides as inhibitors of hepatitis C virus NS3 serine protease. 2005-US17401 2005113581, 20050518., 2005.
36. Healy, M. Government shuts down HIV/AIDS vaccine trial. *Los Angeles Times* 2013.
37. Bell, T. W.; Demillo, V. G.; Schols, D.; Vermeire, K. Improving potencies and properties of CD4 down-modulating CADA analogs. *Expert Opinion on Drug Discovery* **2012,** *7*, 39-48.
38. Demillo, V. G.; Goulinet-Mateo, F.; Kim, J.; Schols, D.; Vermeire, K.; Bell, T. W. Unsymmetrical Cyclotriazadisulfonamide (CADA) Compounds as Human CD4 Receptor Down-Modulating Agents. *J. Med. Chem.* **2011,** *54*, 5712-5721.
39. Vermeire, K.; Bell, T. W.; Choi, H.-J.; Jin, Q.; Samala, M. F.; Sodoma, A.; De Clercq, E.; Schols, D. The anti-HIV potency of cyclotriazadisulfonamide analogs is directly correlated with their ability to down-modulate the CD4 receptor. *Mol. Pharmacol.* **2003,** *63*, 203-210.
40. Vermeire, K.; Schols, D.; Bell, T. W. CD4 down-modulating compounds with potent anti-HIV activity. *Curr. Pharm. Des.* **2004,** *10*, 1795-1803.
41. Vermeire, K.; Princen, K.; Hatse, S.; de Clercq, E.; Dey, K.; Bell, T. W.; Schols, D. CADA, a novel CD4-targeted HIV inhibitor, is synergistic with various anti-HIV drugs in vitro. *AIDS (London, United Kingdom)* **2004,** *18*, 2115-2125.
42. Francois, K. O.; Balzarini, J. Potential of carbohydrate-binding agents as therapeutics against enveloped viruses. *Med. Res. Rev.* **2012,** *32*, 349-387.
43. Boyd, M. R.; Gustafson, K. R.; McMahon, J. B.; Shoemaker, R. H.; O'Keefe, B. R.; Mori, T.; Gulakowski, R. J.; Wu, L.; Rivera, M. I.; Laurencot, C. M.; Currens, M. J.; Cardellina, J. H., II; Buckheit, R. W., Jr.; Nara, P. L.; Pannell, L. K.; Sowder, R. C., II; Henderson, L. E. Discovery of cyanovirin-N, a novel human immunodeficiency virus-inactivating protein that binds viral surface envelope glycoprotein gp120: potential applications to microbicide development. *Antimicrob. Agents Chemother.* **1997,** *41*, 1521-1530.
44. Mori, T.; O'Keefe, B. R.; Sowder, R. C., II; Bringans, S.; Gardella, R.; Berg, S.; Cochran, P.; Turpin, J. A.; Buckheit, R. W., Jr.; McMahon, J. B.; Boyd, M. R. Isolation and Characterization of Griffithsin, a Novel HIV-inactivating Protein, from the Red Alga Griffithsia sp. *J. Biol. Chem.* **2005,** *280*, 9345-9353.
45. Xue, J.; Gao, Y.; Hoorelbeke, B.; Kagiampakis, I.; Zhao, B.; Demeler, B.; Balzarini, J.; LiWang, P. J. The Role of Individual Carbohydrate-Binding Sites in the

Function of the Potent Anti-HIV Lectin Griffithsin. *Mol. Pharmaceutics* **2012,** *9*, 2613-2625.
46. Guo, Q.; Ho, H.-T.; Dicker, I.; Fan, L.; Zhou, N.; Friborg, J.; Wang, T.; McAuliffe, B. V.; Wang, H.-g. H.; Rose, R. E.; Fang, H.; Scarnati, H. T.; Langley, D. R.; Meanwell, N. A.; Abraham, R.; Colonno, R. J.; Lin, P.-f. Biochemical and genetic characterizations of a novel human immunodeficiency virus type 1 inhibitor that blocks gp120-CD4 interactions. *J. Virol.* **2003,** *77*, 10528-10536.
47. Lin, P.-F.; Blair, W.; Wang, T.; Spicer, T.; Guo, Q.; Zhou, N.; Gong, Y.-F.; Wang, H. G. H.; Rose, R.; Yamanaka, G.; Robinson, B.; Li, C.-B.; Fridell, R.; Deminie, C.; Demers, G.; Yang, Z.; Zadjura, L.; Meanwell, N.; Colonno, R. A small molecule HIV-1 inhibitor that targets the HIV-1 envelope and inhibits CD4 receptor binding. *Proc. Natl. Acad. Sci. U. S. A.* **2003,** *100*, 11013-11018.
48. Makinson, A.; Reynes, J. The fusion inhibitor enfuvirtide in recent antiretroviral strategies. *Curr Opin HIV AIDS* **2009,** *4*, 150-8.
49. Sax Paul, E.; DeJesus, E.; Mills, A.; Zolopa, A.; Cohen, C.; Wohl, D.; Gallant Joel, E.; Liu Hui, C.; Zhong, L.; Yale, K.; White, K.; Kearney Brian, P.; Szwarcberg, J.; Quirk, E.; Cheng Andrew, K. Co-formulated elvitegravir, cobicistat, emtricitabine, and tenofovir versus co-formulated efavirenz, emtricitabine, and tenofovir for initial treatment of HIV-1 infection: a randomised, double-blind, phase 3 trial, analysis of results after 48 weeks. *Lancet* **2012,** *379*, 2439-48.
50. Chermann, J. C.; Barre-Sinoussi, F.; Dauguet, C.; Brun-Vezinet, F.; Rouzioux, C.; Rozenbaum, W.; Montagnier, L. *Isolation of a new retrovirus in a patient at risk for acquired immunodeficiency syndrome*; Switzerland FIELD Citation:, 1983; pp 48-53.
51. Rathbun, R. C.; Lockhart, S. M.; Stephens, J. R. Current HIV treatment guidelines - an overview. *Curr. Pharm. Des.* **2006,** *12*, 1045-1063.
52. Mehellou, Y.; De Clercq, E. Twenty-Six Years of Anti-HIV Drug Discovery: Where Do We Stand and Where Do We Go? *J. Med. Chem.* **2010,** *53*, 521-538.
53. Schaefer, W.; Friebe, W. G.; Leinert, H.; Mertens, A.; Poll, T.; Von der Saal, W.; Zilch, H.; Nuber, B.; Ziegler, M. L. Non-nucleoside inhibitors of HIV-1 reverse transcriptase: molecular modeling and x-ray structure investigations. *J. Med. Chem.* **1993,** *36*, 726-32.
54. Balzarini, J. Current status of the non-nucleoside reverse transcriptase inhibitors of human immunodeficiency virus type 1. *Curr. Top. Med. Chem. (Sharjah, United Arab Emirates)* **2004,** *4*, 921-944.
55. Auwerx, J.; Stevens, M.; Van Rompay, A. R.; Bird, L. E.; Ren, J.; De Clercq, E.; Oeberg, B.; Stammers, D. K.; Karlsson, A.; Balzarini, J. The phenylmethylthiazolylthiourea nonnucleoside reverse transcriptase (RT) inhibitor MSK-076 selects for a resistance mutation in the active site of human immunodeficiency virus type 2 RT. *J. Virol.* **2004,** *78*, 7427-7437.
56. Young, S. D. Non-nucleoside inhibitors of HIV-1 reverse transcriptase. *Perspect. Drug Discovery Des.* **1993,** *1*, 181-92.
57. Debyser, Z.; Pauwels, R.; Andries, K.; Desmyter, J.; Kukla, M.; Janssen, P. A. J.; De Clercq, E. An antiviral target on reverse transcriptase of human immunodeficiency virus type 1 revealed by tetrahydroimidazo[4,5,1-jk][1,4]benzodiazepin-2(1H)-one and -thione derivatives. *Proc. Natl. Acad. Sci. U. S. A.* **1991,** *88*, 1451-5.

58. de Bethune, M.-P. Non-nucleoside reverse transcriptase inhibitors (NNRTIs), their discovery, development, and use in the treatment of HIV-1 infection: A review of the last 20 years (1989-2009). *Antiviral Res.* **2010,** *85*, 75-90.
59. Baba, M.; Tanaka, H.; De Clercq, E.; Pauwels, R.; Balzarini, J.; Schols, D.; Nakashima, H.; Perno, C. F.; Walker, R. T.; Miyasaka, T. Highly specific inhibition of human immunodeficiency virus type 1 by a novel 6-substituted acyclouridine derivative. *Biochem. Biophys. Res. Commun.* **1989,** *165*, 1375-81.
60. De Clercq, E. Non-nucleoside reverse transcriptase inhibitors (NNRTIs): past, present, and future. *Chem. Biodiversity* **2004,** *1*, 44-64.
61. Deng, B.-L. C., M. D.; Zhou, Z.; Hartman, T. L.; Buckheit, R. W.; Pannecouque, C.; De Clercq, E.; Fanwick, P. E.; Cushman, M. Synthesis and anti-HIV activity of new alkenyldiarylmethane (ADAM) non-nucleoside reverse transcriptase inhibitors (NNRTIs) incorporating benzoxazolone and benzisoxazole rings. *Bioorg. Med. Chem.* **2006,** *14*, 2366-2374.
62. Esnouf, R. M.; Ren, J.; Ross, C.; Jones, E. Y.; Stammers, D. K.; Stuart, D. I. Mechanism of inhibition of HIV-1 reverse transcriptase by non-nucleoside inhibitors. *Nat. Struct. Bio.* **1995,** *2*, 303-308.
63. Balzarini, J. Strategies to suppress resistance to drugs targeted at human immunodeficiency virus reverse transcriptase by combination therapy. *Commentary. Biochem. Pharmacol.* **1999,** *58*, 1-27.
64. De Clercq, E. The role of non-nucleoside reverse transcriptase inhibitors (NNRTIs) in the therapy of HIV-1 infection. *Antiviral Res.* **1998,** *38*, 153-179.
65. Battegay, M.; Bucher Heiner, C. Antiretroviral monotherapy: should we abandon the principles of successful antiretroviral therapy? *AIDS (London, England)* **2010,** *24*, 1057-9.
66. Gussio, R.; Pattabiraman, N.; Zaharevitz, D. W.; Kellogg, G. E.; Topol, I. A.; Rice, W. G.; Schaeffer, C. A.; Erickson, J. W.; Burt, S. K. All-atom models for the non-nucleoside binding site of HIV-1 reverse transcriptase complexed with inhibitors: A 3D QSAR approach. *J. Med. Chem.* **1996,** *39*, 1645-1650.
67. Zaharevitz, D. W.; Gussio, R.; Wiegand, A.; Jalluri, R.; Nagarauan, P.; Kellogg, G. E.; Pallansch, L. A.; Yang, S. S.; Buckheit Jr., R. W. Discovery of Novel HIV-1 Reverse Transcriptase Inhibitors Using a Combination of 3D Database Searching and 3D QSAR. *Med. Chem. Res.* **1999,** *9*, 551-564.
68. Watanabe, H.; Gay, R. L.; Hauser, C. R. *ortho* Metalation of N-Substituted Benzenesulfonamides by Excess n- Butyllithium. Condensation with Carbonyl Compounds. Cyclizations. *J. Org. Chem.* **1967,** *33*, 900-902.
69. Baker, D. C.; Mayasundari, A.; Mao, J.; Johnson, S. C.; Yan, S. Methods of synthesizing sultams and anti-viral compositions. 1999-US16240 2000004004, 19990716., 2000.
70. Baker, D. C.; Mayasundari, A.; Mao, J.; Johnson, S. C.; Yan, S. Preparation of sultams having antiviral and especially anti-HIV-1 activity. 1999-353900 6562850, 19990715., 2003.
71. Mao, J.; Baker, D. C. Preparation of arylsultams as HIV reverse transcriptase inhibitors. 2000-US7892 2000056332, 20000324., 2000.

72. LeCroix, B. C. M., J.; Riyam, K.; Johnson, S.; Mayasundari, A; Yan, S.; Rowe, A.; Naramore, R.; Baker, D.C. Work Unpublished. In.
73. Wright, J. B. The Preparation of 2H-1,2,3-Benzothiadiazine-1,1-dioxides, 11H-11,11a-dihydrobenzimdazo [1,2-b] [1,2]benzisothiazole-5,5-dioxides, 6H-dibenzo [c,g] [1,2,5]thiadiazocine-5,5-dioxides and 5H-dibenzo [c,g] [1,2,6] thiadiazocine-6,6-dioxides. *J. Heterocycl. Chem* **1968,** *5*, 453-459.
74. Abramovitch, R. A.; Smith, E. M.; Humber, M.; Purtschert, B.; Srinivasan, P. C.; Singer, G. M. 1,2-Benzisothiazole 1,1-dioxides. Synthesis of 3-Alkyl-(or Aryl-)1,2-benzisothizole 1,1-dioxides and Related Compounds. *J. Chem. Soc. [Perkin. 1].* **1974**, 2589-2594.
75. Noyori, R.; Hashiguchi, S. Asymmetric Transfer Hydrogenation Catalyzed by Chiral Ruthenium Complexes. *Acc. Chem. Res.* **1997,** *30*, 97-102.
76. Uematsu, N.; Fujii, A.; Hashiguchi, S.; Ikariya, T.; Noyori, R. Asymmetric transfer hydrogenation of imines. *J. Am. Chem. Soc.* **1996,** *118*, 4916-4917.
77. Stinson, S. C. Fine Chemicals Face Challenges. *C & E News* **1998**, 15-24.
78. Mao, J.; Baker, D. C. A Chiral Rhodium Complex for Rapid Asymmetric Transfer Hydrogenation of Imines with High Enantioselectivity. *Org. Lett.* **1999,** *1*, 841-843.
79. Kafri, R. Design and Synthesis of Novel Sultams: A Family of Non-Nucleoside Reverse Transcriptase Inhibitors and Modeling Studies of a Rhodium Catalyst. University of Tennessee, University of Tennessee, 2007.
80. Mager, P. P. A check on rational drug design: molecular simulation of the allosteric inhibition of HIV-1 reverse transcriptase. *Med. Res. Rev.* **1997,** *17*, 235-276.
81. Cramer, R. D.; Patterson, D. E.; Bunce, J. D. Comparative molecular field analysis (CoMFA). 1. Effect of shape on binding of steroids to carrier proteins. *J. Am. Chem. Soc.* **1988,** *110*, 5959-67.
82. Cramer, R. D., III; Patterson, D. E.; Bunce, J. D. Comparative molecular field analysis (CoMFA). 1. Effect of shape on binding of steroids to carrier proteins. *J. Am. Chem. Soc.* **1988,** *110*, 5959-67.
83. Allinger, N. L.; Chen, K.; Lii, J.-H. An improved force field (MM4) for saturated hydrocarbons. *J. Comput. Chem.* **1996,** *17*, 642-68.
84. Allinger, N. L.; Chen, K.; Katzenellenbogen, J. A.; Wilson, S. R.; Anstead, G. M. Hyperconjugative effects on carbon-carbon bond lengths in molecular mechanics (MM4). *J. Comput. Chem.* **1996,** *17*, 747-55.
85. Nevins, N.; Lii, J.-H.; Allinger, N. L. Molecular mechanics (MM4) calculations on conjugated hydrocarbons. *J. Comput. Chem.* **2004,** *17*, 695-729.
86. Gasteiger, J.; Marsili, M. Iterative partial equalization of orbital electronegativity: a rapid access to atomic charges. *Tetrahedron* **1980,** *36*, 3219-22.
87. Beans, E. J.; Fournogerakis, D.; Gauntlett, C.; Heumann, L. V.; Kramer, R.; Marsden, M. D.; Murray, D.; Chun, T.-W.; Zack, J. A.; Wender, P. A. Highly potent, synthetically accessible prostratin analogs induce latent HIV expression in vitro and ex vivo. *Proceedings of the National Academy of Sciences of the United States of America, Early Edition* **2013**, 1-6, 6 pp.
88. Sharma, B. Anti-HIV-1 drug toxicity and management strategies. *Neurobehavioral HIV Medicine* **2011,** *3*, 27-40.

89. Differding, E.; Lang, R. W. New fluorinating reagents. Part II. Preparation and synthetic application of a saccharin-derived N-fluorosultam. *Helv. Chim. Acta* **1989,** *72*, 1248-52.
90. Ma, S.; He, Q. The cyclopropyl effect on the regioselectivity of coupling reactions involving the lithiation of 1-cyclopropyl-2-arylacetylenes. *Tetrahedron* **2006,** *62*, 2769-2778.
91. Gemal, A. L.; Luche, J. L. Lanthanoids in organic synthesis. 6. Reduction of α-enones by sodium borohydride in the presence of lanthanoid chlorides: synthetic and mechanistic aspects. *J. Am. Chem. Soc.* **1981,** *103*, 5454-9.
92. Almeida, L.; Ioannidis, S.; Lamb, M.; Su, M. Preparation of pyrazolyl-amino-substituted pyrazines for treatment of cancer. 2008-GB1046 2008117050, 20080326., 2008.
93. Gospodarowicz, K.; Holynska, M.; Paluch, M.; Lisowski, J. Novel chiral hexaazamacrocycles for the enantiodiscrimination of carboxylic acids. *Tetrahedron* **2012,** *68*, 9930-9935.
94. Backes, B. J.; Ellman, J. A. An Alkanesulfonamide "Safety-Catch" Linker for Solid-Phase Synthesis. *J. Org. Chem.* **1999,** *64*, 2322-2330.
95. Marcaurelle, L. A.; Bertozzi, C. R. Recent advances in the chemical synthesis of mucin-like glycoproteins. *Glycobiology* **2002,** *12*, 69R-77R.
96. Mende, F.; Seitz, O. 9-Fluorenylmethoxycarbonyl-Based Solid-Phase Synthesis of Peptide α-Thioesters. *Angew. Chem. Int. Ed. Engl.* **2011,** *50*, 1232-1240.
97. Oppolzer, W.; Rodriguez, I.; Starkemann, C.; Walther, E. Chiral toluene-2,α-sultam auxiliaries: asymmetric alkylations, acylations and aldolizations of N-acyl derivatives. *Tetrahedron Lett.* **1990,** *31*, 5019-22.
98. Kulkarni, N. A.; Yao, C.-F.; Chen, K. On the scope of diastereoselective allylation of various chiral glyoxylic oxime ethers with allyltributylstannane in the presence of a Lewis acid and triallylaluminum. *Tetrahedron* **2007,** *63*, 7816-7822.
99. Isleyen, A.; Gonsky, C.; Ronald, R. C.; Garner, P. Efficacious preparation of Oppolzer's glycylsultam via the Delepine reaction. *Synthesis* **2009**, 1261-1264.
100. Liu, Z.; Mehta, S. J.; Hruby, V. J. Strategies for Asymmetric Synthesis of Amino Acids with γ,δ-Unsaturation. *Organic Preparations and Procedures International* **2012,** *44*, 222-255.
101. Oppolzer, W.; Moretti, R.; Thomi, S. Asymmetric alkylations of a sultam-derived glycinate equivalent: practical preparation of enantiomerically pure α-amino acids. *Tetrahedron Lett.* **1989,** *30*, 6009-10.
102. Josien, H.; Lavielle, S.; Brunissen, A.; Saffroy, M.; Torrens, Y.; Beaujouan, J.-C.; Glowinski, J.; Chassaing, G. Design and Synthesis of Side-Chain Conformationally Restricted Phenylalanines and Their Use for Structure-Activity Studies on Tachykinin NK-1 Receptor. *J. Med. Chem.* **1994,** *37*, 1586-601.
103. Basha, A.; Lipton, M.; Weinreb, S. M. A mild, general method for conversion of esters to amides. *Tetrahedron Lett.* **1977**, 4171-4.
104. Noyori, R.; Tomino, I.; Tanimoto, Y.; Nishizawa, M. Asymmetric synthesis via axially dissymmetric molecules. 6. Rational designing of efficient chiral reducing agents. Highly enantioselective reduction of aromatic ketones by binaphthol-modified lithium aluminum hydride reagents. *J. Am. Chem. Soc.* **1984,** *106*, 6709-16.

105. Hutchins, R. O.; Abdel-Magid, A.; Stercho, Y. P.; Wambsgans, A. Asymmetric reduction of phosphinyl imines with hydride reagents. Enantioselective synthesis of chiral primary amines. *J. Org. Chem.* **1987,** *52*, 702-4.
106. Haskel, A.; Keinan, E. TPM: a new protecting group for alkynes. *Tetrahedron Lett.* **1999,** *40*, 7861-7865.
107. Hayashi, Y.; Yamaguchi, H.; Toyoshima, M.; Okado, K.; Toyo, T.; Shoji, M. Formal Total Synthesis of Fostriecin by 1,4-Asymmetric Induction with an Alkyne-Cobalt Complex. *Chem.--Eur. J.* **2010,** *16*, 10150-10159, S10150/1-S10150/134.
108. Greenfield, H.; Sternberg, H. W.; Friedel, R. A.; Wotiz, J. H.; Markby, R.; Wender, I. Acetylenic dicobalt hexacarbonyls. Organometallic compounds derived from alkynes and dicobalt octacarbonyl. *J. Am. Chem. Soc.* **1956,** *78*, 120-4.
109. Helal, C. J.; Magriotis, P. A.; Corey, E. J. Direct Catalytic Enantioselective Reduction of Achiral α,β-Ynones. Strong Remote Steric Effects Across the C-C Triple Bond. *J. Am. Chem. Soc.* **1996,** *118*, 10938-10939.
110. Lumbroso, A.; Cooke, M. L.; Breit, B. Catalytic Asymmetric Synthesis of Allylic Alcohols and Derivatives and their Applications in Organic Synthesis. *Angew. Chem. Int. Ed. Engl.* **2013,** *52*, 1890-1932.
111. Charette, A. B.; Francoeur, S.; Martel, J.; Wilb, N. New family of cyclopropanating reagents: synthesis, reactivity, and stability studies of iodomethylzinc phenoxides. *Angew. Chem. Int. Ed. Engl.* **2000,** *39*, 4539-4542.
112. Schaumberg, J. P.; Hokanson, G. C.; French, J. C.; Smal, E.; Baker, D. C. 2'-Chloropentostatin, a new inhibitor of adenosine deaminase. *J. Org. Chem.* **1985,** *50*, 1651-6.
113. Pirrung, M. C. *The Synthetic Organic Chemists' Companion*. 2007; p 198 pp.
114. Frija, L. M. T.; Fausto, R.; Loureiro, R. M. S.; Cristiano, M. L. S. Synthesis and structure of novel benzisothiazole-tetrazolyl derivatives for potential application as nitrogen ligands. *J. Mol. Catal. A Chem.* **2009,** *305*, 142-146.

# Appendix

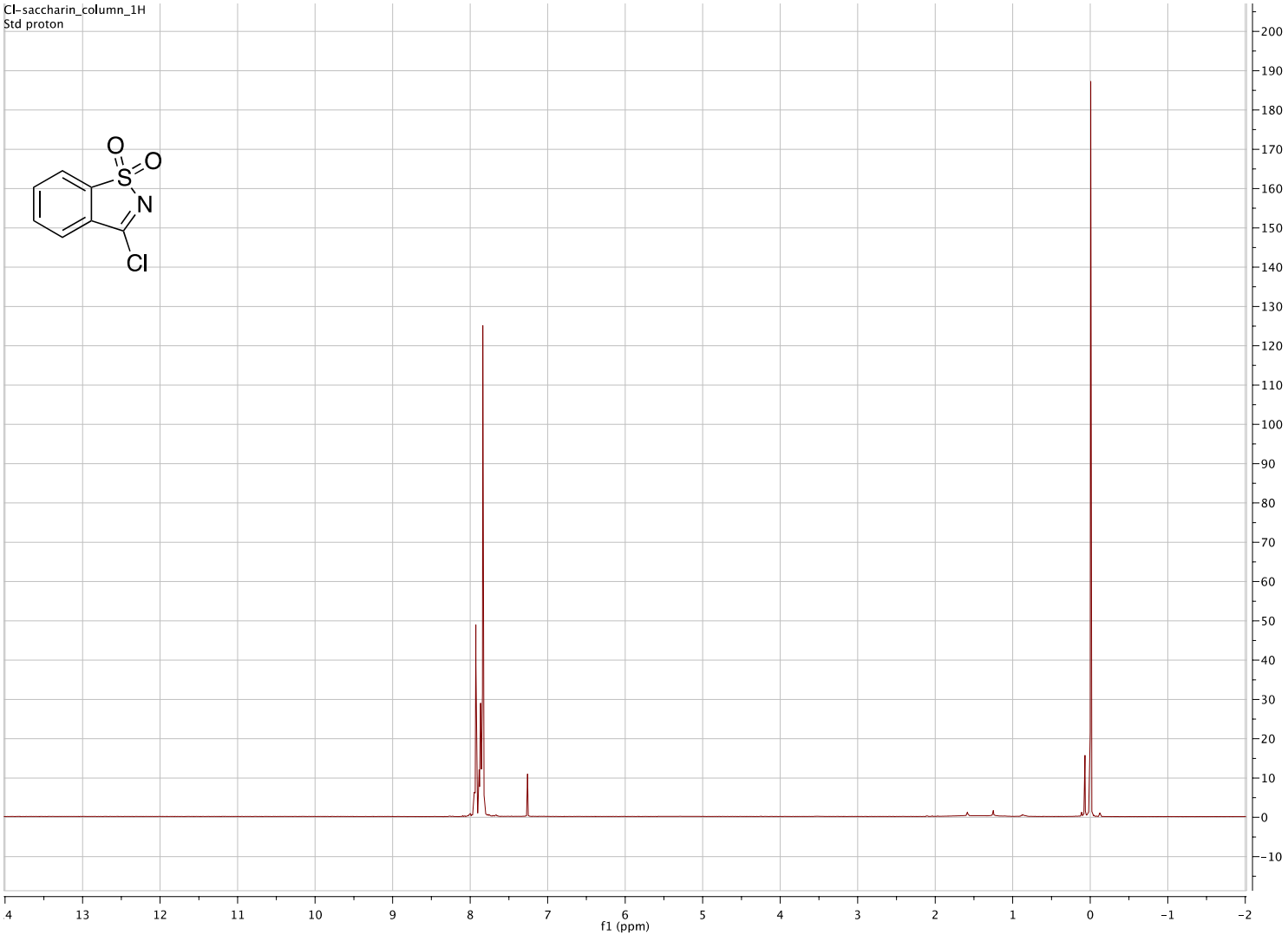


$^{1}$H NMR (500 MHz, $CDCl_3$) of 3-chloro-1,2-benzisothiazole 1,1-dioxide

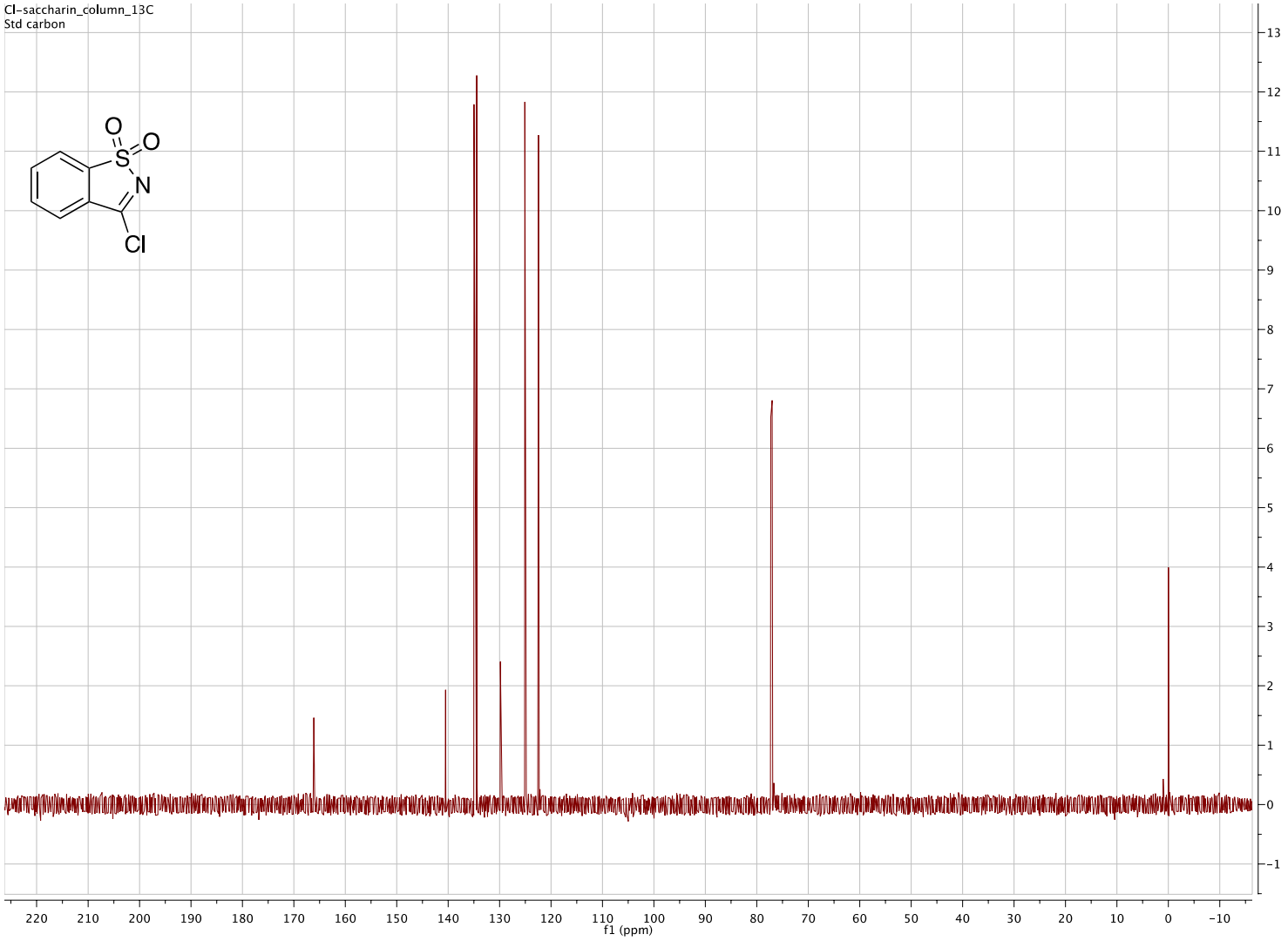


$^{13}C$ NMR (500 MHz, $CDCl_3$) of 3-chloro-1,2-benzisothiazole 1,1-dioxide

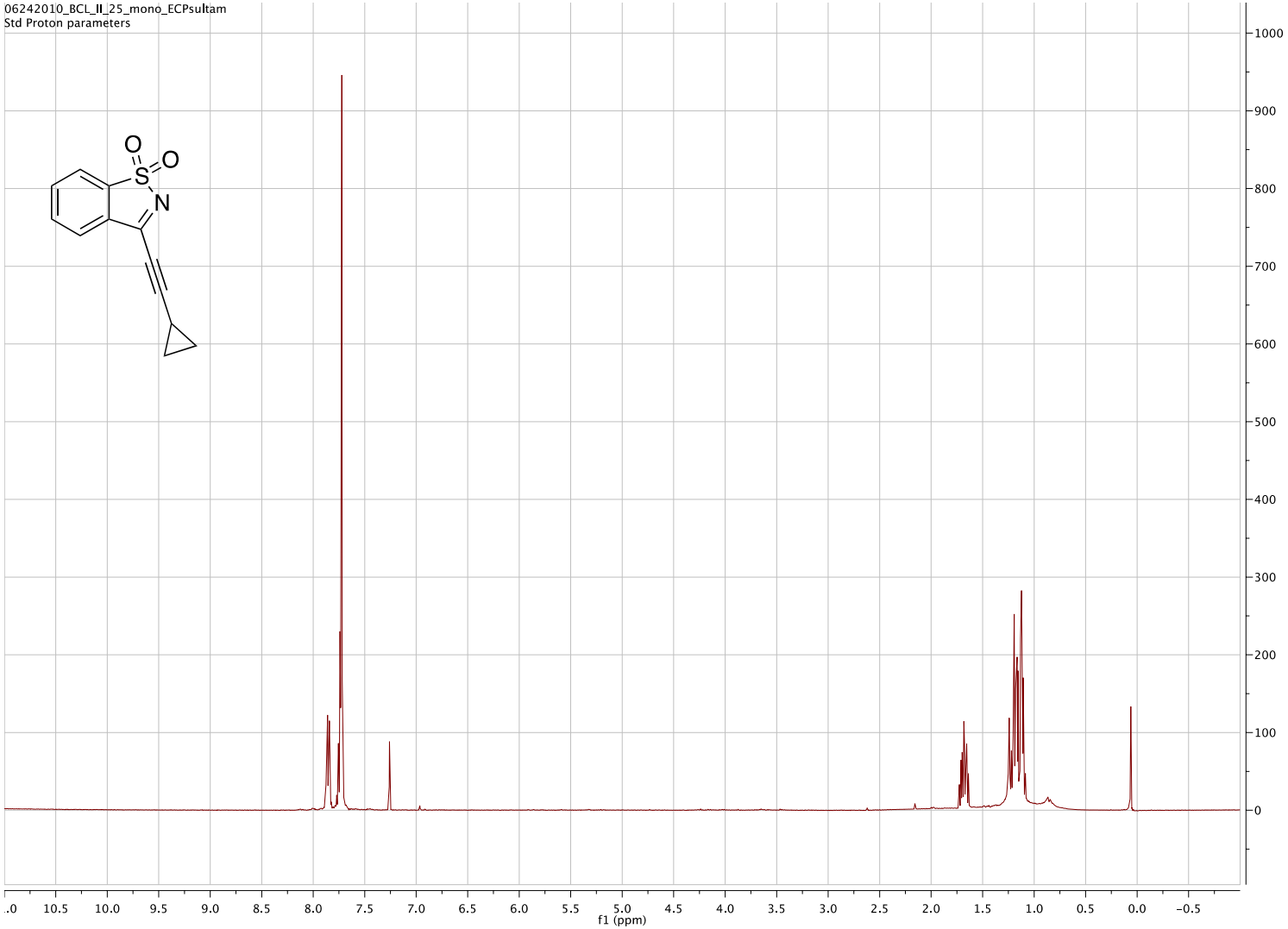


$^{1}$H NMR (500 MHz, $CDCl_3$) of 3-cyclopropylethynyl-1,2-benzisothiazole 1,1-dioxide

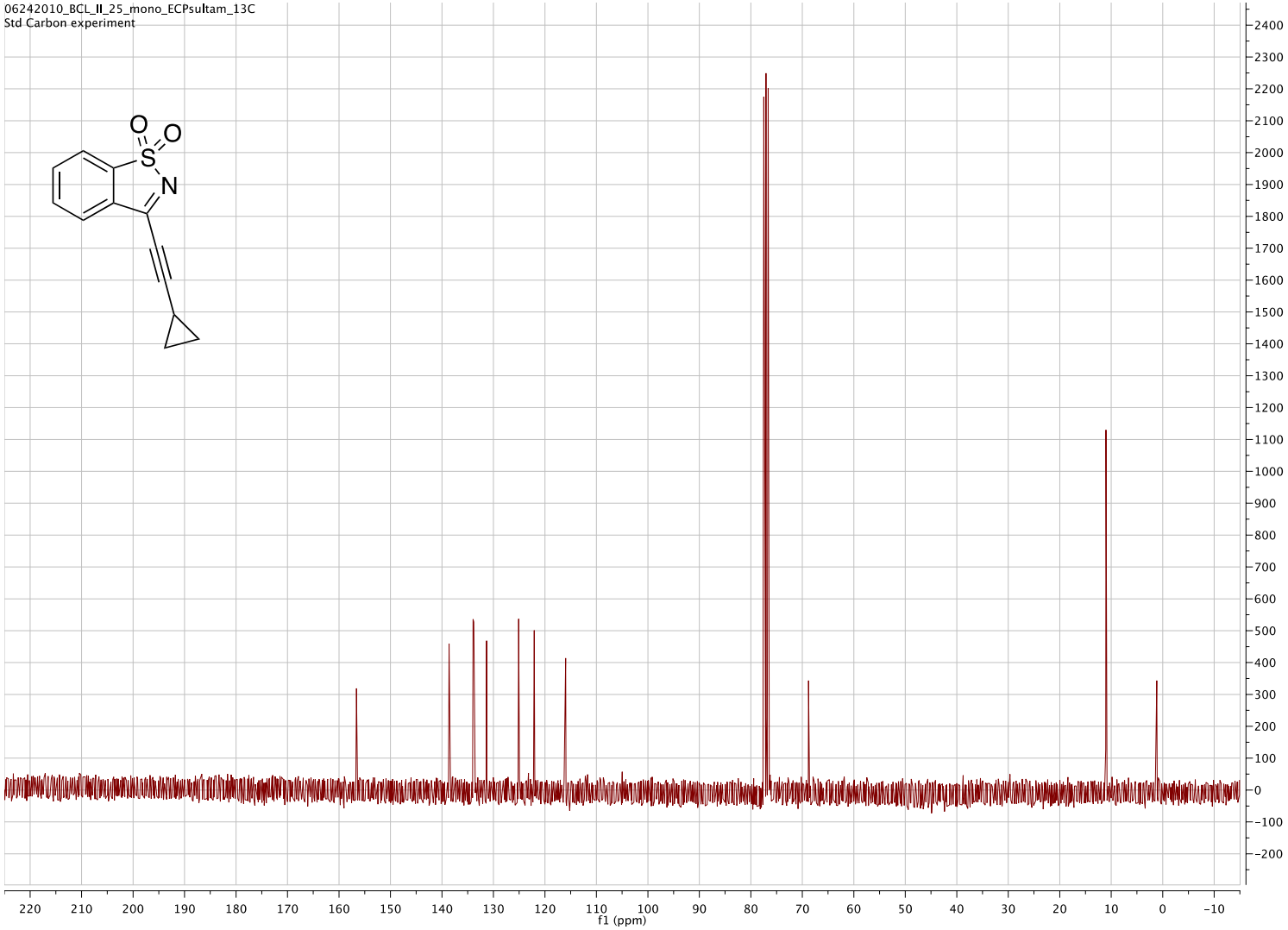


$^{13}C$ NMR (500 MHz, $CDCl_3$) of 3-cyclopropylethynyl-1,2-benzisothiazole 1,1-dioxide

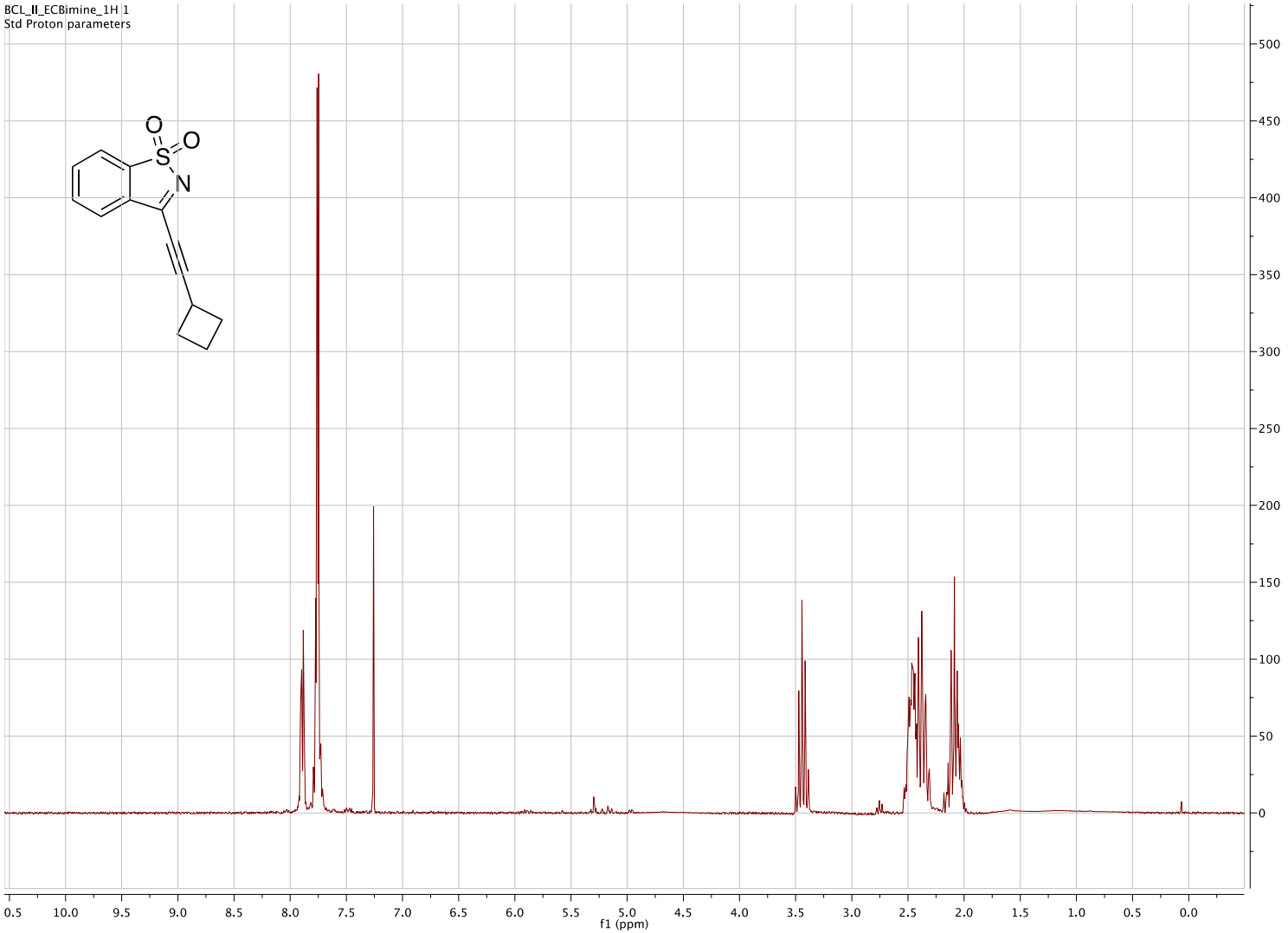


$^{1}$H NMR (500 MHz, $CDCl_3$) of 3-(cyclobutylethynyl)-1,2-benzisothiazole 1,1-dioxide

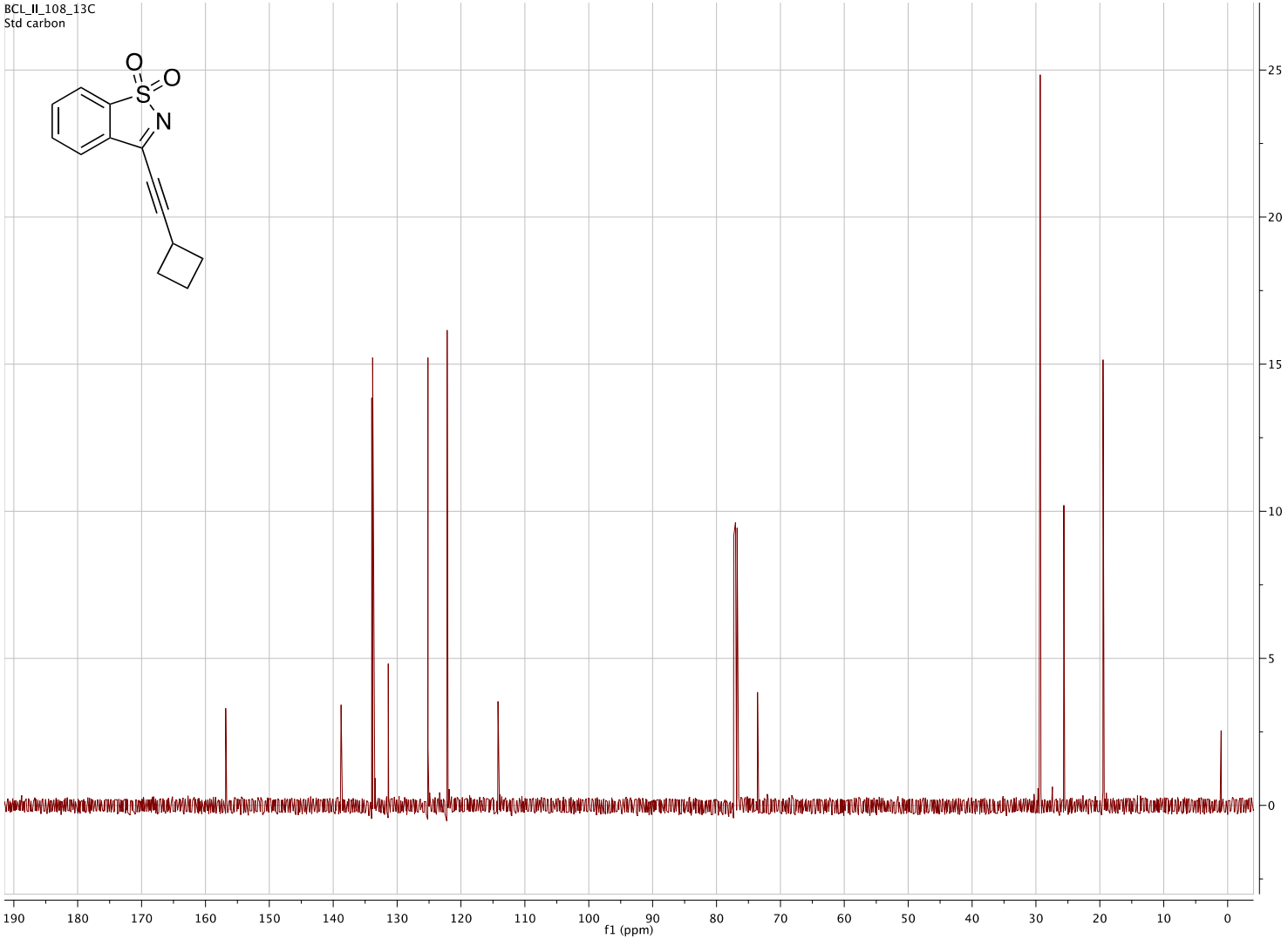


$^{13}C$ NMR (500 MHz, $CDCl_3$) of 3-(cyclobutylethynyl)-1,2-benzisothiazole 1,1-dioxide

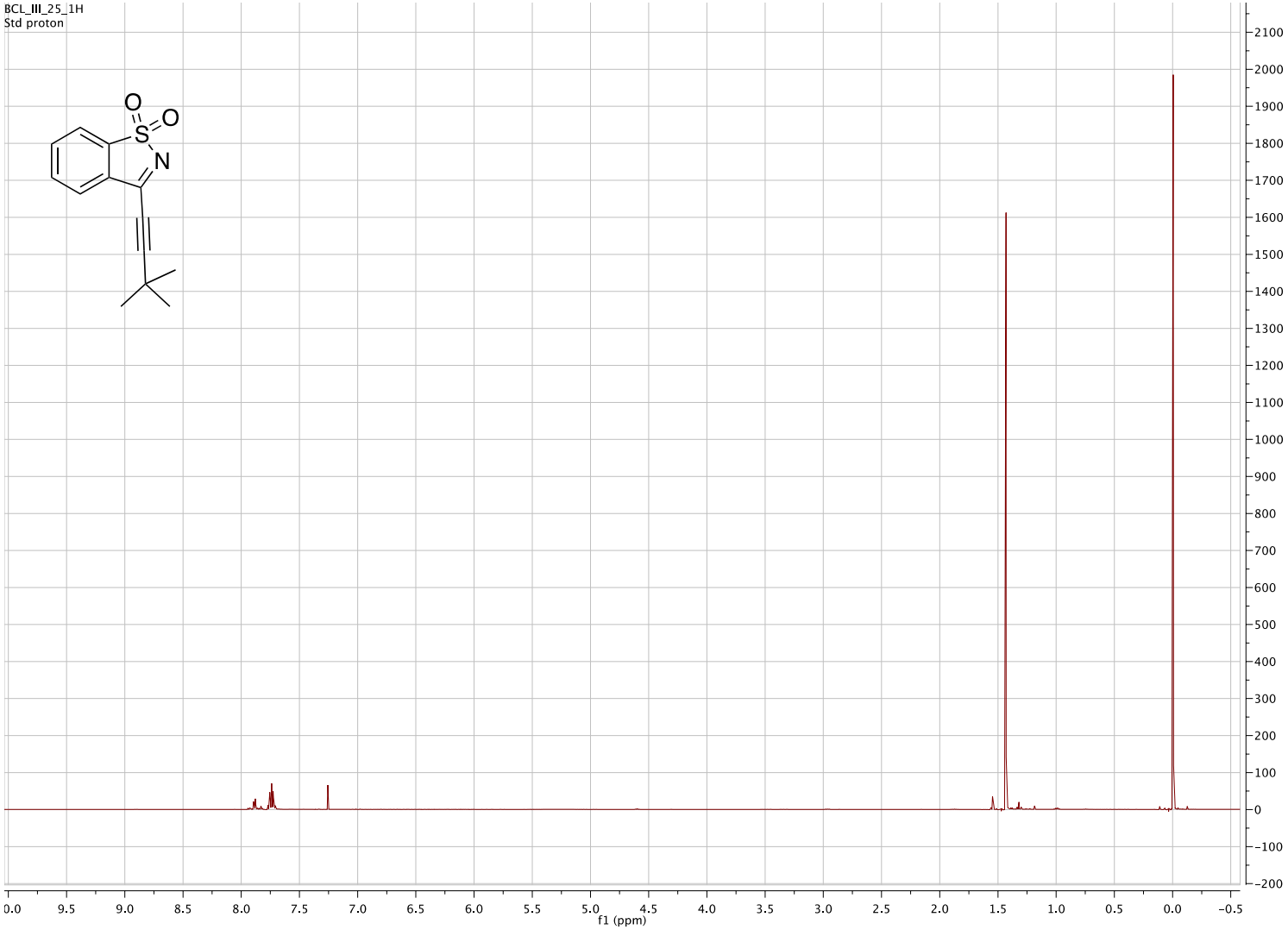


$^{1}$H NMR (500 MHz, $CDCl_3$) of 3-(*tert*-butylethynyl)-1,2-benzisothiazole 1,1-dioxide

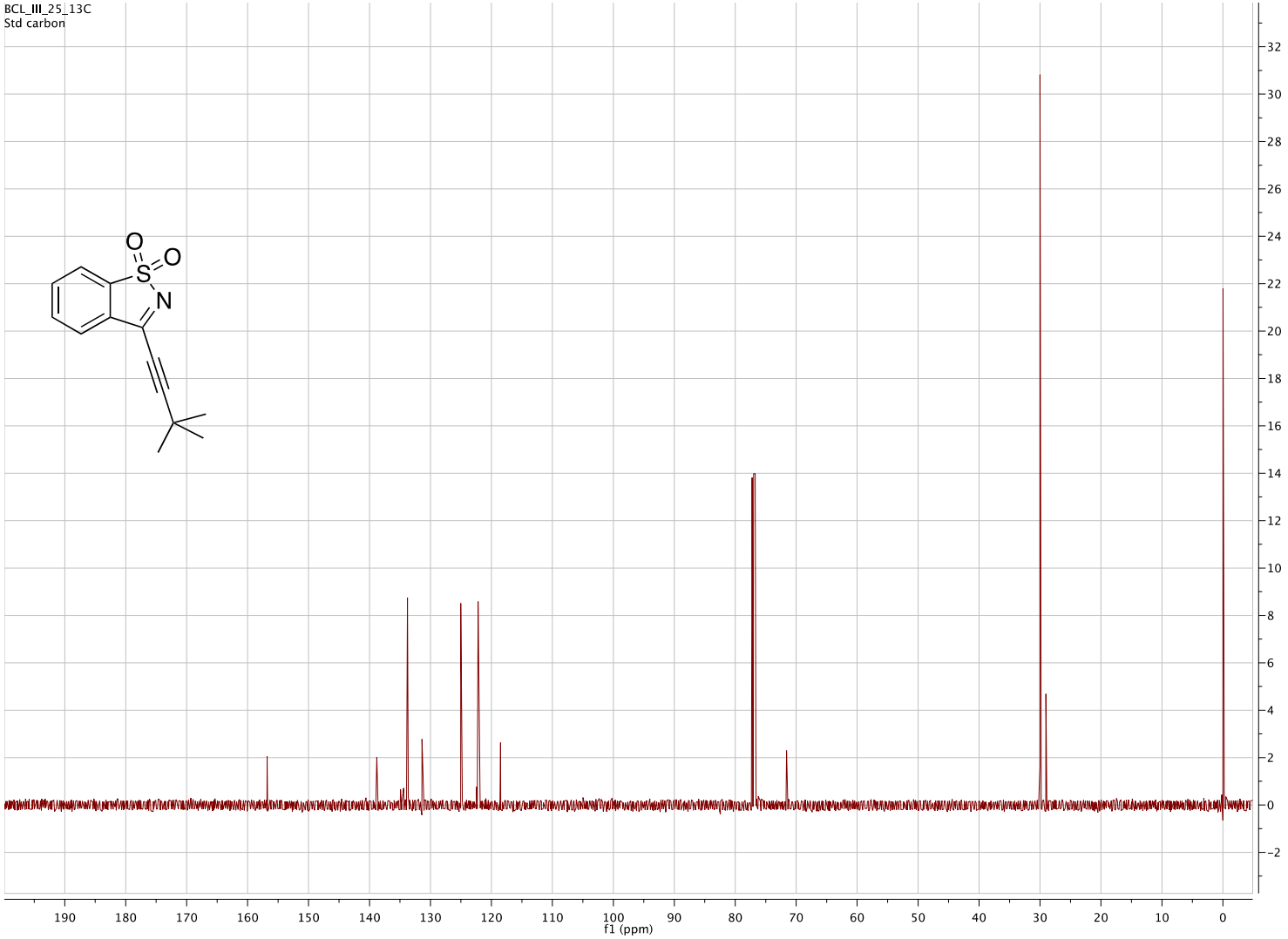


$^{13}C$ NMR (500 MHz, $CDCl_3$) of 3-(*tert*-butylethynyl)-1,2-benzisothiazole 1,1-dioxide

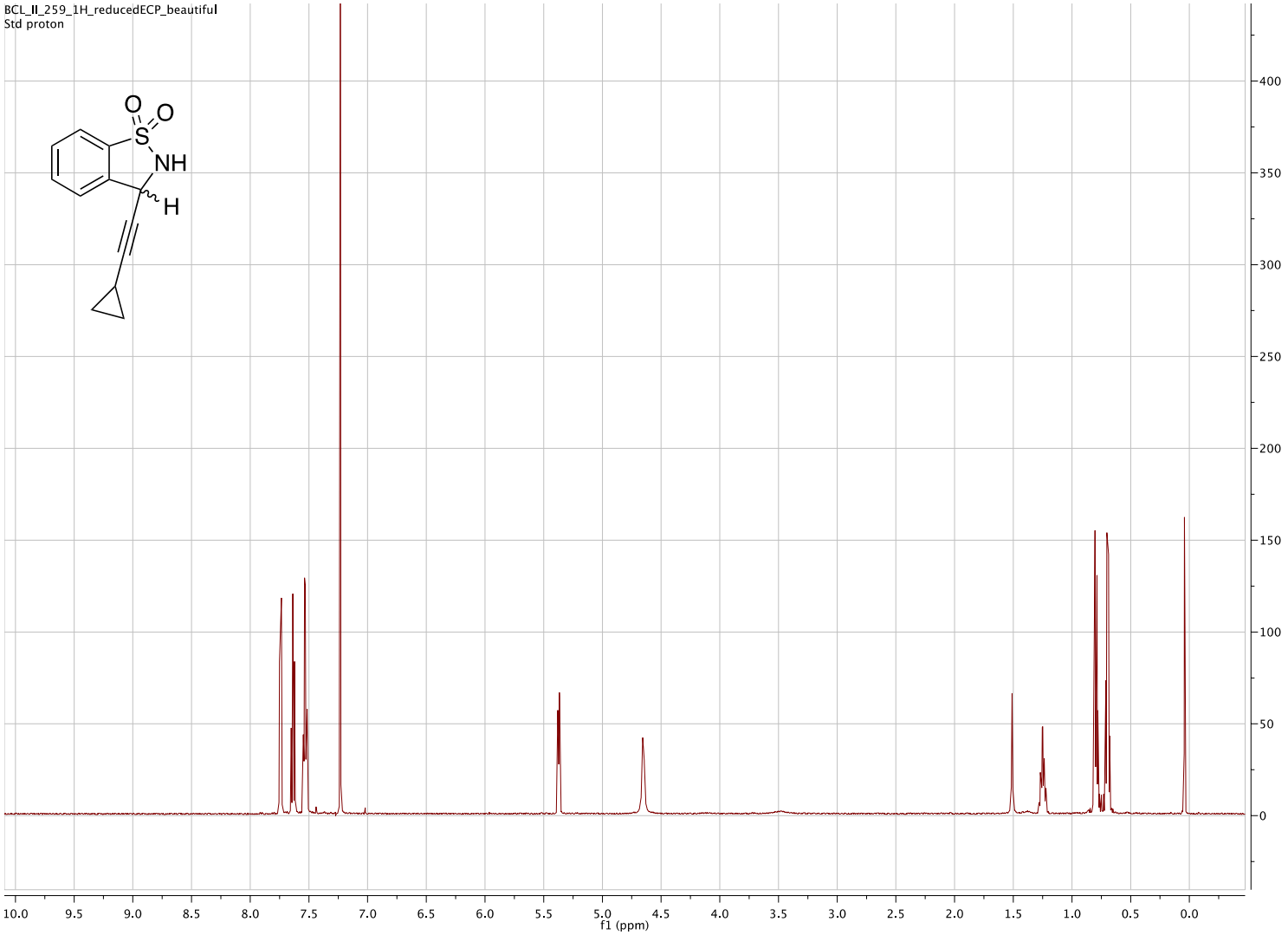


$^{1}$H NMR (500 MHz, $CDCl_3$) of 3-(cyclopropylethynyl)-2,3-dihydro-1,2-benzisothiazole 1,1-dioxide

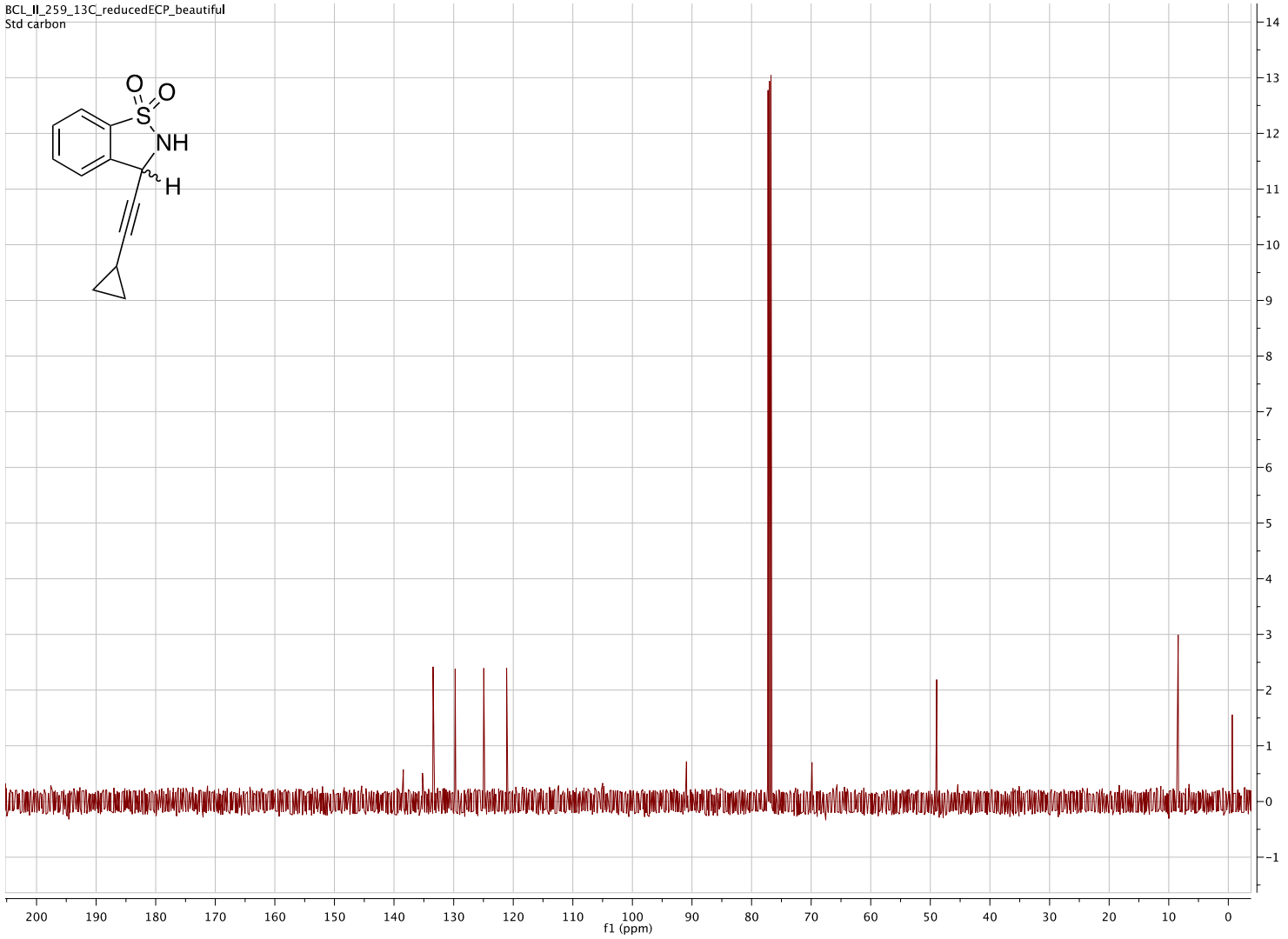


$^{13}C$ NMR (500 MHz, $CDCl_3$) of 3-(cyclopropylethynyl)-2,3-dihydro-1,2-benzisothiazole 1,1-dioxide

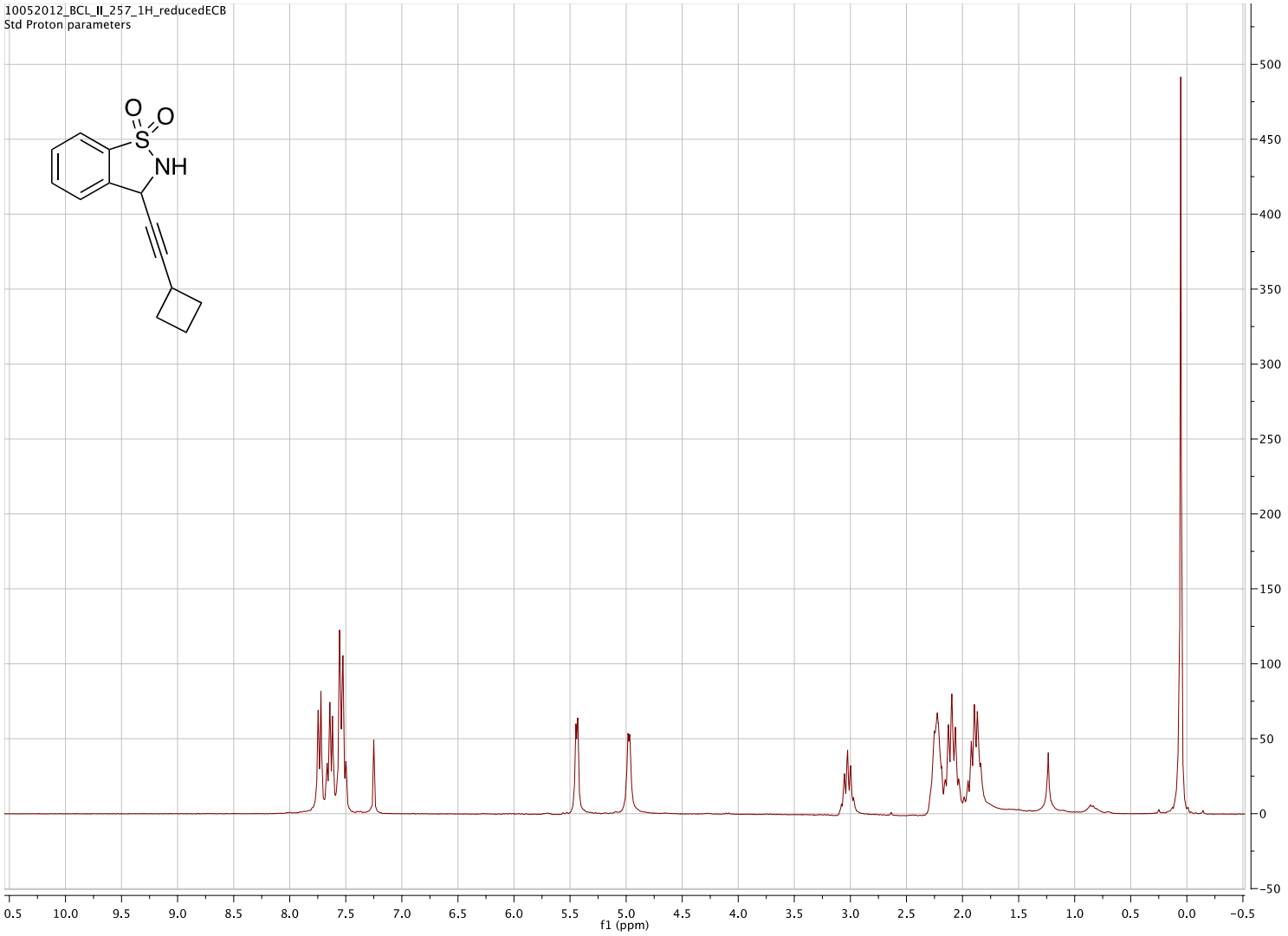


$^{1}$H NMR (500 MHz, $CDCl_3$) of 3-(cyclobutylethynyl)-2,3-dihydro-1,2-benzisothiazole 1,1-dioxide

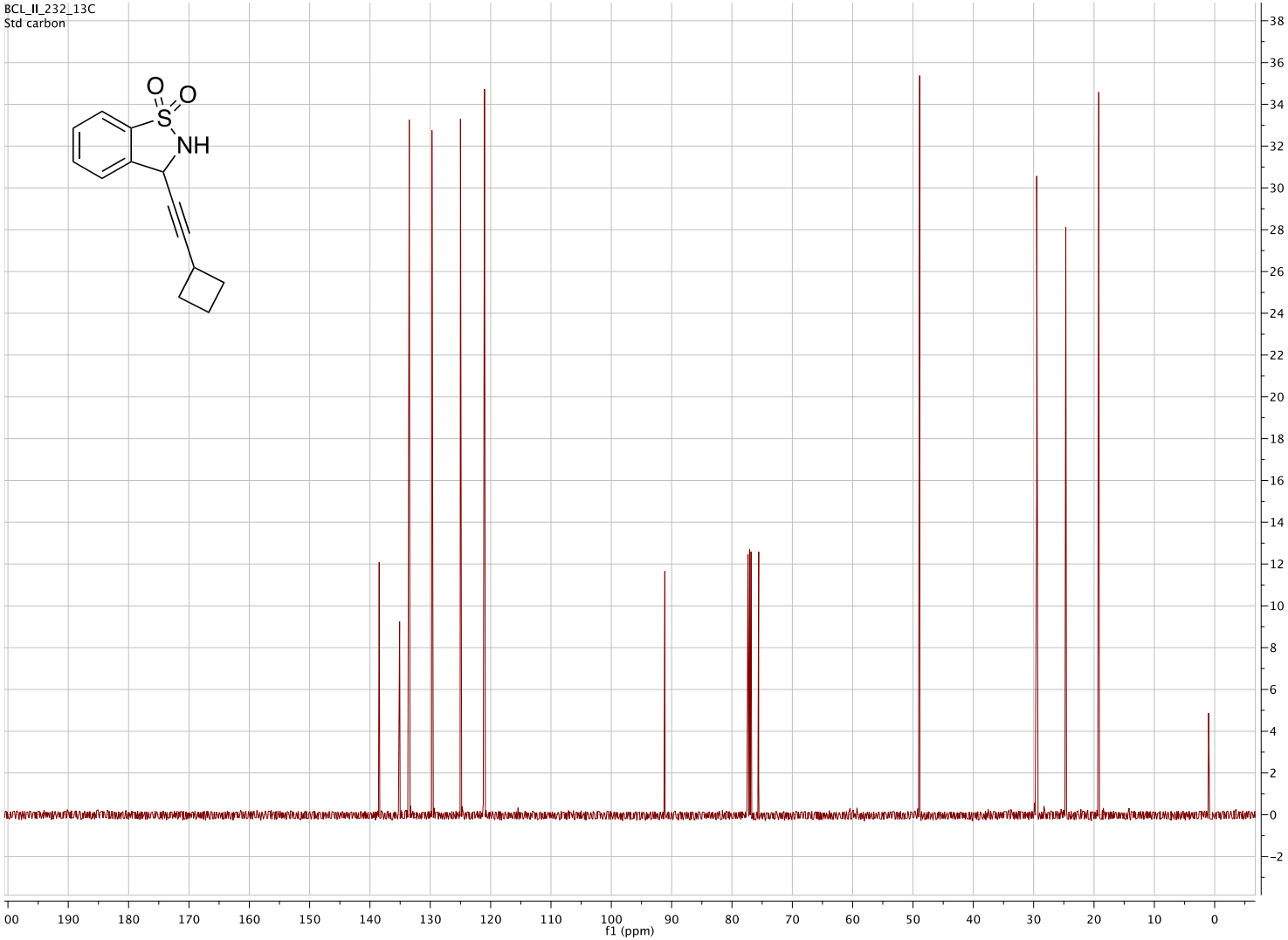


$^{13}C$ NMR (500 MHz, $CDCl_3$) of 3-(cyclobutylethynyl)-2,3-dihydro-1,2-benzisothiazole 1,1-dioxide

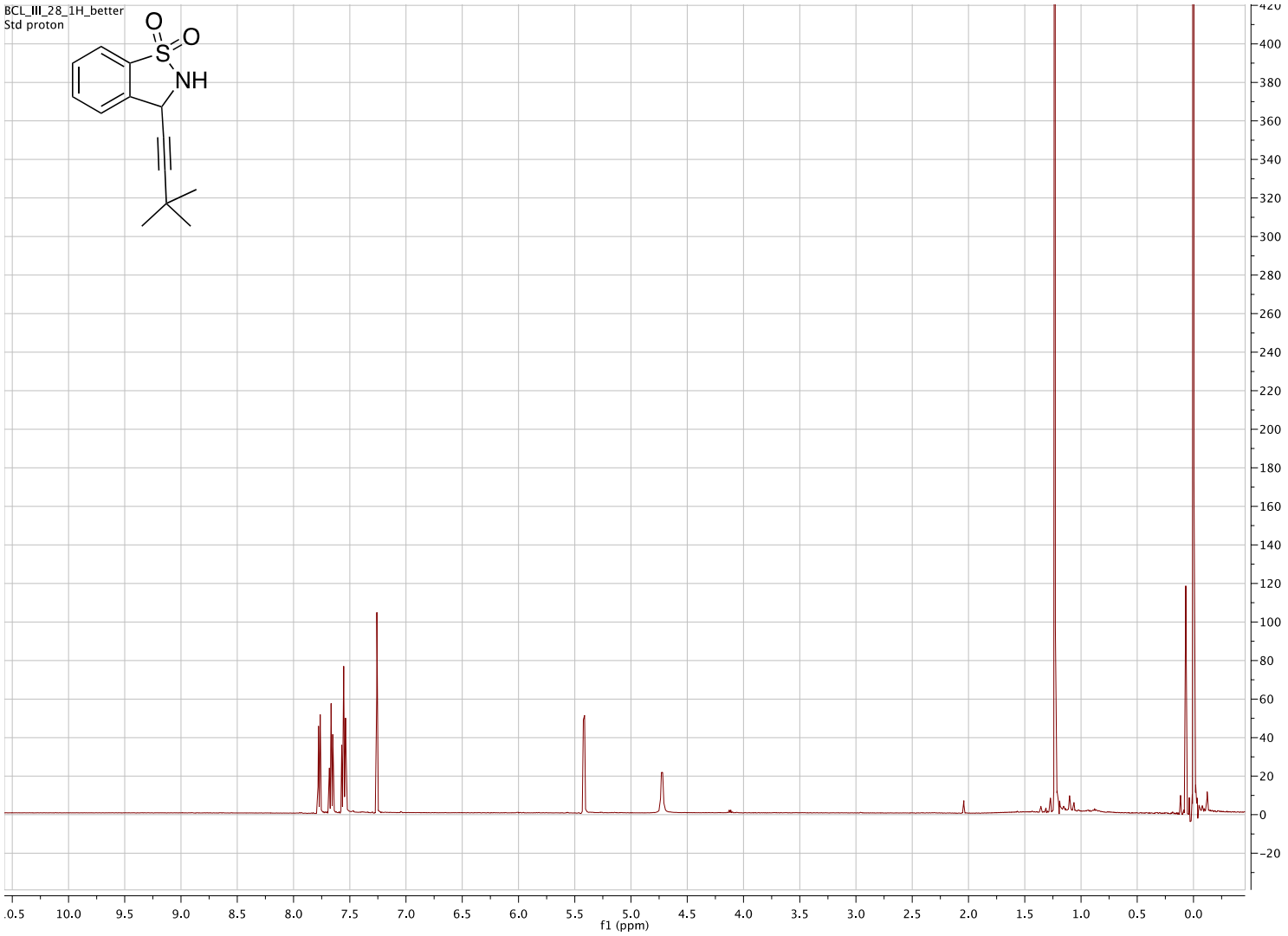


$^{1}$H NMR (500 MHz, $CDCl_3$) of 3-(*t*-butylethynyl)-2,3-dihydro-1,2-benzisothiazole 1,1-dioxide

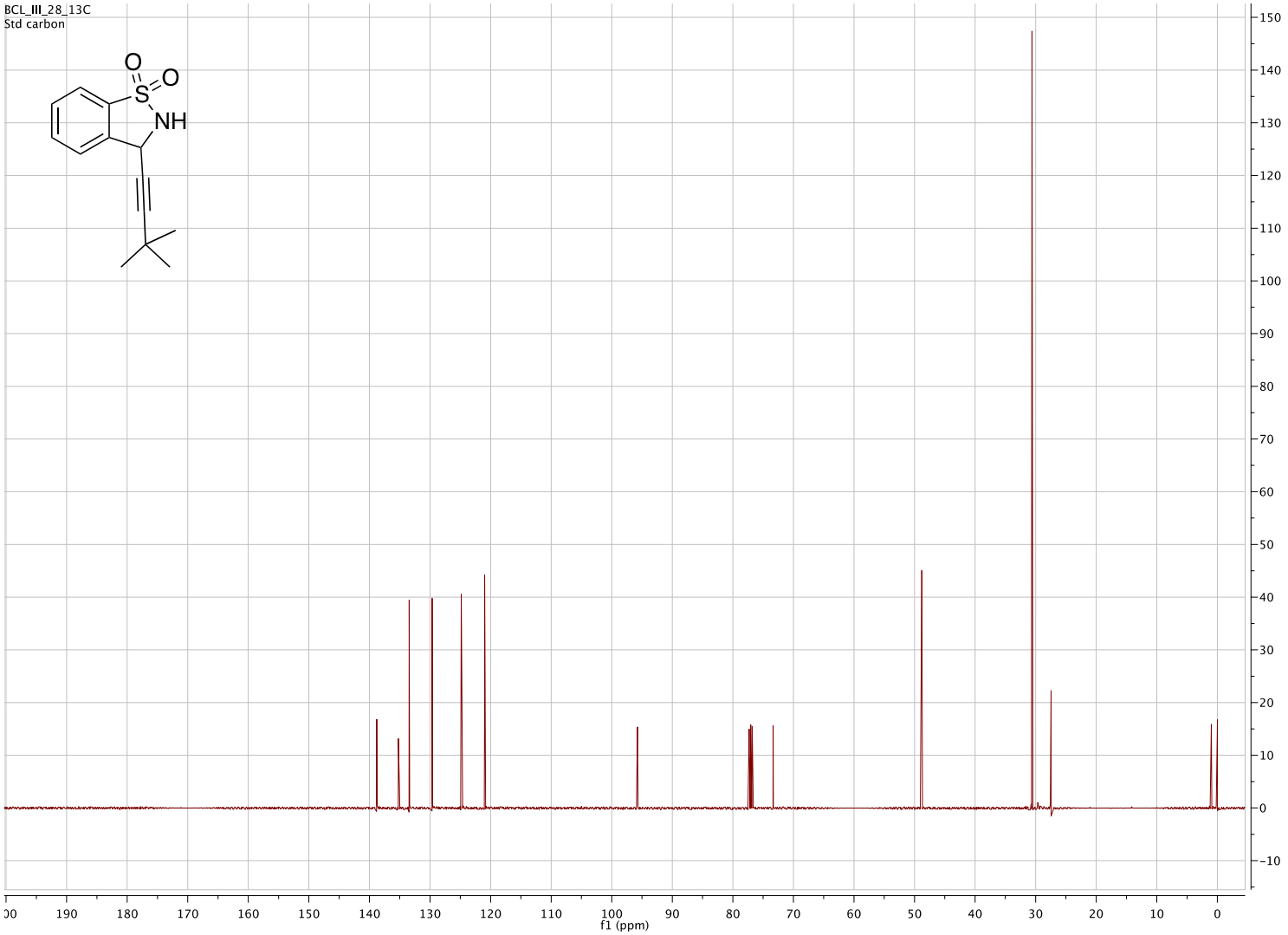


$^{13}C$ NMR (500 MHz, $CDCl_3$) of 3-(*t*-butylethynyl)-2,3-dihydro-1,2-benzisothiazole 1,1-dioxide

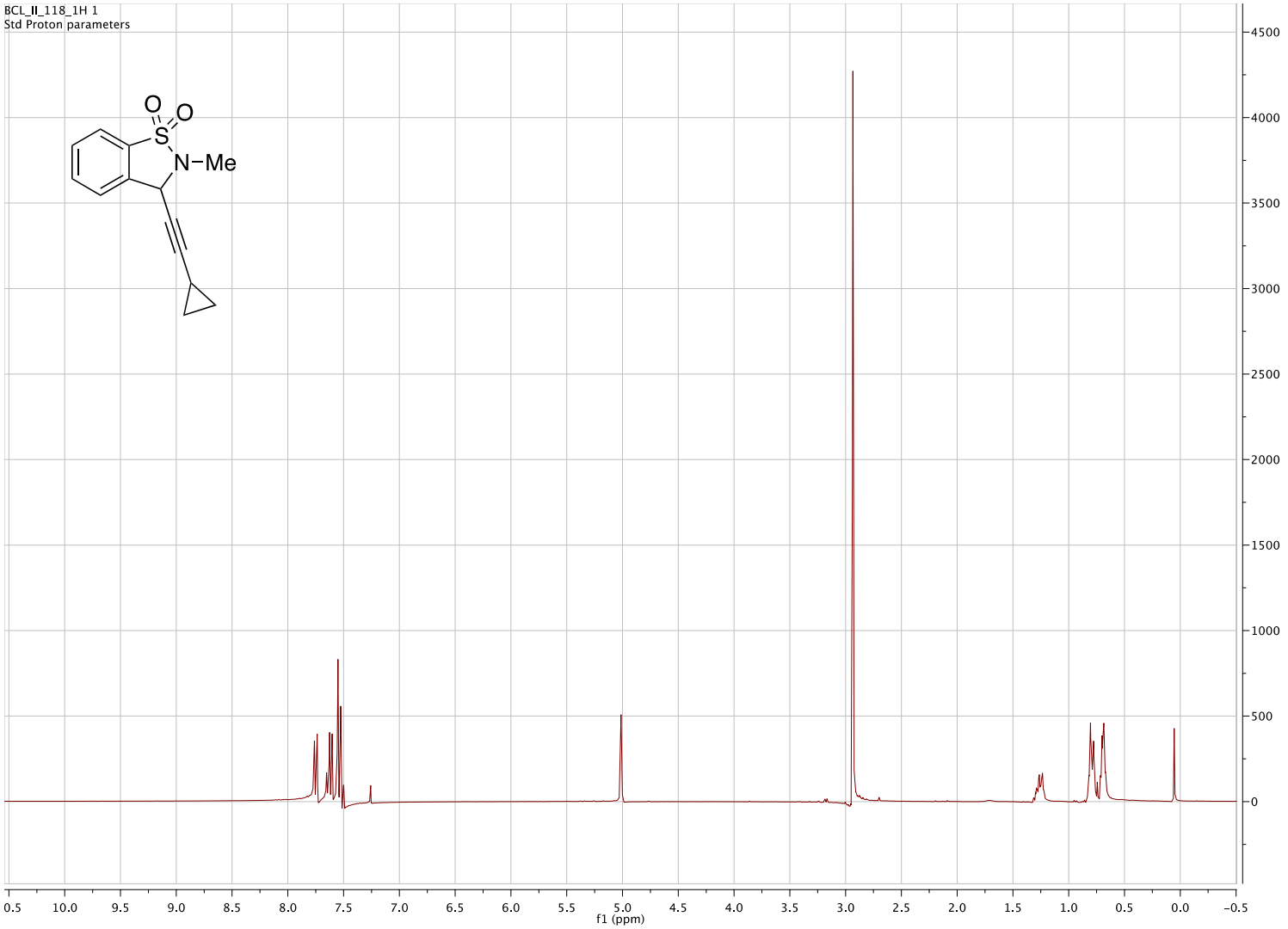


$^{1}$H NMR (500 MHz, $CDCl_3$) of 3-(cyclopropylethynyl)-2,3-dihydro-3-methyl-1,2-benzisothiazole 1,1-dioxide

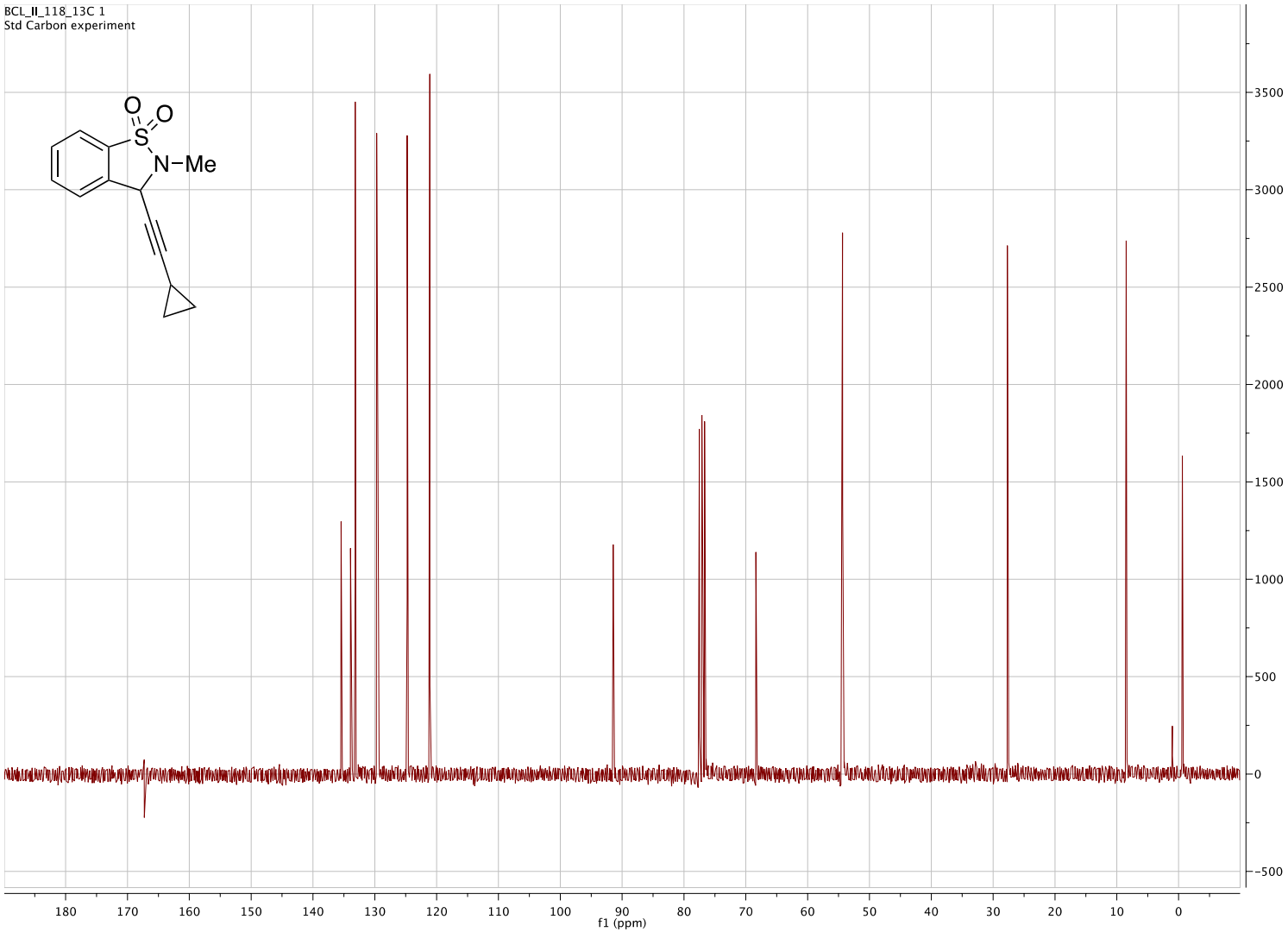


$^{13}C$ NMR (500 MHz, $CDCl_3$) of 3-(cyclopropylethynyl)-2,3-dihydro-3-methyl-1,2-benzisothiazole 1,1-dioxide

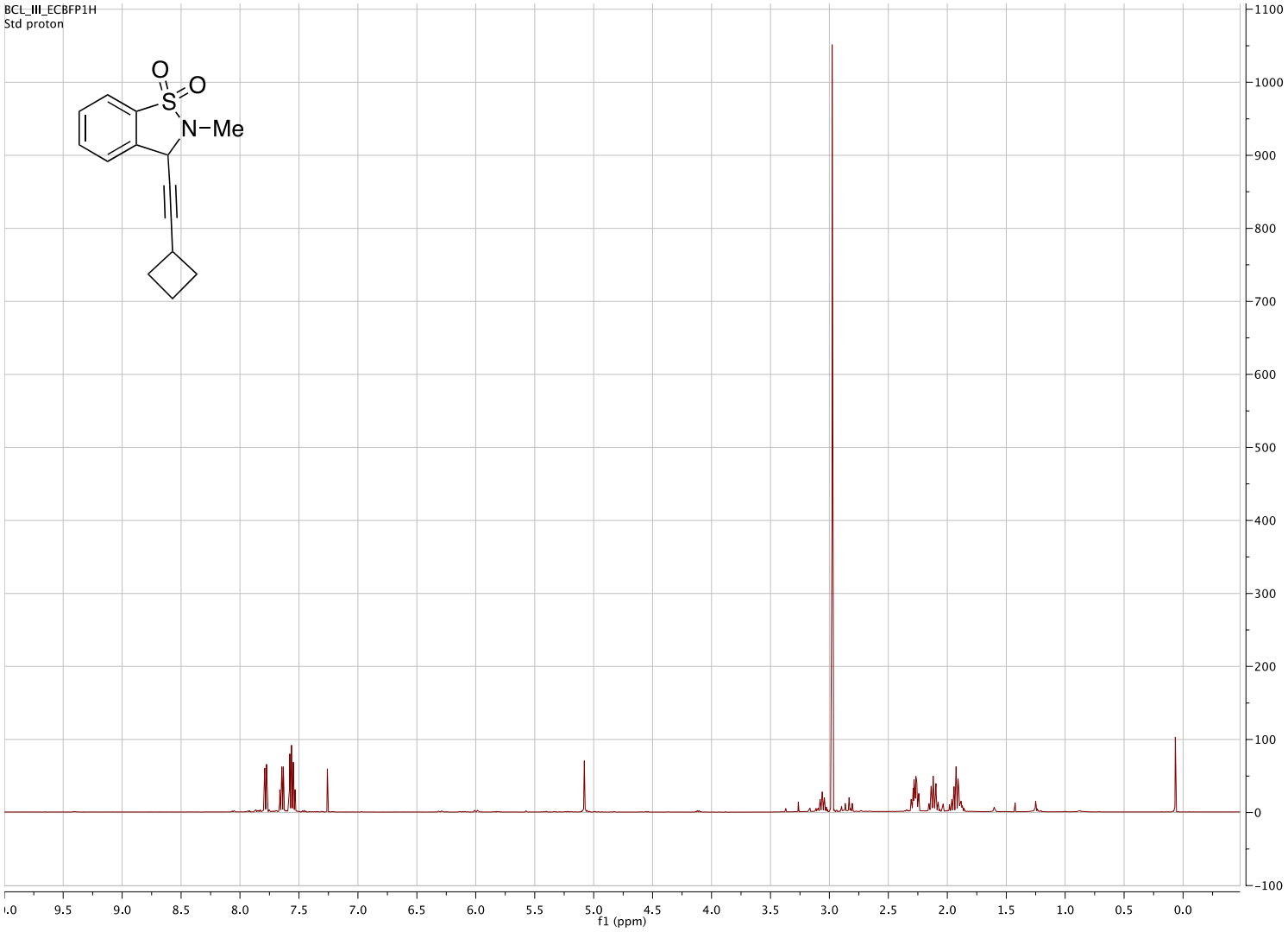


$^{1}$H NMR (500 MHz, $CDCl_3$) of 3-(cyclobutylethynyl)-2,3-dihydro-2,methyl-1,2-benzisothiazole 1,1-dioxide

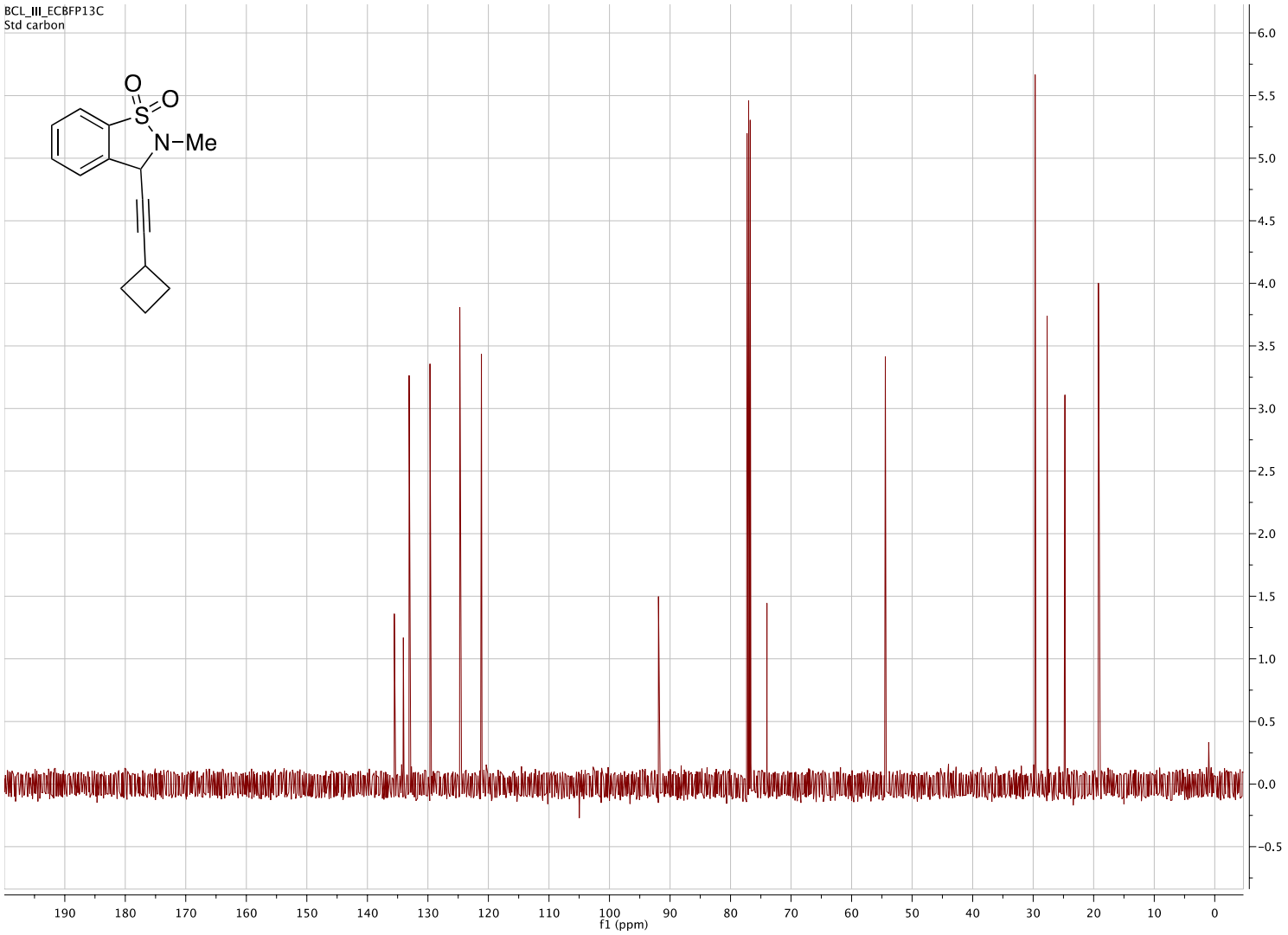


$^{13}C$ NMR (500 MHz, $CDCl_3$) of 3-(cyclobutylethynyl)-2,3-dihydro-3-methyl-1,2-benzisothiazole 1,1-dioxide

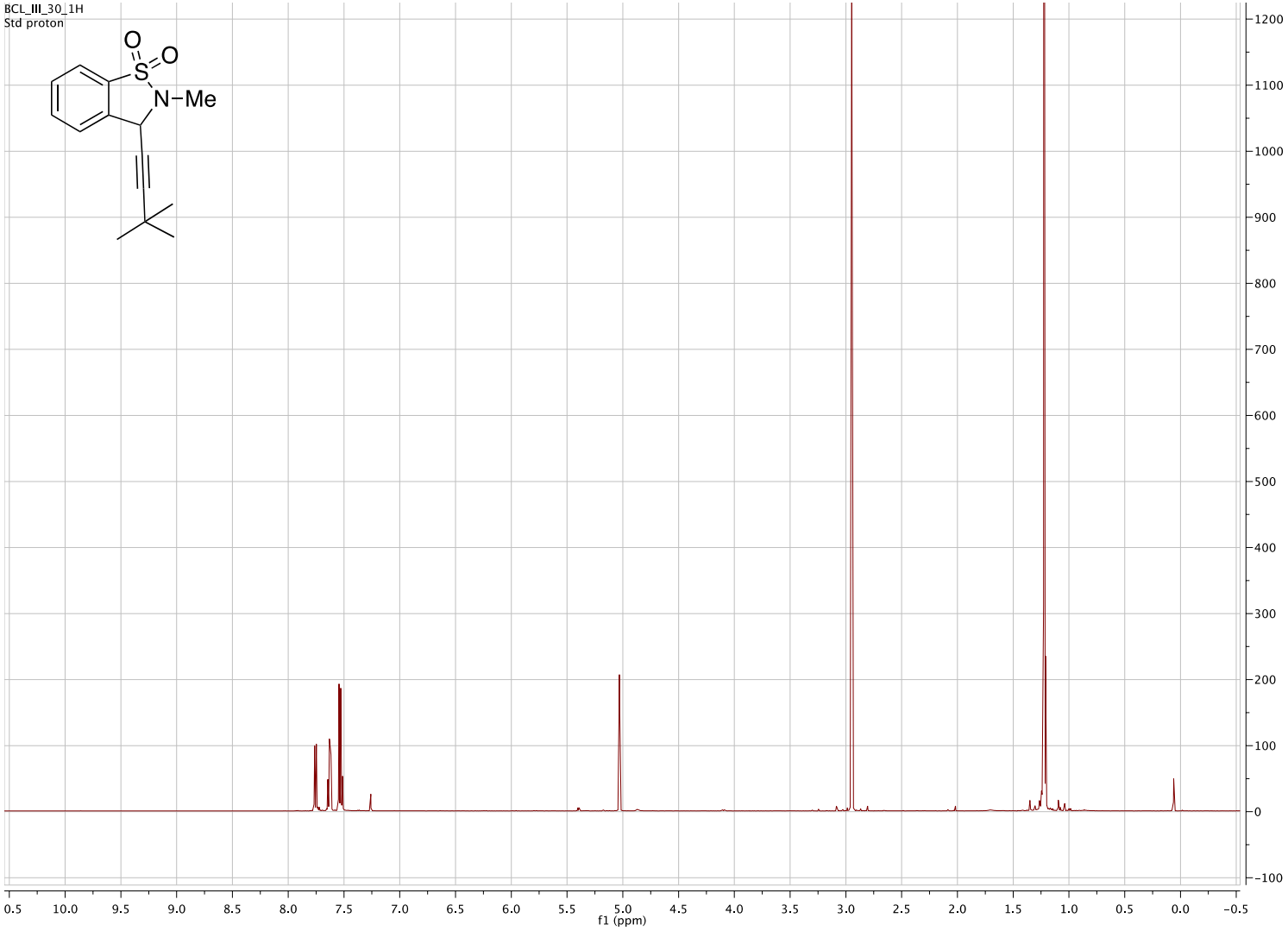


$^{13}$C NMR (500 MHz, $CDCl_3$) of 3-(*t*-butylethynyl)-2,3-dihydro-2,methyl-1,2-benzisothiazole 1,1-dioxide

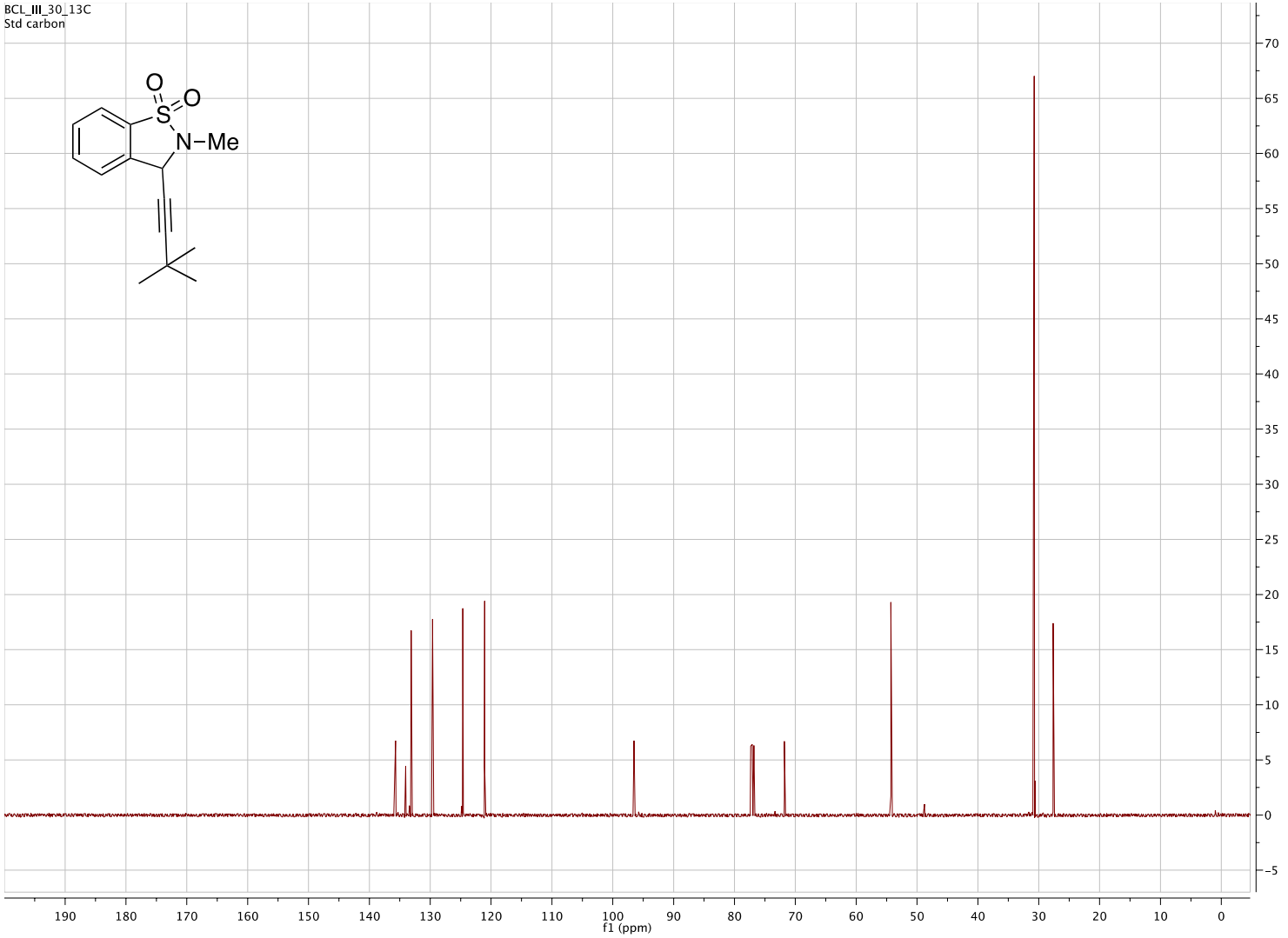


$^{13}C$ NMR(500 MHz, $CDCl_3$) of 3-(*t*-butylethynyl)-2,3-dihydro-2,methyl-1,2-benzisothiazole 1,1-dioxide

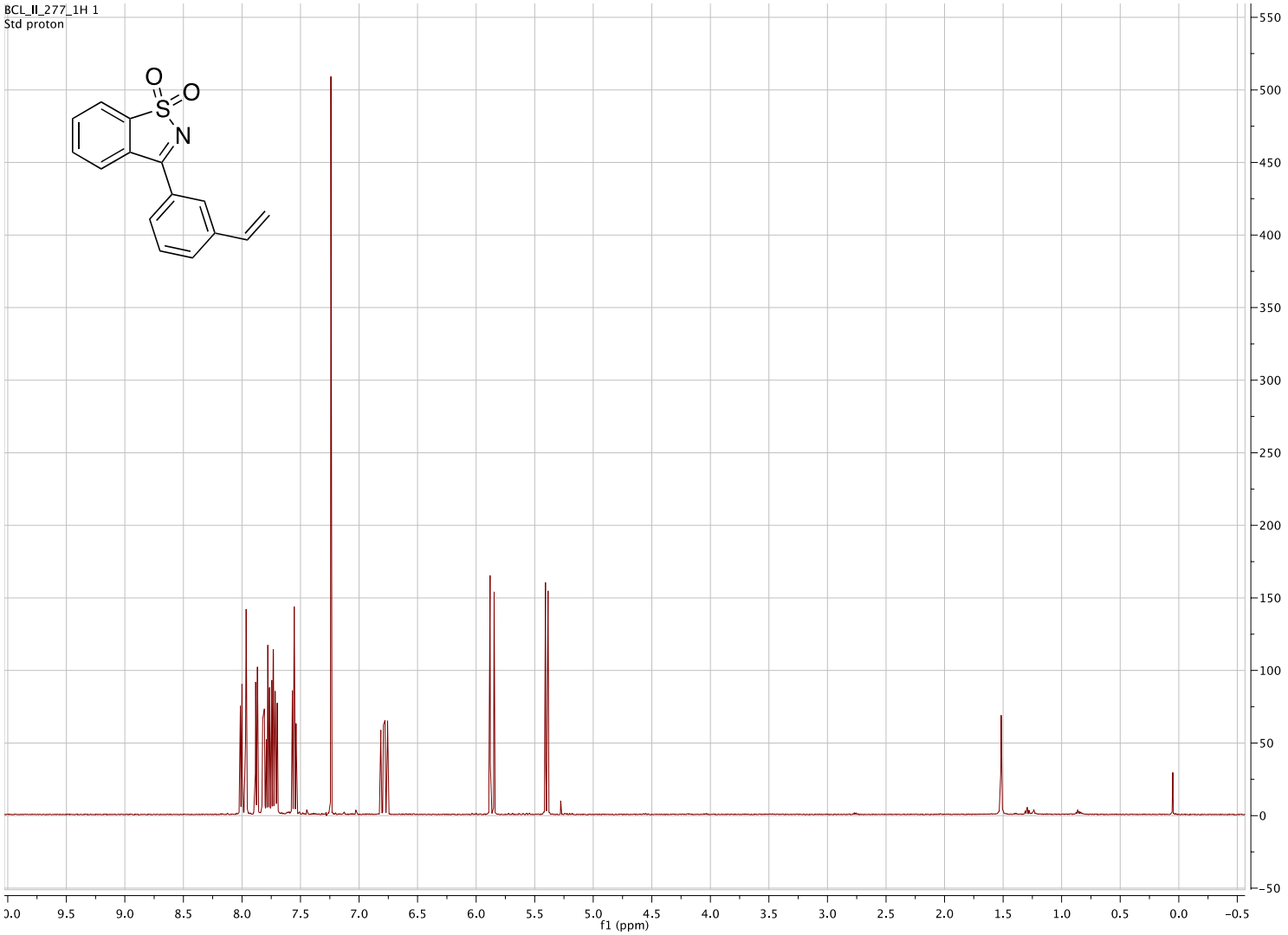


$^1$H NMR (500 MHz, $CDCl_3$) of 3-(3-vinylphenyl)-1,2-benzisothiazole 1,1-dioxide

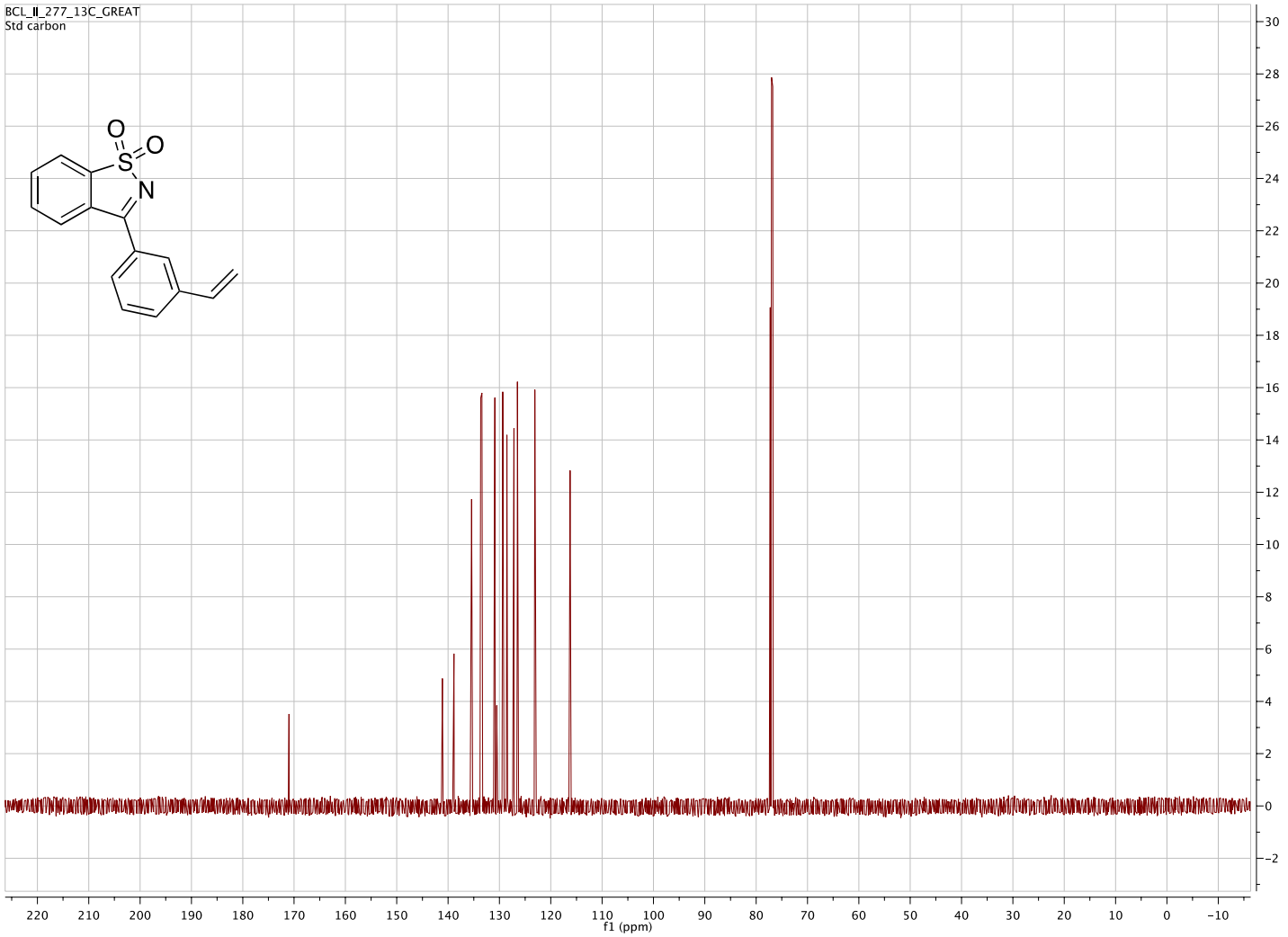


$^{13}C$ NMR (500 MHz, $CDCl_3$) of 3-(3-vinylphenyl)-1,2-benzisothiazole 1,1-dioxide

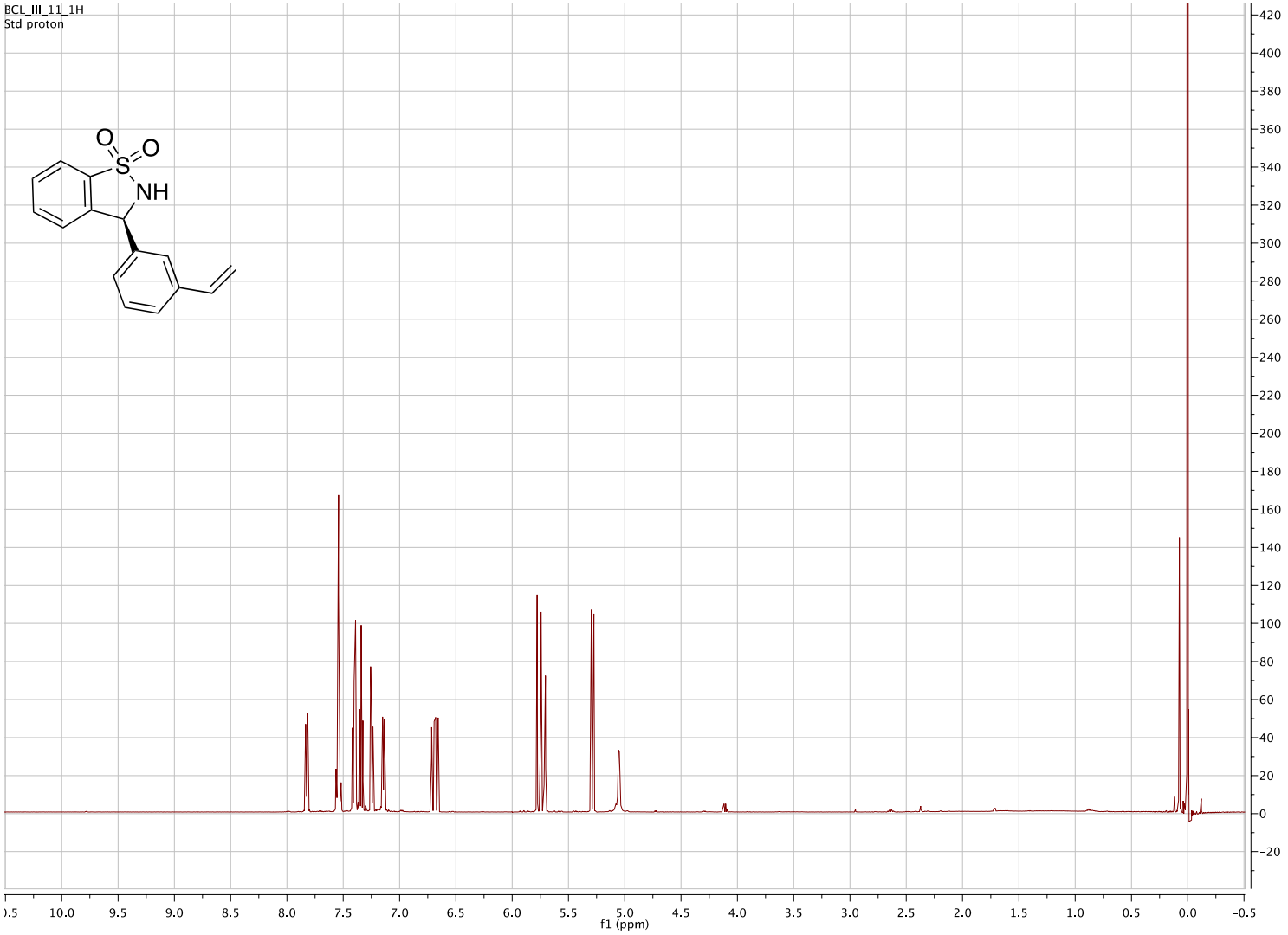


$^{1}$H NMR (500 MHz, $CDCl_3$) of (*S*)-3-(3-vinylphenyl)-2,3-dihydro-1,2-benzisothiazole 1,1-dioxide

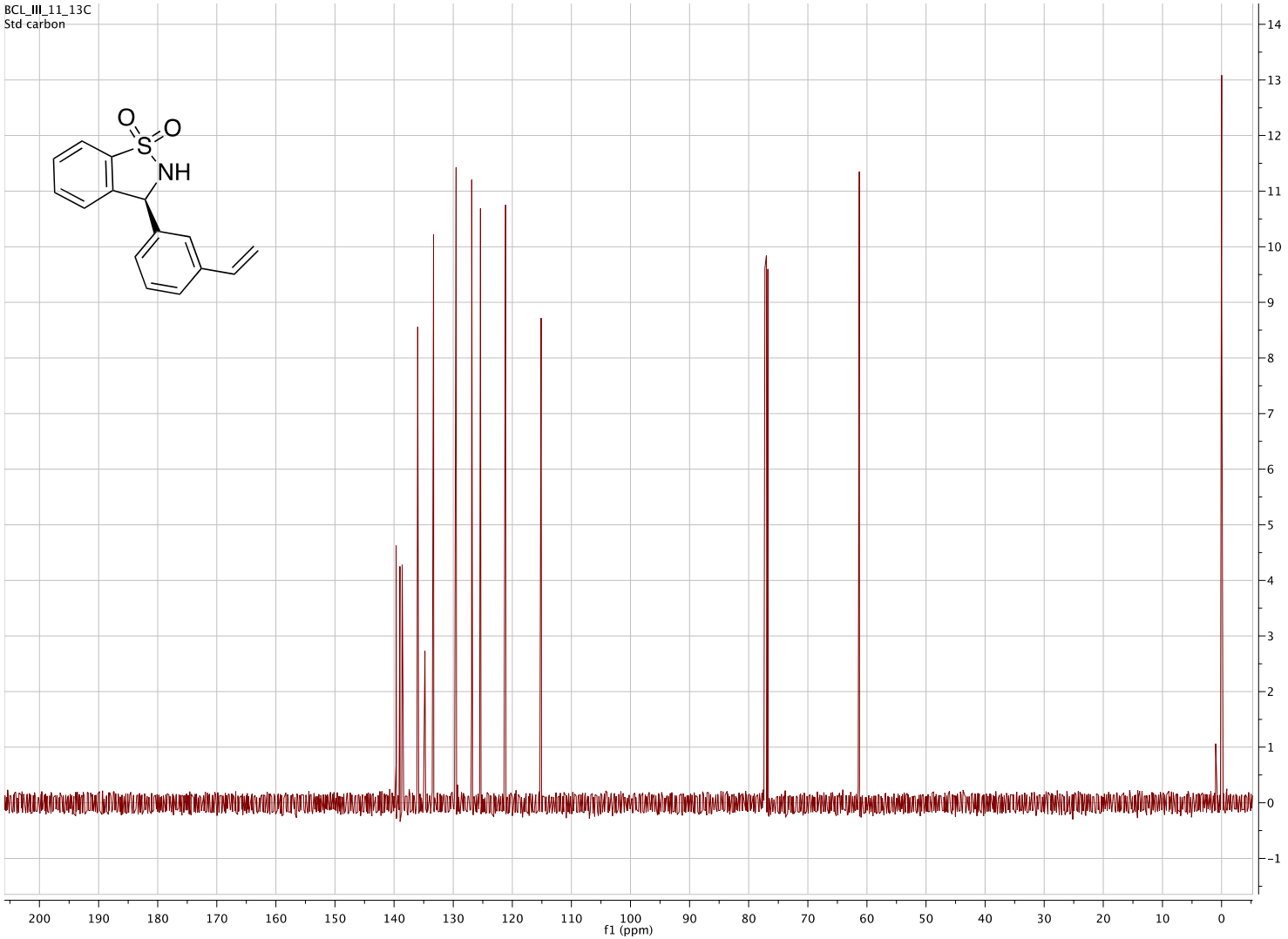


$^{13}C$ NMR (500 MHz, $CDCl_3$) of (*S*)-3-(3-vinylphenyl)-2,3-dihydro-1,2-benzisothiazole 1,1-dioxide

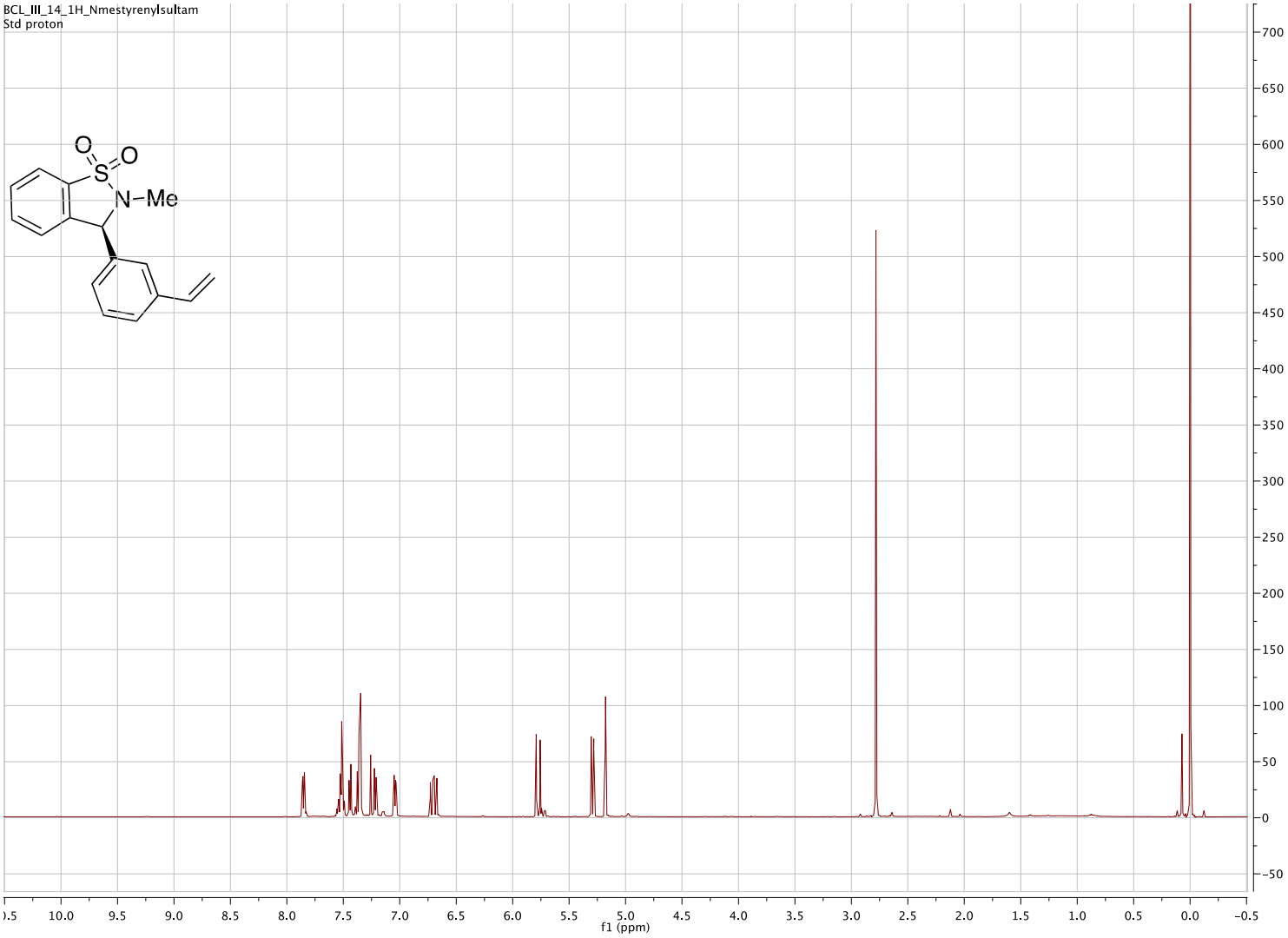


$^{1}$H NMR (500 MHz, $CDCl_3$) of (*S*)-2-methyl-3-(3-vinylphenyl)-2,3-dihydro-1,2-benzisothiazole 1,1-dioxide

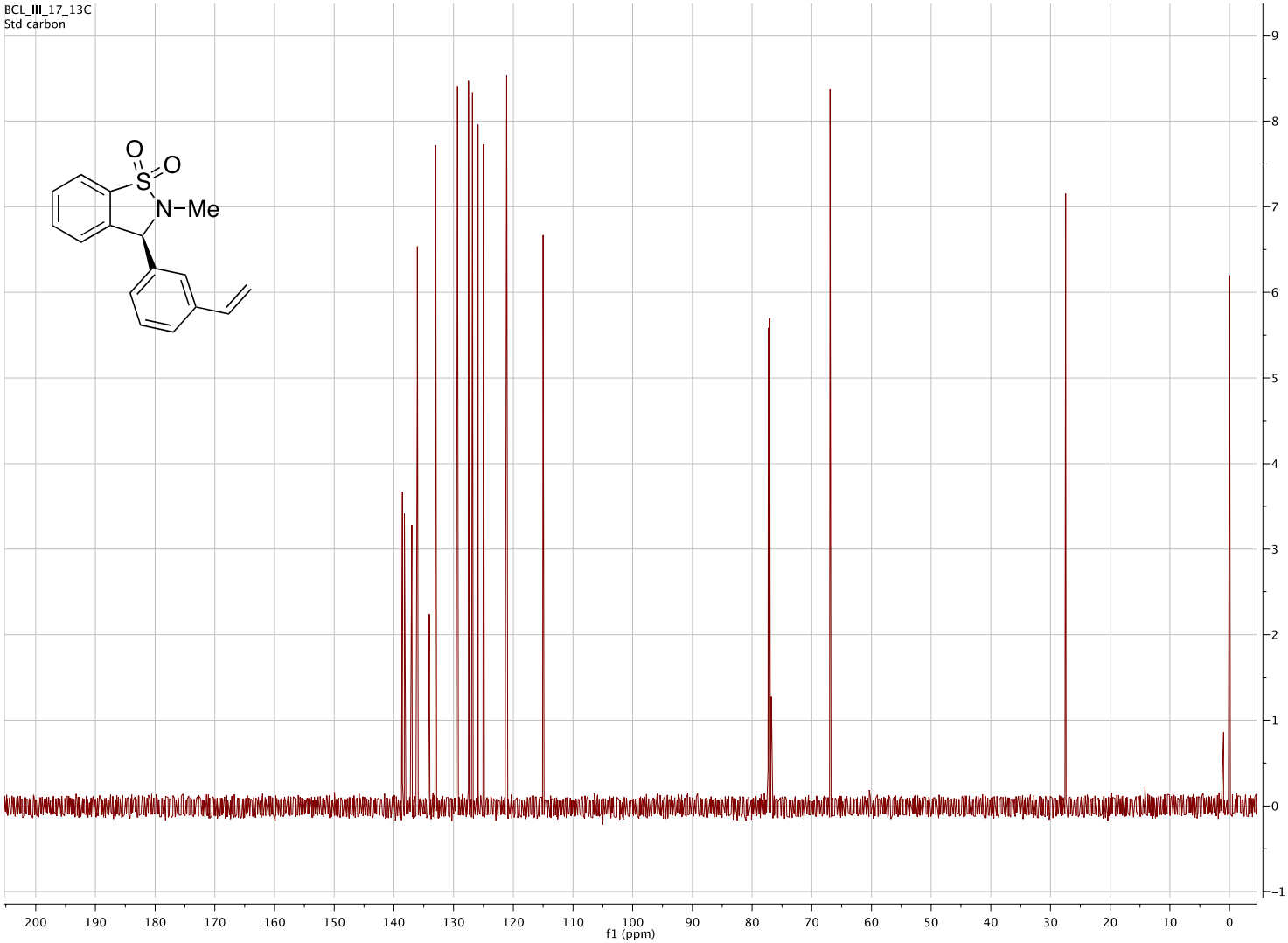


$^{13}C$ NMR (500 MHz, $CDCl_3$) of (*S*)-2-methyl-3-(3-vinylphenyl)-2,3-dihydro-1,2-benzisothiazole 1,1-dioxide

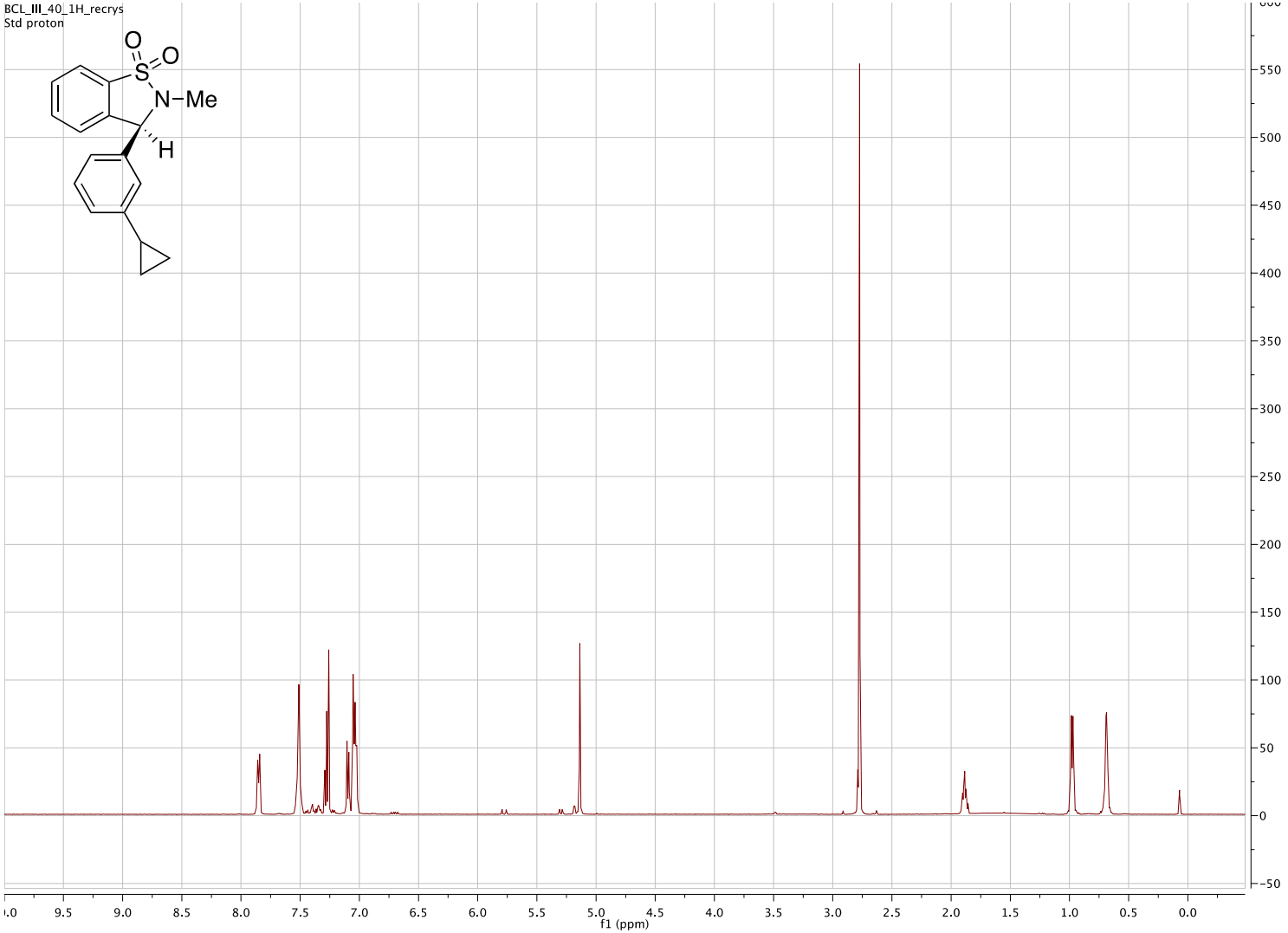


$^{1}$H of (500 MHz, $CDCl_3$) (*S*)-3-(3-cyclopropylphenyl)-2,3-dihydro-2-methyl-1,2-benzisothiazole 1,1-dioxide

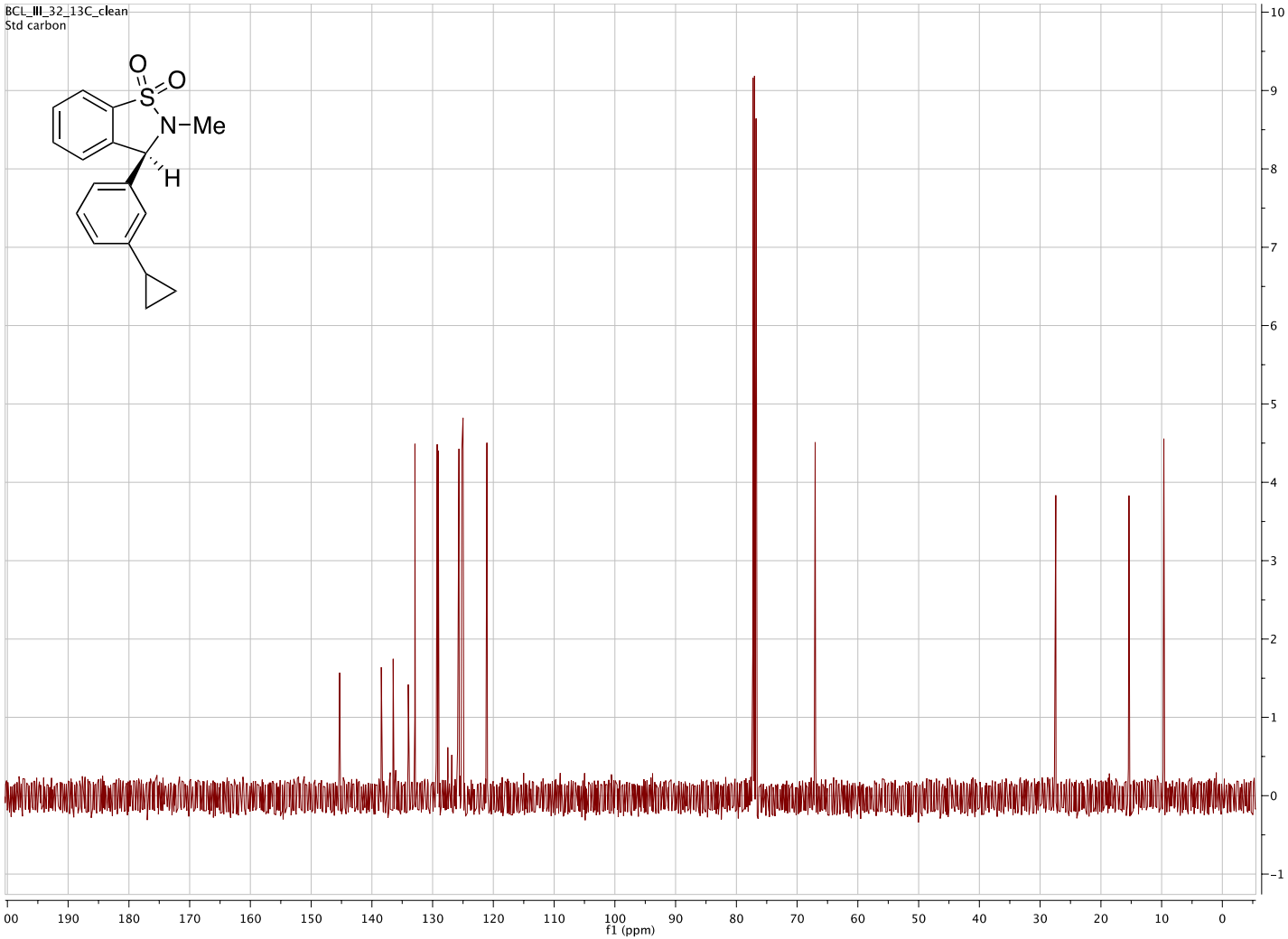


$^{13}C$ NMR (500 MHz, $CDCl_3$) of (*S*)-3-(3-cyclopropylphenyl)-2,3-dihydro-2-methyl-1,2-

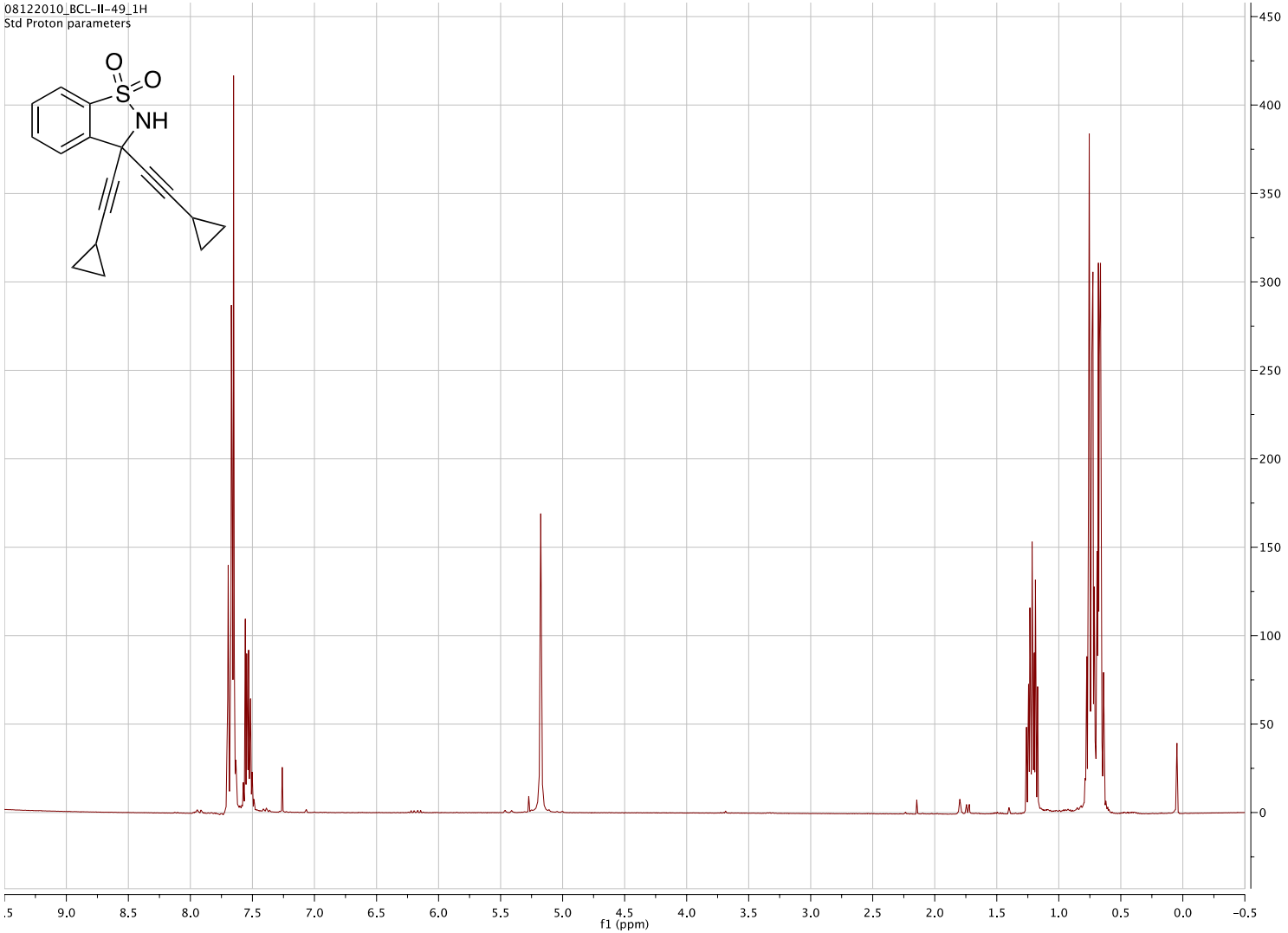


$^1$H NMR (500 MHz, $CDCl_3$) of 3,3-bis (cyclopropylethynyl)-2,3-dihydro-1,2-benzoisothiazole

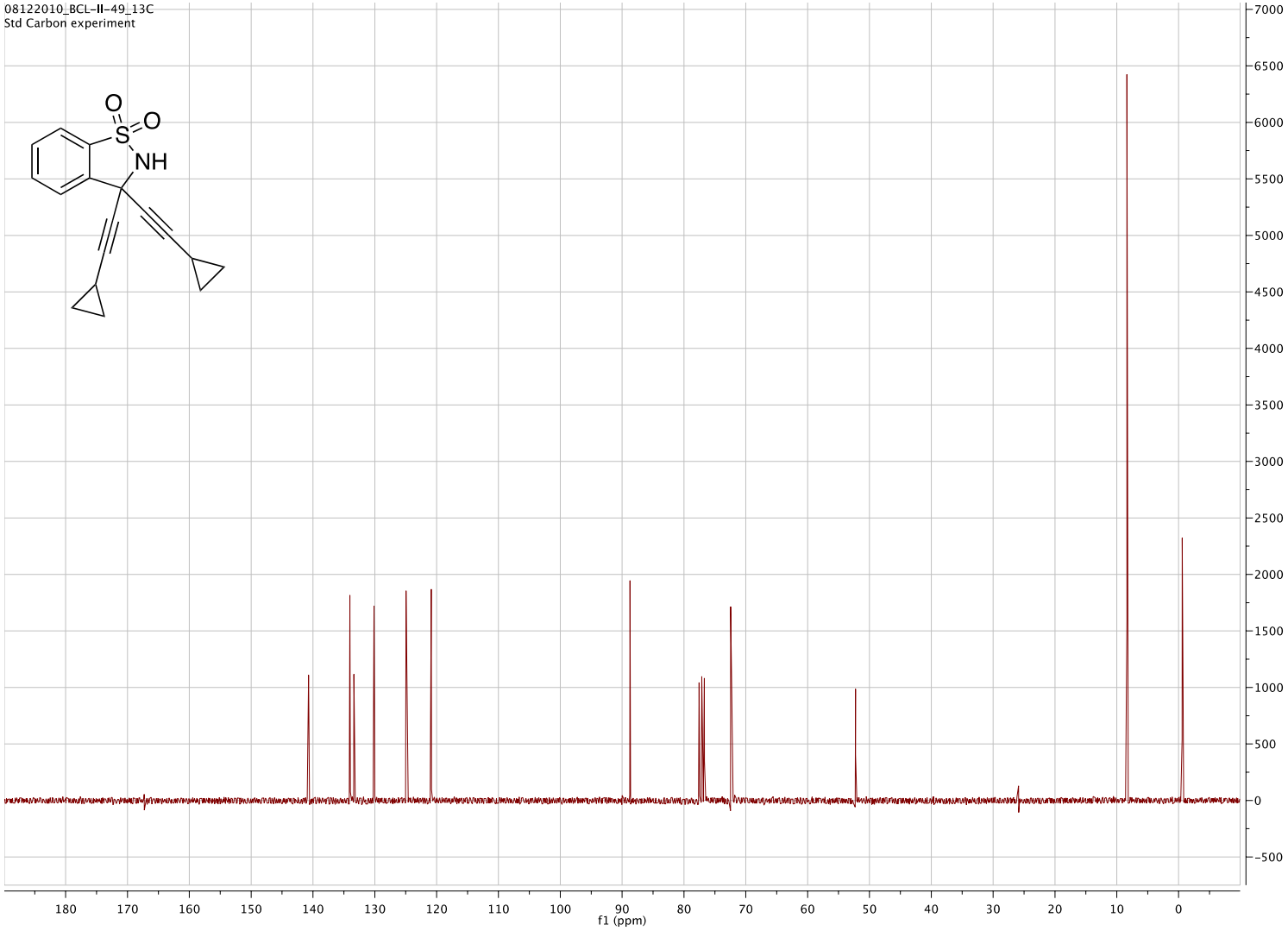


$^{13}C$ NMR (500 MHz, $CDCl_3$) of 3,3-bis (cyclopropylethynyl)-2,3-dihydro-1,2-benzisothiazole 1,1-dioxide

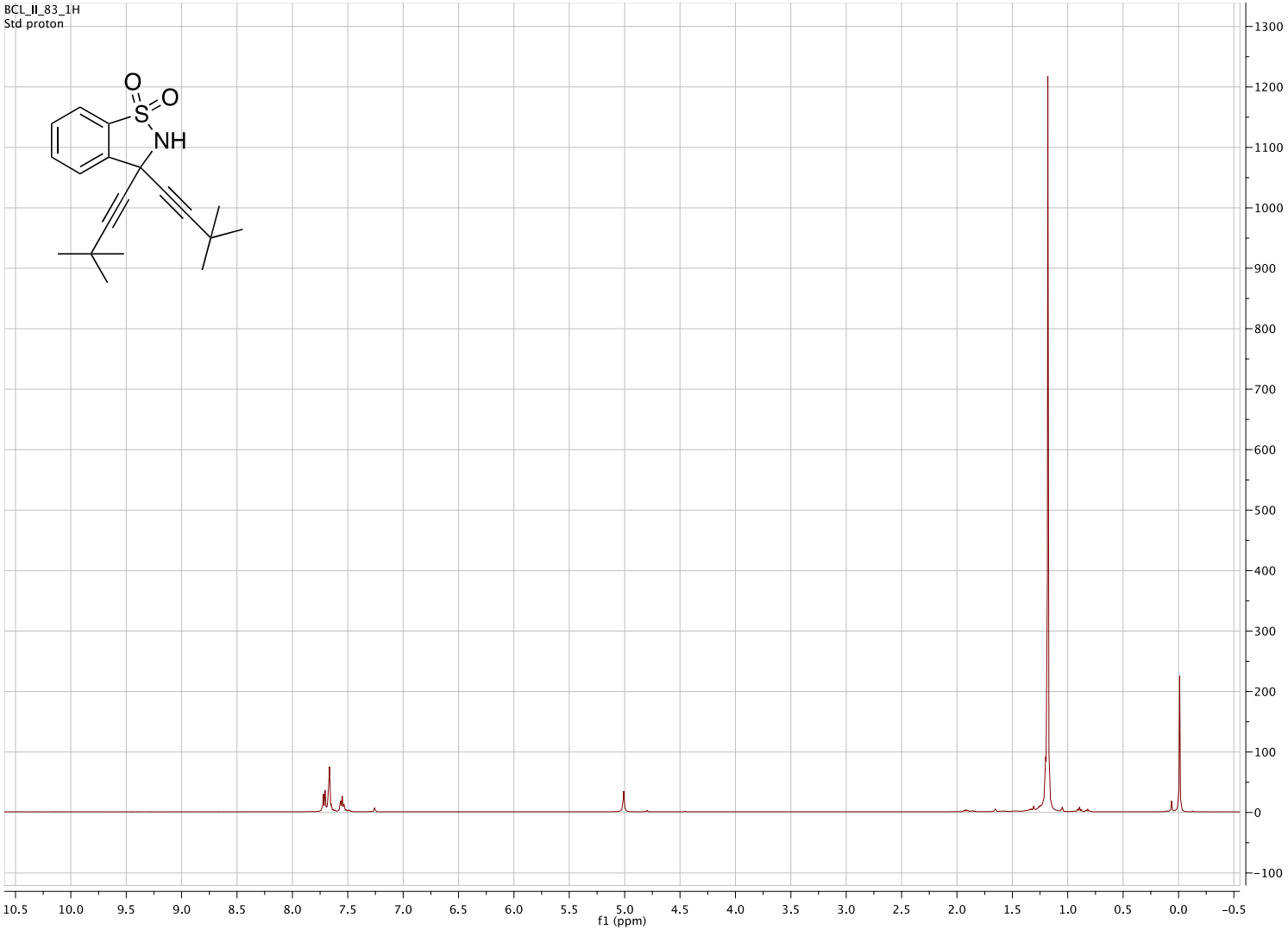


$^{1}$H NMR (500 MHz, $CDCl_3$) of 3,3-bis (*t*-butylethynyl)-2,3-dihydro-1,2-benzisothiazole 1,1-dioxide

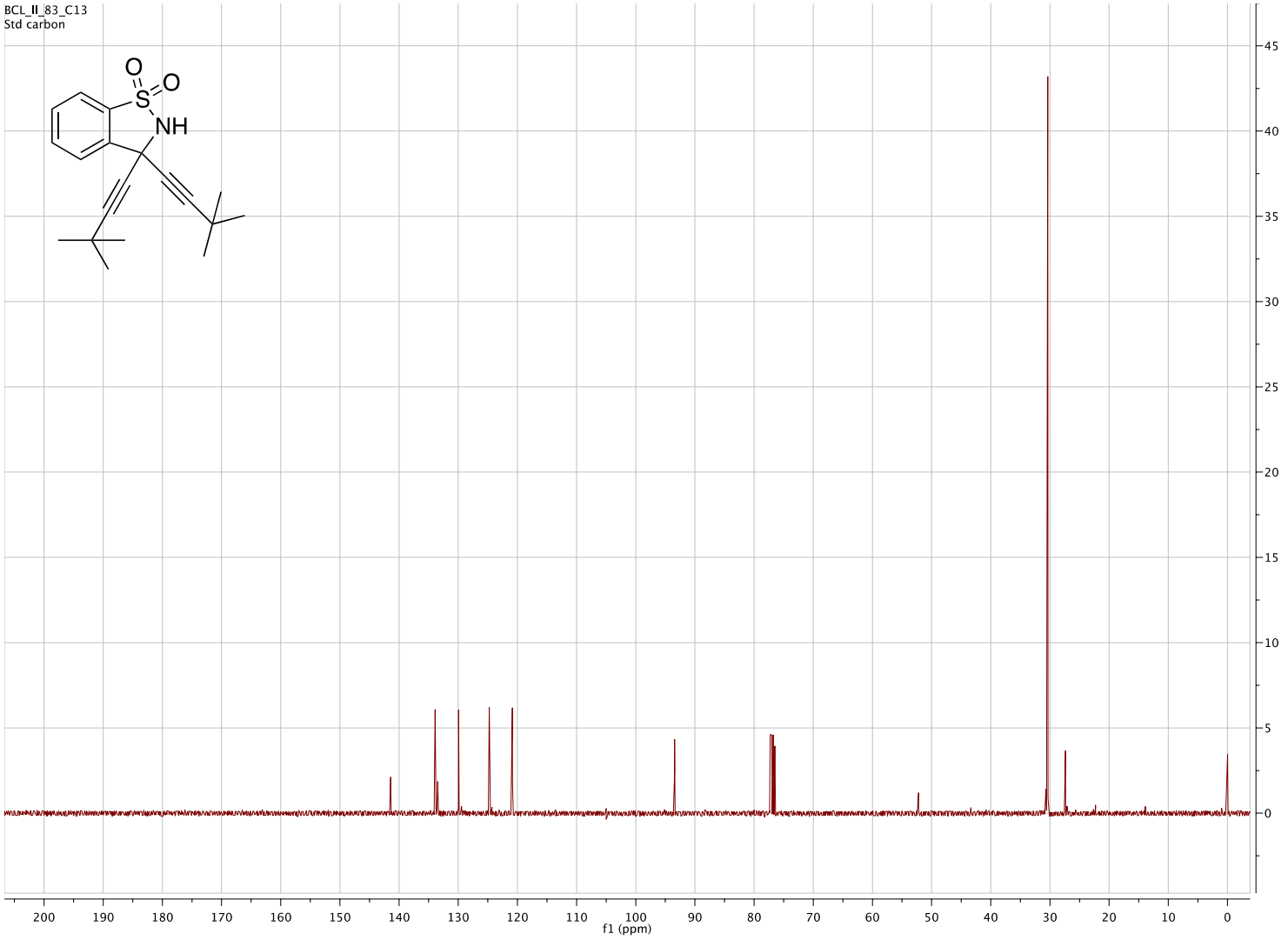


$^{13}C$ NMR (500 MHz, $CDCl_3$) of 3,3-bis (*t*-butylethynyl)-2,3-dihydro-1,2-benzisothiazole 1,1-dioxide

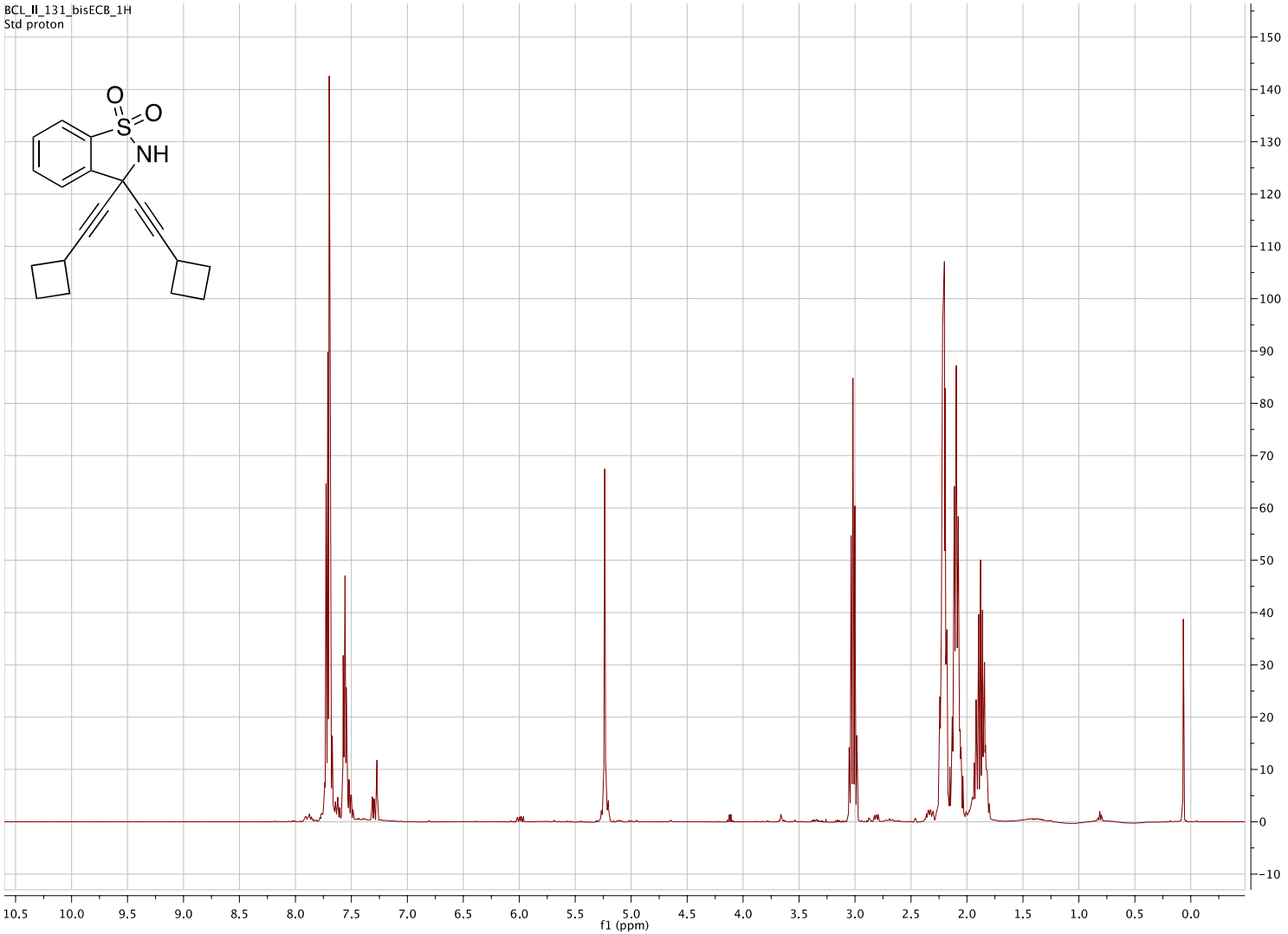


$^{1}$H NMR (500 MHz, $CDCl_3$) of 3,3-bis (cyclobutylethynyl)-2,3-dihydro-1,2-benzoisothiazole 1,1-dioxide

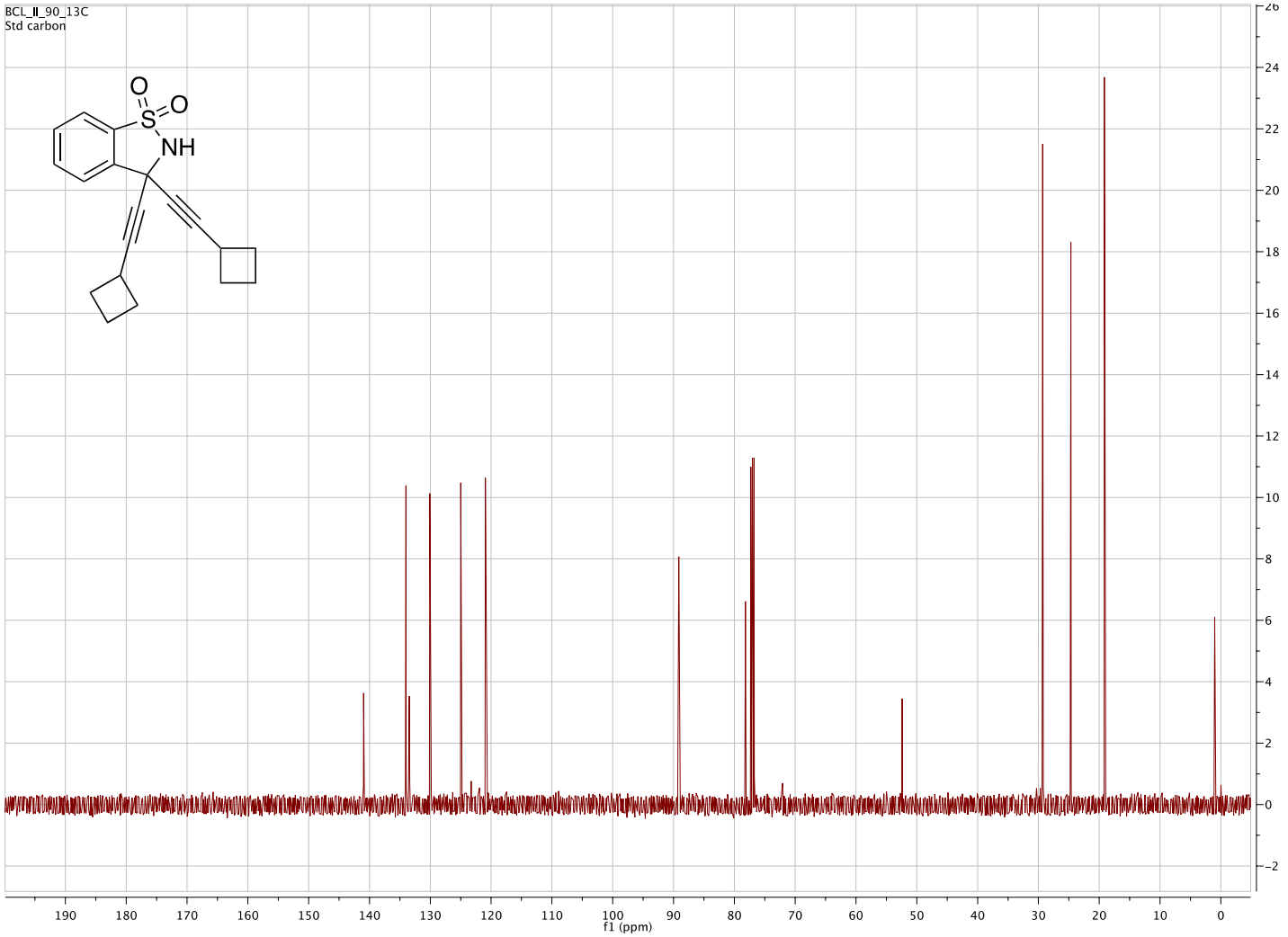


$^{13}C$ NMR (500 MHz, $CDCl_3$) of 3,3-bis (cyclobutylethynyl)-2,3-dihydro-1,2-benzoisothiazole 1,1-dioxide

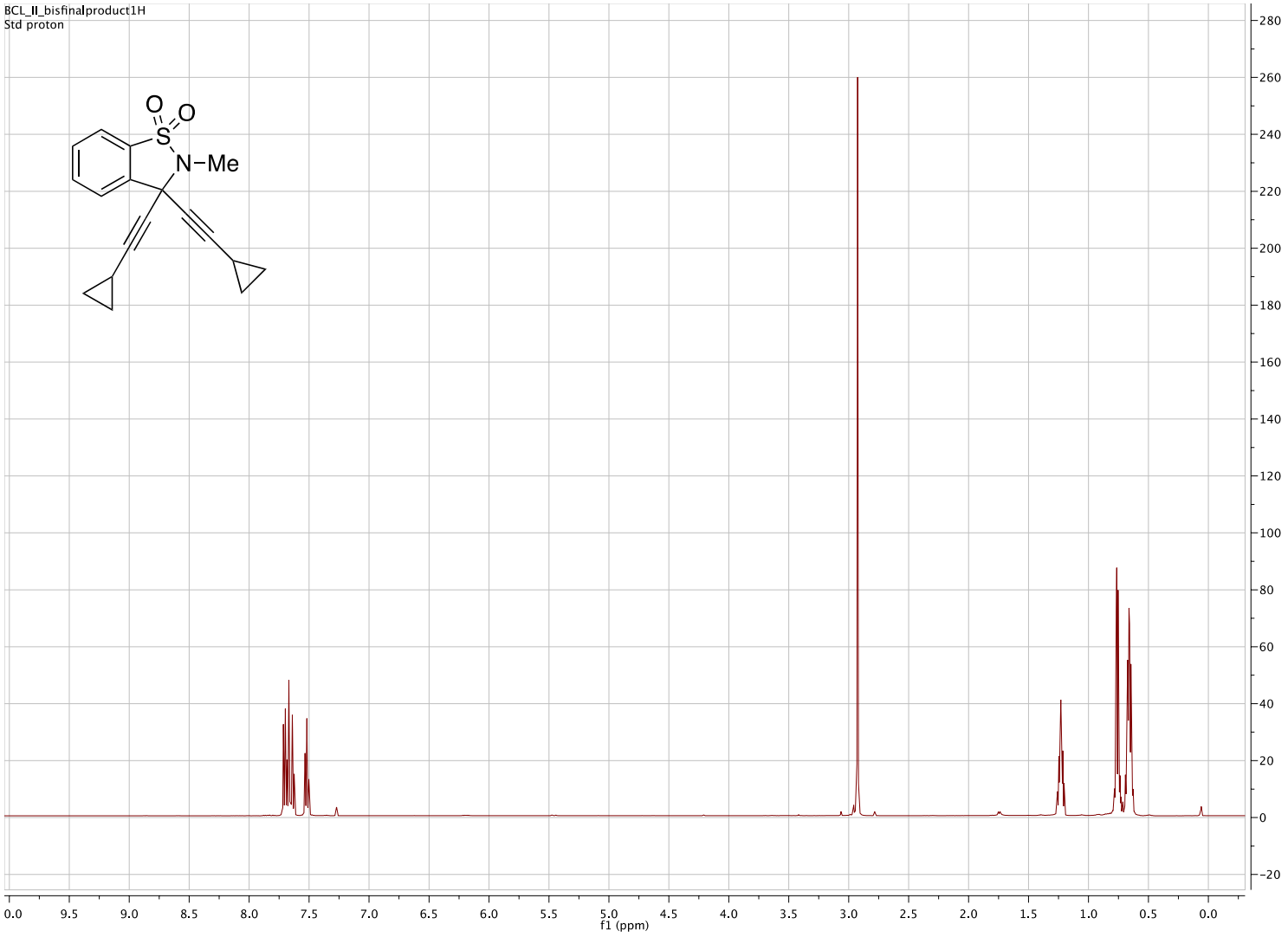


$^{1}$H NMR (500 MHz, $CDCl_3$) of 3,3-bis (cyclopropylethynyl)-2,3-dihydro-2-methyl-1,2-benzoisothiazole 1,1-dioxide

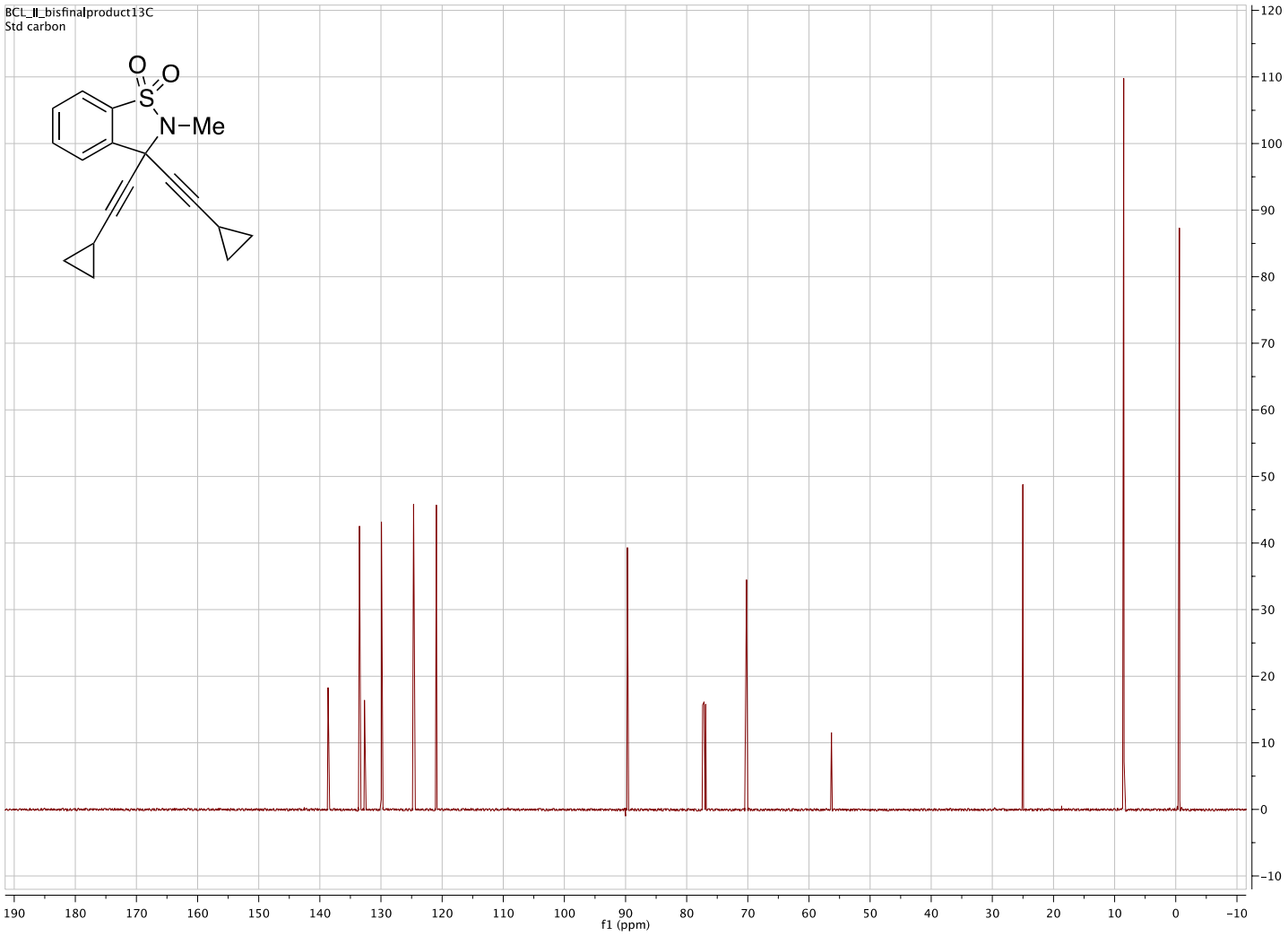


$^{13}C$ NMR (500 MHz, $CDCl_3$) of 3,3-bis (cyclopropylethynyl)-2,3-dihvdro-2-methvl-1.2-benzoisothiazole 1.1-dioxide

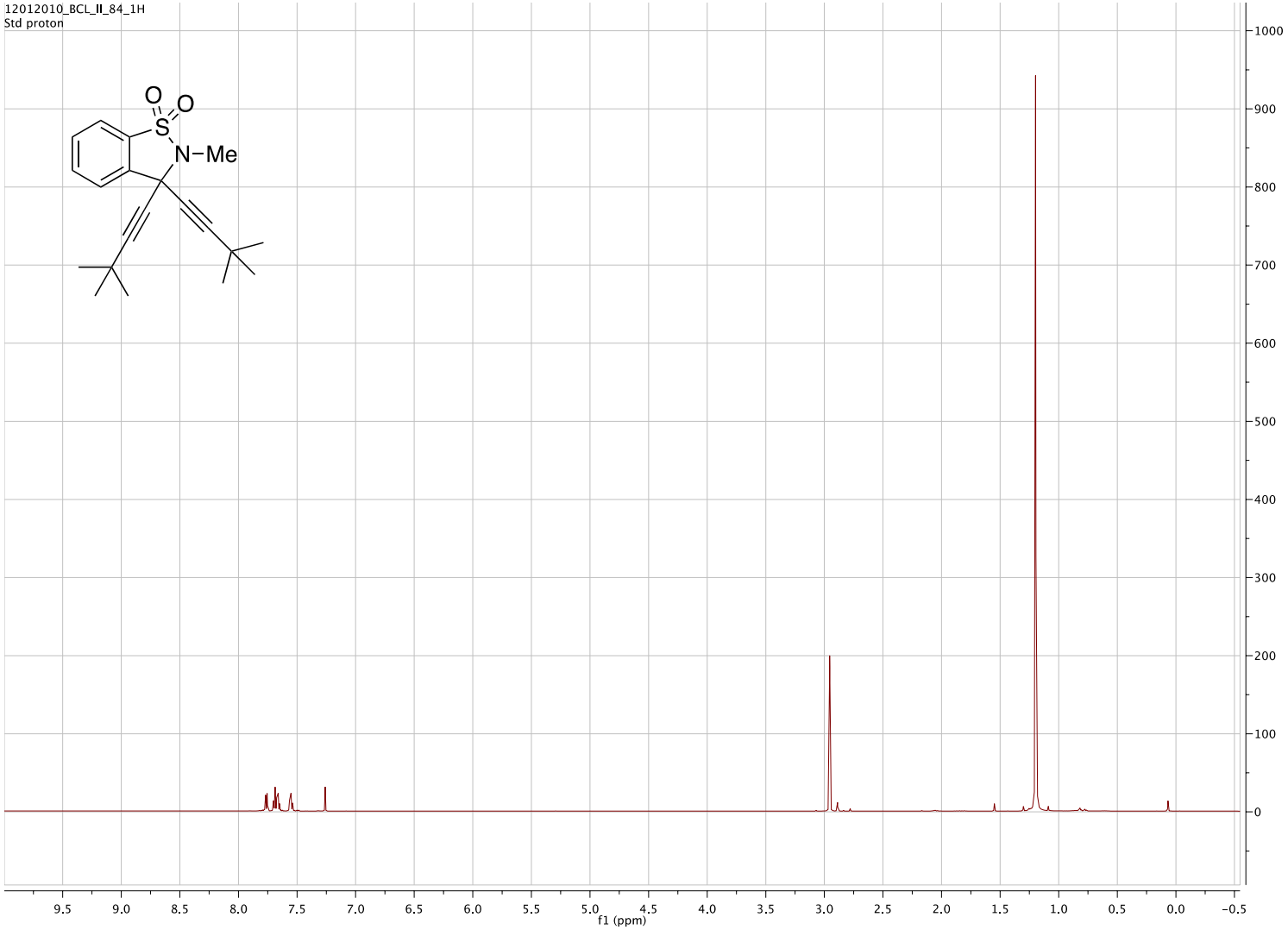


$^{1}$H NMR (500 MHz, $CDCl_3$) of 3,3-bis (*t*-butylethynyl)-2,3-dihydro-2-methyl-1,2-benzoisothiazole 1,1-dioxide

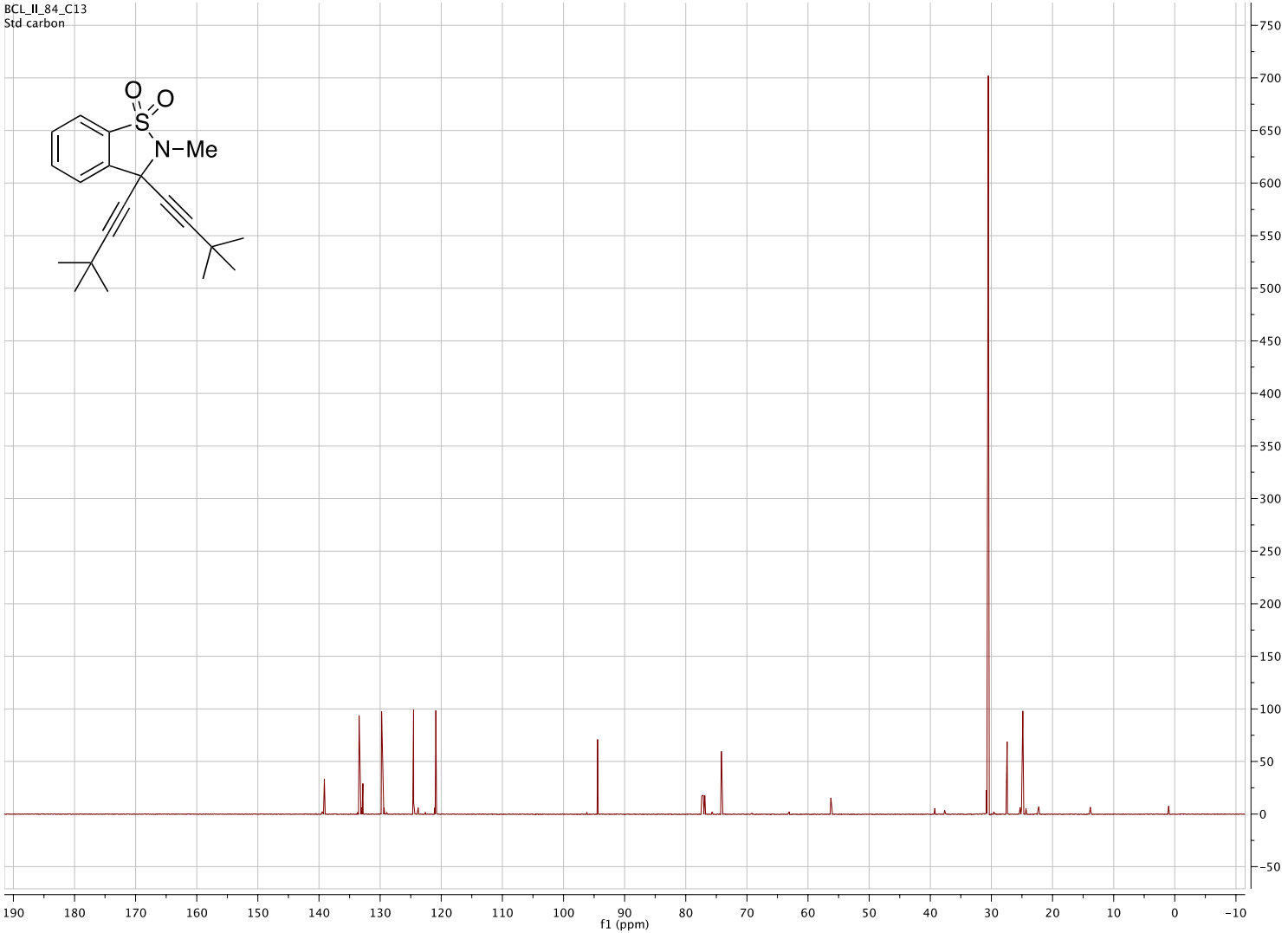


$^{13}C$ NMR (500 MHz, $CDCl_3$) of 3,3-bis (*t*-butylethynyl)-2,3-dihydro-2-methyl-1,2-benzoisothiazole 1,1-dioxide

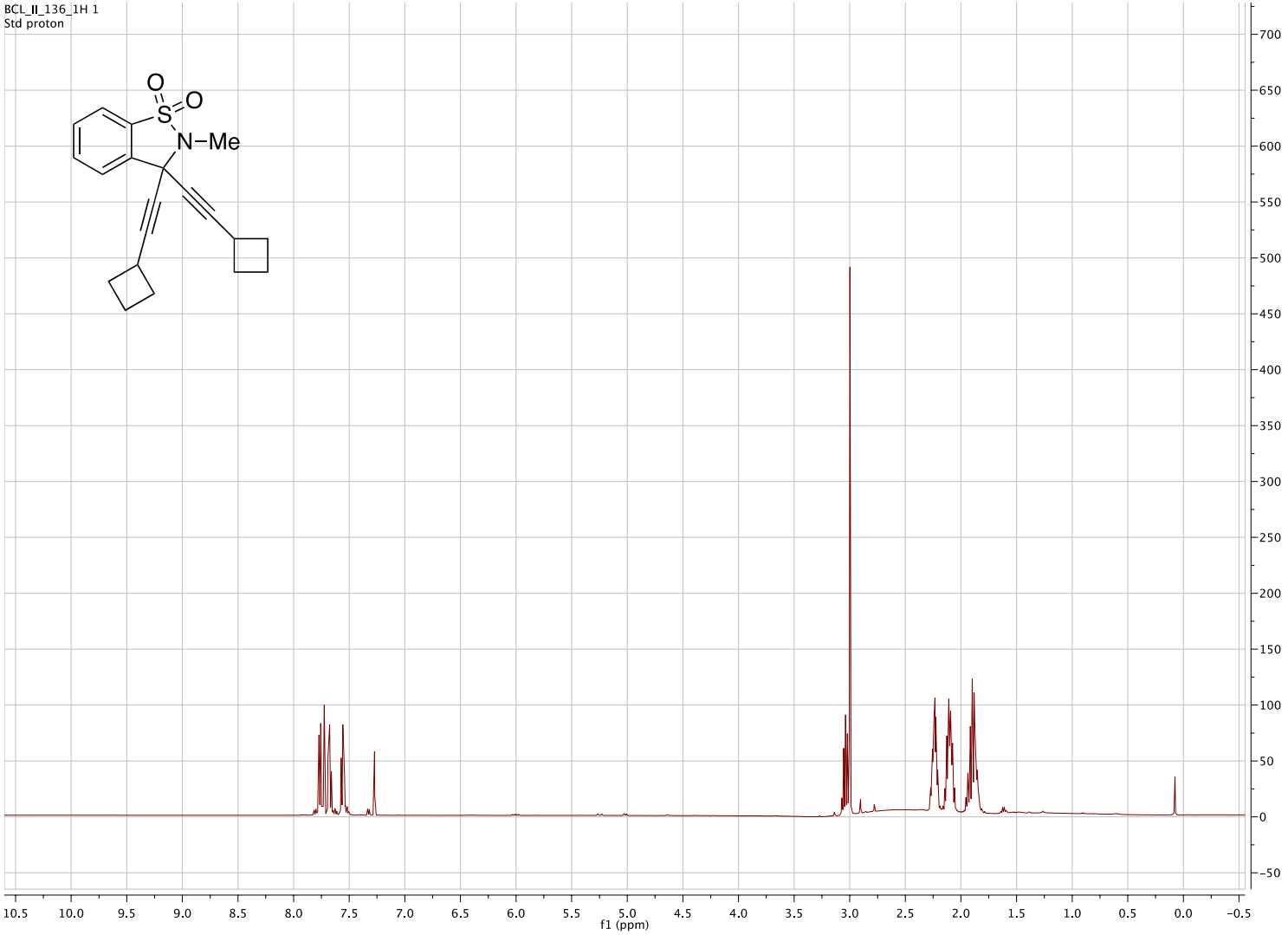


$^{1}$H NMR (500 MHz, $CDCl_3$) of 3,3-bis (cyclobutylethynyl)-2,3-dihydro-2-methyl-1,2-benzoisothiazole 1,1-dioxide

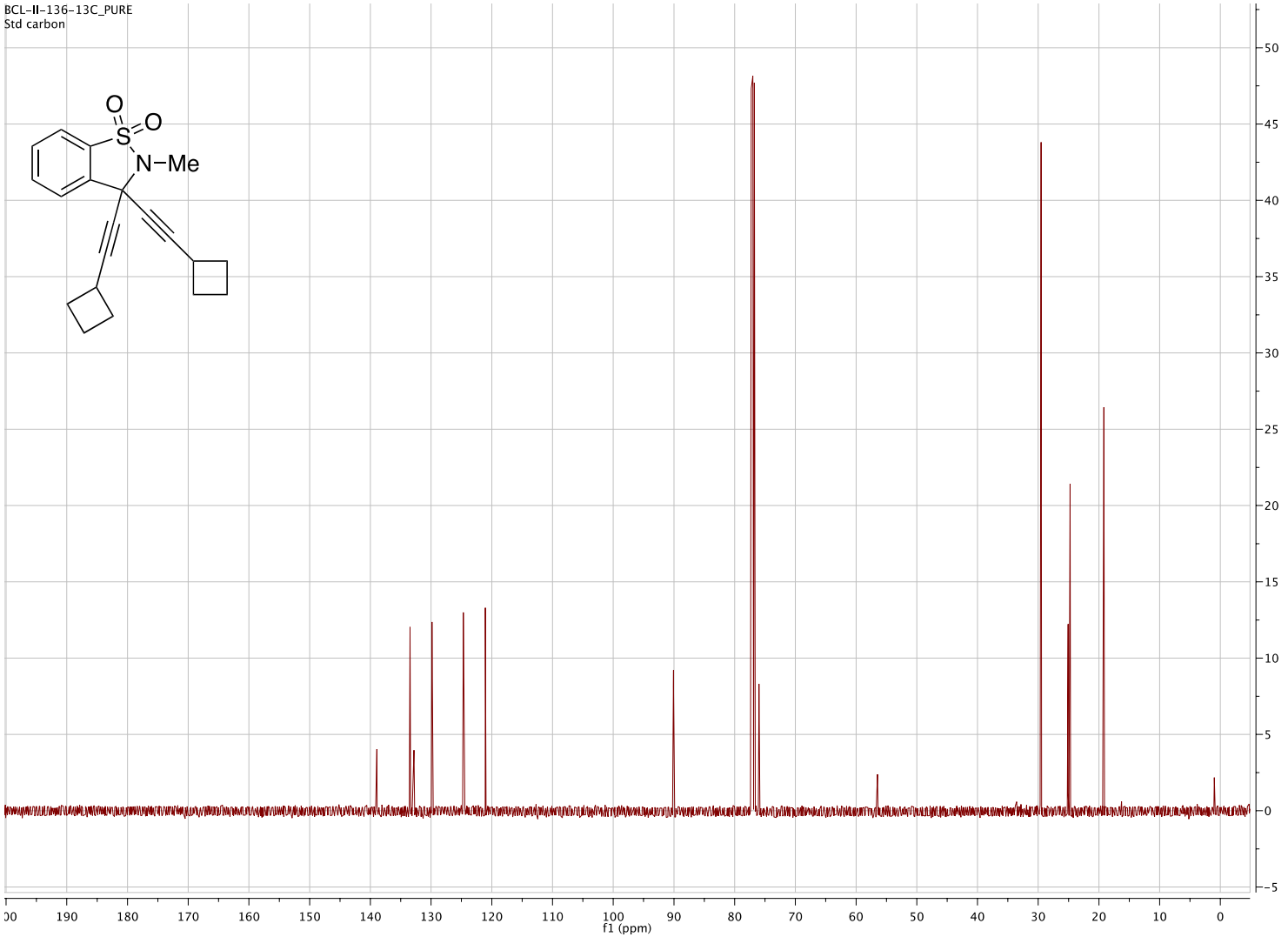


$^{13}C$ NMR (500 MHz, $CDCl_3$) of 3,3-bis (cyclobutylethynyl)-2,3-dihydro-2-methyl-1,2-benzoisothiazole 1,1-dioxide

# VITA

Chad LeCroix was born in Decatur, Alabama on November 8, 1985. He attended St. Ann's Catholic School for K-4 grade, and he finished his Elementary school years at Brookhill Elementary in Athens, AL. He then attended Athens Intermediate and Middle Schools followed by Athens High School where he graduated in May of 2004. It was in eleventh grade with Mrs. Jacquelyn Allen at Athens High School where he first learned chemistry, and he continued his studies in chemistry by taking the dual enrollment course offered at Athens High School through Calhoun Community College. Chad attended Birmingham-Southern College in Birmingham, AL for his undergraduate coursework. While at BSC, he took organic chemistry under Dr. David J. A. Schedler. Dr. Schedler's courses are what first motivated Chad to major in Chemistry, but it was performing research under Dr. Schedler in the Summer of 2007 until May 2008 that convinced Chad that organic chemistry was what he wanted to do. After graduating in May 2008, Chad was enrolled in the graduate school at the University of Tennessee, Knoxville, and joined Dr. David C. Baker's group to work on drug design and synthesis of anti-HIV reverse transcriptase inhibitors. Chad completed the doctorate requirement in July 2013 and officially received his diploma in December 2013.